Measurements in Geochemical Carbon Dioxide Removal

Measurements in Geochemical Carbon Dioxide Removal

1st Edition

September 2023

Measurements in Geochemical Carbon Dioxide Removal

James S. Campbell[1*], Laura Bastianini[1], Jim Buckman[1], Liam A. Bullock[2], Spyros Foteinis[1], Veronica Furey[1], Jess Hamilton[3,4], Kirsty Harrington[1], Olivia K. Hawrot[1], Phil Holdship[5], William J. Knapp[6], Cara N. Maesano[7], Will M. Mayes[8], Philip A.E. Pogge von Strandmann[9] Tom Reershemius[10], Georgina M. Rosair[1], Fiona Sturgeon[11], Connor Turvey[12], Sasha Wilson[12], Phil Renforth[1*]

1. Heriot-Watt University, Edinburgh, EH14 4AS, UK
2. Geosciences Barcelona (GEO3BCN), CSIC, Lluis Solé i Sabarís s/n, 08028 Barcelona, Spain
3. ANSTO – Melbourne 800 Blackburn Rd, Clayton VIC 3168, Australia
4. Monash University, Clayton VIC 3168, Australia
5. Department of Earth Sciences, University of Oxford, South Parks Road, Oxford OX1 3AN, UK
6. Department of Earth Sciences, University of Cambridge, Downing Street, Cambridge, CB2 3EQ, UK
7. RMI, 22830 Two Rivers Road, Basalt, CO 81621, USA
8. School of Environmental Sciences, University of Hull, Cottingham Road, Hull HU6 7RX, UK
9. MIGHTY, Institute of Geosciences, Johannes Gutenberg University, Mainz, Germany
10. Department of Earth and Planetary Sciences, Yale University, 210 Whitney Ave, New Haven, CT 06511, USA.
11. Environmental and Biochemical Sciences, The James Hutton Institute, Aberdeen AB15 8QH, UK
12. Department of Earth and Atmospheric Sciences, University of Alberta, Edmonton, AB, T6G 2E3, Canada

Corresponding authors
*james.campbell@hw.ac.uk
*p.renforth@hw.ac.uk

How to cite:

Campbell, J.S., Bastianini, L., Buckman, J., Bullock, L.A., Foteinis, S., Furey, V., Hamilton, J., Harrington, K., Hawrot, O.K., Holdship, P., Knapp, W.J., Maesano, C.N., Mayes, W.M., Pogge von Strandmann, P.A.E., Reershemius, T., Rosair, G.M., Sturgeon, F., Turvey, C., Wilson, S., Renforth, P. 2023. *Measurements in Geochemical Carbon Dioxide Removal*. 1st Edition. Heriot-Watt University. DOI 10.17861/2ge7-re08 Available from https://doi.org/10.17861/2GE7-RE08.

Forewords

The need for effective approaches to carbon dioxide (CO_2) from the atmosphere (or 'CDR') has become an important part of climate policy for nations to meet their net zero climate targets. With global deployment of CDR the order 10–20 billions of tonnes CO_2 per year by mid-century. CDR includes a range of technologies, such as direct air capture, blue carbon, biochar, and afforestation. One particular pathway gaining increasing attention is geochemical CDR, which uses alkaline minerals to remove and store CO_2. Research suggests geochemical CDR technologies could make substantial contributions to CDR over the coming decades, possibly scaling to billions of tonnes CO_2 per year. However, important challenges remain for their safe and effective deployment. Regulatory hurdles and limited demand could potentially impede the large-scale deployment of geochemical CDR, and robust methods of monitoring, reporting, and verification are required. This is particularly important for industry and regulators who will need to develop confidence in robust certification and viable business models to accelerate widely implementation of these approaches.

This report was coordinated by researchers as part of the Industrial Decarbonisation Research and Innovation Centre (IDRIC, http://www.idric.org). Based in the UK and launched in 2021, IDRIC is a key player pioneering whole system decarbonisation solutions, providing evidence on their effectiveness to industry and policy makers. It is doing this by accelerating the green industrial revolution through collaboration with over 200 partners and stakeholders. These include academic institutions, industry, community representatives and policy makers who are all striving to address urgent innovation priorities. IDRIC is part of the UK Industrial Decarbonisation Challenge and funded by the UK Research and Innovation (UKRI). The Challenge provides £210 million, matched by £261 million from industry, to enable the delivery of a wide range of projects to ensure four decarbonised clusters by 2030 and one net-zero industrial cluster by 2040.

Collaboration among experts from various fields will be essential for the international validation, verification, and enhancement of geochemical CDR. This guide's aim is to provide a tangible resource that bridges theory and practice, offering tools to support the ongoing efforts to counteract the impacts of climate change. I am confident that this guide represents a key step to accelerate the pace and scale of deployment of geochemical CDR to meet our global climate targets.

Prof. Mercedes Maroto-Valer, FRSE
Director for the Industrial Decarbonisation Research and Innovation Centre
Heriot-Watt University, Edinburgh, United Kingdom, September 2023

The inspiration behind this document was initially in response to the numerous enquiries we often receive from industry on suitable methods of accounting for carbon dioxide removal in alkaline waste materials. While we were putting together this report,

it became increasingly clear that this information is required for all geochemical-based carbon dioxide removal approaches, particularly to support the ongoing work in developing robust methods of monitoring, reporting, and verification. As such, the scope of the document was expanded to cover a wide range of measurement approaches. While this is not exhaustive, we believe that this is the most comprehensive account of collated measurement techniques for geochemical CDR (as standard operating procedures, SOPs). These SOPs are intended to offer guidance for specialists both in academia and industry, encompassing sampling of solids and liquids, analysis of physical characteristics of alkaline materials, determination of elemental composition, examination of mineralogy, quantification of stored mineralised CO_2, and measurement of alkalinity generation in waters/solutions. These SOPs are designed to provide general methods while highlighting potential pitfalls, offering a practical foundation for measurement activities in the realm of geochemical CDR.

We hope that this 1st Edition, which we have made freely available to the community, will be further developed and improved in response to the needs of the geochemical CDR field. We are eternally grateful to our co-authors who have brought diverse expertise in geochemical CDR to this project and have made outstanding contributions to the document, without whom this report would not have been possible. We welcome anyone from the community who has comments or thoughts on this Edition, or who would like to contribute to further editions, to contact us.

Prof. Phil Renforth and Dr James Campbell
Lead Authors
Heriot-Watt University, Edinburgh, United Kingdom, September 2023

Interest, research, and investment in geochemical carbon dioxide removal (CDR) is accelerating rapidly. Effective deployment of CDR will require rigorous measurement, reporting, and verification (MRV), but much work remains to ensure that geochemical measurements are used effectively. We are excited by the release of the first edition of *"Measurements in Geochemical Carbon Dioxide Removal"*, which provides a timely synthesis of technical best practices and is freely accessible to the public.

Although the field of CDR as a whole is still nascent, a handful of resources have been developed to help teach and guide the science. The *CDR Primer*, for example, provided a high-level synthesis of CDR science across a range of pathways, creating a shared knowledge base for scientists and practitioners from different disciplines. We see this new report serving a similar function, but at a more detailed level, providing a much-needed summary of "what can we measure" and "how can we measure it" for geochemical CDR. While it might seem obviously useful, detailed resources that fully connect the "what," the "why," and the "how" of scientific measurements are rare. Journal articles, for example, often say what was measured, but assume the reader knows about the underlying analytical techniques. Alternatively, they go into the details of a measurement method but without giving context for why it matters. This report should serve as a resource for all members of the geochemical CDR community,

helping them learn about relevant analytical techniques and make more effective and informed decisions about implementation and deployment.

Regardless of the CDR pathway, planning for the future requires solid technical foundations. By synthesising geochemical measurement best practices, this resource helps build that foundation for geochemical CDR. We hope that *"Measurements in Geochemical Carbon Dioxide Removal"* will support the development and implementation of rigorous MRV standards, and that similar efforts might emerge across other CDR pathways in the future.

Dr Tyler Kukla, Freya Chay, and Dr Jeremy Freeman
CarbonPlan
September 2023

Contents

Executive summary

Geochemical carbon dioxide removal (CDR) technologies capture and store carbon dioxide (CO_2) from the atmosphere using alkaline materials that are rich in calcium (Ca) and magnesium (Mg). Alkaline materials include natural rocks such as basalt, industrial by-products such as steel slag, or artificially generated and industrially produced materials such as lime. Geochemical CDR technologies speed up the reactions of such materials with air or other CO_2-bearing gases, and convert the CO_2 into solid carbonate minerals or dissolved inorganic carbon in the ocean. Gigatonne (Gt) scale removal is potentially possible with geochemical CDR owing to the abundant quantities of alkaline materials, in addition to durable carbon storage over thousands of years.

Interest in geochemical CDR has expanded considerably over the past 5 years, as researchers and practitioners explore its feasibility. However, further research, development, and deployment of geochemical CDR may be limited by a lack of robust and standardised approaches to measurement. In this work, aspects of measurement in geochemical CDR are considered with the objectives of i) accounting for carbon accumulation in a material or solution, ii) assessing the capacity of the material to react with CO_2, iii) understanding how material properties may impact the speed of reaction with CO_2, iv) collecting sufficient information on a material to aid in the design of a reaction process, and v) collecting sufficient information such that risks associated with a mineral can be assessed. In order to help meet these objectives, materials properties must be collected via analytical techniques.

Here we present guidance for the application of these analytical techniques in the form of standard operating procedures (SOPs), tailored to meet the needs of geochemical CDR projects. The collection of accurate data obtained through standardised methods could facilitate project feasibility, design and operation, carbon accounting, and foster regulatory confidence in the industry. Given the often-heterogeneous nature of alkaline materials and the range of technologies that might facilitate their reaction with CO_2, this document is for guidance only and the protocols should be adapted to suit the needs of the user. As the field innovates, we anticipate updating this report with additional operating procedures, and welcome such contributions to future editions.

1. Introduction

Owing to the increasing concentration of atmospheric carbon dioxide (CO_2) of anthropogenic origin and its connection with climate change, there is a need for technologies which can capture and store CO_2 from the air (termed carbon dioxide removal, CDR). There are several pathways for CDR including direct air capture (DAC), blue carbon, biochar, afforestation, reforestation, soil carbon sequestration, and ocean fertilisation (Bui and Mac Dowell, 2022; National Academies of Sciences, Engineering, and Medicine, 2021; Wilcox et al., 2021).

Geochemical CDR refers primarily to those approaches which use abundant alkaline minerals as part CO_2 removal or storage (Campbell et al., 2022). These include 'in situ', 'ex situ', and surficial CO_2 mineralisation, enhanced weathering (EW) in soils, and ocean alkalinity enhancement (OAE) (see Section 2 for a primer on geochemical CDR). Geochemical CDR may also encompass forms of DAC that utilise alkaline materials such as magnesia (McQueen et al., 2020), lime (Lackner et al., 2001) or mine tailings (Kelemen et al., 2020) in a series of carbonation/calcination cycles to produce high concentration CO_2 for use or storage. Together, geochemical CDR technologies have the potential to remove and permanently store large quantities of CO_2 as carbonate minerals or dissolved ocean bicarbonate (Maesano et al., 2022).

Over the next few decades, geochemical CDR technologies have the potential to grow from (kilotonne) kt CO_2 yr^{-1}, toward (megatonne) Mt CO_2 yr^{-1}, and possibly to (gigatonne) Gt CO_2 yr^{-1} removal (Maesano et al., 2022). However, for geochemical CDR, limiting factors for upscaling may result from a lack of demand, or from prohibitive regulation (e.g., OAE), rather than technological barriers or material scarcity. Addressing both demand and regulatory progress requires robust measurement, verification, and reporting (MRV) frameworks, as also highlighted in a recent "CDR Knowledge Gap Database" (Frontier, 2022). Buyers (be it public or private) should be satisfied that carbon credits purchased from geochemical CDR companies provide durable, net greenhouse gas (GHG) removals, and that any negative externalities (and co-benefits) are well understood.

Although recent work considers MRV for soil EW (PuroEarth, 2022; Wolf et al., 2023), in situ (subsurface) CO_2 mineralisation (Ratouis, 2022), CO_2 mineralisation in concrete (Verified Carbon Standard, 2019), DAC (Pretorius, 2022), and best practice guides for OAE research (Ho et al., 2023), there is a need for a reference document which specifically discusses measurement aspects relevant to MRV frameworks.

To address part of this gap, aspects of measurement relevant to geochemical CDR are extensively covered with the goal of providing a reference guide to geochemical CDR measurement. It is intended that this volume will provide new specialists (both in industry and academia) with the tools to be able to construct systems of measurement for

geochemical CDR experiments or field trials. Specifically, we consider the following, aided by 'standard operating procedures' (SOPs):

1. Sampling of solids and liquids.
2. Physical characteristics of solid alkaline materials, e.g., porosity (SOP 1), particle size (SOP 12) and surface area (SOP 13), which are needed to assess rates of reaction with CO_2.
3. Elemental composition, e.g., cation measurement, which is necessary to understand the maximum potential of the feedstock to capture and store CO_2 (SOP 2–5, and 11).
4. Mineralogy – which is useful for understanding the rate of reaction of the feedstock and identifying the types and stability of carbonate mineral products (SOP 6–8).
5. Quantification of the stored mineralised CO_2 which may be crucial in determining or proving the total CO_2 that has been captured and stored (SOP 9–11).
6. Measurement of waters/solutions for determination of alkalinity generation and thus potential for CO_2 capture and storage in the form of dissolved bicarbonate (SOP 3–5 and 14–16) or the contribution of a range of other anions (SOP 17).

SOPs are procedures specific to an operation that describe the activities necessary to complete tasks in accordance with industry regulations, provincial laws, or within a business or organisation. Many of the SOPs provided in this document have been used for decades, but have been tailored to meet the needs of geochemical CDR. Further, these SOPs have, in some cases, been updated to include the accumulated experience of the authors and any recent advances and state of the art instrumentation. Although the SOPs take the analyst through the entire analytical procedure, they are not instrument specific. Thus, the exact procedures used will differ between instruments. Furthermore, sample preparation will also differ depending on the nature of the material. For example, potential asbestos-hosting materials may need special sampling and preparation methods for safety purposes.

The main purpose of the SOPs in this document is to provide guidance on geochemical CDR measurements while highlighting potential pitfalls. To achieve this, the SOPs are not overly prescriptive. In addition to the SOPs, we contextualise measurements relevant to geochemical CDR, including carbon accounting, life cycle assessment (LCA), and sampling. The SOPs provided here are the first attempt to provide measurement advice and will be updated and refined over time, particularly in response to evolving experience and demand of the emerging geochemical CDR industry. The international validation, verification, and updating of these SOPs will require collaboration from a number of experts working in different fields.

Although this document is focussed on CDR i.e., CO_2 that has been captured directly, or indirectly (e.g., DAC), from air, the SOPs may also be relevant for permanent storage of CO_2 that would otherwise be emitted (emissions reduction) e.g., mineralisation of CO_2 from flue gases into alkaline materials. Many of the SOPs contained in this document are applicable to geochemical CDR technologies generally (e.g., carbon mineralisation, EW, OAE, some DAC

processes) as described in the primer (see Section 2). However, subsurface (in situ) CO_2 mineralisation is only briefly considered in this document. For in situ CO_2 mineralisation, a combination of reactive and non-reactive tracers, mass balances, and geochemical modelling, rather than frequent physical sampling, are likely to dominate measurement activity (Matter et al., 2016). Thus, this document is predominantly designed for geochemical CDR technologies taking place at the Earth's surface.

1.1 How to use this document

This document provides an overview of geochemical CDR approaches (Section 2) and how these are considered within MRV protocols (Section 3). An introduction to materials and site investigation is also provided (Section 4), and those objectives that relate to geochemical measurements are expanded upon (Sections 5, 6 and 7). SOPs are included within the Supplementary Information but are summarised in Figure 1.

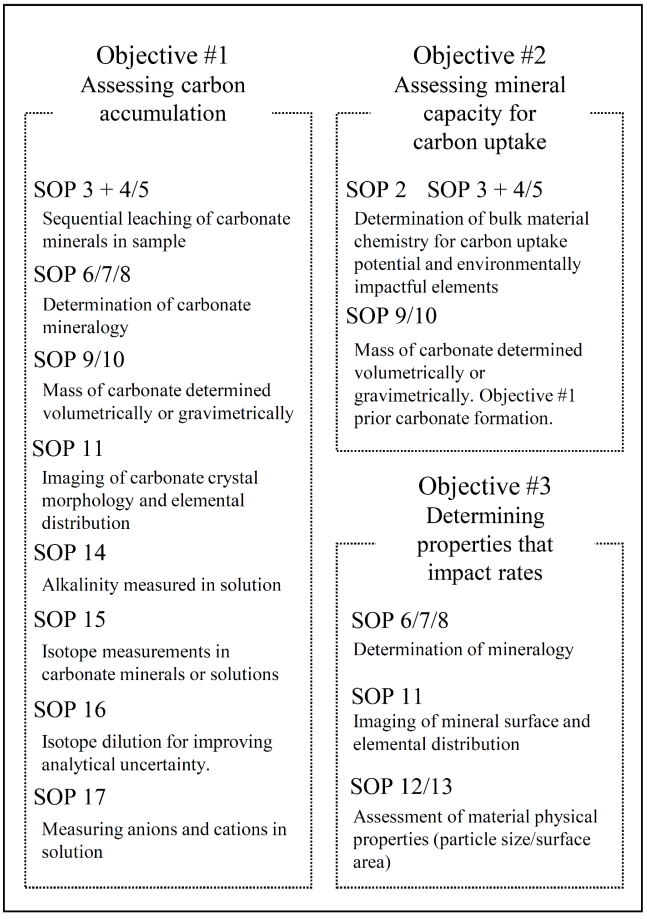

Figure 1. An overview of geochemical CDR measurement SOPs and how these relate to the objectives of a site or material investigation (see Section 4 for an overview of objectives).

2. Geochemical CDR primer

2.1 Introduction

Geochemical CDR is a group of technologies that remove CO_2 from air, directly or indirectly, using (large) quantities of alkaline (Ca- and Mg-rich) materials which include natural alkaline rocks (e.g., peridotite, basalt, or limestone), or artificial materials such as industrial by-products and wastes (e.g., mine tailings and slags), or tailored alkaline materials (e.g., lime). These technologies include in situ, ex situ, and surficial CO_2 mineralisation (see Figure 2), where CO_2 is stored as solid carbonate minerals; OAE, where CO_2 is stored as dissolved ocean bicarbonate; and EW, where CO_2 can be stored as dissolved bicarbonate (in the ocean, eventually), but also as carbonate minerals in soil. Geochemical CDR may also encompass some forms of DAC (e.g., those that use ambient carbonation of solid alkaline materials).

In carbonate mineral formation (e.g., Eq. 1), in theory, 1 mole of CO_2 can be removed for every 1 mole of alkaline metal, creating one molecule of a highly stable carbonate mineral with storage times on the order of >10^6 years.

$$Mg_2SiO_{4(s)} + 2CO_{2(g)} \rightarrow 2MgCO_{3(s)} + SiO_{2(s)} \quad \text{Eq. 1}$$

For bicarbonate creation (e.g., Eq. 2), in theory, 2 moles of CO_2 can be removed for every alkaline cation (and one mole for each alkali cation, e.g., Na), with storage times on the order of 10^4 to 10^5 years.

$$Mg_2SiO_{4(s)} + 4CO_{2(g)} + 4H_2O_{(l)} \rightarrow 2Mg^{2+}_{(aq)} + 4HCO^{-}_{3(aq)} + H_4SiO_{4(aq)} \quad \text{Eq. 2}$$

The longevity of the CO_2 stored via geochemical CDR could be attractive to buyers of CO_2 removal credits who are concerned about the durability of CO_2 storage. MRV protocols for CO_2 mineralisation technologies ought to be more straightforward than for EW and OAE, given that products are in their immobile solid form and unlikely to be highly dispersed in the environment. Regardless, all geochemical CDR approaches will have their own unique MRV challenges.

2.2 Resources

Natural alkaline rocks and minerals. A mineral is an inorganic solid with distinctive composition, atomic structure, and physicochemical properties, whereas rocks are natural assemblages of minerals. Natural alkaline minerals are often silicate-based minerals, which are rich in alkaline earth metal cations such as Ca and Mg. Other natural Mg- and Ca-rich alkaline minerals may include carbonates and aluminosilicates, and less so oxides and hydroxides. These minerals are found in alkaline rocks, including: (i) igneous rocks, such as

basalt and peridotite, (ii) metamorphic rocks, such as serpentinite, and (iii) sedimentary rocks such as limestone or dolomite. Basic igneous and metamorphic rocks typically contain 15–28% MgO, 1–15% CaO, and 46–54% SiO_2 (among other minor components), whereas ultrabasic rocks typically contain 35–46% MgO, 5–15% CaO, and 42–48% SiO_2 (Sen, 2014). Rocks such as these are primarily mined and processed by the construction aggregates industry, whose annual capacity exceeds 50 Gt (Sverdrup et al., 2017), suggesting that marginal increases in production would be sufficient to reach the Mt CO_2 $yr.^{-1}$ scale using geochemical CDR technologies.

Artificial alkaline materials can also be used for geochemical CDR. These typically include wastes or by-products of industrial processes, such as landscaping or quarrying, or even artificial materials tailored for specific industrial applications (Dijkstra et al., 2019). It is often more appropriate to use 'materials' than 'minerals' as not all of these are crystalline. On a global scale, it is estimated that 7 Gt of these alkaline material by-products and wastes are produced annually, with a combined potential to capture and store 2.9–8.5 Gt CO_2 $yr.^{-1}$ by 2100 (Renforth, 2019). These materials generally have little commercial value and are often deposited in managed heaps, submerged in ponds, or buried. While weathering takes place slowly without intervention, most legacy deposits may be only partially reacted with CO_2, suggesting substantial potential for additional CO_2 removal. For example, 40–140 years after the deposition of a 30 Mt slag deposit in Consett, UK, only ~3% of its CO_2 sequestration potential has been achieved (Mayes et al., 2018; Pullin et al., 2019). The reactivities of artificial alkaline materials are typically greater than natural minerals, partly caused by larger surface areas and higher crystal disorder (La Plante et al., 2021). These materials may be less abundant than natural rocks and contain potentially toxic metals, limiting the applicability of some materials to uncontrolled weathering in the open environment. Artificial materials may also include tailored minerals, for example lime (CaO) and magnesia (MgO) which are produced via the calcination of their respective carbonate rocks, i.e., limestone and dolomite. These have even higher reactivities than slags and mine tailings and can be used in some geochemical CDR approaches (Kheshgi, 1995; McQueen et al., 2020).

2.3 CO_2 mineralisation

Ex situ mineralisation. Ex situ CO_2 mineralisation involves reaction of high surface area alkaline materials with CO_2-rich gases in reactors (Gerdemann et al., 2007; Lackner et al., 1995). For this, alkaline material feedstocks are usually transported to a site of CO_2 production. While ex situ processes could be integrated with existing sources of concentrated CO_2 (e.g., industry), co-deployment with DAC may also be possible. Lab and pilot tests have been performed using crushed rocks rich in olivine (Kwon et al., 2011), serpentine (Nduagu et al., 2012; Park and Fan, 2004; Wang and Maroto-Valer, 2011), and wollastonite (Daval et al., 2009; Huijgen et al., 2006) as well as mine tailings (Bodénan et al., 2014) and iron and steel slags (Yadav and Mehra, 2017). High temperatures and pressures, high CO_2 partial pressures, additives, and mechanical or heat activation are often needed to

enhance the rate of reaction with CO_2 (Domingo et al., 2006; Fabian et al., 2010; Farhang et al., 2019; Krevor and Lackner, 2011; Li et al., 2019; Li and Hitch, 2018).

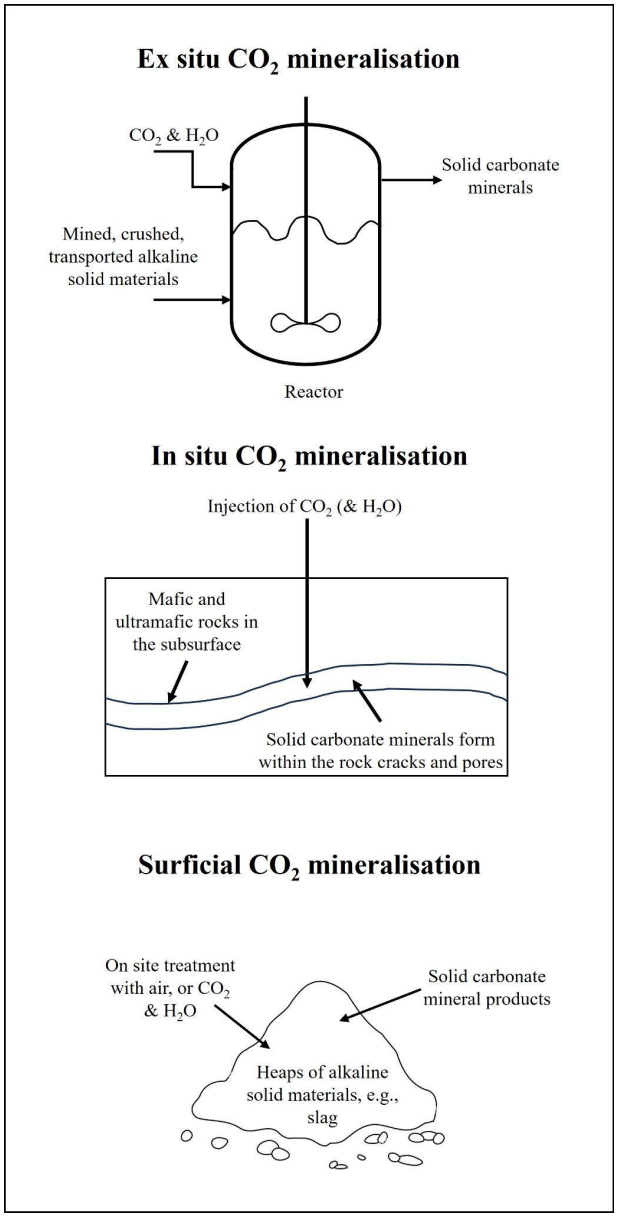

Figure 2. Schematic of three main approaches for achieving CO_2 mineralisation.

Ex situ processes can be broadly categorised as either "direct" or "indirect." Direct ex situ CO_2 mineralisation occurs in one single step, as a gas-solid (Kwon et al., 2011; Liu et al., 2018) or as a gas-liquid-solid process (Benhelal et al., 2019b; Li et al., 2019). Indirect ex situ CO_2 mineralisation involves multiple steps, including the extraction of Mg and/or Ca from the mineral feedstock, followed by reaction with CO_2. Multistep approaches usually involve some pH swing using chemical reagents such as hydrochloric acid (Ferrufino et al., 2018; Lackner et al., 1995), acetic acid (Kakizawa et al., 2001), ammonium salts (Highfield et al., 2012; Wang

and Maroto-Valer, 2011), ammonia and brine (based on solvay process) (Huang et al., 2001), or molten salt ($MgCl_2.nH_2O$) (Wendt et al., 1998). Direct mineralisation requires pure CO_2 for reaction (necessitating integration with DAC, or bioenergy with carbon capture and storage (BECCS), or another process that directly or indirectly captures atmospheric CO_2 for CDR), whereas some indirect processes produce reactive alkaline hydroxides that may be suitable for direct reaction with atmospheric CO_2. Ex situ approaches can also produce useful carbonated products (Fernández Bertos et al., 2004; Hills et al., 2020; Qiu, 2020). Quantification of the stored CO_2 for ex situ processes, which typically occur on a smaller scale than other geochemical CDR technologies within closed reactors, should be relatively straightforward by simple mass balances. Concrete curing type processes may require more involved MRV protocols (Verified Carbon Standard, 2019).

In situ mineralisation. In situ CO_2 mineralisation involves the injection of CO_2 (as a gas, or pre-dissolved in water) into subsurface alkaline geological rock formations such as basalt or peridotite, where the CO_2 reacts with alkaline earth metal cations (namely Mg^{2+}, Ca^{2+}, Fe^{2+}), forming stable carbonate minerals (Kelemen et al., 2020; Kelemen and Matter, 2008; Ratouis, 2022). In situ CO_2 mineralisation requires careful site selection, monitoring, and engineering to ensure that the injected CO_2 remains trapped in mineral form and does not lead to unintended environmental or geological consequences. Drill cores can be used to obtain physical solid samples. However, relatively small amounts of carbonate minerals are precipitated compared to the surrounding rock formation, limiting the representativeness of physical sampling. Geochemical monitoring can be achieved by installing sensors within boreholes that can offer real-time data on various parameters such as pressure, temperature, and chemical composition. Tracer techniques involve injecting a known quantity of a traceable substance along with the CO_2 during the injection process. As the CO_2 reacts with minerals and forms carbonates, the tracer substance's movement and distribution can be tracked. This helps researchers determine the extent of CO_2 spread, the reaction rates, and the overall progress of CO_2 mineralisation. Tracers may be reactive such as Ca isotopes, or $^{14}CO_2$ (radiocarbon), or non-reactive tracers (e.g., SF_6) (Matter et al., 2016). For example, certain Ca-isotope ratios rapidly increase with pH and calcite saturation state, indicating calcite precipitation. Geophysical methods involve using various techniques to measure changes in the physical properties of the storage site, which can provide valuable information about the behaviour of stored CO_2. For example, seismic surveys use sound waves to create images of subsurface structures, helping to track the movement and distribution of CO_2 within the geological formations. Gravity measurements can detect changes in the density of rocks due to CO_2 injection and mineralisation, offering insight into the extent of carbonation. Remote sensing can help monitor surface deformation, temperature changes, and even chemical interactions between the stored CO_2 and the geological formations. These satellite-based observations contribute to the overall understanding of the carbonation process over larger spatial scales. The aforementioned approaches to monitoring can provide real physical data that can be fed into computational models to simulate the complex interactions between CO_2, minerals, and fluids within the

geological formations. These models integrate geological, hydrological, and geochemical data to predict how the stored CO_2 will evolve over time. They assist in estimating reaction rates, potential migration pathways, and the long-term stability of mineralised carbon. Model predictions can then be compared to real-world monitoring data for validation and refinement.

Surficial mineralisation. This form of mineralisation involves reaction of air, or CO_2-bearing gases or fluids, with high surface area natural alkaline rocks, mine tailings or other alkaline industrial by-products/wastes, in large piles, heaps, or in controlled spaces such as closed ponds or greenhouses, forming carbonate minerals. Surficial processes occur more slowly than ex situ processes and they generally require less intensive reaction conditions, with carbon removal occurring over weeks to months, rather than minutes or hours. Surficial approaches allow minerals to be carbonated near to their site of mining (natural rocks) or production (artificial materials), thus reducing mineral transportation costs. Like ex situ approaches, surficial approaches enable the sale of the carbonated materials, for example, as aggregates for the building and construction sector (Huntzinger et al., 2009a; Huntzinger, et al., 2009b; Liu et al., 2021). One surficial method was investigated by (Myers and Nakagaki, 2020) who proposed a gas-solid reaction of crushed basalt, or slag, spread thinly in vertical tiers in a greenhouse. Solar panels drive fans which continuously supply fresh air over the layers of material and trays of water provide the necessary humidity. Other surficial approaches have investigated carbonation of existing mafic and ultramafic mine tailings (Kelemen et al., 2020; Mervine et al., 2017, 2018; Power et al., 2010, 2013, 2020; Wilson et al., 2014) and industrial wastes such as slag (Stolaroff et al., 2005). In general, most industrial wastes and by-products present certain advantages for surficial mineral carbonation due to their wide availability, relatively low cost, and good reactivity (Renforth, 2019). CO_2 availability is often the limiting factor in ambient weathering of mine tailings and other industrial alkaline wastes (Pullin et al., 2019; Wilson et al., 2009). Therefore, increasing the CO_2 supply in surficial processes using DAC to provide a more concentrated stream of CO_2 (e.g., 1–10 %) could lower overall costs compared to reliance on ambient air (Kelemen et al., 2020). [While higher purity CO_2 could theoretically be used, significant losses could occur in open systems]. The availability of humidity in the air could also be limiting in some cases, with some studies quoting a minimum requirement of 55–60% relative humidity required for carbonation reactions to take place (Erans et al., 2020; Samari et al., 2020). Surficial mineral carbonation of anthropogenic waste materials may serve a dual purpose, since waste management can be materialised (via a reduction in liability associated with hazardous materials) in addition to CO_2 removal. This may be achievable at greater scale, and lower cost, compared to ex situ approaches. Carbonation reduces the pH of these wastes, and potentially reduces the mobility of toxic metals (Mayes et al., 2008) and destroys (and potentially encapsulates) some of the hazardous asbestiform minerals of relevant mine tailings (Bobicki et al., 2012). Measurement work related to surficial mineralisation is slowly emerging based on standard analytical techniques as well as some more novel approaches

(Knapp et al., 2023; MacDonald et al., 2023; Mayes et al., 2018; Turvey et al., 2017; Wilson et al., 2006).

2.4 Enhanced weathering in soils

Over the past two decades, research on EW has grown exponentially (Minx et al., 2017). The body of literature encompasses several mesocosms (Amann et al., 2020; Buckingham et al., 2022; Haque et al., 2019; Jariwala et al., 2022; Reershemius et al., 2023; ten Berge et al., 2012; Vienne et al., 2022), laboratory (Renforth et al., 2015; Renforth and Manning, 2011) and modelling (Beerling et al., 2020; Cipolla et al., 2021; Kantzas et al., 2022; Kanzaki et al., 2022; Strefler et al., 2018; Taylor et al., 2017) studies. However, these studies report varied results for the weathering rate of different minerals, and in consequence, broad estimations on the CO_2 sequestration potential (Larkin et al., 2022).

There are currently ongoing and planned field trials (Bijma et al., 2021; Haque et al., 2020; Vink et al., 2022), which aim to test the feasibility of EW and develop MRV protocols. For example, inorganic carbon uptake via EW can be assessed by measuring the alkalinity content in soil pore solution for smaller-scale trials, and alkalinity runoff to the catchment area for large-scale deployments. However, frequent alkalinity sampling and analyses can be expensive and time consuming. It has been suggested that electrical conductivity could be a good predictor for alkalinity, simplifying the monitoring process (Amann and Hartmann, 2022). Nevertheless, to successfully calibrate these two variables, a comprehensive database for different combinations of soil type, climate, vegetation cover and diversity, topography, and hydrology is needed. Other studies focus on determining the physical and chemical properties of the rock used for EW by investigating aspects such as mineralogy, particle size and surface area of the rock, and using 1D reactive transport models of soil processes to simulate inorganic CDR potential via cation flux (Kemp et al., 2022; Lewis et al., 2021). Zhang et al. (2022) suggest that a more realistic estimation of the CDR potential of EW can be achieved by accounting for processes that occur in the drainage waters, since the cations derived from weathering could potentially be precipitated in drainage waters resulting in CO_2 release into the atmosphere. Reershemius et al. (2023) quantify weathering rates by focusing on mass-balancing within the soil, i.e., by measuring the difference in feedstock concentration before and after weathering. Both the sampling and the timescales of CO_2 sequestration via EW can vary significantly depending on site-specific conditions. As such, the MRV framework must report site and time specific rates of feedstock weathering, while being cost effective and minimally invasive.

As well as investigating the rate of weathering and CO_2 uptake, MRV protocols for EW should also include monitoring the potential environmental impact, including the release of heavy metals (Haque et al., 2020; ten Berge et al., 2012) and feedstock run-off into waterways which can increase turbidity impacting aquatic ecosystems (Morgan, 1987; Pulido et al., 2012; Wyatt and Stevenson, 2010).

2.5 Ocean alkalinity enhancement

The ocean's carbonate system consists of dissolved inorganic carbon (DIC) species, including carbon dioxide ($CO_{2(aq)}$), bicarbonate ions (HCO_3^-), and carbonate (CO_3^{2-}) ions, which exist in equilibrium with one another. By adding alkali or alkaline substances, this equilibrium can be shifted from $CO_{2(aq)}$ towards bicarbonate and carbonate ions, thus enabling further CO_2 drawdown from the atmosphere (Renforth and Henderson, 2017). This process is referred to as ocean alkalinisation or OAE. There are several different substances that can be added to the ocean to achieve OAE: i. sodium hydroxide ($NaOH_{(aq)}$) – produced by electrochemical splitting of brines (de Lannoy et al., 2018), ii. lime ($CaO_{(s)}$), slaked lime ($Ca(OH)_{2(s)}$), and brucite ($Mg(OH)_{2(s)}$) – produced by mining, grinding and calcination of limestone and dolomite (Kheshgi, 1995; Renforth et al., 2013), iii. ikaite ($CaCO_3.6H_2O$) – produced by hydration of limestone (Renforth et al., 2022), iv. mined and crushed natural minerals such as olivine which are added to high energy beaches and coastal shelves where they undergo weathering (Hangx and Spiers, 2009). Other methods include accelerated weathering of limestone (Rau et al., 2007). OAE pathways are summarised in Figure 3.

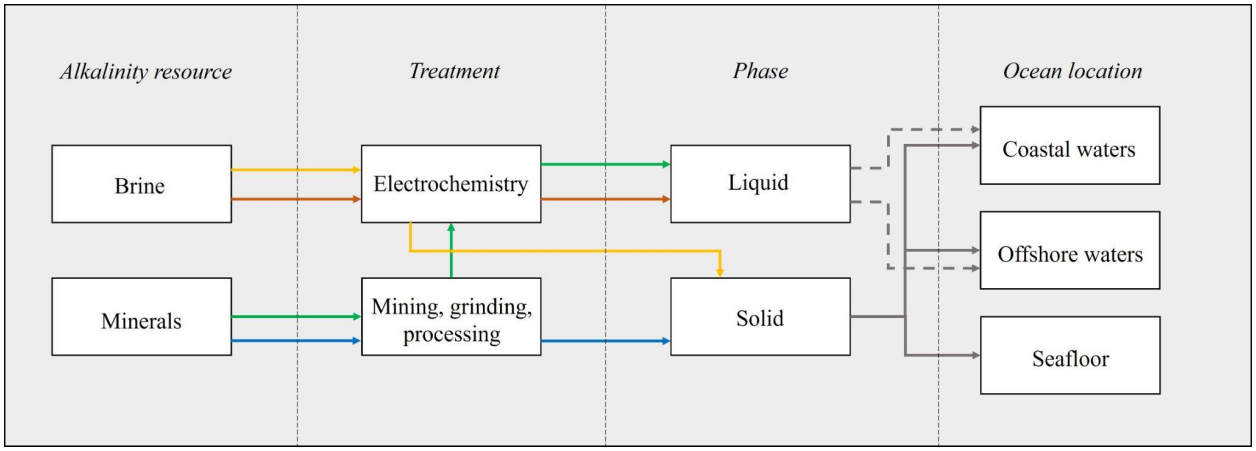

Figure 3. Summary of OAE approaches where each coloured arrow represents a different pathway (adapted from Eisaman et al. (2023)).

While this document is relevant for the analysis of OAE approaches, a comprehensive best practice guide for measurement of the ocean carbonate system has already been produced for ocean acidification research (Dickson et al., 2007), a recent review of OAE was included in a consensus report (National Academies of Sciences, Engineering, and Medicine, 2021), and a best practice guide is being developed for research in this field (Oschlies et al., 2023).

3. Monitoring, reporting, and verification

3.1 Introduction

Principles. Monitoring, reporting, and verification, sometimes referred to as measurement, reporting, and verification and popularly known as MRV, is an evolving and contested term. Broadly, it refers to processes for measuring GHG emissions reduction or removal activities and reporting the results of those activities to regulators, market participants, or other institutions or stakeholders, for example communities local to where the activities being measured are taking place. Various actors have proposed a range of principles or criteria for what effective CDR practices should achieve. Again, this is an evolving area of debate, but there is broad agreement and well-grounded arguments for carbon removal operations to assess:

> *Life cycle carbon emissions or carbon penalty:* Effective CDR approaches must remove more CO_2 from the atmosphere than the carbon dioxide equivalent (CO_2eq) they release during all steps of their setup, operation, and decommissioning.
>
> *Additionality:* Determination of human-induced atmospheric CO_2 drawdown resulting from a given operation, against a counterfactual scenario without human involvement.
>
> *Durability:* Approximate duration of carbon storage, post operation.
>
> *Leakage:* Assessment of reversal of stored carbon to be re-released into the atmosphere as CO_2, during operation. For geochemical CDR, leakage can occur when dissolved bicarbonate is removed from solution through carbonate precipitation, or if dissolved bicarbonate or precipitated carbonate minerals interact with strong acids.
>
> *Environmental impacts:* Assessment of the positive and negative impacts on the surrounding environment as a result of an operation.
>
> *Social and community impacts:* Evaluation of both positive and negative social, economic, and public health impacts of an operation that can affect local communities.

Importance of confidence in MRV. The role of MRV in geochemical CDR serves to establish net GHG negativity for any given carbon removal project using state-of-the-art techniques underpinned by rigorous science, and to provide a framework for, and verification against, a

set of standards and accepted practices in order to meet the needs of other stakeholders across society, and to substantiate an overall societal benefit. MRV provides confidence to private and/or public funders of CDR activities. Done well, MRV can address concerns about the efficiency of geochemical CDR approaches and their capacity for safely and durably removing atmospheric CO_2. Public trust is essential in scaling up CDR, and while previous disputes (Greenfield, 2023) surrounding carbon credits may not be directly applicable to geochemical processes, as a novel approach to drawing down CO_2 from the atmosphere, commercialisation of geochemical CDR projects is still reliant on proving itself credible.

Geochemical CDR activities are expected to be funded initially through voluntary carbon markets, and eventually through compliance markets and government procurement (Maesano et al., 2022), where the unit of sale is one carbon credit, represented by 1 metric tonne of carbon dioxide equivalent (CO_2eq). Thus, projects need to determine costs per tonne of atmospheric CO_2 removed, requiring reliable quantification to properly assess the overall net negativity of a project, accounting for the parameters described above. This quantification must be externally verified and certified in order to qualify for purchase by the majority of buyers of carbon credits. From a legal perspective, MRV is also essential as buyers of carbon removal credits are transferring carbon liability to the removal operator/developer.

Though MRV is necessary to support geochemical CDR as a growing industry, its application in the field is not straightforward. The group of stakeholders involved in creating, validating, verifying, and certifying carbon credits is large and varied, while the details of the process can be obscure and even the terms 'monitoring' or 'measurement', 'reporting', and 'verification' can mean different things to different stakeholders. Further confusion can arise when 'measurement' refers to modelled results, or ongoing monitoring, rather than discrete measurement activities.

Beyond the quantification itself, embedded into the MRV process is adherence to standards, ensuring the quality and validity of a removal project. Such quality metrics include durability of carbon storage and additionality of the removal activity, but also bounds on environmental and social impacts. Ideally, an additional level of governance, one that sits outside of the carbon credit value chain, sets these standards and addresses accounting challenges.

This section seeks to introduce MRV, as well as highlight the carbon accounting practices that are necessary for CDR measurement. Reporting and verification will be discussed only briefly to provide context. As this document focuses on geochemical CO_2 removal, this chapter assumes that carbon removal credits are derived from such processes and therefore does not consider carbon credits derived from avoidance or reduction activities, nor does it consider potential nuances of other forms of CDR. Discussion of both standards for quality, as well as the market mechanisms of purchasing and trading carbon credits or offsets, are outside the scope of this report.

3.2 From carbon removal to carbon credits

MRV is the means by which excess atmospheric CO_2 transitions to a commoditized product. In general, creating carbon credits requires a multi-step process to measure, model, and/or monitor the total amount of CO_2eq that is removed over a period of time, report these findings, and finally, have them verified by an accredited third party before obtaining certified carbon credits. This process has been developed through the voluntary carbon market (World Bank, 2022) for carbon credits that relate primarily to emissions reduction, not removal (Lovell, 2010), and is now being applied across CDR (Arcusa and Sprenkle-Hyppolite, 2022). MRV for geochemical CDR is expected to follow a similar procedure.

A high-level depiction of the carbon crediting process is given in Figure 4. Once a CDR developer is confident their process can quantifiably remove CO_2, independent assessment is required to validate their process, verify, and certify the credits. This independent assessment is conducted primarily through the use of *methodologies*, which are documents that lay out requirements and procedures to establish boundaries for the project, assess baselines, and determine additionality, as well as to quantify movement of CO_2 and lay out which parameters need to be measured and how they should be reported. Through the development of methodologies, the methodology proponent is challenged to demonstrate the parameters, criteria, and operations they will use to calculate removals for their process, as well as how it complies with accepted standards and practices. These methodologies are usually specific to a particular type of project and are essentially guides for how, and under which conditions, to conduct certain types of carbon removal operations.

The full MRV process can be lengthy and goes beyond CO_2 measurement. Even the creation of methodologies involves multiple parties across the MRV process chain as shown in Figure 4. Methodologies must be validated by an accredited validation and verification body (VVB) before projects proceed with operations in order to ensure that the methodology – and any projects that use it – adhere to best practices and environmental standards. A VVB is also needed to verify that the methodology was followed during and after operations, and in some cases to scientifically corroborate quantitative results with additional measurements. Once verified, a certifying body is then able to issue a specific number of credits corresponding to the tonnage of net CO_2 removed. Credits can then be listed on a registry, allowing them to be sold.

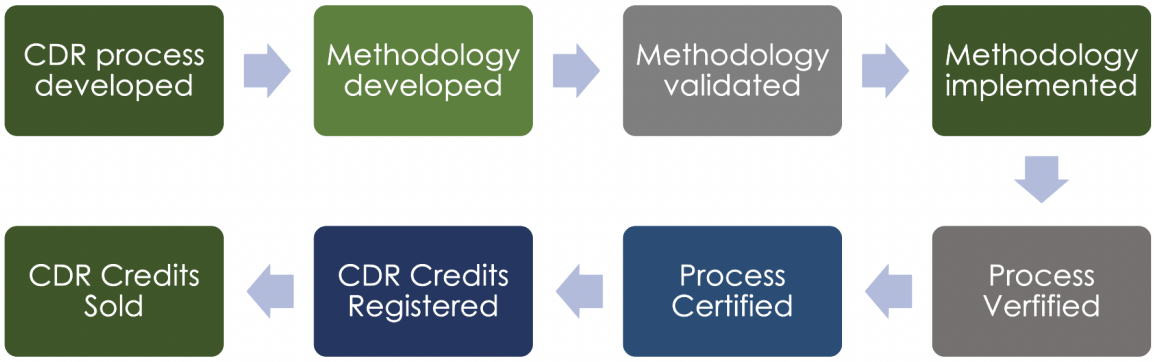

Figure 4. High level overview of the steps required to create carbon removal credits from a CDR process. Methodologies are created to provide a how-to guide for the entire carbon removal operation, ideally according to accepted standards. Methodologies must be validated by an external party before it is implemented and carbon removal takes place. External parties are also required to verify that the methodology, and all protocols within, have been complied with, at which point credits can be certified and registered for sale.

It is tempting to think of MRV as a process that starts with quantitative measurement, flows into reporting of those measurements, and ends with a verification of those measurements, as the name implies. However, MRV is doing several things: Ensuring technical aspects are up to date and acceptable in practice, ensuring adhesion to standards, ensuring compliance with local laws, assessing baselines and additionality, defining measurement procedures, tolerances, and uncertainties, defining monitoring procedures and timelines, as well as establishing reporting and data requirements. While arduous, project compliance with the overall MRV procedure is important in order to establish trust and to safeguard against potential risks and unforeseen issues. While still new, there are a handful of emerging methodologies that cover geochemical processes, such as CO_2 mineralisation in concrete (Verified Carbon Standard, 2019), enhanced weathering (PuroEarth, 2022) and more are expected as new companies begin to implement geochemical CDR for the purpose of generating carbon credits.

It is, indeed, the quantity of net CO_2 removed that matters most in the context of keeping within climate change targets. But in order for a CDR project to confer an overall net benefit to communities, and to effectively operate under the inherent uncertainty associated with deployment conditions and other limiting factors, the measurement, reporting, and verification steps all need to fall within a wider procedure, one that also ensures environmental and human safety.

Given that the MRV process contains so many opportunities for uncertainties to propagate (CarbonPlan, 2022), robust and accurate measurements are important. As science and technology advances, MRV methodologies will need to be continually reviewed and updated.

This document is focused on the current state of the art of measurement techniques used within geochemical CDR, as well as relevant carbon accounting practices, that are embedded into methodologies. MRV for carbon reduction, and particularly removal ventures, is a complicated and evolving process with many degrees of freedom. However, for some geochemical processes, it is possible to have a clear understanding of how CO_2 is drawn down and stored, and quantification may be reassuringly straightforward.

3.3 Carbon accounting

Carbon accounting is the means by which quantities of removed CO_2 are balanced against any GHG emissions that occurred as a result of implementing the removal process. A generic approach to carbon accounting in geochemical CDR would include the following steps:

1. Full LCA to quantify the CO_2eq that is emitted by the CDR operation, including the emissions arising after its lifespan (e.g., during decommissioning and future monitoring activities).
2. Robust assessment of baseline carbon removal to support assessments of additionality, and CO_2 drawdown rates as a function of time.
3. Ensure that the durability of the storage and the associated leakages are those considered in project planning and the LCA, in order to ensure no additional carbon emissions will enter the atmosphere during the lifespan of the geochemical CDR activity.

There is a need for standardised practices for both qualitative and quantitative measurements to enable companies and regulators to determine the amount of CO_2 that has been captured and stably stored as minerals. There will be losses in the supply chain and uncertainty limits and tolerances need to be defined.

For a geochemical CDR activity to be net negative, i.e., remove more carbon than it emits during its life cycle, the amount of CO_2eq that is removed and stored and/or avoided must be larger than the amount of CO_2eq that is emitted from its full supply chain (Eq. 3). For geochemical CDR activities, the main focus is the CO_2eq stored component, which is the amount of carbon that is removed from the atmosphere and stored as solid minerals and/or dissolved ocean bicarbonate. This is in contrast to the avoided emissions components, which are the amounts of (additional) fossil carbon that are prevented from entering the atmosphere in the first place.

It is possible for a CDR activity to also result in avoided emissions, and therefore both carbon removal and avoidance should be accounted for, though separately. However, in both removal and avoidance cases the life cycle carbon emissions, along with other emissions that are attributed to the entire lifespan of the geochemical CDR activity (see Section 5) should be accurately quantified and accounted for.

The total impact on atmospheric CO_2 concentrations can be defined as:

$$E_{total} = [E_{removed} + E_{avoided} - E_{LC}] \quad \text{Eq. 3}$$

where

- E_{total} = net CO_2eq removed and/or avoided, which is the amount of all GHG emissions that have been removed and/or avoided and permanently stored by the mineral carbonation activity.
- $E_{removed}$ = CO_2eq removed from the atmosphere and stored as *new* stable carbonate minerals and dissolved forms such as carbonate alkalinity.
- $E_{avoided}$ = CO_2eq prevented from entering the atmosphere as a result of the activity (certified emissions reductions).
- E_{LC} = life cycle carbon emissions generated from all activities undertaken during and after the lifespan of the carbonation activity.

All terms are expressed in mass units, e.g., t CO_2eq.

When presenting the values from Eq. 3, it is important to distinguish between $E_{removed}$ and $E_{avoided}$ (both should be reported) given that they pertain to separate climate targets (Wilcox et al., 2021). Calculating $E_{removed}$ usually begins with estimating the uptake potential ('C_{pot}' mineral carbonate and 'E_{pot}' bicarbonate, see Section 6, Eq. 5 and 6) of the material under study, which is the theoretical amount of carbon that the material (minerals) can store per unit of mass before reaction with CO_2. This value must be adjusted based on efficiency, taking into account the inefficiencies of the engineering system under study, as well as any physical and chemical limitations that affect reaction rates. The amount of carbon that might be lost in the short-term (e.g., shortly after carbonate mineral or alkalinity formation, some CO_2 might be re-emitted to the atmosphere) must be subtracted to account for possible losses, aka leakage (Eq. 4). X_{pot} (=C_{pot} or E_{pot}), as well as any losses (e.g., CO_2 evasion in drainage waters), can be estimated using the SOPs described in this document and will not be elaborated on in this section. How measurement systems are employed to estimate efficiency (conversion extent) is beyond the scope of this document.

$$E_{removed/avoided} = [X_{pot} * Conversion\ extent] - Losses\ (aka\ leakage) \quad \text{Eq. 4}$$

Time dependence of the carbonation or enhanced weathering potential of the proposed feedstock minerals is also relevant in terms of determining a carbon credit.

Different protocols can be employed to quantify the CO_2eq that is permanently removed and/or avoided, as well as the life cycle emissions of the geochemical CDR activity (Table 1).

Table 1. Summary of commonly used protocols for carbon accounting.

Protocol	Description	Reference
GHG Protocol	Global standard framework jointly developed by the World Resources Institute and the World Business Council for Sustainable Development for quantifying and reporting greenhouse gas emissions from the private or/and public sectors.	GHGProtocol (2023)
ISO 14064	Specifies the principles and requirements, at the organisation and project levels, for GHG emissions quantification and reporting guidelines on accounting and reporting.	ISO (2018b)
ISO 14067	Quantifies and reports GHG emissions at the product level.	ISO (2018a)
ISO 14040 & ISO 14044	The LCA methodology provides a systematic and robust analysis for the quantification of the GHG emissions as well as of other environmental impacts.	ISO (2006a, 2006b)

For estimating the life cycle carbon emissions (E_{LC}) of the geochemical CDR activity and also estimating the emissions reductions and removals, the GHG Protocol, which is a standard for corporate accounting (quantification) and reporting of GHG emissions, can be used (GHGProtocol, 2023). The GHG Protocol discerns emissions into three different Scopes. Specifically, direct emissions produced from the CDR developer's owned or controlled sources are classified as Scope 1 and these include emissions from stationary and mobile (vehicles) combustion, along with fugitive and process emissions. Indirect emissions, those not produced by the CDR developer, can include those from energy purchases (electricity, steam, heat/cooling), which fall under Scope 2 (only the emissions from energy generation itself and not transmission and distribution losses and upstream emissions are considered, i.e., generation-only emission factors are used). All other indirect emissions from upstream and downstream activities fall under Scope 3, which discerns between 15 categories such as the emissions from capital goods and from fuel- and energy-related activities that are not Included in Scope 1 or Scope 2 (GHGProtocol, 2023).

Alternatively, the ISO 14064 standard, which specifies principles and requirements for GHG quantification and reporting at the organisation and project level and provides the principles, requirements, and guidelines for validating and verifying the estimated GHG emissions, can be used (ISO, 2018b). Although less extensive than the GHG Protocol in identifying indirect emissions, as it does not make a distinction between Scope 2 and Scope 3, the ISO 14064 Standard provides a level of formal verification by including guidance for independent validation.

Similarly to ISO 14064, the ISO 14067 standard also provides carbon footprint verification, but additionally allows for the analysis of full or partial life cycle stages and also includes

reporting of stored biogenic carbon (ISO, 2018a). It does not, however, cover delayed emissions or delayed removals, and treats all GHG emissions as released or removed at the beginning of the assessment.

For this reason, LCA, which is a robust and versatile framework for estimating carbon and environmental footprints, can be used as it allows for both spatial and temporal differentiation of the characterisation model, i.e., delayed emissions and/or removals can be included in the analysis. This is of prime concern in many geochemical CDR activities, since carbon mineralisation and EW can be slow processes and therefore time to full (maximum capacity) conversion of the mineral might extend to decades or even hundreds of years.

The LCA framework has been detailed in ISO 14040 and ISO 14044 (ISO, 2006a, 2006b), with the first describing the principles and framework and the second specifying requirements and providing guidelines. Furthermore, apart from the carbon footprint, LCAs can also estimate additional environmental impacts, such as impacts on eutrophication and (eco)toxicity. This is of major importance for some geochemical CDR activities, since, for example, certain minerals can include in their matrix (heavy) metals, which, if released to the environment, can induce toxicity impacts that are not captured by carbon accounting alone. Other approaches and frameworks, such as ISO 14080 (ISO, 2018c) which provides guidance for GHG management and related activities, and national carbon footprint standard such as PAS 2050 (UK) and BP X30-323 (France), have also been developed, but their detailed discussion is beyond the remit of this document.

In LCA, environmental impacts, including the carbon footprint, are quantified using life cycle impact assessment (LCIA) methods. Determining E_{LC} through LCA requires a detailed analysis of all energy and materials flows of the geochemical CDR system and their transformation using LCIA methods, to carbon balances and other environmental impacts using emissions factors. For this reason, a system boundary must be clearly defined, preferably conducting a 'cradle to grave' assessment, i.e., full LCA, that includes all main inputs, outputs, and process steps. For example, for processes using mined rocks, GHG emissions from mining, crushing, and grinding must be accounted for. On the other hand, where the feedstock minerals are industrial wastes, such as slag, GHGs released by their production can be outside the LCA boundary and therefore do not need to be accounted for.

In more detail, a system boundary for an ex situ carbon mineralisation system would include mineral mining and processing (e.g., crushing), transportation of materials, as well as the reactor itself and all relevant emissions, whereas for surficial mineral carbonation, the boundary could be restricted to the reactor itself, particularly when waste materials are used, which are not attributed the environmental burdens of their production process. In both cases, transport and other possible emissions should be also included in the analysis. If the mineral is further valorised (CCU), then avoided emissions could also be credited to the system, as long as additionality is ensured, and the valorisation pathway does not cause the release of the captured carbon back to the atmosphere (durability).

A full LCA for the geochemical CDR activity, following the guidelines of the ISO 14040/44 is the responsibility of the CDR developer, however LCAs may be conducted by external parties if in-house expertise is not available. The LCA should include all GHG emissions for the process and for consistency, results should be reported in CO_2eq removed/avoided. LCIA methods that include a wide range of impacts are preferable.

Additionality should also be considered, as minerals may already be weathering naturally, albeit slowly, and this CO_2 must be subtracted during the accounting process (and measured through establishing a baseline of background weathering e.g., (Bach, 2023)). Furthermore, double counting must be avoided by drawing the system boundaries carefully, so that an emission or the removal itself is not accounted for or credited twice e.g., in EW carefully accounting for the fraction of stored carbonate minerals in soil and the fraction of bicarbonate ions that will reach the oceans versus simply summing up the theoretical potential for both.

3.4 Standardisation in geochemical CDR

As a prerequisite to MRV, an agreed upon set of standards, by which practitioners should operate, should be developed by a financially disinterested party. In this regard, a relevant standard by the International Organisation for Standardisation (ISO), where technical and scientific open questions are addressed, could be helpful, since this could set up the best practices for MRV.

While ISO standards exist for GHG emissions and removals and for LCA (Table 1), there is as yet no set of standards focused on best practices for implementing CDR (CarbonPlan, 2023) or MRV (Ausra, 2023). Such standards may be the most effective if they are specifically tailored for CDR projects and include requirements on durability, additionality, leakages, environmental impacts, as well as measurement uncertainty tolerance (Stripe, 2023). In the absence of such robust standards, current buyers of CDR credits are left to determine their own standards and quality metrics regarding the origin and robustness of the CDR credits based on ideals and preferences. This requires a level of expertise and good will, which is neither realistic for a growing market nor conducive to its growth.

Despite the lack of market standards, carbon removal credits are still being developed and sold through the voluntary carbon market or directly from CDR companies to buyers (Smith et al., 2023). The pressure for CDR credits to be robust is especially high given the current level of scrutiny of carbon credits more generally and accusations of greenwashing (Greenfield, 2023; Song and Temple, 2021). Diligent MRV can ensure such quality and generate trust in the overall system, which is imperative if carbon markets are necessary to fund CO_2 removal activities.

4. Site and material investigation, design, and sample acquisition

Deployment and monitoring of geochemical CDR will occur at a specific location or 'site'. There are established commercial protocols for acquisition of samples for geotechnical and geoenvironmental site investigation (British Standards Institution, 2015). The objectives of these protocols are to ascertain the suitability of a site for development, aid in the design and construction, and predict risks. While these protocols are not directly transferable for geochemical CDR, they provide a useful framework for the assessment and ongoing monitoring of a location for deployment. The scope and depth of the work should extend only so far as the requirements needed for CDR monitoring and verifying and other socio-environmental impacts, and thus must be tailored to the geochemical CDR approach. Adapting from the BS5930 framework (British Standards Institution, 2015), we propose the following objectives for a site, material, or project investigation for geochemical CDR:

1. **Carbon accumulation and uptake.** To assess how much CO_2 has accumulated (as new carbonate minerals) or removed and transported in drainage waters (as dissolved bicarbonate) as a result of reaction with the material.
2. **Carbon dioxide removal potential of alkaline materials.** To assess the maximum potential of the feedstock alkaline material for reaction with CO_2.
3. **Mineralogy of the material.** To assess material properties (particularly the mineralogy) that might impact the maximum rate of accumulation.
4. **Design.** To enable, if required, the adequate and economic design of a process/project in which additional CO_2 may be sequestered. This may include the acquisition of material in which to base the design and location of a pilot experiment, or develop a baseline for site characteristics prior to treatment.
5. **Risk.** To evaluate, if required, the possible risks associated with additional reaction with CO_2. This may include assessing the environmental impact of potential leachates on local surface and groundwaters, geotechnical risks from carbonation, and possible hazards to human health.

The first three pertain to all sites (and are discussed in Sections 5, 6 and 7), whereas #4 and #5 may be appropriately applied to sites in which further reaction with CO_2 is planned. Similar to BS5930, we propose that site investigation be carried out in two stages:

Stage 1: Desk study and site reconnaissance. This should be undertaken at the beginning of the investigation, with the purpose of describing, in as much detail as necessary, the geoenvironmental context of the site (geological setting, existing data, inferred or possible drainage water geochemistry, inferred or possible solid material mineralogy/geochemistry, site hydrology/hydrogeology) and include anything that may constrain activity in Stage 2 (risks associated with contamination, environmental, ecological, or social considerations).

Stage 1 should conclude with the development of a conceptual/observational ground/ocean/sediment model that has been supported by site reconnaissance, and recommendations should be made for Stage 2. While it is possible that the scope of a site investigation may be less encompassing for distributed geochemical CDR (e.g., EW, ocean liming) when deployed at scale, carefully curated site information will be essential for pilot research and development during the calibration and verification of ground models.

Stage 2: Detailed investigation. This should include solid and/or liquid sampling (described in detail below), but potentially including topographic, hydrographic, or geophysical surveying. A protocol for how samples are collected needs to be established (we provide an overview of sample requirements in SOP 1). This protocol is a predetermined procedure for selection, withdrawal, preservation, transportation, and preparation of the samples. How a sampling protocol is exercised will depend on the nature of the project and should consider the number, size, and location of samples, as well as instructions for the compositing or reductions of these samples for laboratory analysis. Sample collection and choice of analytical method will depend on the acceptable level of uncertainty in the results. Sample collection will depend on the nature of the alkaline material. For example, mine tailings are often stored in large tailings storage facilities and may be deposited as dewatered paste, dry stacks, or slurries (Davies, 2011; Davies et al., 2010; Fourie, 2009; Furnell et al., 2022) and certain sampling approaches are recommended (Amacher and Brown, 2000; Blight, 2009). For carbonation of minerals in controlled reactors, samples could be withdrawn at periodic intervals for analysis, in combination with real time monitoring equipment, as is the case with any continuous or batch industrial processes.

Samples should be stored with a unique identification – a number or code, and data management practices implemented to ensure traceability between sample metadata and results. Samples should be stored such that there is no possible contamination. Plastic bags or containers are recommended for storage. The samples' sensitivity towards light, heat, moisture, air, and other chemical and physical effects should be considered for appropriate storage. Many alkaline materials, such as slag and mine tailings, are stable under ambient conditions and basic storage is sufficient. For more reactive materials, such as lime, samples must be stored in conditions of low humidity (< 20% RH) and low CO_2 so that hydration and carbonation is negligible prior to analysis. Desiccant materials such as silica gel or zeolites can be used to create the necessary atmosphere. Even under such conditions, a holding time should be determined. The holding time is defined as the maximum period of time that can pass from sampling to measurement before the sample has changed significantly (3 standard deviations less than the initial value) (Prichard and Barwick, 2007). Ideally, samples should be analysed as soon as possible after collection/receipt. Where appropriate, refrigeration can be used to minimise the impact of biological activity during prolonged storage. Samples must be disposed of in accordance with local or regional regulations.

4.1 Solids sampling

Sampling of solid material is the process of taking a small portion of material in order to infer characteristics of the whole or 'bulk' material. In commercial ground investigation it is typical to sample <2% of the bulk material. While the analytical result may depend on the analysis method, it will always depend on the sampling procedure. Improvements to the analytical methods used may not improve analytical outcomes if the uncertainty or error introduced by sampling is large.

There are four types of sample: i) representative, that which is typical of the parent material ii) selective, that which has been deliberately chosen iii) random, that which has an equal chance of being obtained, and typically employed when less is known about the bulk material and iv) composite, which is a combination of the above and may provide statistically meaningful results while focusing collection on only a part of the bulk material. For example, legacy deposits of alkaline materials such slag and mine tailings can range from 10s to 1000s of metres in length and 10s to 100s of metres in depth. Such legacy deposits may exhibit physical and chemical heterogeneity, owing to the compositional variations in the original rock feedstocks and other input fluxes, as well as operating conditions during their industrial processing and variation in weathering during storage. As such, each sample may represent a snapshot in time and thus one or two samples are highly unlikely to be representative of the bulk deposit. Instead, multiple samples should be obtained which span the full extent of the deposit. This can be performed by randomly selecting collection points (unbiased), or by separating the deposit into multiple cells and taking a sample from each cell (biased). Random or unintelligent sampling can miss "hot spots" of high or low carbonation, which may be possibly detected through selective sampling.

If the component of interest is low concentration and the material is heterogeneous, then more samples will be needed to be representative of the bulk. The rate of carbonation will determine how frequently samples must be withdrawn. For some "rapid" mineralisation processes, samples will need to be withdrawn frequently; whereas for slower mineralisation processes samples can be taken at intervals of weeks to months. A separate sampling plan may need to be devised after completion of the mineral carbonation activity for the purposes of ensuring long-term stability of the mineralised CO_2.

For deeper deposits, coring or drilling may be needed to collect buried material, especially if the topmost few cm's are likely to be highly weathered. Soil and vegetation may need to be removed from the surface of alkaline material deposits during shallow sampling.

For some analytical methods, several grams of subsample are needed, and since more than one analytical method is usually performed, some with several repeats, collecting 100 g of sample or greater is recommended. Depending on the *sensitivity* of the analytical techniques then more or less sample mass may be required. For legacy deposits, samples of

greater than 100 g are recommended, from which subsamples can be withdrawn for analysis (see SOP 1 for more information on sample sizes).

The particle size of the deposit should also be considered when sampling. For example, the smallest fraction (often the fraction < 2 mm) usually determines the material's reactivity. This fraction will likely provide the "best-case" scenario for carbonation potential of the deposit. On the other hand, finer material may already be altered and contain secondary minerals, which the larger grains do not. Thus, the analyst may wish to also collect larger fractions, in which case a greater mass of sample will be needed.

4.2 Solution sampling

Similar to solid sampling, water samples represent only a small fraction of the total material, and chemistry and characteristics are inferred. In advance of sampling, non-reactive sample containers should be cleaned and dried. Sample containers and their method of preparation are constrained by the analyte (Table 2). Sample sizes on the order of 50–100 mL are usually sufficient for most analysis, although additional samples may be required for highly dilute trace metals. For best practice for seawater sampling and measurement, see Dickson et al. (2007).

Gloves should be worn to avoid contamination, and as personal protection when sampling hazardous waters. It is essential to consult the specific requirements of the laboratory conducting the analysis, as they may have bespoke recommendations for sample bottle types and materials.

The appropriate sampling locations based on the study objectives should be selected, and consider hydrology, geology, land use, and potential sources of contamination. The sampling campaign should aim for representative sampling by selecting sites that reflect the range of conditions or variables of interest.

Groundwater sampling. Fretwell et al. (2006) outlines a useful guide to implementing a groundwater monitoring programme including design, construction, maintenance, and decommissioning. Extraction of water from a borehole can be achieved using a bailer, submersible pump, or dedicated groundwater well. Purging the pump or well before sampling to remove any stagnant water or residue is recommended.

Surface water sampling. Automated water sampling units can be installed to obtain liquid samples in real-time, and can be programmed to do this for fixed intervals of flow or time ('composite sampling', (British Standards Institution, 2018, 2023)). Samples can be periodically retrieved, with the interval depending on the stability of the analyte in the sample. Alternatively, 'spot' samples can be hand collected. Spot samples should be collected in clean containers, which have been rinsed at least three times with water at the sampling location. Sampling containers should be fully submerged to reduce air contact, and care

should be taken to minimise head space in the container. Sampling near shorelines, where water quality may differ from the main body of water, should be avoided. When collecting composite samples, a depth-integrating sampler could be used or multiple samples at different depths could be taken.

Porewater sampling. A range of methods can be employed for sampling water from granular materials (Di Bonito et al., 2018). Rhizon sampler is a common 'tension' method, which uses a porous tube that is gently inserted into the soil at the desired sampling depth. A syringe is attached to the Rhizon sampler. The syringe will create negative pressure when it is drawn which will extract the soil pore water (~1 mL min^{-1}). The negative pressure will draw the soil pore water into the sampler through its porous membrane. This may need to be repeated until sufficient sample volume is collected.

River sampling. River chemistry can vary significantly along stream due to various inputs from tributaries and point sources. When selecting a possible sampling site, it is important to consider these inputs as they can cause misinterpretation of the chemical data obtained. Sampling along a downstream transect, as well as these additional input sources, can be valuable for obtaining information about chemical change with distance. Identifying the flow rate at the sampling site may also be required if the concentration data obtained from sampling (often in mmols L^{-1} or mg L^{-1}) must be converted to flux estimates (mmols s^{-1} or mg s^{-1}). It may be helpful to select a sampling site close to a known flow monitoring station, if available.

Samples should be retrieved from a flowing section of the river, away from the shoreline (or large confluences if appropriate), and any potential point sources or large confluences that might influence chemistry. As with surface water samples, water should be collected using clean containers which have been rinsed at least three times with local river water, and if possible, filtered on site using syringes, also pre-rinsed with river water. Some research may also require the collection of suspended sediment during a river sampling campaign. This can be retrieved as a 'spot' sample in a clean, large container to be filtered off site, typically using electric filtration devices. Alternatively, Van Dorn samplers can be used to capture the compositional heterogeneity of suspended sediment with depth (Wren et al., 2000).

Effective solution sampling plans will also measure and record field parameters at the time of sampling, including temperature, pH, electrical conductivity, dissolved oxygen, and turbidity, using the appropriate portable metres. These parameters provide contextual information and can help in data interpretation. There is also benefit to measuring alkalinity in the field using either a portable spectrophotometer (expensive), or titrating using the gran method (inexpensive) (see SOP 14). Samples that have been stored for a while prior to alkalinity titration can evolve from that measured in the field for various reasons (i.e., due to exchange with the head space within the container, or the precipitation of secondary carbonates).

Quality control measures should be included to ensure data reliability. For instance, duplicate samples, field blanks (unused containers exposed to the sampling environment), and reference standards for calibration purposes should be collected. These measures help identify and account for any potential contamination or analytical errors.

Table 2. Sample vessel, preparation and preservation methods for a range of common analyte types.

Analyte	Storage vessel material	Vessel preparation method	Sample preservation method
General water chemistry	Polyethylene (HDPE) or glass bottles: Used for general water chemistry analysis, including pH, conductivity, and alkalinity.	Rinse in deionised or MQ water at least three times and oven dry.	Filtration (<0.45 µm), fill container so that no head space remains.
Major cations and dissolved Metals	Acid-washed, HDPE bottles: pre-cleaned bottles are typically used to remove potential contaminants.	(i) Rinse in MQ- water and oven dry. (ii) leave a 2–5% nitric acid solution in the container for ~24 hours. (iii) final rinse in MQ- water and dry.	Filtration (<0.45 µm), fill container so no head space remains. Acidify + refrigeration.
Major anions/ nutrients (i.e., nitrate, phosphate)	HDPE bottles: For most nutrient analysis, light sensitive amber HDPE bottles are suitable. For ultra-low-level analyses, specialised trace-metal-clean containers may be required.	Rinse bottles with DI or MQ-water at least three times and dry.	Filtration (<0.45 µm), fill container so that no head space remains. Refrigeration.
Trace metals and metal isotopes	For trace metal analysis at low concentrations, acid-cleaned HDPE bottles or fluoropolymer bottles (e.g., Teflon).	Bottles rinsed with 2–5% nitric acid to remove contaminants. For highly dilute analytes, distilled acid may be required.	Filtration (<0.45 µm). Fill the container so that no head space remains. Acidify + refrigeration.
Organic compounds (e.g., volatile organic compounds)	Amber glass bottles with Teflon-lined caps are commonly used to store water samples for organic compound analysis. The amber glass provides protection against light-induced degradation, while the Teflon-lined caps prevent contamination.	Check with the laboratory performing the analysis as the method may differ. Some laboratories will provide pre-cleaned bottles ready for sampling.	Do not filter. Fill the container so that no headspace remains. Add two drops of HCl and cap. Agitate and check that there are no air bubbles. Chill immediately on sampling. For detailed information, see (Shelton, 1997).
Microbiological analysis	Sterile polyethylene bottles to minimise the risk of bacterial or fungal contamination.	Typically autoclave at 120–130°C, 100–200 kPa for 15–30 minutes.	Refrigeration.

5. Objective #1: Carbon accumulation and uptake

5.1 Carbonate mineral identification and quantification

Mass of carbonate and its mineralogy. Solid products of mineral carbonation include carbonate minerals such as calcite ($CaCO_3$), magnesite ($MgCO_3$), dolomite ($(CaMg)(CO_3)_2$), and various hydrated magnesium carbonates, e.g., hydromagnesite ($Mg_5(CO_3)_4(OH)_2{\cdot}nH_2O$), and nesquehonite ($MgCO_3.3H_2O$). These are stable enough to be stored for long time periods. Other carbonate minerals such as siderite ($FeCO_3$), dawsonite ($NaAl(CO_3)(OH)_2$), and ankerite ($Ca(Fe,Mg,Mn)(CO_3)_2$) can act as stores of carbon, but are usually only stable in subsurface environments (Hellevang et al., 2005; Snæbjörnsdóttir et al., 2014; Yu et al., 2020). Common carbonates of Mg and Ca are given in Table 3, along with their free energies and enthalpies of formation. Other elements may also form stable carbonate minerals (e.g., strontium, barium, cadmium, cobalt, copper, lead, manganese, nickel, uranium, zinc) but their abundance, stability, or toxicity limit their application for large-scale reaction with CO_2.

Table 3. Metal carbonates with formula masses, Gibbs free energies of formation, enthalpies of formation and the temperature range of CO_2 release during heating.

Mineral	Formula	Molar Mass	ΔG_f	ΔH_f	Calcination temp. (°C)*
Calcite	$CaCO_3$	100.09	-1128.5	-1207.4	800–950
Dawsonite	$NaAl(CO_3)(OH)_2$	143.00	-1786.0	-1964.0	>800**
Dolomite	$CaMg(CO_3)_2$	184.41	-2161.3	-2324.5	600–800
Hydromagnesite	$Mg_5(CO_3)_4(OH)_2.4H_2O$	546.54	-5864.16	-6514.9	–
Magnesite	$MgCO_3$	84.32	-1029.5	-1113.3	620–650
Monohydrocalcite	$CaCO_3.H_2O$	118.11	-1361.6	-1498.3	–
Nesquehonite	$MgCO_3.3H_2O$	138.38	-1723.8	-1977.26	–
Rhodochrosite	$MnCO_3$	114.95	-819.1	-892.9	>480***
Siderite	$FeCO_3$	115.86	-682.8	-755.9	>500 †
Strontianite	$SrCO_3$	147.63	-1137.6	-1218.7	924–1233
Tricarboaluminate	$Ca_6Al_2(CO_3)_3(OH)_{12}.26H_2O$	1147.11	-14536.0	–	–
Witherite	$BaCO_3$	197.34	-1132.2	-1210.9	800–1300

*Temperatures of calcination in a furnace are dependent on the heating rate, gas composition and the purge gas flow rate, as well as the sample mass, surface area, and the type and quantity of impurities **Lundvall et al. (2019) ***Tu et al. (2022) † Luo et al. (2016)

A range of analytical techniques can be used for carbonate mineral identification and quantification, some of which are summarised in Table 4, however, there is no ideal approach. The suitability of a method will depend on what degree of accuracy and precision is required in the measurement and the availability and cost of analytical instrumentation. For example, is quantification of the total inorganic carbon (TIC) sufficient, or more information is needed on the types and quantities of carbonate minerals? Is the carbonate material being sold, e.g., as aggregates for the construction sector, and therefore must meet certain criteria? The cost and environmental impact of the analysis will also need to be considered. It may be necessary to use two or more techniques to provide assurance in the accuracy of the measurement. Data may also be needed on the origin of the carbonate minerals e.g., are these a result of captured anthropogenic CO_2 or are they formed as a result of precipitation from pre-existing natural sources of DIC? The main approaches for identification and quantification of carbonate minerals are summarised below.

Thermogravimetric analysis (TGA) uses the same principle as loss on ignition (LOI) except that the mass of the sample is measured continuously and precisely in real time. Furthermore, greater control of the furnace environment (temperature, gas type and flow) is possible with modern TGA instruments. Small masses (few mg) minimise heat and mass transfer effects compared to LOI. By numerically differentiating the mass with respect to time (or temperature) the discrete stages of the decomposition can (usually) be observed. These data can in some cases be used to help identify carbonate minerals due to their characteristic decomposition temperatures ranges.

Powder X-ray diffraction is perhaps the most common technique for identification of solid powdered materials. It is non-destructive and works best for materials which are crystalline (carbonate minerals will often have well-defined crystal structures enabling easy identification in most cases). The method involves firing of X-rays of a particular wavelength at a sample and recording the diffracted X-rays that are detected at a specific angle, which will be determined by the identity of crystalline minerals present in the sample. It may be difficult to identify carbonate minerals when they are in small quantities (<1000 ppm) (Kemp et al., 2022). It can also be used for quantitative analysis (see Supplementary Information – Box 6.1), but this requires far more niche expertise than other methods (Turvey et al., 2017; Turvey et al., 2018b; Wilson et al., 2006).

Fourier transform infrared (FTIR) spectroscopy is another useful technique for carbonate mineral identification. This method allows a good preservation of the sample with minimum preparation. Furthermore, all the carbonate bands are easily identifiable in the mid-infrared region, hence are very distinguishable from other minerals (Kim et al., 2021). FTIR can also be used to provide quantitative results if necessary. Diffuse reflectance infrared Fourier transform spectroscopy (DRIFTS) is a type of FTIR which allows identification and quantification of calcite and dolomite (Bruckman and Wriessnig, 2013; Tatzber et al., 2007). It is not necessary to dilute the sample in infrared transparent material, which is time-saving in the preparation of the sample and the latter is not destroyed after analysis (So et al., 2020).

Traditionally, the quantity of mineralised CO_2 has been determined by measuring the amount of CO_2 gas created during acid, or heat decomposition.

Volumetric calcimetry is a method in which samples are digested in strong acid and the volume of CO_2 released is determined from its proportionality to a change in the height of the water level in the column of the calcimetry apparatus (see Supplementary Information – SOP 9). This method has considerable shortcomings, particularly its inability to distinguish between organic and inorganic carbon, leading to significant overestimates. However, it is a straightforward, low-tech, and inexpensive technique that may be useful when the sample under consideration is simple, low in organic matter, and already well-characterised by other methods.

Loss on ignition (LOI) is another straightforward approach, whereby samples are heated in a furnace: first, to 500°C to estimate weight loss due to organic combustion; then, to 900°C to determine weight loss due to carbonate mineral decomposition. This method may provide better estimates of the inorganic carbon content than volumetric calcimetry. However, results can still be significantly inaccurate (Kemp et al., 2022). This is due to a number of factors: mass change due to release of water, dehydroxylation of clays and other minerals, etc. Furthermore, several carbonate minerals, e.g., magnesite, may decompose in the same range as organic combustion, and redox reactions of metal oxides may further complicate the analysis. LOI is useful for analysis of many samples simultaneously which are well characterised, or have a few components (e.g., limestone).

Table 4. Summary of analytical tools for identification and quantification of mineral carbonates.

Analytical tool	Identification (I) or Quantification (Q)	Description	Sensitivity	Advantages, disadvantages and use case
TGA (SOP 10)	Q	Continuous measurement of mass vs. time/temperature while heating the sample. As the sample heads up minerals decompose and release volatiles at certain characteristic ranges. The TGA records the mass change that occurs at these events, which can then be used to infer the starting mass of the decomposing minerals.	<1000 ppm $CaCO_3$	Manipulation of control variables such as heating rate, gas flow rate, and gas type (CO_2, Air, O_2 or N_2) (Kemp et al., 2022; Warne, 2005) can aid in peak (dm/dt vs. t) separation, helping to distinguish simultaneous reactions and thus aid in identifying and quantifying carbonate minerals. However, a CO_2 atmosphere could cause carbonation <600°C, observed as mass gain, and lead to overestimates of carbonate content at >600°C. The addition of differential thermal analysis or differential scanning calorimetry provides information on heat flow enabling identification of exothermic (e.g., combustion) and endothermic reaction (e.g., $CaCO_3$ decomposition). Dehydroxylation reactions (release of H_2O) overlap with decomposition of magnesite and potentially other carbonates in which case TGA-MS may be needed. TGA with infrared heating can provide greater sensitivity than traditional wire resistance heating due to better temperature control.
TGA-MS (Box 10.2)	Q	Continuous measurement of mass vs. time/temperature with analysis of gas composition by mass spectrometry.	<100 ppm $CaCO_3$	By adding mass spectrometry greater sensitivity is enabled (Haines, 2002; Kemp et al., 2022; Sutter et al., 2017). High precision, good for quantification of carbonate minerals in small quantities thus suitable for surficial CO_2 mineralisation activities and enhanced weathering. Requires some skill in interpretation.
XRD (SOP 6)	I (and Q see Box 6.1)	A rotating sample is hit with an X-ray beam, an X-ray detector is used to detect at what angles X-rays are diffracted from the sample. As each mineral has a unique set of diffraction angles (due to its composition and crystal structure) they can be identified and quantified.	<1000 ppm depending on nature of the sample	Most commonly used tool for identification of major minerals. Also useful for quantification (Turvey et al., 2017; Turvey et al., 2018a, 2018b; Wilson et al., 2006).

Raman (SOP 7)	I	Raman spectroscopy is a method based on molecular spectroscopy using the interaction of light with matter to characterise a material.	–	This is a technique which preserves the sample with minimum sample preparation. It is straightforward to distinguish carbonate from other minerals with this method since the bands of the carbonates have distinct positions. Mineralogical and geochemical studies have been conducted with Raman analyses for a long time, but recently portable devices have been made for new applications (Kim et al., 2021).
FTIR (SOP 8)	Q and I	The FTIR analysis method uses infrared light to scan test samples and observe chemical properties.	–	FTIR is a fast method, which does not need much sample (~ 1 mg) and creates characteristic carbonate bands. Diffuse reflectance infrared Fourier transform spectroscopy (DRIFTS) is a type of FTIR which allows identification and quantification of calcite and dolomite (Bruckman and Wriessnig, 2013; Tatzber et al., 2007). It is not necessary to dilute the sample in infrared transparent material, which is save-timing in the preparation of the sample and the latter is not destroyed after analysis.
SEM-EDX (SOP 11)	Q and I	A microscopy technique that combines high-resolution imaging with elemental analysis. Firing a focused electron beam at the sample's surface generates X-rays, allowing for the identification and quantification of its elemental composition.	1 µm spatial resolution, ~1000 ppm detection limit	Requires thin sections or polished blocks. Analysis can be expensive and time consuming.
Volumetric calcimetry (SOP 9)	Q	Measurement of volume of evolved CO_2.	1% $CaCO_3$	No complex equipment necessary. Useful for quantifying the carbonate content of large numbers of simple, well characterised samples with high % of carbonate minerals, with low organic matter content. H^+ consumption by non-carbonate minerals may lead to underestimates (Pillot et al., 2014; Wang et al., 2012).
Loss on ignition (Box 10.3)	Q	Point measurement of mass loss vs time/temperature.	–	Useful for quantifying the carbonate content of large numbers of simple, well characterised samples with high % of carbonate minerals with high decomposition temperatures e.g., $CaCO_3$. Interference from dehydroxylation.

Isotopes of carbonate minerals. Carbon and oxygen isotopes can be used in the analysis of mineral carbonates due to their natural abundance and distinct isotopic fractionation behaviour during carbonation (e.g., Craig (1953); Hudson (1977)). Stable carbon isotopes (^{13}C and ^{12}C) and oxygen isotopes (^{18}O and ^{16}O) exhibit isotopic fractionation, which reflects the preferential incorporation of specific isotopes into carbonate mineral phases. In addition, the variable concentration of these isotopes in the reactants can also be useful in determining the provenance and formation environment (Andrews, 2006), which is particularly important in distinguishing between newly formed carbonate and lithogenic carbonate (e.g., limestone). By measuring and comparing isotopic compositions, the sources of CO_2 can be discerned and the evolution of isotopic signatures during carbonation reactions can be traced. Previous work has investigated consistent stable C and O isotopic fractionations in carbonates formed in hyper alkaline materials and drainage waters (Andrews et al., 1997; Dietzel et al., 1992; Gras et al., 2017; Krishnamurthy et al., 2003; Macleod et al., 1991; O'Neil and Barnes, 1971; Renforth et al., 2009; Turvey et al., 2018a; Wilson et al., 2010), which can be attributed to the uptake/diffusion, and hydroxylation, of atmospheric CO_2.

The radiogenic carbon isotope (carbon-14, ^{14}C) is formed in the upper atmosphere through the interaction of cosmic rays with nitrogen-14 (^{14}N). It is then taken up by plants through photosynthesis and enters the carbon cycle. The decay of the radiogenic carbon when it is incorporated into organic carbon has been used to estimate the time since the organic matter formed (e.g., Hajdas et al. (2021)). Similarly, radiogenic carbon in carbonate minerals can be used to distinguish between new and old carbonate (e.g., limestone) (Knapp et al., 2023; Washbourne et al., 2015; Wilson et al., 2010).

Metal isotope ratios are widely used in the analysis of mineral carbonates to gain insight into geological processes, environmental conditions, and dating of carbonate minerals. Common isotope measurements in carbonates include strontium (Sr), Mg and Ca. Sr is a naturally occurring element with four stable isotopes: ^{84}Sr, ^{86}Sr, ^{87}Sr, and ^{88}Sr (^{87}Sr is radiogenic, derived from the decay of rubidium-87). Variation in the ratio of Sr isotopes is primarily due to the differences in the initial isotopic composition of the source material (e.g., Dart et al. (2007)). Calcium has several stable isotopes, including ^{40}Ca, ^{42}Ca, ^{43}Ca, ^{44}Ca, and ^{46}Ca, and ^{48}Ca with sufficient half-life to be considered stable for most analysis. Calcium isotope ratio can be used to quantify biomineralisation, sediment diagenesis, and fluid-rock interactions (Fantle and Tipper, 2014; Kump et al., 2013; Pogge von Strandmann et al., 2019). Magnesium has three stable isotopes: ^{24}Mg, ^{25}Mg, and ^{26}Mg. Magnesium isotope ratios are used in the analysis of mineral carbonates due to their variation in source rock (Li et al., 2010), and their sensitivity to environmental and biological processes (Black et al., 2006). This fractionation can be influenced by factors such as temperature, pH, precipitation rates, and biological activity (AlKhatib and Eisenhauer, 2017a, 2017b; Mavromatis et al., 2013; Opfergelt et al., 2014; Pogge von Strandmann et al., 2019). Given that numerous multi-isotope transition metals are incorporated into carbonates there is a range of isotope systems that may be analysed.

Three possible methods of tracing carbon sources are compared in Figure 5. First is measuring the stable C and O isotope composition ($\delta^{13}C$ and $\delta^{18}O$) of carbonates. The premise of this method is that the combined $\delta^{13}C$ and $\delta^{18}O$ composition of mineralised CO_2 (in $CaCO_3$) reflects a mixture between some modern source of CO_2, i.e., what is intended to be mineralised for CDR, and an old source of CO_2, i.e., an additional source of DIC that is not intended to be mineralised, e.g., dissolution of a limestone. Atmospheric CO_2 (once hydroxylated) and soil-respired CO_2, have a distinctly negative $\delta^{13}C$ and $\delta^{18}O$ composition ($\delta^{13}C$ = -25 ‰ and $\delta^{18}O$ = -20‰) when compared to more old sources of DIC such as limestones, which generally reflect the $\delta^{13}C$ and $\delta^{18}O$ composition of the seawater within which the carbonate was formed ($\delta^{13}C$ = ~0 ‰ and $\delta^{18}O$ = -2 to +1.5 ‰, (Hudson, 1977). The disparity in $\delta^{13}C$ and $\delta^{18}O$ compositions of modern and old sources of DIC to a system suggests that a simple mixing relationship between the different sources of carbon in a system may be derived. However, previous attempts at doing this have yielded large uncertainties (Falk et al., 2016; Knapp et al., 2023; Mayes et al., 2018; Renforth et al., 2009) because $\delta^{13}C$ and $\delta^{18}O$ isotopes are unlikely to be solely influenced by conservative mixing between two chemically distinct endmembers (Knapp et al., 2023). Instead, $\delta^{13}C$ and $\delta^{18}O$ are influenced by a myriad of processes including non-equilibrium fractionation effects (i.e., kinetic fractionation), and partial DIC equilibration during CO_2 hydroxylation into solution (Falk et al., 2016). The result of these undesired effects is a large range in $\delta^{13}C$ and $\delta^{18}O$ isotope composition of carbonates precipitated in soils (Renforth et al., 2009), and streams (Knapp et al., 2023), producing large uncertainties during carbon source apportionment (e.g., Figure 5).

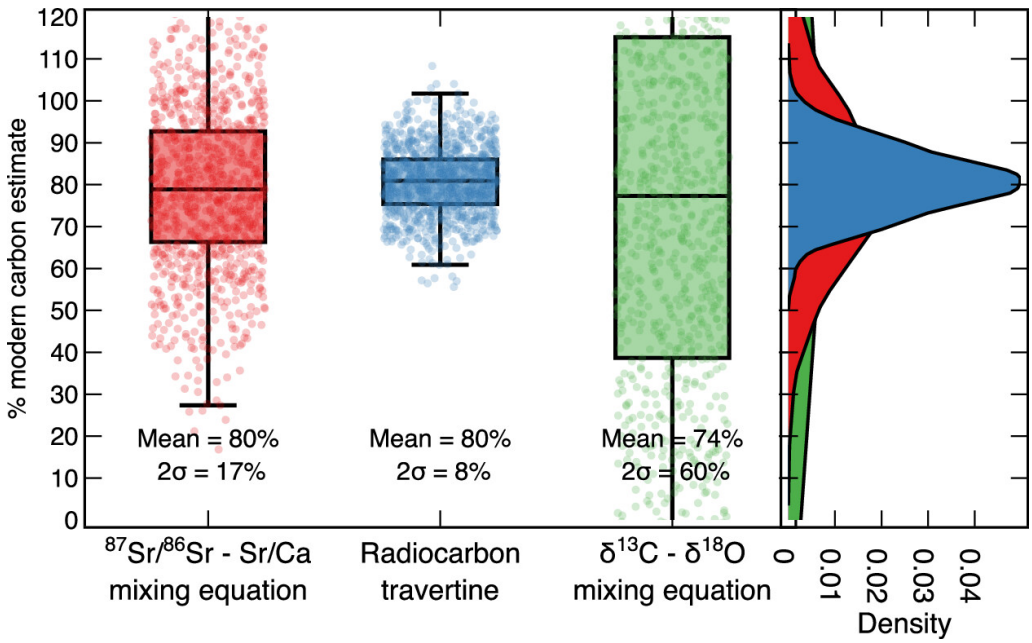

Figure 5: A comparison of three plausible models for carbon source apportionment from Knapp et al. (2023). The different approaches were tested on authigenic $CaCO_3$ deposits in Howden Burn, a stream draining a legacy iron and steel making slag deposit at the ex-Consett steel works site in Consett, Co. Durham, UK.

A second method for carbon source apportionment is provenance tracing using $^{87}Sr/^{86}Sr$ and trace metals relative to Ca (Sr/Ca). This method is particularly useful for discerning between carbonate and silicate weathering in EW settings (Larkin et al., 2022). As previously mentioned, the weathering of a carbonate lithology is half as impactful as weathering a silicate lithology. Silicate and carbonate lithologies have a distinct $^{87}Sr/^{86}Sr$ and Sr/Ca composition (Palmer and Edmond, 1992), owing to silicates being Sr-rich and derived from the mantle, which is a radiogenic source of Sr, and carbonates being relatively Sr-poor and derived from seawater, which is less radiogenic than the mantle. Therefore, in a similar way to $\delta^{13}C$ and $\delta^{18}O$, a mixing relationship can be established between plausible water-rock interactions, which have different implications for CDR. For creating mixing models $^{87}Sr/^{86}Sr$ presents a distinct advantage over $\delta^{13}C$ and $\delta^{18}O$, as $^{87}Sr/^{86}Sr$ behaves conservatively during mineral dissolution and carbonate precipitation reactions. This makes $^{87}Sr/^{86}Sr$ insensitive to kinetic isotope effects. Because of this conservative behaviour, uncertainties related to kinetic isotope effects are mitigated, and the main source of uncertainty is analytical error. This reduces 2σ uncertainties 3-fold compared to $\delta^{13}C$ and $\delta^{18}O$ measurements (Figure 5). However, a caveat of this approach is that all plausible mineral dissolution reactions in the system must be known, and the $^{87}Sr/^{86}Sr$ composition of all materials contributing Sr to solution must be characterised to satisfy mass-balance.

The final approach to be discussed is measuring the radiocarbon activity of authigenic $CaCO_3$. This technique can be considered a 'gold-standard' for carbon source apportionment, because radiocarbon simplifies a complicated set of water-rock interactions into a binary set of endmembers – modern or geological carbon. This makes proving additionality substantially easier because i) baseline mixes of carbon can be straightforwardly compared to post process mixes of carbon, and ii) achieving mass balance with respect to sources of carbon is not necessary, assuming the carbon in the system is a homogeneous mixture. A radiocarbon measurement of recent carbonate precipitates and waters provides a substantially improved estimate of modern carbon (Figure 5). 2σ uncertainties are halved in comparison to $^{87}Sr/^{86}Sr$-Sr/Ca mixing models, and almost 8 times improved compared to $\delta^{13}C$ and $\delta^{18}O$ mixing models. However, cost is critical for scaling MRV solutions. The clarity provided by using radiocarbon must be squared against the cost of the analysis versus other less costly solutions. Although radiocarbon measurements are relatively routine, costs are still > $100 per sample, which is likely similar to a carbon credit certificate. It is recommended that radiocarbon be used initially and then sparingly, to fully understand carbon source apportionment during geochemical CDR and prove additionality, before cost-effective alternatives to tracing additional carbon be used. A full synthesis of isotope tracers in geochemical CDR can be found in Knapp et al. (2023).

5.2 Quantifying CO_2 uptake during weathering

Measurements of drainage waters to quantify natural weathering have been reported for decades and remain the focus of a field of environmental sciences (Nesbitt et al., 1980). Continental weathering has been measured in river waters through various methods.

Major ion chemistry and alkalinity. Chemical elements such as Ca, Mg, Na, potassium (K), silicon (Si), and HCO_3^- are often released through weathering processes. By measuring the concentrations of these ions in river waters, it is possible to estimate the extent of continental weathering. The transport of these ions from the weathering environment (e.g., soils or material deposits) into drainage waters and rivers will be influenced by the complex interaction of soil processes and water flow (Harrington et al., 2023; Knapp and Tipper, 2022). Weathering of alkaline minerals and materials results in an increase in alkalinity of the drainage solutions. While a comprehensive definition of alkalinity includes the concentration of numerous base pairs (see SOP 14), HCO_3^-, and CO_3^{2-} are the primary anions in many alkaline natural or anthropogenic waters, although the contribution of other anions may lower or limit the weathering efficiency (SOP 17).

Stable isotopes. Stable isotopes of a range of elements, such as oxygen ($^{18}O/^{16}O$), strontium ($^{87}Sr/^{86}Sr$), magnesium ($^{26}Mg/^{24}Mg$) and lithium ($^{7}Li/^{6}Li$) can be used to measure artefacts of continental weathering. Isotopic signatures of river waters can reflect the source and history of the water, including the degree of interaction with weathering materials, or the formation of secondary minerals in soils and drainage waters (Pogge von Strandmann et al., 2021; Tipper et al., 2012).

Sediment load. River waters transport sediments eroded from the continents, and the composition of these sediments can indicate the degree of continental weathering. By measuring the sediment load in river waters and analysing the mineralogy of the sediments, inferences on upstream weathering are possible (Lipp et al., 2020; von Blanckenburg, 2006). Higher sediment loads and a greater presence of weathered minerals suggest more intense continental weathering.

Solid-phase mass balance/measurements of cation loss from soils. The extent of weathering of a rock feedstock can be calculated by measuring the difference in the amount of a mobile element in the feedstock after weathering, relative to before weathering. Highly mobile elements include alkali and alkaline earth metals (e.g., Ca, Mg, Na) that balance bicarbonate ions in the silicate weathering reaction. The loss of these elements from feedstocks can therefore be directly converted into an amount of initial CO_2 uptake, correcting for weathering by non-CO_2-derived acidity (Beerling et al., 2023; Kantola et al., 2023; Reershemius et al., 2023; Wolf et al., 2023).

This calculation relies on comparing equivalent quantities of rock feedstock in-situ, before and after weathering. Samples of a representative soil baseline are collected from the field

before mineral addition, and compared to the chemistry of the rock feedstock and to samples of soil from the field after mineral addition and weathering. These samples are first homogenised. Then, a leach is performed to remove metal ions held at soil exchange sites. Finally, a total digest is performed, and the concentration of elements is determined (using inductively coupled plasma-mass spectrometry (ICP-MS and/or ICP-OES) for maximum resolvability). In order to quantify the amount of feedstock present in a sample, an elemental tracer is measured that is present in both soil and feedstock in resolvable amounts, and that displays immobile behaviour during weathering – i.e. generally remains in the solid phase, for example titanium (Ti) (Brimhall and Dietrich, 1987; Chadwick et al., 1990; Esson, 1983).

6. Objective #2: Carbon dioxide removal potential of alkaline materials

Three main approaches for determining the elemental composition of solid alkaline material feedstocks are considered here: 1. Energy dispersive X-ray fluorescence (EDXRF); 2. Sample digestion in acid and analysis through inductively coupled plasma-optical emission spectroscopy (ICP-OES); and 3. Sample digestion in acid and analysis through ICP-MS (see Supplementary Information SOP 2–5). Some of the main features of these analytical techniques are compared in Table 5. The most suitable method will depend on the nature of the geochemical CDR activity, the accuracy and precision needed, the number of samples, and the overall cost, among other things. Flame atomic absorption spectroscopy (AAS) provides a cost-effective method for elemental analysis; however, it is not considered here since its usage has declined due to greater sensitivity and faster sample throughput of the abovementioned analytical techniques.

Determining the composition of the feedstocks mineral matter is crucial for assessing its potential for CO_2 removal and storage. It is also an input parameter for kinetic and mass transfer models which predict the rate of carbonation. Depending on the type of activity, it may also be necessary to understand the trace element concentrations, e.g., cadmium (Cd), lead (Pd), nickel (Ni), etc, for environmental and human health purposes. The atomic composition is also useful when determining the crystallography by powder X-ray diffraction (PXRD) (See Supplementary Information – SOP 6) and for corroborating the results of thermogravimetric analysis-mass spectrometry (TGA-MS) (see Supplementary Information – SOP 10) via mass balances.

Solid samples can be analysed directly by XRF with little to no sample preparation, although melting the sample using a flux and creating a homogenised glass bead can improve reproducibility (Ichikawa and Nakamura, 2016). For ICP-OES and ICP-MS, however, samples must first be aerosolised. To achieve this, solids are commonly converted into solutions using lithium borate fusion and digested in nitric acid.

Once obtained the elemental composition data (after conversion into their corresponding oxides) can be fed into the extended Steinor equations (Eqs. 5 and 6) in order to determine the maximum carbonation potential (C_{pot}) and enhanced weathering potential (E_{pot}) respectively (Renforth, 2019). [Note, these equations are not applicable to EW of alkali or alkaline carbonates]. The maximum carbonation potential is the maximum theoretical amount of CO_2 that can become mineralised by a material and this is mainly dependent on the Mg and Ca concentration of a material. The enhanced weathering potential (E_{pot}) is the maximum amount of carbon that can be removed and stored as HCO_3^- in solution i.e., each alkali cation (Na^+, K^+, etc) is charge balanced by one HCO_3^- and each alkaline cation (Mg^{2+},

Ca^{2+}, ect) is charge balanced by two HCO_3^-. [In reality, values are less than 2, owing to the carbonate buffering system].

Table 5. Comparison of three analytical techniques for elemental analysis of materials.

	EDXRF	ICP-OES	ICP-MS
Destructive (D) or non-destructive (ND)	ND (D if using a fusion)	D	D
Cost	Low–Moderate	Moderate	High
Cost per sample	Low	Moderate	High
Dynamic range of measurement	100% to sub ppm	10 ppb–10,000ppm	<1 ppt–1000ppm
No. samples per day	50–100 [>1000 for handheld devices]	2000–2500	1000
Sample preparation	None (lithium borate fusion can be used for homogenisation)	Lithium borate fusion and acid digestion	Lithium borate fusion and acid digestion
Tolerance to dissolved solids	–	High	Low
Number elements measured	>100	74	86
Operator skill	Low to medium	Medium	High
Isotopic analysis	No	No	Yes
Lab or Field	Lab and field	Lab	Lab

CO_2 mineralisation, also known as mineral carbonation, involves reaction of CO_2 (and H_2O) with alkaline minerals to form solid carbonate minerals. A theoretical 1 mole of CO_2 is captured per mole of Mg or Ca. The carbonation potential (C_{pot}) is expressed in kg of CO_2 per tonne of alkaline solid material (kg CO_2 t^{-1}):

$$C_{pot} = \frac{M_{CO_2}}{100}.(\alpha\frac{CaO}{M_{CaO}} + \beta\frac{MgO}{M_{MgO}} + \gamma\frac{SO_3}{M_{SO_3}} + \delta\frac{P_2O_5}{M_{P_2O_5}}).10^3 \quad \text{Eq. 5}$$

where CaO, MgO, SO_3, P_2O_5 are the elemental concentrations of Ca, Mg, sulphur (S), and phosphorus (P), expressed as oxides, M_x is the molecular mass of those oxides; coefficients α, β, γ and δ, consider the relative contribution of each oxide as a function of pH (see Figure. 6).

The coefficients γ and δ are negative as the carbonation potential is reduced by stronger acids of S and P, which are occasionally found in alkaline minerals (see Figure 6).

During mineral dissolution (without carbonate precipitation), CO_2 and H_2O react with alkaline minerals to form dissolved species including bicarbonate. The enhanced weathering potential (E_{pot}) can be expressed in kg of CO_2 per tonne of alkaline solid material (kg CO_2 t^{-1}):

$$E_{pot} = \frac{M_{CO_2}}{100} \cdot \left(\alpha \frac{CaO}{M_{CaO}} + \beta \frac{MgO}{M_{MgO}} + \varepsilon \frac{Na_2O}{M_{Na_2O}} + \theta \frac{K_2O}{M_{K_2O}} + \gamma \frac{SO_3}{M_{SO_3}} + \delta \frac{P_2O_5}{M_{P_2O_5}}\right) \cdot \eta \cdot 10^3 \quad \text{Eq. 6}$$

where CaO, MgO, Na_2O K_2O, SO_3, P_2O_5 are the elemental concentrations of Ca, Mg, Na, K, S, and P, expressed as oxides, M_x is the molecular mass of those oxides; coefficients α, β, ε, θ , γ and δ consider the relative contribution of each oxide as a function of pH (see Figure 6), and η is the molar ratio of CO_2 to divalent cation sequestered during enhanced weathering. Eq. 2 (See Section 2 Geochemical CDR Primer) implies that η=2; however, due to buffering in the carbonate system, the value is likely between 1.4 and 1.7 for relevant environments, and typical ranges of pCO_2 and temperature (Hartmann et al., 2013).

As an example calculation for C_{pot} and E_{pot} (Eq. 7–10), the composition of red mud, relevant to geochemical CDR, is CaO (5.7), MgO (0.3), Na_2O (5.2), K_2O (0.4) and SO_3 (0.1) where values given as % wt, coefficients are 1, 1, 1, 1, -1 at a pH of 7 for each of the elements respectively (see Figure 6).

$$C_{pot} = \frac{44}{100} \times \left(1\frac{0.057}{56.08} + 1\frac{0.003}{40.30} + (-1)\frac{0.001}{80.06}\right) \times 10^3 \quad \text{Eq. 7}$$

$$C_{pot} = 47.5\ kgCO_2\ t^{-1} \quad \text{Eq. 8}$$

$$E_{pot} = \frac{44}{100} \times \left(1\frac{0.057}{56.08} + 1\frac{0.003}{40.30} + 1\frac{0.052}{61.97} + 1\frac{0.004}{94.2} + (-1)\frac{0.001}{80.06}\right) \times 1.5 \times 10^3 \quad \text{Eq. 9}$$

$$E_{pot} = 129.4\ kgCO_2\ t^{-1} \quad \text{Eq. 10}$$

For all materials, E_{pot}>C_{pot}. However, for red mud, the difference between E_{pot} and C_{pot} is higher than other alkaline materials because of the high concentration of Na present.

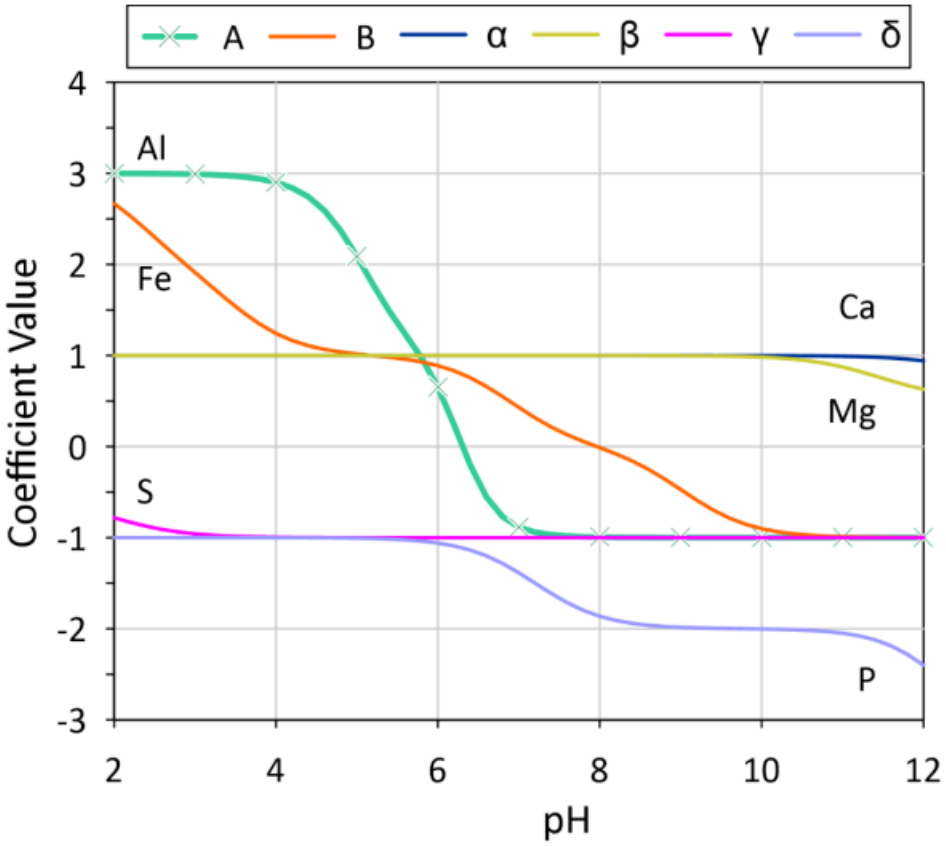

Figure 6. Variation in coefficients used to calculate the carbonation (C_{pot}) and enhanced weathering (E_{pot}) potentials. A coefficient value greater than zero increases the material carbon sequestration potential whereas a value less than zero reduces it. The value over the range of the dissolution environment pH is shown at a standard temperature and pressure. Note for Na_2O and K_2O the coefficients ε and θ are = 1 for pH<12 (republished with permission from Renforth (2019)).

7. Objective #3: Mineralogy of the material

While not as essential for MRV as carbonate mineral identification and quantification, determining the bulk mineralogy of an alkaline material is still important for i) determining the most suitable approach to carbonation, ii) estimating total carbon sequestration potential and carbon sequestration rates, and iii) identifying the presence of mineral phases that may negatively impact the carbon sequestration efficiency of the material.

The bulk mineralogy of a material intended for use as a geochemical CDR feedstock is one of the most fundamental controls on carbon sequestration potential. This is not only because different minerals have a range of elemental compositions (controlling the total abundance of divalent cations available for reaction), but because variability in their crystal structures (how atoms are bonded together) causes them to have wildly different dissolution rates and reaction kinetics. For example, 100 g of pure chrysotile ($Mg_3Si_2O_5(OH)_4$), a serpentine mineral, has the same total mass and contains the same amount of Mg as a mixture of 63 g of brucite ($Mg(OH)_2$) and 37 g of quartz (SiO_2), but would not produce the same carbon sequestration rate at Earth surface conditions due the much greater reactivity of brucite (Lu et al., 2022).

Bulk mineralogy is also important as certain carbon sequestration techniques will only be appropriate for specific bulk mineralogies. Techniques that operate at low temperatures and pressures have the advantage of minimising energy usage (important while the world is far from 100% renewable energy), but they tend to be the most selective in terms of their required mineralogy, often relying on highly reactive minerals to achieve significant carbon drawdown (Lu et al., 2022). Techniques that operate at higher temperatures and pressures, or those that require additional materials (such as strong acids), are less reliant on a specific mineralogy but they have greater energy and material costs. Table 6 lists some of the most common Ca- and Mg-minerals used in carbon sequestration feedstocks and lists their most appropriate CDR technologies.

For determining the bulk mineralogy of a material, a variety of analytical tools can be used, many of which are summarised below in Table 7. The most important consideration is typically the time, resources, and access to the analytical techniques and expertise. Assuming these considerations are not an issue, the analytical techniques that will provide the most useful information are PXRD, quantitative X-ray diffraction XRD (qXRD) (see SOP 6) and quantitative evaluation of materials by scanning electron microscopy (QEMSCAN). These techniques are heavily automated, making analysis and interpretation time relatively short. They can also provide bulk mineralogy of powdered samples (PXRD) or thin sections (QEMSCAN). In many cases, either of these techniques will provide robust answers for the main questions that bulk mineralogy can answer, including quantifying presence or absence of reactive Ca/Mg minerals (e.g., lime, periclase, brucite, forsterite, serpentine), pre-existing carbonate minerals, and any other phases of interest or concern.

Table 6. Common Ca- and Mg-rich mineral sources for carbon sequestration and their most appropriate CO_2 capture applications.

Mineral(s)	Formula	Feedstock	Applications
Lime	CaO	Recycled cement	DAC cycling (Chrissafis, 2007) ambient air capture; flue gas capture (Gupta and Fan, 2002)
Portlandite	$Ca(OH)_2$	Recycled cement, industrial wastes	DAC cycling (Nikulshina et al., 2007) EW; ambient air capture (Morales-Flórez et al., 2011) flue gas, OAE (Caserini et al., 2021)
Wollastonite	$CaSiO_3$	Skarn	EW (Haque et al., 2020; Stubbs et al., 2022) ambient air capture; flue gas capture; acid leaching and carbonation, (Zhang et al., 2010); heat treatment and carbonation (Huijgen et al., 2006).
Gypsum	$CaSO_4 \cdot 2H_2O$	Evaporites, some porphyries	Electrolytic carbonation (Lammers et al., 2023)
Periclase	MgO	Metamorphosed limestones and dolomites	DAC cycling (McQueen et al., 2020); flue gas capture.
Brucite	$Mg(OH)_2$	Serpentinites, some kimberlites	EW (Stubbs et al., 2022) ambient air capture (Turvey et al., 2018a), flue gas capture (Hamilton et al., 2020; Lu et al., 2022)
Forsterite	Mg_2SiO_4	Basalts, serpentinites	EW (Stubbs et al., 2022) High temperature/pressure flue gas capture (Wang and Dreisinger, 2022) acid leaching and carbonation; OAE (CEW) (Meysman and Montserrat, 2017)
Serpentines	$Mg_3Si_2O_5(OH)_4$	Serpentinites, kimberlites	EW (Stubbs et al., 2022), Flue gas (Lu et al., 2022) acid leaching and carbonation (Lu et al., 2022), heat treatment and carbonation (Benhelal et al., 2018; Benhelal et al., 2019a).
Iowaite–woodallite	$Mg_6Fe_2Cl_2(OH)_{16} \cdot 4H_2O$ $Mg_6Cr_2Cl_2(OH)_{16} \cdot 4H_2O$	Serpentinites	EW; ambient air capture (Turvey et al., 2018a), flue gas capture (Lu et al., 2022), acid leaching and carbonation; heat treatment and carbonation; anion exchange (Turvey et al., 2018a).
Ca/Mg smectites (e.g., saponite)	$M^{m+}_{x/m}Mg_3(Al_xSi_{4-x})O_{10}(OH)_2 \cdot nH_2O$ where M is a labile interlayer cation	Kimberlites, weathered basalts, many sedimentary rocks	Cation exchange (Zeyen et al., 2022)
Ca-feldspar	$CaAl_2Si_2O_8$	Basalts, gabbros	Acid leaching and carbonation
Chlorites	$Mg_5Al(AlSi_3O_{10})(OH)_8$	Widespread in multiple rock types	Acid leaching and carbonation
Talc	$Mg_3Si_4O_{10}(OH)_2$	Serpentinites, kimberlites	Acid leaching and carbonation
Amphiboles	$n Ca_2Mg_5Si_8O_{22}(OH)_2$ where n is an empty atomic position	Widespread in multiple rock types	Acid leaching and carbonation

Table 7. Summary of analytical tools for bulk mineralogy determination.

Analytical Tool	Description	Sensitivity	Advantages	Disadvantages	Use Case
PXRD (SOP 6)	A rotating sample interacts with an X-ray beam, an X-ray detector is used to detect the angles at which X-rays are diffracted from the sample. As each mineral has a unique set of diffraction angles and intensities (due to its crystal structure and composition) they can be identified and quantified.	<1 wt. % in complex mineralogical samples	Can be used on a wide variety of sample types including crushed rock samples (tailings), slag and soil. Identification and determination of relative mineral abundances is fast and simple.	Relatively low sensitivity, quantitative analysis involving complex samples (especially those containing amorphous materials or clay minerals) requires specialised analytical knowledge.	Typical analysis method for multiple crushed or fine-grained samples.
TGA (SOP 10)	Continuous measurement of mass vs. time/temperature while heating the sample. As the sample is heated minerals decompose and release volatiles at certain characteristic ranges of temperature. The TGA records the mass change that occurs at these events, which can then be used to infer the starting mass of the decomposing minerals.	<1000 ppm $CaCO_3$	Can provide highly accurate quantification of abundances for certain phases.	Cannot be used to identify minerals, requires other analytical techniques to determine the bulk mineralogy. Also requires calibration curves to be constructed when trying to quantify new minerals.	Highly accurate quantitative analysis for specific important minerals (e.g., brucite or periclase, and carbonates).
Optical microscopy	Traditional microscope that creates a magnified image of the sample using light. Minerals are identified using their optical properties.	1000× magnification	Inexpensive and easily accessible. Provides textural information. Can be used to obtain compositional information about some minerals (e.g., feldspars).	Relatively low magnification, cannot be used to identify very fine-grained materials. Challenging to obtain quantitative abundance information.	Need to get mineralogical and textural information with limited access to equipment or funding.
SEM (SOP 11)	A microscope that uses a beam of electrons instead of light to	1–20 nm resolution	Higher magnification than optical microscopy.	Cannot give quantitative abundance	Need textural information to

	create a magnified image of the target, produces higher magnification images than a traditional light microscope.			information.	supplement XRD data.
SEM-EDX (SOP 11)	SEM with energy dispersive spectroscopy (EDX) capabilities. EDX measures the energy of emitted electrons from samples and uses the characteristic energy levels to determine the elemental composition of the sample.	1 µm spatial resolution, ~1000 ppm detection limit	Can provide chemical information for each of the phases visible in the SEM image.	Only produces information about which elements are present and their relative abundances Does not explicitly identify minerals. Can be expensive and time consuming.	Want to be able to infer mineralogy from elemental composition of phases seen in SEM.
QEMSCAN	A combined SEM, 4 X-ray detectors and software identification package that scans and then automatically identifies minerals on a pixel-by-pixel basis.	~4 µm spatial resolution, ~1000 ppm detection limit	Highly automated, explicitly identifies minerals, determines their abundances, and provides textural context that can be useful to assess reactivity.	Requires development and calibration of in-house databases for mineral identification. Can be expensive and time consuming.	Highly detailed mineralogical analysis when time and cost are not issues.

8. Summary

Geochemical CDR has the potential to be deployed at significant scale and make a meaningful contribution to meeting carbon removal goals in the coming decades. Essential to effective implementation is the introduction of robust methods of monitoring carbon dioxide removal or storage, which provides confidence in the efficacy of the approach, and underpins its relationship with incentivisation strategies (e.g., compliance and voluntary markets, government procurement schemes).

This document presented guidance for best-practice in measurements of geochemical CDR approaches with the objectives of i) accounting for carbon accumulation in a material or solution, ii) assessing the capacity of the material to react with CO_2, iii) understanding how material properties may impact the speed of reaction with CO_2, iv) collect sufficient information on a material to aid in the design of a reaction process, and v) collect sufficient information to quantify risks associated with using a material. Methods of measurement vary with approach, and this document is intended to support others that detail best practices for research or protocols for monitoring, reporting and verification.

Methods for assessing material chemistry, mineralogy, and physical properties are included through SOPs contained within the Supplementary Information. They represent the approaches used by the authors to undertake research within geochemical CDR. It is anticipated that these will be updated and supplemented as the field develops, and we welcome collaboration for future editions of the document.

Acknowledgements

Phil Renforth (PR) and James Campbell acknowledge funding from the Industrial Decarbonisation Research Centre (EP/V027050/1) as the primary support for this work, though Wave #1 Project 21. Cara Maesano would like to thank Daniel Pike for his help in reviewing and editing Section 3 and acknowledges funding from the Grantham Foundation for the Protection of the Environment. PR and Laura Bastianini acknowledge funding from ClimateWorks Foundation and Climate Pathfinders Foundation (Novel Materials for Ocean Alkalinity Enhancement Project). PR and Spyros Foteinis acknowledge funding from the European Union's Horizon 2020 Research and Innovation Program under grant 869357 (project OceanNETs: Ocean-based Negative Emission Technologies—analysing the feasibility, risks, and co-benefits of ocean-based negative emission technologies for stabilising the climate). Liam Bullock is funded under H2020-EU.1.3.2. (DETAILS Project, grant agreement ID: 101018312). Philip Pogge von Strandmann is funded by ERC grant 682760 CONTROLPASTCO2. Connor Turvey and Sasha Wilson were funded by the Grantham Foundation for the Protection of the Environment, through a Discovery Grant from the Natural Sciences and Engineering Research Council of Canada, and by the Canada Research Chairs Program.

Author contributions

James S. Campbell – Conceptualised the report, scoped and outlined its contents, edited the report, contributed to Sections 1, 2, 4, 5, 6 and SOPs 4, 6, 9, 10, and 12.
Laura Bastianini – Contributed to Section 5, and SOPs 7, 8, and 14.
Jim Buckman – Contributed to SOP 11.
Liam A. Bullock – Contributed to SOP 13.
Spyros Foteinis – Edited the report and contributed to Section 3.
Veronica Furey – Contributed to Section 2.
Jess Hamilton – Contributed to SOP 2.
Kirsty Harrington – Contributed to Section 4.
Olivia K. Hawrot – Contributed to SOP 9.
Phil Holdship – Contributed to SOPs 4 and 5.
William J. Knapp – Contributed to Section 4 and SOP 15.
Cara Nichole Maesano – Contributed to Section 3.
Will Mayes – Contributed to SOP 8.
Philip A.E. Pogge von Strandmann – Contributed to SOP 15.
Tom Reershemius – Contributed to Section 4 and SOP 16.
Georgina Rosair – Contributed to SOP 6.
Fiona Sturgeon – Contributed to SOP 4.
Connor Turvey – Contributed to Sections 5 and 7, and SOP 6 and 10.
Sasha Wilson – Contributed to Section 7 and SOP 6.
Phil Renforth – Conceptualised the report, scoped and outlined its contents, edited the report, contributed to Sections 1, 2, 4, 5 and SOPs 1, 2, 3, 12, 14, 17.

Supplementary Information

SOP 1 – Sample collection, preparation, and physical properties

Methods of sample acquisition are described in Section 4, but the approximate quantities needed for the range of analytical techniques described in the SOPs is presented in Table 1.1.

Table 1.1. Sample size requirements for a range of measurement approaches used in geochemical carbon dioxide removal.

Measurement/ preparation method	Sample size required	Notes
X-ray fluorescence (SOP 2)	10–15 g	–
Acid digestion/ sequential extraction (SOP 3)	0.5 g	–
ICP-OES (SOP 4)	1–10 mL	Assuming an aspiration rate of ~1 mL s^{-1} for 1 minute measurement time. Lower aspiration rates/quicker measurement rates are possible.
ICP-MS (SOP 5)	1–10 mL	Assuming an aspiration rate of ~1 mL s^{-1} for 1 minute measurement time. Lower aspiration rates/quicker measurement rates are possible.
XRD (SOP 6)	~2 g	Smaller grain size is best, coarse samples will need to be milled.
Raman spectroscopy (SOP 7)	NA	Laser spot size 10s µm, possible to analyse single crystals.
FTIR (SOP 8)	NA	–
Volumetric calcimetry (SOP 9)	1–10 g	On the order of 50–200 mg of carbonate.
TGA (SOP 10)	~50 mg	Smaller grain size is best, coarse samples will need to be milled.
SEM (SOP 11)	0–10 g	Amount of material varies from a single particle of powder (micron to mm), to something that may be several cm in size.
Particle size determination (SOP 12)	~100 g	For < 2 mm, for larger particle sizes more material is required.
BET (SOP 13)	50 mg–1 g	Sufficient total surface area to reduce pressure within the instrument.
Total alkalinity (SOP 14)	20–200 mL, filtered solution	Smaller sample sizes to 10s mL are possible with larger analytical error.
Stable and radiogenic carbonate isotopes (SOP 15)	10s mg of carbonate	–
ID-ICP-MS (SOP 16)	–	Sample procedure follows acid digestion.
Ion chromatography (SOP 17)	1–10 mL	–

S1.1 Physical properties of solid samples

Bulk density. Bulk density is the total mass of a defined volume of mineral material. It includes the volume occupied by solid, liquid, and gas of a material. It can be measured at a field site by inserting a metal or plastic tube into a material (with known length and internal diameter), removing the material, and weighing the contents. For materials that are insufficiently cohesive to be extracted this way, a sand cone test (D18 Committee, 2016) may be performed.

Moisture or water content. Water content (w) definition: the mass of water which can be removed from the mineral sample by heating at 105°C, expressed as a percentage of the dry mass (often referred to as 'moisture content'). The water content is determined by oven drying the material overnight at 105 – 110°C, for gypsum rich materials a lower temperature <80°C must be used.

Specific gravity. The specific gravity (G_s) is the ratio between the density of a solid and that of water (sometimes referred to as 'particle density'). The principle behind the determination of G_s is to determine the volume of a known mass of solid particles, and divide this density by the density of water.

G_s is determined using two (or more) 50- or 100-mL density bottles (pycnometers) with stoppers. Ensure the pycnometers and stoppers are clean and dry. Wash with a small amount of methanol if required. Weigh the pycnometers and stoppers and record their mass (m_1). Add a sample of oven-dried granular material until the pycnometer is around 1/3 full, replace the stopper, and weigh (m_2). Add deionised/distilled water until the solid sample is completely submerged and place into a vacuum desiccator, depressurise and leave overnight. Shake the bottle gently, and return to the vacuum desiccator for a further 24 hours. The aim of this procedure is to completely remove air that might be trapped between the solid grains, which are the largest source of error. Remove the pycnometer from the desiccator and fill to top with deionised water. Allow the sample to stand for an hour or so before replacing the stopper. Replace the stopper and weigh (m_3). Empty the contents of the pycnometer, clean with deionised water, and refill with only deionised water. Replace the stopper and weigh (m_4). Specific gravity is calculated using Eq. 1.1.

$$G_s = \frac{m_2 - m_1}{(m_4 - m_1) - (m_3 - m_2)} \qquad \text{Eq. 1.1}$$

Calculation of porosity and void ratio. While the volume of the void space within a granular mineral material can be measured, it is easier and usually more convenient to calculate it from more easily measured parameters. The void ratio (the volume of voids per volume of solid) is calculated using specific gravity (G_s), moisture content (w), and the relative density of water to bulk density) (ρ_w/ρ_b) (Eq. 1.2).

$$e = G_s + (1 + w)\frac{\rho_w}{\rho_b}$$ Eq. 1.2

Porosity (n) can be determined from the void ratio (Eq. 1.3).

$$n = \frac{e}{1+e}$$ Eq. 1.3

The saturation ratio of the bulk material (S_r) can be determined using Eq. 1.4 (an S_r = 1 indicates that the volume of the voids is completely filled with water).

$$S_r = \frac{w \cdot G_s}{e}$$ Eq. 1.4

SOP 2 – Energy dispersive X-ray fluorescence (EDXRF)

S2.1 Scope and field of the application

This SOP describes how to identify and quantify carbonate minerals contained within alkaline materials using an analytical technique known as energy dispersive X-ray fluorescence (EDXRF). There are two main types of X-ray fluorescence that are commonly used for identification and quantification of minerals whose difference lies in the type of detection system: Energy Dispersive (EDXRF) and wavelength dispersive X-ray fluorescence (WDXRF). This SOP deals only with EDXRF (which enables simultaneous multi-element detection, is lower-cost, more transportable, and used in the vast majority of applications. In contrast, WDXRF systems analyse one or a few elements at high resolution and sensitivity, but are more expensive and less commonly used). Generally, elements lighter than Mg cannot be detected. Field XRF is also discussed (see Box 2.1).

S2.2 Principle

EDXRF is a non-destructive analytical method that provides information on the elemental composition via the interaction of radiation with the atoms of a mineral sample. When a material is excited by X-ray radiation, an inner shell electron may be lost/ionised. An electron in an outer electronic orbital moves to replace the missing inner electron, and in doing so, releases energy ('fluorescence'). The atomic electronic orbitals are known and fixed, and thus produce unique characteristic fluorescent signatures. By analysing the fluorescence emitted from the excited sample, the elemental composition can be determined.

The importance of escape depths. When we irradiate a sample with X-rays, samples with high average atomic number tend to absorb X-rays more strongly than samples with low average atomic number. This influences the penetration depth of the primary X-ray. By the same token, the fluorescent X-rays emitted within this penetration depth may be either re-absorbed within the sample, or if generated from a shallower location than the 'escape depth', may escape the sample and be detected. The escape depth can be calculated from the rock density and chemical composition (Ichikawa and Nakamura, 2023) and varies with atomic number. For example, in an average igneous rock, Mg Kα (fluorescent energy 1.04 keV) has an escape depth of 5 µm, while Ca Kα (3.69 keV) escape depth is 35 µm and Fe Kα (6.4 keV) is 84 µm. Heavier elements like Sr Kα have a much greater escape depth of 840 µm (Ichikawa and Nakamura, 2023). As such, an XRF detector receives a greater proportion of signal from higher energy fluorescent X-rays emitted by high atomic number elements compared to lower energy fluorescent X-rays from low atomic number elements. For this reason, standard materials are used to calibrate results and account for this effect.

Practically, it is important to consider escape depth for sample preparation. The smallest escape depth is the limiting factor, and so for reliable XRF analysis, the sample should be prepared such that it has a flat surface, and is homogenous with smaller particles than this limiting depth. As this is challenging to achieve in practice, quantitative results for low energy fluorescent elements should be considered with more caution.

S2.3 Instrumentation

X-ray source. A vacuum X-ray tube generates X-rays with energies on the order of 20–60 kV by accelerating electrons between a cathode and anode (see Figure 2.1). Common target materials for the anode include tungsten, molybdenum, or rhodium. These materials produce characteristic X-rays when bombarded by high-energy electrons accelerated within the tube. Higher energy sources (e.g., up to 50 keV) will allow detection of higher atomic number elements (the irradiating X-rays must exceed the absorption energy of elements of interest to generate fluorescence), however the use of a higher energy source comes at the expense of sensitivity to low atomic number elements. High intensity low-energy X-ray sources (e.g., 1-10 keV) are used to improve sensitivity to low atomic number elements. Some instruments incorporate multiple target materials to provide a broader range of sensitivity.

Sample holder. The sample holder is a device that securely holds the sample during analysis and ensures proper alignment with the X-ray source and detector. The holder may be designed to accommodate different sample forms, such as powders, pellets, or liquids. It is important to position the sample at a fixed distance and angle relative to the X-ray tube and detector for consistent analysis.

X-ray detection system. The X-ray detection system is responsible for capturing the emitted X-rays and converting them into measurable signals. Proportional counters are commonly used in EDXRF instruments, e.g., silicon drift detectors (SDD), that measure charge produced when its atoms are ionised from incident X-rays emitted from the sample. When an X-ray interacts with the SDD, it produces electron-hole pairs, generating an electrical signal proportional to the energy of the incident X-ray.

Signal processing and analysis. The electrical signals from the detector are processed and analysed using dedicated electronics and software. The detector signals are amplified, digitised, and converted into a spectrum representing the X-ray energies detected. Signal processing techniques, such as pulse height analysis, are employed to discriminate X-ray signals from background noise and improve signal-to-noise ratio. Specialised software is used to analyse the acquired spectrum, identify characteristic peaks, and quantify the elemental composition of the sample based on calibration curves.

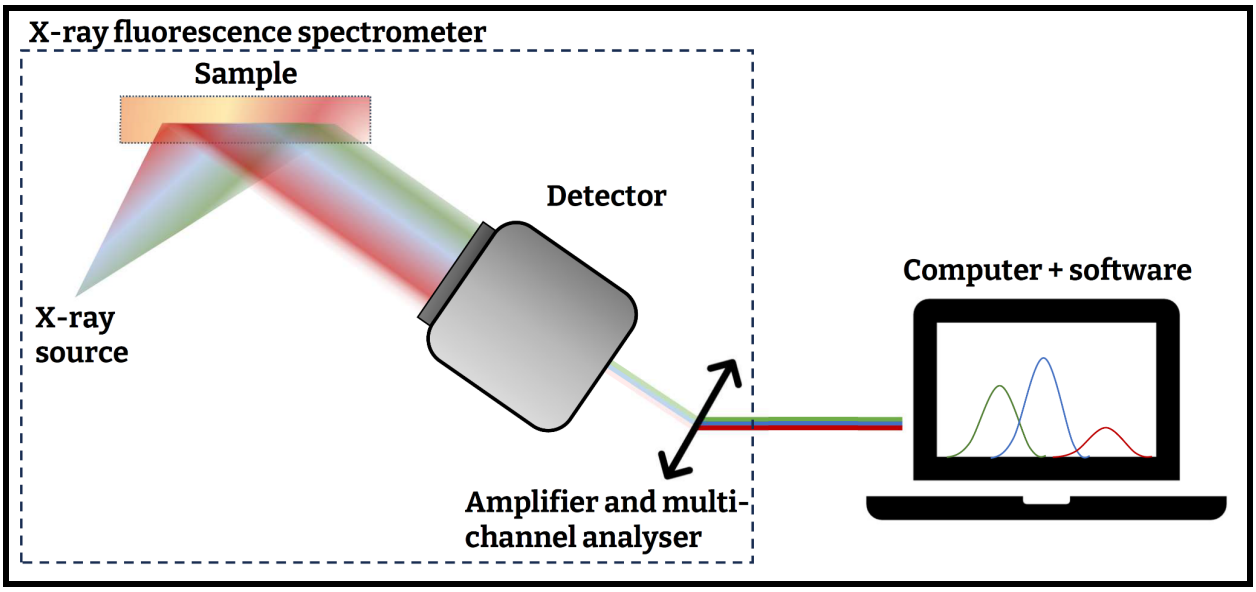

Figure 2.1. Simplified diagram of energy dispersive X-ray fluorescence instrumentation in operation adapted from Khalid et al. (2011).

S2.4 Sample preparation

For XRF, sample preparation is a critical factor controlling the reliability and accuracy of quantitative results. Having said that, the technique is often used with minimal or no sample preparation in order to get quick, semi-quantitative information about the elemental composition of a sample.

The two most common ways to prepare samples are as pressed powders or glass fusion. Fused beads allow for the detection of major elements with the advantage of higher repeatability. Drawbacks include greater time and material preparation costs, the necessary dilution of the sample for bead preparation, such that trace elements are often not determined, and can pose a risk of loss of reactive elements (e.g., C, O, N).

Pressed powders allow for the detection of a wider range of elements, but care is required in the preparation of the sample surface. Ideal samples exhibit fine and uniform particle size, high degree of homogeneity, homogenous mixing with a binder agent (e.g., wax, cellulose, boric acid, starch) at an appropriate ratio, and consistency in the amount of material used and pressure applied to produce pellets with uniform thickness and surface roughness.

It is essential to appropriately calibrate the instrument. Check standards should be used to confirm accuracy. Samples <10 mm in the smallest dimension and >2-mm thick are optimal for EDXRF analyses (Davis et al., 1998; Lundblad et al., 2007). With recent developments in digital EDXRF instrumentation and tube collimation, it is possible to analyse to sizes of 2 mm, e.g., ThermoScientific Quant'X EDXRF at Berkeley (see also Hughes et al. (2010))

Typically, methods for XRF analysis on mineral materials using fusion beads (e.g., British Standards Institution (2009); ISO (2010, 2021)) suggests mixing 5–10 parts of lithium borate flux with 1 part sample, and a releasing agent of ammonium iodide or lithium iodide. 100g of sample should be milled and sieved to <150 µm, although only 5–10g may be needed for pellet creation (for reactive materials, this should be done as quickly as possible to avoid the contact with the atmosphere), and heated to >1000°C in a platinum-gold, platinum-rubidium crucible.

Excellent resources are available in the literature including detailed sample preparation guides e.g., Ichikawa and Nakamura (2023).

S2.5 Standards and calibration

When selecting standards for XRF analysis, it is crucial to consider factors such as traceability, reliability, stability, and compatibility with the sample matrix. All standards and samples should be presented for analysis in a reproducible and identical way, so standards should ideally have similar physical and chemical characteristics to the samples (particle size and homogeneity, composition (e.g., distribution of high and low absorbing elements), and preparation style. It is also recommended to consult recognized organisations, manufacturers, and scientific literature to identify appropriate standards for specific applications and analytical needs.

Certified Reference Materials (CRMs). CRMs are highly characterised materials with known and certified elemental compositions. They are produced and certified by reputable organisations such as the National Institute of Standards and Technology (NIST) or the International Atomic Energy Agency (IAEA). CRMs are routinely used for calibrating XRF instruments, validating analytical methods, and verifying the accuracy and precision of results.

Geological reference materials. Geological reference materials are specifically designed to simulate geological samples and are commonly used in mineral exploration, mining, and geosciences. These materials represent different geological matrices, such as ores, rocks, soils, and sediments, and cover a broad range of elements and concentrations. Well-established geological reference materials, such as those offered by the Geological Survey of Canada (GSC) or the United States Geological Survey (USGS), are widely used in the mineral analysis industry.

Synthetic standards. Synthetic standards are artificially prepared materials that mimic the elemental composition and matrix of the samples of interest. They are typically used when certified reference materials are not available for a specific application or when a specific matrix needs to be closely matched. Synthetic standards are particularly useful for calibration, method development, and quality control purposes. If preparing these as

pressed powder, good control over particle size, homogeneity, packing density is needed. In contrast, the fusion bead process makes synthetic standard preparation easier.

Internal standards. Internal standards are elements or compounds added to the sample or calibration standards to compensate for matrix effects and instrumental variations. They are typically elements present at known concentrations that are not of primary analytical interest. They are less costly than CRMs and can be benchmarked at the beginning and throughout analysis to check for drift and consistency of measurements.

Calibration. Calibration should be performed approximately yearly or following replacement of the source or detector. This is done by analysing CRMs that contain a broad range of elements, and more than two standards per element are required (Yatkin et al., 2015).

S2.6 Procedure

The exact operation and user interface may vary depending on the specific XRF analyser model and manufacturer. It is advisable to consult the instrument's user manual and guidelines for precise operating instructions. However, the following outlines a broad method for operation:

1. Prepare the sample according to the recommended sample preparation procedures (see above).
2. Place the sample in the appropriate sample holder, ensuring that it is aligned with the X-ray source and detector for accurate analysis.
3. Access the control interface of the XRF analyser, which can be a software interface or a control panel on the instrument.
4. Specify the measurement parameters, such as the analysis mode (e.g., spot analysis, mapping, or line scan), measurement time, and any additional settings required for the specific analysis. Some analysers may offer pre-configured analysis modes based on the sample type or application to simplify the setup process.
5. Initiate the measurement process, and the X-ray tube in the analyser emits X-rays with specific energies (or wavelengths in the case of WDXRF).
6. The X-rays penetrate the sample, causing the sample atoms to undergo X-ray absorption and subsequent emission of characteristic fluorescent X-rays.
7. The X-ray detector captures the emitted X-rays and converts the X-ray energy into electrical signals, which are then amplified and processed by the analyzer's electronics.
8. Data is processed in a multichannel analyser that produces a data spectrum for energies emitted from the sample, and converted to voltage pulses in the detector.

S2.7 Data presentation

For alkaline materials, and geological samples generally, EDXRF results for major elements are usually reported as common oxides (see Table 4.2 for examples) but may also be given as the elements. These common oxides include Al_2O_3, CaO, Cr_2O_3, Fe_2O_3, FeO, K_2O, MgO, MnO, Na_2O, P_2O_5, SO_3, SiO_2, TiO_2. It is common to include mass loss on ignition (LOI, see Box 10.3) in the results. The sum of the oxide concentrations and the LOI should be 100% of the mass of the original sample. Trace elements are often reported as elements rather than oxides, and the limit of detection for each element should be stated alongside the results.

Box 2.1 – Field portable XRF

A portable XRF analyser is a compact and handheld instrument designed for on-site or field-based elemental analysis (Kalnicky and Singhvi, 2001). It offers the capability to determine the elemental composition of various materials quickly and non-destructively. The X-ray tube is typically operated at low power and is designed for safe and efficient operation in portable instruments. To initiate a measurement, the user typically places the portable XRF analyser in contact with the sample surface or holds it close to the sample. The analyser may have an adjustable measurement window or a collimator to restrict the analysis area and focus the X-ray beam. The user interface of the portable XRF analyser allows for easy setup and selection of analysis parameters, such as measurement time, calibration settings, and analysis mode.

Portable XRF analysers find applications in various industries, including mining, environmental analysis, archaeology, alloy analysis, and quality control. Their portability, ease of use, and rapid analysis capabilities make them ideal for on-site measurements and non-destructive testing in diverse field settings.

S2.8 Advantages and disadvantages

It is important to consider advantages and disadvantages in relation to the specific analytical requirements, sample characteristics, and desired outcomes when deciding whether XRF analysis is suitable for a particular application.

XRF analysis is a non-destructive technique, and the sample remains intact and can be further utilised or preserved for other analyses. It can analyse a wide range of elements, from low atomic number elements like magnesium (although with difficulty) to high atomic number elements like uranium. It covers a significant portion of the periodic table, allowing for comprehensive elemental analysis. The analysis can provide quantitative information about the elemental composition of a sample. Calibration curves and standards can be used to accurately determine elemental concentrations. XRF requires minimal sample

preparation compared to some other techniques. For many applications, samples can be analysed directly or with minimal grinding, reducing time and effort.

XRF is less accurate for the analysis of light elements (atomic number less than 11) due to their weak X-ray emissions and overlap with background signals. Quantitative analysis of light elements may require more advanced techniques or additional sample treatment. XRF analyses only the surface layer of the sample, typically in the range of a few micrometres to several millimetres. It may not provide information about the bulk composition or variations within the sample. The analysis can be influenced by the matrix composition of the sample, leading to potential interferences or inaccuracies. Correction algorithms or calibration standards may be required to address these matrix effects. XRF analysis can be sensitive to sample geometry, including the sample thickness, density, and homogeneity. Variations in sample presentation can affect the accuracy and precision of results.

The difficulty in detecting Mg requires greater care in optimising both sample preparation and analytical processes when using this technique to quantitatively measure Mg-rich feedstocks or carbonated products. Calcium or other trace elements may be used as elemental proxies.

Another important note is that XRF cannot measure carbonate, thus the reported metal oxide abundances must be used in conjunction with other information (TGA, LOI, total carbon analysis, XRD, etc) to constrain mass balance calculations when estimating the abundance of existing carbonates in feedstock materials, and when assessing the abundance and type of carbonate products (e.g. Ca, Mg and Fe carbonates which may also be variably hydrated).

S2.9 Quality assurance

XRF should only be operated by those who have obtained appropriate training and, where necessary, certification. Methods will be calibrated and checked against international standards. The standards are used to calibrate trace elements. Elements without overlaps are fitted (unconstrained) to a linear least squares fit. Multiple linear least squares fits are used to align overlapping items. Compton ratioing is used in both cases to adjust the matrix (Harvey and Atkin, 1985). According to the XRF-1 I User Guide, updating intensities from a standard in the driver file allows for the calibration of main elements (Criss, 1985). Sources of uncertainty that could exist include choosing a peak and background counting time on a representative sample. The inaccuracy from counting statistics will grow if samples with fewer of the constituent elements of interest are analysed, which will result in low precision. Furthermore, the signal from measured elements may overlap unexpectedly or incorrectly.

SOP 3 – Acid digestion and sequential extraction

S3.1 Scope and field of application

Acid digestion and sequential extraction has been used for decades to measure the inorganic composition of mineral solids. The techniques involve completely or partially dissolving a solid sample with a volume of corrosive solvent (Table 3.1), and analysing the solvent using a method of solution analysis (see SOP 4, 5, and 15), and reviewed by (Hu and Qi, 2014).

S3.2 Principle

Minerals are sparingly soluble in water (e.g., 10 mg of calcite in 1 L of pure water), and the rate of dissolution is slow. Furthermore, the equilibrium of silicate minerals with water can result in the supersaturation of secondary minerals (e.g., silica, clays, carbonates). Digesting mineral solids in aqueous solvents overcomes these limitations, and given sufficient solvent, it may be possible to completely dissolve a small quantity of solid. Subsequent chemical analysis of the liquid will reveal the chemical constituent of the solid. Given that mineral solids are typically composed of phases with variable solubility in different solvents, it is possible to tailor the digestion to analyse the chemical composition of specific components of the solid.

S3.3 Sample Preparation

Solids should be collected as described in SOP 1, oven dried (105°C to constant mass), crushed and powdered to < 63 µm (Balaram and Subramanyam, 2022). While most (clean) standard laboratory grinding apparatus are suitable for major element determination, it may be a potential source of contamination for less abundant elements. Performing the procedure with standard materials will help assess the suitability of the experimental protocol.

S3.4 Procedure

A typical recipe for the digestion of silicate and carbonate rocks is as follows (from Totland et al. (1992)). 0.5 g of powdered sample is placed into a beaker and moistened with 1–2 mL of deionized water. 10 mL of HF + 4 mL of $HClO_4$ is added and the sample is oven dried (this should be repeated 3–4 times). 10 mL of 5 mol kg^{-1} HNO_3 is added and gently heated, and then transferred to a 50 mL volumetric flask and made up with dilute HNO_3.

It is possible to achieve complete mineral dissolution by melting the material at high temperature and dissolving the resulting glass bead in a strong acid (Ingamells, 1970). For silicate minerals, a flux is required (commonly lithium borate or metaborate). 0.1 g of

powdered sample is mixed with 0.3 g of flux and placed into a non-wetting (5% gold) platinum crucible and heated to 1050°C until the powder has completely melted (~15 minutes). The melt is then poured into 50 mL of 5 mol kg^{-1} HNO_3, continuously stirred for 30–60 min at 60°C to aid dissolution. Samples should be diluted as required for analysis using ICP-MS or ICP-OES (see SOP 4 and 5).

Table 3.1. A summary of strong acids used to dissolve minerals/rocks for analysis, adapted from Hu and Qi (2014).

Acid	Typical digestion concentration (mol kg^{-1})	Notes
Nitric (HNO_3)	16	Oxidising, decomposing carbonates and sulphide minerals. Stable matrix for ICP-MS.
Perchloric ($HClO_4$)	12	Oxidising and dehydrating, can form insoluble salts of K, Rb, and Cs, highly reactive with some salts and organic material.
Hydrofluoric (HF)	29	Can break down Si-O bonds, but readily forms insoluble salts. Highly corrosive and toxic.
Aqua Regia (HNO_3-HCl)	16 HNO_3 – 12 HCl at a ratio of 1:3	Strongly oxidising, and should be prepared directly before use.

In addition to assessing the bulk composition of a material, it is often useful to determine the chemical composition of specific phases or materials within a complex mixture. Sequential leaching has been extensively used for this purpose (Tessier et al., 1979), which involves exposing a solid material to increasingly stronger solvents and analysing the resulting solution. Table 3.2 presents a typical set of extraction steps for metals bound to exchange sites, carbonates, iron oxides, and organic material.

Table 3.2. A summary of a sequential extraction procedure for mineral materials, adapted from Kumkrong et al. (2021).

Step	Solvent (concentration)	Notes
Exchangeable	Sodium acetate (1 mol kg^{-1}) ~ pH 8	1 g of solid sample + 8 mL of solvent. 1 hr dissolution time + 30 min centrifuge.
Carbonate	Sodium acetate (1 mol kg^{-1}) ~ pH 5 (adjusted with acetic acid)	8 mL of solvent. 5 hr dissolution time + 30 min centrifuge.
Iron or manganese Oxides	Hydroxylammonium chloride (0.04 mol kg^{-1}) in 25% acetic acid	20 mL of solvent at 96°C for 6 hr + 30 min centrifuge.
Organic/Sulphides	Nitric acid (0.02 mol kg^{-1}) + Hydrogen peroxide (30%) + at pH 2	3 mL nitric acid + 5 mL of hydrogen peroxide. 15 min idle + 3 hr at 85°C.
Residual	HF + $HClO_4$	As described above.

SOP 4 – Inductively coupled optical emission spectrometry (ICP-OES)

S4.1 Scope and field of the application

This SOP provides a thorough guide for analysis of solid (and liquid) samples by inductively coupled plasma optical emissions spectroscopy (ICP-OES). ICP-OES is a term used interchangeably with inductively coupled atomic emissions spectroscopy (ICP-AES). ICP-OES is most suited for analysis of metals in concentrations greater than 5 % by wt. If the elements of interest are in lower concentration than the instrument's lower detection limit, then ICP-MS may be preferable (see SOP 5). Thirty-nine elements can be quantified by ICP-OES analysis including aluminium, antimony, arsenic, barium, beryllium, cadmium, calcium, chromium, cobalt, copper, iron, lead, lithium, magnesium, manganese, mercury, molybdenum, nickel, phosphorus, potassium, selenium, silica, silver, sodium, strontium, thallium, tin, titanium, vanadium and zinc (see Briggs (2002)), bismuth, gallium, sulphur, tungsten, yttrium and zirconium (see US-EPA (2007)).

S4.2 Principle

Plasma is the fourth state of matter and comprises a stream of highly energised, charged particles. Inductively coupled plasma (ICP) is a type of plasma that is created by electromagnetic induction by combining a high frequency RF radiation within an enclosed metal coil, to a supply of a stable non-reactive gas (predominantly argon). After its formation the plasma is stabilised at very high temperatures and can be sustained if the RF and gas supplies are maintained. The plasma is particularly energetic, and as such provides an ideal ion source for trace element mass spectrometry analysis, where nearly all elements are atomized and ionised.

ICP-OES measures the atomic concentrations of a sample by studying its emitted light when heated to high temperatures. The sample is converted into an aerosol, and the fine droplets are ionised in an argon plasma. Once in their ionised state, the atoms or ions can decay to lower energy levels through radiative emission. The light that is emitted by the energised plasma is directed to a diffraction grating which separates it into its spectral lines. The spectral lines and their intensities are characteristic of the types and concentrations of elements in the sample. ICP-OES requires element standard solutions of a known concentration. Samples must be in the aqueous phase, therefore insoluble solid samples must be prepared via acid digestion (for rock and mineral samples this is usually with prior lithium borate fusion, see SOP 3). OES uses only the visible and ultraviolet parts of the electromagnetic spectrum (wavelengths of 130–800 nm).

S4.3 Instrumentation

Typical ICP-OES instruments are composed of several main components (see Figure 4.1). A peristaltic pump withdraws liquid samples to the nebuliser which converts the solution into a fine aerosol. The aerosol is sprayed into a high-energy argon plasma generated by high power radio frequency or microwave which causes gas ionisation. Interactions between the plasma and the sample result in degradation of the sample to its individual elements, causing emission of a characteristic optical signal. The emitted light is sent to a diffraction grating and prism which separates it into spectral lines picked up by the detector (see (Levine, 2021)). Software converts the spectral lines into concentration units. The instrument must be periodically purged. Prior to using the instrument, it is purged with argon gas for 30–60 minutes, and periodically thereafter. Glassware should be checked daily, and pump tubing should be replaced weekly. The background equivalent concentration should also be checked on a daily basis. BEC is a ratio of the counts per second obtained by aspirating a blank solution and the slope of the calibration curve.

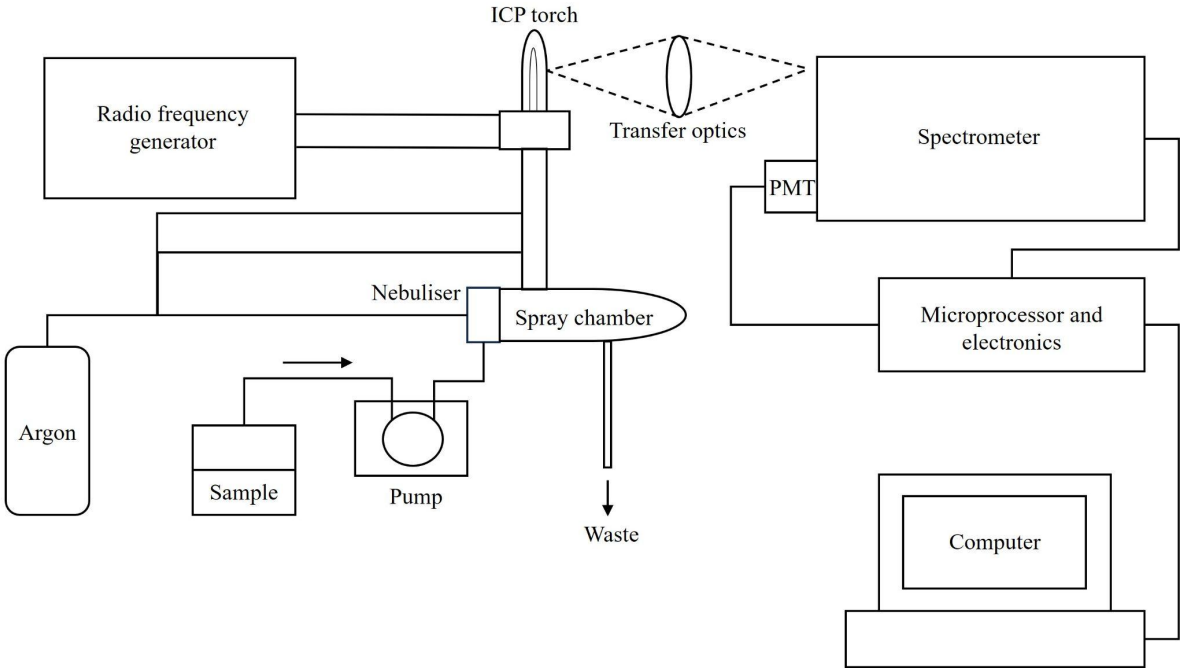

Figure 4.1. Simplified schematic of ICP-OES instrumentation.

S4.4 Sample Preparation

Sample preparation will depend on the type of sample being analysed. Most importantly the samples must be in liquid form with dissolved solids of no more than 30% (samples with high dissolved solids should be diluted with deionized water prior to analysis). Aqueous samples can be introduced into a plasma directly, and often without dilution. They are typically acidified with nitric acid (HNO_3) to ensure that their elemental components remain

in solution. A nitric acid or aqua regia digest is often used for soil and sediment samples, however rock or minerals will need a more robust digestion technique such as lithium metaborate fusion (see SOP 3). For example, a 0.25 g olivine sample should be first milled and mixed with 1.25 g $LiBO_2$ and fused in a furnace (e.g., Katanax X-300 X-Fluxer). The sample can be placed in the furnace at 1000°C for 6.5 min before the resulting melt is poured into a beaker containing 8% HNO_3. The sample dissolves in the dilute acid, which can be transferred to a 250 mL flask and made up to mark.

S4.5 Procedure

Calibration. In order to calibrate the ICP-OES instrument for analysis, standard solutions containing the elements of interest must be prepared, at concentrations that will encompass the levels expected to be present in the samples. Standard and Quality Control solutions should be made up from stock solutions that are traceable to reputable standards (e.g., those supplied by NIST). However, a range of sources should be used for standard and QC solutions. Multi-point calibrations can be plotted by diluting the most concentrated standard. Standards should be matrix matched to the samples as much as possible to account for nebuliser and plasma related effects. Limits of detection (LoDs) are routinely calculated as three times the standard deviation of 10 blank analyses. This applies to both ICP-MS (see SOP 5) and ICP-OES instrumentation.

Table 4.1. Limits of detection (mg L^{-1}) for Perkin Elmer NexION 2000 ICP-OES.

Element	Limit	Element	Limit
Al	0.0009	Mn	0.00002
As	0.00001	Na	0.002
B	0.001	Ni	0.00005
Ca	0.007	P	0.001
Cu	0.00002	Pb	0.0001
Fe	0.005	Si	0.003
K	0.002	Sr	0.00002
Mg	0.0001	Zn	0.0004

For demonstration, an olivine sample was digested by $LiBO_2$ fusion and analysed using the Perkin Elmer AVIO 500 ICP-OES for Al, Ba, Ca, Cr, Fe, K, Mg, Mn, Na, P, Si, Sr, Ti. An argon humidifier and nebuliser for high dissolved solids was used for this analysis due to the nature of the matrix. Standard and QC solutions were matrix-matched to the samples. LODs were not applied to this data and mg L^{-1} results were used to calculate and report both mg kg^{-1} and oxide data. LODs are listed in Table 4.1. As samples were diluted x5 prior to analysis any reported LODs will be x5 the LODs.

Internal standards. Users are encouraged to utilise an internal standard to adjust for variability between samples and variations in processing, particularly to remove unwanted interferences before analysis. Scandium-32 and yttrium-33 are often used internal standards given that their wavelengths do not coincide with those of other atoms in the sample.

S4.6 Data presentation

Results of aqueous samples are usually expressed as mg L^{-1} or ppm, which for solid samples that have been digested can be multiplied up to mg kg^{-1} results. For rock or mineral samples, such as the olivine sample in this example, the % oxide values can be calculated by multiplying mg kg^{-1} data by oxide ratios (Table 4.2).

Table 4.2. Composition data for olivine sample determined through acid digestion and ICP-OES.

Element	Concentration (mg kg^{-1})	Element (expressed as an oxide)	Concentration (wt. %)
Al	3839	Al_2O_3	0.73
Ba	20	BaO	0.002
Ca	1786	CaO	0.25
Cr	3377	Cr_2O_3	0.5
Fe	45870	Fe_2O_3	6.56
K	328	K_2O	0.04
Mg	287523	MgO	47.7
Mn	707	MnO	0.09
Na	653	Na_2O	0.09
Ni	2349	NiO	0.3
P	ND	P_2O_5	ND
Si	166088	SiO_2	41.9
Sr	22	SrO	0.003
Ti	77	TiO_2	0.01
Total	n/a	Total	98.2

The sample was analysed in triplicate and average values are reported. ND = Not detected
Concentration data (mg kg^{-1}) was used to derive oxide concentrations.

S4.7 Advantages and disadvantages

One major advantage of using ICP-OES over atomic absorption spectroscopy (AAS) is that the plasma provides enough heat to ionise multiple elements simultaneously as well as all atoms and ions emitting their characteristic radiation at the same time. This means that as well as observing several elements at the same time, multiple wavelengths of the same element can also be observed (Charles and Fredeen, 1997). ICP-OES is often compared to ICP-MS (see SOP 5). Rather than using emitted light, ICP-MS separates the components of

plasmolysed samples by their mass-to-charge ratio. ICP-MS instruments can obtain concentrations as parts per trillion whereas ICP-OES is limited to parts per billion, but best suited to ppm. Therefore, ICP-MS is preferred where the element of interest is in very low concentration. However, ICP-OES has a higher tolerance for total dissolved solids (TDS) (up to 30% TDS) than ICP-MS (up to 0.2%) and therefore sample dilution is often needed for ICP-MS. Further, ICP-MS is usually more expensive and requires greater technical expertise.

S4.8 Quality assurance

Quality control samples need to be analysed to prove the validity of the sample preparation as well as the analytical precision. Other concerns in analysing ICP-OES data relate to potential interferents and their ability to compromise the system performance. If available, a Certified Reference Material (CRM) should also be analysed with the samples to check that the chosen digestion process has worked correctly.

SOP 5 – Inductively coupled plasma mass spectrometry (ICP-MS)

S5.1 Scope and field of the application

Inductively coupled plasma mass spectrometry (ICP-MS) is a powerful analytical technique used to examine low-abundance elemental compositions in a sample. It is particularly useful for the measurement of trace metals in a variety of sample types, where it can accurately operate within a concentration window that spans over nine orders of magnitude, in addition to providing detection limits below pg g^{-1} concentrations (e.g., the rare earth elements). Many ICP-MS systems have the capability to analyse both solid and liquid matrices, where the former is conducted by coupling the instrument with a laser ablation unit. Laser Ablation ICP-MS is particularly useful for determining the spatial distribution of trace and major elements in samples (Kang et al., 2004), and can also be used to map such concentrations in a substrate, for example, in bio and medical sciences (Becker et al., 2010). Finally, certain ICP-MS systems can also be employed to simultaneously measure different isotopes of a particular element. Known as Isotope ratio ICP mass spectrometry, or Multi-Collector ICP-MS, this important technique will be discussed separately (see SOP 15).

S5.2 Principle

In mass spectrometry ions are measured according to their mass-to-charge ratio (m/z). As discussed above (SOP 4), the argon plasma transfers many elements into the mass spectrometer in an ionised state, where it is important to minimise such oxidation reactions to the release of more than one electron (i.e., to only transfer M1+ ions into the mass spectrometer. This is normally controlled through careful optimisation of the plasma and should be about 97% efficient.

When the ions enter the mass spectrometer they are focused and channelled towards the mass filter for mass separation. Mass filtering is predominantly conducted using a quadrupole: a device comprising four metal rods, two connected to a constant DC current and two connected to a varying AC current. The AC current cycles over a period of a few microseconds, where within each such succession individual masses, corresponding to a particular element, are able to resonate without restriction through the four rods for a small fraction of time. This fixed time is unique per mass and thus allows discrimination within the mass spectrometer so that elemental concentrations can be determined for a particular sample.

S5.3 Instrumentation

Instrumentation supporting the ICP part of the ICP-MS is identical to ICP-OES (please see Figure 4.1 in SOP 4). Ions enter the mass spectrometer via the interface, where the majority of the M1+ ions pass through the centre orifice of the cones. Once inside the mass spectrometer they are focused and, in many cases, deflected by the high voltage electronic components, to eliminate the transfer of light and neutral species further into the instrument. The channelled ion beam then enters the reaction/collision cell, which can be filled with reactive or inert gases (namely NH_3 and He respectively). These gases enable the dissociation of undesirable molecules – polyatomic ions that form within the cooler regions of the plasma, which often cause interference on analyte M+ ions within the mass spectra. After the enhanced ion beam has exited the cell, it is then directed towards the quadrupole for mass filtering and then finally to the secondary electron multiplier for detection. The software then converts the detector counts per second values into concentrations (Figure 5.1).

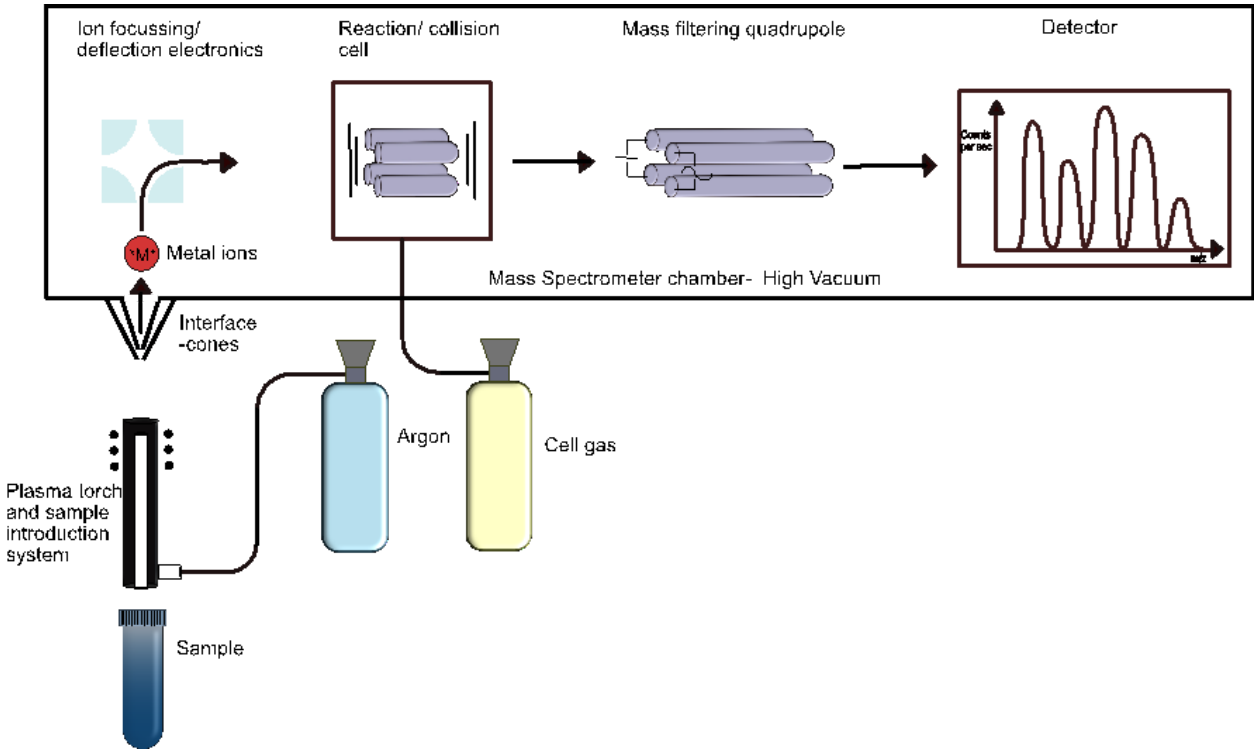

Figure 5.1. A simplified schematic of the operations of inductively coupled plasma mass spectrometry.

Optimisation. Before any samples can be measured the instrument should be optimised to check that the following criteria are met with a certified tuning solution (varies between manufacturer):

1. Torch aligned to maximum sensitivity.
2. Nebuliser gas optimised for the highest sensitivity, but to a rate that oxide production is at an adequate rate. Indium is often used as a proxy element for determining the maximum sensitivity and cerium for oxide production rate. Cerium's most abundant isotope has a mass of 140 AMU, so its oxide forms at AMU 156. By measuring both masses the oxide formation rate by the ratio of 156/140 can be determined and should be <0.03 for optimum performance.
3. Tuned deflection and focusing voltages for optimum ion transfer through the mass spectrometer.
4. Adequate stability checked from the measurement of at least 5 replicates from the tuning standard. Normally the relative standard deviation from the five measurements should be less than 3%.

S5.4 Procedure

Calibration. ICP-MS is not an absolute quantitative analytical technique, therefore it requires calibration prior to use. As previously mentioned above ICP-MS is a type of mass spectrometry that provides linear working ranges that are greater than nine orders of magnitude. Therefore, linear regression calibrations are an ideal approach to convert signals from the detector into concentrations in the samples. Calibrant solutions ($n \geq 5$) should be prepared from NIST certified standards (e.g., Merck Certipur or Spex Certiprep) and diluted to form a range of concentrations that encompass the likely concentrations within the sample working solutions. Adequate linear regression lines drawn after the calibration should achieve correlation coefficients >0.9995.

Internal standards. Plasma suppression/ enhancements often occur during analysis by ICP-MS. Such measurement artefacts are caused by differences in the sample matrix and can be a source of error if it is not corrected. One way to mitigate this is to 'matrix-match' the blanks and standards to the samples (often known as standard addition). This methodology works adequately when the matrix within a sample set is well defined and consistent (e.g., when measuring sea waters), although in reality this is often not the case, where sample sets may contain varying matrix compositions. Instead, internal standards are often used (note this can also be adopted to the standard addition approach too).

Internal standards are elements that are doped into all of the samples, blanks and standards at the same concentrations. These elements should not be present in the samples and should be easily detectable by the ICP-MS.

The following metals are frequently used as internal standards in ICP-MS: Indium, rhodium, iridium and rhenium. These four elements are generally found in ultra-trace or negligible concentrations in many environments/ applications and are also very sensitive by this technique. This series of elements also comprise different first ionisation energies (energy required to relinquish a valent electron and become an M+ ion), with indium imparting the lowest value and iridium the highest: therefore, providing pairings based upon the element's first ionisation energy and mass. For example, rhodium has a similar first ionisation energy to many of the first-row transition elements. As it is also similar in mass it will be an ideal choice as an internal standard for these elements.

Once doped into all of the solutions to be measured in the analytical run the instrument software will allow you to assign an element as the internal standard. Then any changes that may occur to the plasma chemistry during the analytical run will be constrained by corrections to the signal obtained in the nearest blank.

As previously highlighted it is important to ensure that the total dissolved solids of the samples are within the acceptable range for ICP-MS analysis (i.e., less than 0.2%) to ensure that any internal standard corrections are minimal. Generally, suppression/ enhancement normalisations by the internal standards should be limited to ±25%.

S5.5 Results presentation

The results of ICP-MS are usually presented as mass spectrum which is a plot of intensity vs. the mass-to-charge ratio. The instrument software can also adapt this layout to present concentrations per sample, after converting counts per second data into concentrations, providing blank subtractions and correcting for internal standards.

S5.6 Advantages and disadvantages

Analyte sensitivity is one of the main advantages of this technique, where many instruments are able to detect some heavy metal elements below pg g^{-1} concentrations. In order to achieve such low detection performance, the mass spectrometer firstly operates at a high vacuum, in order to maximise transmission along the flight tube. Coupling the high voltage electronics and the high energy inductively-coupled plasma – ICP-MS succeeds as being the most sensitive inorganic analytical technique, where it is able to operate over nine orders of magnitude. Therefore, this enables the instrument to determine concentrations accurately and precisely for a sample set that may contain many elements distributed over wide concentration ranges.

However, a noticeable limitation in ICP-MS is its ability to tolerate samples containing high total dissolved solids (TDS). At the interface of the ICP-MS the instrument contains a set of cones that are used to separate unwanted sample material away from the ion transfer beam. When TDS concentrations exceed 0.2% sample deposition at the interface region occurs

excessively, which begins to negatively impact on the instrument performance through drift, contamination and space-charge effects (Barros et al., 2020). This TDS threshold is much lower than ICP-OES, so it is important that considerations are made and that samples are adequately diluted prior to measurement.

S5.7 Quality Assurance

Quality control standards are vital elements of an analytical run. Not only do they verify the calibration of the instrument, but they also provide an important measure for uncertainty propagation. Standards prepared from a different source to those used to prepare the calibration standards are ideal to verify the validity of the calibration. Simply preparing one standard within the range of the calibration is sufficient to determine this.

In order to calculate the uncertainties from the preparation and analytical method, a certified reference material (CRM) should also be measured. Any type of material can be purchased as a CRM from manufacturers such as NIST and LGC Standards. Such CRM's will have an available certificate of analysis, which lists the certified components. Many present data on trace element concentrations and generally a wide range of elements are certified. A suitable CRM should be digested and measured with the samples and the results determined in a similar fashion to the other samples within the set. Data on the analytical precision can be determined from the relative standard deviation from a series of replicates ($n \geq 5$) and the accuracy calculated by comparing the mean value of the replicates to the certified concentration.

SOP 6 – Powder X-ray diffraction spectrometry (PXRD)

S6.1 Scope and field of the application

This SOP describes the method for qualitative analysis of the bulk mineralogy of alkaline solid materials using powder X-ray diffraction (PXRD). Quantitative XRD analysis is also possible and is covered in Box 6.1. XRD is especially useful for identification of fine-grained materials such as mine tailings and weathering products which have crystalline structures, such as calcite, even when present in small quantities. However, some alkaline materials such as blast furnace slag can contain considerable fractions of non-crystalline material (e.g., glasses or gels) which will not diffract X-rays in a consistent pattern, potentially complicating data interpretation. PXRD can also be used to determine the crystal size via the Scherer equation (Patterson, 1939). Information on the elemental composition and geological or material history of the sample is useful prior to analysis for determining between multiple minerals that appear identical or very similar in an X-ray diffractogram. For samples containing substantial quantities of Fe, Co or Ni, an XRD instrument with a cobalt radiation source is preferred to copper in order to reduce the impact of background interference (Mos et al., 2018). Powder XRD is primarily a lab-based technique, although field based XRD instruments have been used previously to identify the formation of carbonate minerals in mine wastes (Turvey et al., 2017). For analysis of clay-rich samples, specific sample preparation techniques are required, examples of which are given by the USGS (U.S. Geological Survey, report by Poppe et al. (2001)).

S6.2 Principle

Many solid materials are crystalline, meaning they have a regular and repeating arrangement of atoms determined by their crystal structure and elemental composition. When X-rays of a given specific wavelength λ, are fired at a crystalline solid, some of them will hit the individual atoms within the crystal and diffract. Most of the time these diffracted X-ray will destructively interfere, and no obvious X-ray signal will be produced. However, at specific angles between the incident X-rays and the samples θ, the X-rays will constructively interfere according to Bragg's law (Figure 6.1) and will produce an X-ray signal that can be detected by an X-ray detector.

Bragg's Law is satisfied when $2d(\sin\theta) = n\lambda$, where λ is the X-ray wavelength, n is an integer, d is the distance between planes of atoms within the crystal structure and θ is the angle between the incident X-ray and the plane of the crystal surface.

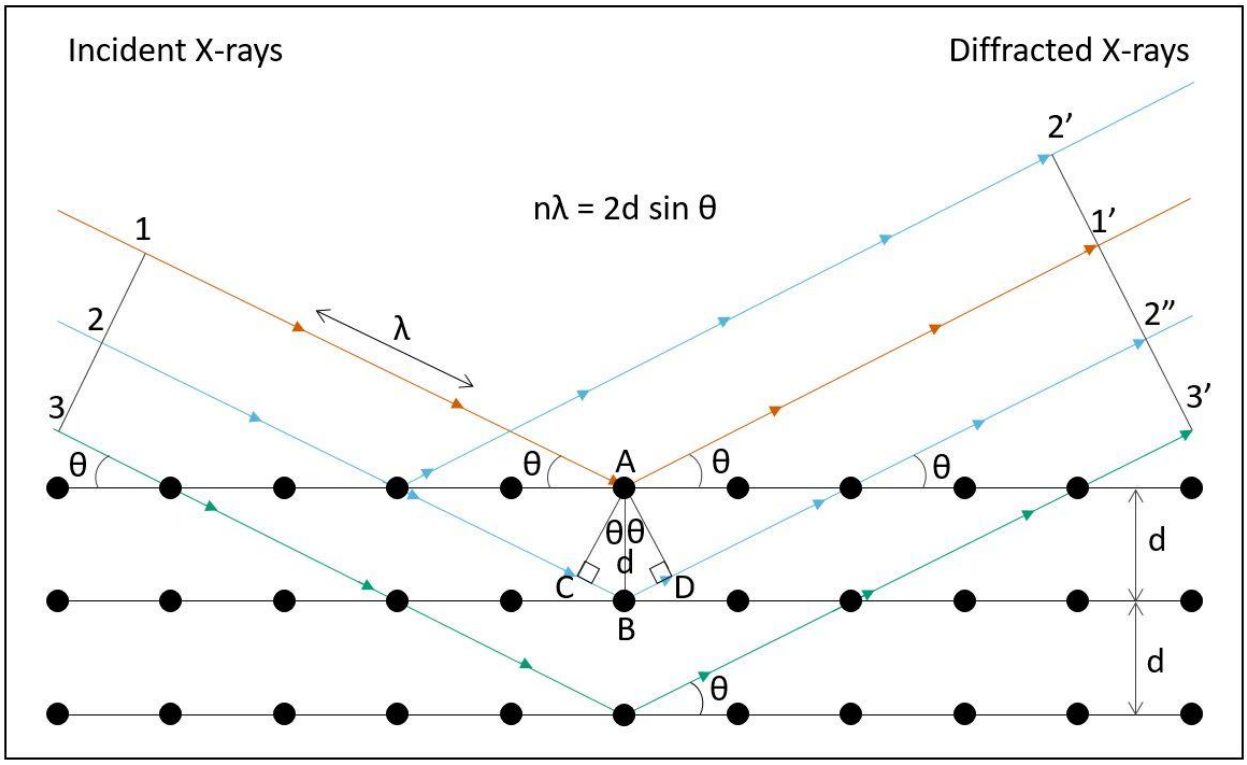

Figure 6.1. Diagram showing how X-rays interact with a crystalline solid and then diffract representing 'Bragg's Law'.

By scanning over a wide array of different angles an XRD instrument can determine when a material is undergoing destructive interference (background signal) and when it is undergoing constructive interference (XRD peaks), this information is recorded as a diffractogram (Figure 6.3). Each material will have a unique pattern of XRD peaks, known as its diffraction pattern, determined by its crystal structure and elemental composition, as they will dictate interatomic distances within the crystal structure. This means that even crystalline materials with the same composition can have different diffraction patterns due to their different atomic arrangements, e.g., quartz and cristobalite are both composed of SiO_2 but have unique diffraction patterns (Milonjić et al., 2007). Amorphous or poorly crystalline materials lack a periodic array with long-range order, so they will not produce an X-ray pattern with characteristic sharp peaks.

An XRD pattern is usually interpreted with the aid of pattern matching software such as DIFFRAC.EVA or HighScore which compare the pattern with a reference database such as the Crystallography Open Database (COD) or Powder Diffraction File (PDF). Search and match software helps the analyst determine what phases are present in a sample by quickly comparing the *d* spacing of the unknown sample to those of known materials in the PDF. The

angle, shape and height of an XRD peak all provide useful information about the crystalline components in a material.

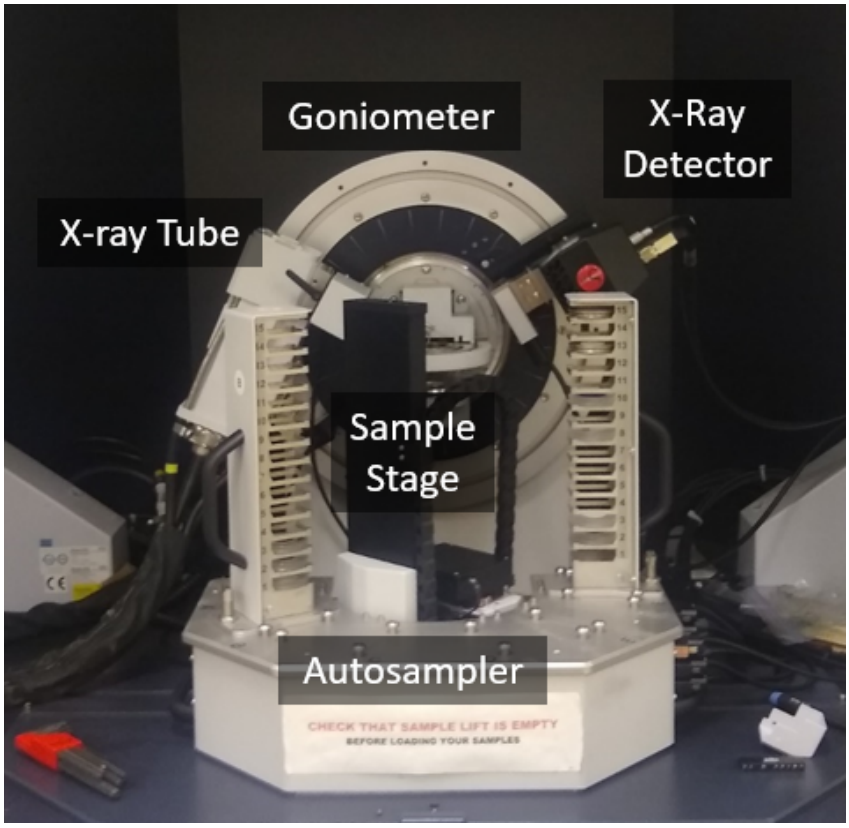

Figure 6.2. The interior of a typical A-ray diffractometer showing the X-ray source, goniometer, sample stage, detector and autosampler.

S6.3 Instrumentation

Typical laboratory-based X-ray diffraction instruments are composed of four main components: the X-ray tube, a sample holder, goniometer and a detector (see Figure 6.2). In the X-ray tube a filament is heated producing electrons which are then accelerated by an applied voltage. The electrons bombard a target composed of a specific metal target (Cu, Fe, Cr, Mo or Co) producing characteristic X-ray radiation. The most common X-ray tubes in laboratory settings are Co and Cu. Two intense peaks are observed in X-ray spectrum when these elements are bombarded – K_α and K_β. The K_α X-rays can be divided into $K_{\alpha 1}$ and $K_{\alpha 2}$ radiation, and the latter is removed by a crystal monochromator (which reduces intensity) or by using software correction. The powder sample is then illuminated with these monochromatic X-rays. The X-ray tube and the detector move on a goniometer in a synchronised rotational motion in a vertical plane orthogonal to the surface of the sample to maintain the same sample penetration over the scan range. In some diffractometers the source remains stationary, and the sample mount is tilted. The intensity of the scattered

radiation is recorded by the detector and converted to a count rate which is processed by a computer. The emitted signal is recorded and graphed, and software enables the peaks to be matched with those in a powder diffraction database.

S6.4 Sample preparation

In powder XRD, the aim of sample preparation is to reduce the size of crystallites and ensure they are randomly oriented, to maximise the number of grains contributing to the diffraction pattern and ensure good counting statistics. Reducing the grain size of crystallites can be achieved by a number of methods, micronisation using a micronising mill in ethanol is the most preferred method, if that option is not available grinding the sample into a fine powder (~10 µm) using a corundum pestle and mortar is acceptable. High energy methods of grinding, e.g., ball-milling, can lead to the destruction of existing phases and creation of amorphous phases and so should be avoided.

Once the sample has been reduced in particle size, it needs to be mounted in such a way to ensure randomly oriented crystallites. There are a variety of different sample holders produced by various manufacturers. The best sample holders for ensuring randomly oriented crystallites are back loading or side loading cavity mounts. When loading such mounts the entire well should be filled, lightly packed (so not too deform the sample or induce preferred orientation), and made flush with the outer disc, while loading against a rough surface such as frosted glass or carborundum sandpaper to ensure the surface crystallites are randomly oriented (Turvey et al., 2018b; Wilson et al., 2006). If such mounts are not available or for smaller samples then the next best alternative are front loading disk mounts or smear mounts using a zero-background plate, where the sample is adhered to a flat surface using iso-propyl alcohol as the medium. In some cases, alcohols may react with some alkaline materials such as $NaFeO_2$ (Campbell, 2019), and petroleum jelly may be used as an alternative adherent. For quantitative XRD on clays, alternative means of sample preparation may be needed such as spray drying (see Box 6.1).

S6.5 Calibration & Quality Assurance

XRD instruments should be calibrated whenever an X-ray tube is replaced and whenever the instrument's geometry is changed (for example if a high temperature analysis stage is added or removed), it should also be re-calibrated regularly (every ~1–3 months) even if no major changes to the instrument have occurred.

For the calibration a known crystal standard is required (typical crystal standards include LaB_6, SiO_2, etc.) with documentation from either NIST or the diffractometer manufacturer (Cline et al., 2013). The documentation is essential as it is needed to check the results of the instrument including peak positions, peak shapes and peak intensities against the expected values.

S6.6 Procedure

All XRD instruments have safety interlocks with LEDs to indicate whether the X-ray shutter is open or closed. Assuming the X-ray shutter is closed and safe, the protective screens or doors can be opened, and the sample disc is secured into position. The screen doors are closed and locked to protect the user. Proprietary software is used to select the scan parameters: scan angle 2θ range – typically 5–70°; step size – typically 0.5°; the step time – typically 1 s. Usually, pre-made protocols with set parameters are available. When the scan commences the LED light should light up indicating the instrument is now irradiating the sample with X-rays. Once the scan is complete, the sample holder should be removed from the machine, the powder sample safely disposed of, or stored away, and the sample holder cleaned with ethanol, and returned to the lab. Ensure the XRD diffraction pattern is saved ready for peak matching analysis.

S6.7 Data analysis and presentation

Diffraction patterns are matched using peak-matching software. This process is more efficient when the elemental composition of the sample and likely mineral phases are known. Using appropriate chemical and other database filters is important to eliminate suggested phases that have similar X-ray patterns to what is seen in the pattern but will not be found in the sample (e.g., you want to remove *explosives* and *pharmaceuticals* as potential suggestions when analysing geological samples). When presenting data, it is better to display multiple scans on the same plot ('diffractogram') such that common peaks can be labelled without repetition (see Figure 6.3). Peaks are usually labelled with a letter, e.g., C for calcite, or a symbol, with a corresponding key. Ideally the intensity scale should be the same for each sample but if one sample has a particularly weak signal it may need to be rescaled for the purposes of presentation. All peaks should ideally be assigned to a particular phase. If any peaks remain unidentified, they should be labelled as such. Although all peaks should be identified, not all peaks need to be labelled in the final presentation if it will interfere with overall readability and presentation of the data. Depending on the analyst's intention, certain peaks may need to be highlighted, e.g., newly forming calcite, to draw attention to the important mineral reactants and products, while other peaks can be left unlabelled to simplify the image. The exact patterns that were used to match the data (either from the PDF or another database) should be included in the text of the document. Ideally, raw data and matched peaks should be made available in supplementary information or appendices for the purpose of data transparency. Intensity (y axis) can be reported as the raw X-ray counts, counts per second, or converted to relative intensity (%). The x axis can be presented as 2θ angle, θ angle or as d-spacing.

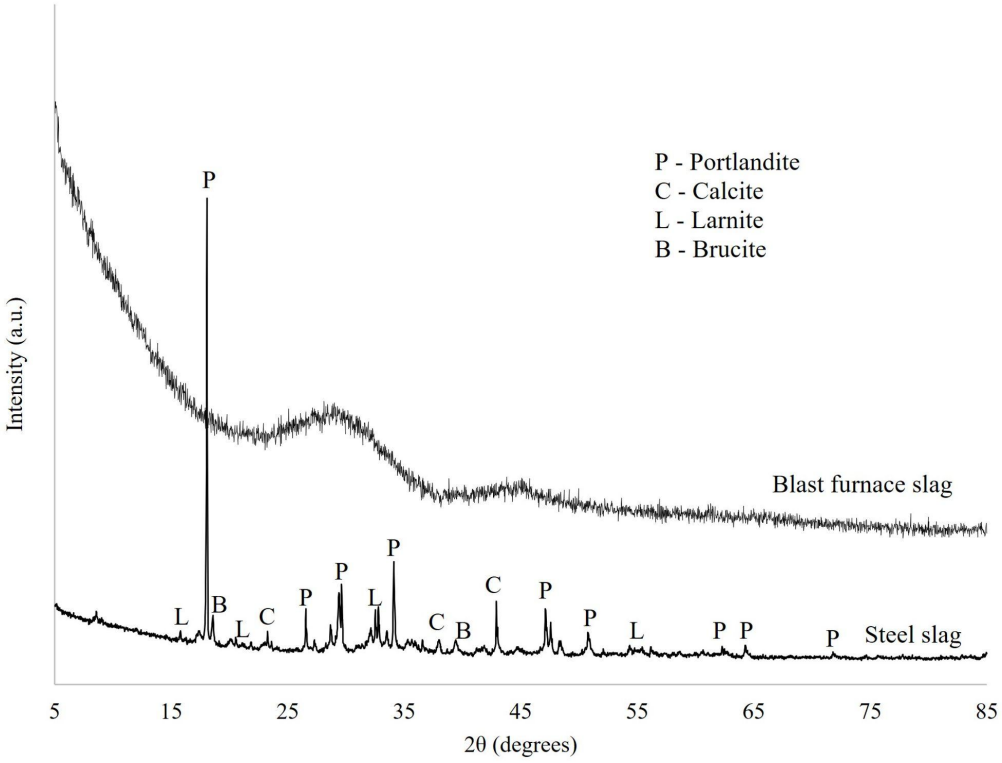

Figure 6.3. X-ray diffractogram for steel slag and blast furnace slag sourced from Turkey. Peaks related to the minerals portlandite, calcite, larnite and brucite are seen in the data for the steel slag. The data for the blast furnace slag is typical of amorphous materials (no long-range crystallinity).

S6.8 Advantages and disadvantages

Powder XRD has many advantages; it is rapid (<1 hr), and non-destructive with little sample preparation required than other methods of mineralogical identification like modal mineralogy, EDX and QEMSCAN. Qualitative data interpretation is reasonably straightforward and unambiguous. XRD requires a fairly large sample (~2 g) although there are methods for obtaining quality data for mg amounts (see sample preparation above).

However, there are also some issues with XRD. Quantitative analysis (see Box 6.1) is significantly more complex in terms of the time and expertise required to produce good results. It also has a relatively high detection limit of 0.1 wt. %, even under ideal circumstances (León-Reina et al., 2016). XRD is also a predominantly lab-based technique and samples must be taken from the field to the lab for analysis; however portable X-ray diffractometers are starting to appear on the market.

Box 6.1 – Quantitative X-ray diffraction

In addition to qualitative analysis, crystalline materials can also be analysed quantitatively by XRD. Quantitative XRD is possible because the peak intensities of a given mineral in the diffractogram are proportional to the weight percent of that particular mineral in the sample. However, peak intensities are also a function of the mineral's absorption coefficient, particle size, degree of crystallinity and the preferred orientation of the sample (Alexander and Klug, 1948; Chung, 1974; Rietveld, 1969), this means that compared to qualitative analysis quantitative XRD requires more specialised expertise to produce accurate results (Omotoso et al., 2006).

There are a variety of quantitative XRD methods including the internal standard method (Alexander and Klug, 1948), reference intensity ratio method (Chung, 1974) and the Rietveld method (Rietveld, 1969). Of these the Rietveld method is the most popular in modern XRD analysis, it uses least squares refinement to compare a hypothetical diffractogram to the diffractogram being analysed and alters various parameters (including mineral abundance) to produce a diffractogram that is as close to the experimental data as possible.

The Rietveld method relies on good counting statistics and data quality for the method to be successful. Therefore, successful quantification of minerals in a sample depends greatly on the method of sample preparation, back loading against sandpaper or frosted glass has been shown to be effective for producing good quality data (Turvey et al., 2018b; Wilson et al., 2006). Spray drying is an alternative method to loading against a roughened surface method to achieve completely random orientation of crystallites, however it requires specific sample preparation equipment that may not be present in all laboratories (Hillier, 1999).

When presenting quantitative XRD results a simple table of values is often used with each sample and its various mineral abundances being presented. In addition, when using the Rietveld method it is best practice to report the weighted pattern residual (R_{wp}), kai squared (χ^2), weighted Durbin-Watson statistic (d), and estimated standard deviation for each analysis. These values are generated by the Rietveld analysis software.

Quantitative XRD analysis is possible even in samples that contain amorphous material, however it requires advanced analytical techniques such as including internal standards (Wilson et al., 2006) or the use of the PONKCS method (Scarlett and Madsen, 2006). Such analyses also require a higher degree of training and expertise to produce results that can be relied upon (Omotoso et al., 2006).

SOP 7 – Raman spectroscopy

S7.1 Scope and field of application

Raman spectroscopy uses the interaction of light with matter to characterise a material in the same way as FTIR. The main difference between both techniques is that Raman spectroscopy is based on a light scattering process, and IR spectroscopy on absorption of light. Both methods have specific spectrum diagnostic of distinct vibrations of a molecule and allow the characterisation of a substance. Yet, Raman spectroscopy can provide information about lower frequency modes and thus insight into crystal lattice structure. Raman spectroscopy is therefore relevant to follow crystallisation processes and useful in determining both reaction mechanisms and kinetics.

Identification of carbonate minerals. Raman spectroscopy is a useful technique for carbonate identification. The carbonate bands in the mid-infrared region are distinguishable from other minerals by their distinct positions (Kim et al., 2021). Mineralogical and geochemical research has been pursued for a long time with Raman analysis of carbonates, but recent portable devices have allowed the exploration of new applications.

The R-3c group corresponds to the crystallisation of rhombohedral carbonate including calcite, magnesite, siderite, and rhodochrosite whereas dolomite and ankerite have different symmetry given the substitutions by divalent atoms such as Ca, Mg, Fe, and Mn in the crystal structure. Recent studies have shown the efficiency of Raman's spectroscopy to identify carbonates, but this was restricted to a few groups of solid solutions using laboratory devices.

The D3d group represents the calcite structure through six Raman active modes in a Raman spectrum (Figure 7.1). In the calcite Raman spectrum, the peaks associated to translational (T) and librational (L) lattice mode from the external vibration of the CO_3 group are at 154 and 279 cm^{-1}. The out-of-plane bending (v4) and most intense stretching (v1) internal vibration modes are respectively corresponding to the positions 710 and 1083 cm^{-1} (Figure 7.1). These two peaks range from 710 to 738 cm^{-1} (m4) and 1082 to 1100 cm^{-1}.

S7.2 Principle

Raman spectroscopy's principle is based on the Rayleigh scattering process whereby most of the photons are dispersed or scattered at the same energy as the incident photons when light interacts with molecules in a gas, liquid, or solid phase. Among these photos, a small quantity (1 photon in 10 million) will scatter at a different frequency than the incident photon through a process named the Raman effect. The Raman shift corresponds to the

difference between the energy of the incident photon and the energy of the scattered photon.

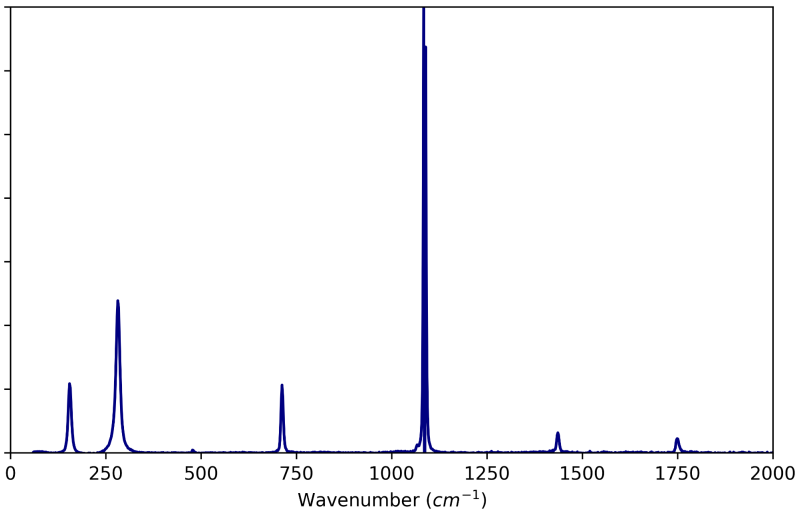

Figure 7.1. Raman spectrum of synthetic analytical grade calcium carbonate. This spectrum shows intensities at 281, 712, and 1086 cm^{-1}, which are characteristic of calcite. Reprinted with permission from Mikkelsen et al. (1999). Copyright 2023 American Chemical Society.

S7.3 Instrumentation

One of the main components of a Raman spectrometer is the laser which infers an excitation source resulting in the Raman scattering (Figure 7.2). The most common wavelengths of 532 nm, 785 nm, 830 nm and 1064 nm are employed by solid state lasers in modern Raman instruments. Fibre optic cables transmit and collect the laser energy to and from the sample respectively. Rayleigh and anti-Stokes scattering are eliminated by an edge filter. The light is captured by a CCD detector to obtain the Raman spectrum. A molecular video including information about kinetics and mechanisms during a reaction can be exploited from a spectrum acquired consistently over the course of an experiment.

S7.4 Procedure

Accurate examination of solid samples can be undertaken with the same setting. A sample holding compartment is needed where the laser beam is deflected through a microscope. The sample itself is pressed into a tiny sample cup that can be easily fitted into the object holder of the microscope. In addition to the adjustment procedure described previously, the solid sample is brought into focus by using a pilot lamp in the visible spectrum. Once in focus, the laser beam is routed through the optical system of the microscope.

Figure 7.2. Photo depicting a Renishaw InVia Raman spectrometer at Heriot-Watt University.

S7.5 Quality assurance

Multiple trials should be made by using several layers of 10% absorbers into the light path prior to the microscope to prevent vaporisation of the sample and coating of the microscope's objective lens (due to the intense laser light).

SOP 8 – Fourier transform infrared spectroscopy (FTIR)

S8.1 Scope and field of application

Fourier transform infrared (FTIR) spectroscopy, also known as FTIR analysis, is an analytical technique used to identify organic, polymeric, and inorganic materials (such as carbonate minerals). FTIR analysis uses infrared emissions to scan samples and observe chemical properties.

S8.2 Principle

Infrared radiations of about 10,000 to 100 cm^{-1} are sent by the FTIR device through a sample and some radiations are either absorbed or transmitted. The sample molecules convert the absorbed radiation into rotational and/or vibrational energy. The detector produces a spectrum as a result ranging from 4,000 cm^{-1} to 400 cm^{-1}. Each molecule or chemical structure will be associated with a specific spectrum. Therefore, FTIR analysis constitutes a very efficient instrument for chemical identification.

S8.3 Instrumentation

Typically for FTIR in the field, an instrument such as the Agilent 4300 Handheld Portable FTIR is used for identification of the material on the field and the peaks might be analysed and identified by the MicroLab FTIR Agilent Software. This innovative approach minimises the risk of alteration of transient mineral phases such as ikaite ($CaCO_3.6H_2O$) after sampling for instance. Alternatively, a PerkinElmer Frontier FTIR might be used for characterisation of the material at the laboratory (Figure 8.1).

Figure 8.1. Photo depicting a PerkinElmer FTIR spectrometer at Heriot-Watt University.

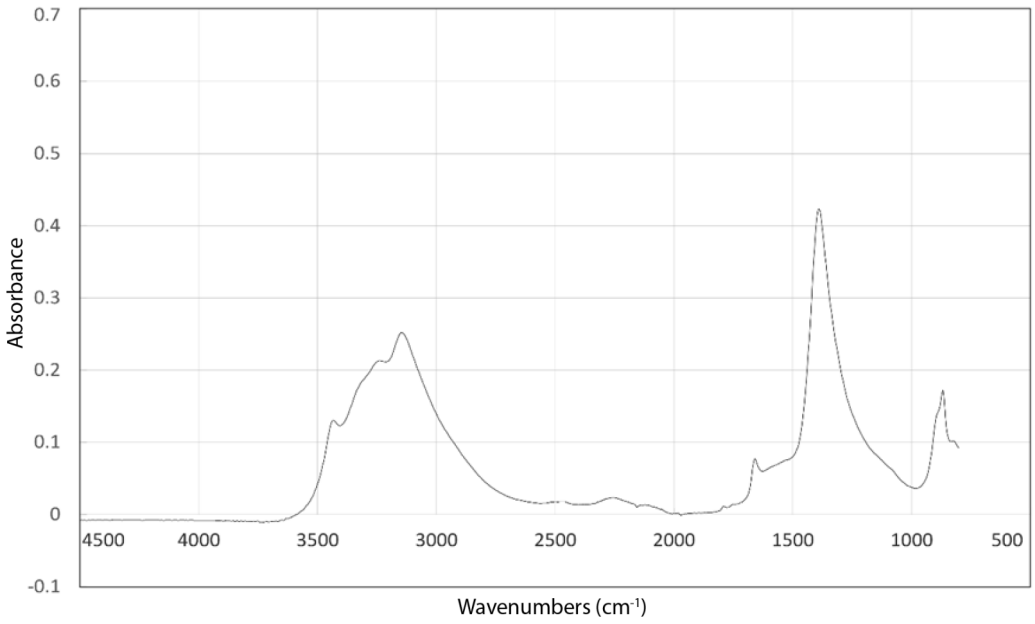

Figure 8.2. FTIR spectrum of a sample of the hydrated calcium carbonate known as ikaite.

S8.4 Procedure

Before identification by attenuated total reflectance Fourier transform infrared spectroscopy (ATR-FTIR), the sample must be air-dried on site and the measurement surface cleaned with ethanol (10 mL g^{-1} of sample) using wipes. Initial scans check for interferences by water molecules (peak absorption at 3182 cm^{-1}) should be undertaken which helps verify that the sample was dried.

S8.5 Identification of carbonate minerals

The FTIR spectrum of ikaite shows absorptions at 718, 1485, and 3182 cm^{-1} (Figure 8.2). The latter peak is typical of O-H stretching and indicates the presence of abundant formation water. Absorption at 1485 cm^{-1} reflects asymmetric CO3 stretching. Absorption at 718 cm^{-1} is symmetric CO3 deformation, which is correct for ikaite but is not reported from amorphous calcium carbonate (ACC) and is present at lower wavenumber in monohydrocalcite.

The infrared spectrum measured from the calcite reference is recognisable by four internal vibration modes of CO_3^{2-} at 1396 cm^{-1} (asymmetric stretching, v3), 1089 cm^{-1} (symmetric stretching, v1), 872 cm^{-1} (asymmetric bending, v2) and 713 cm^{-1} (symmetric bending, v4) (Figure 8.3). The two bending bands v2 and v4 are narrow and sharp. The v3 band is identifiable by a strong and very broad feature in the infrared spectrum and the intensity of the v1 band is very weak.

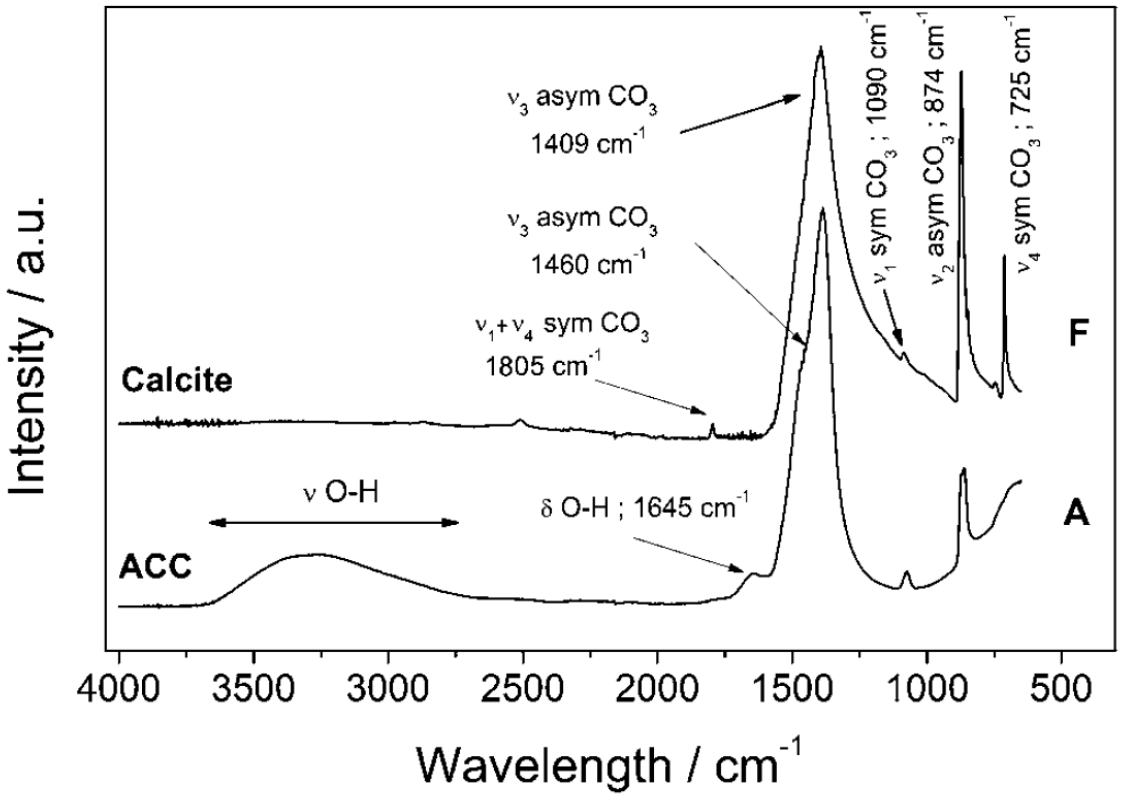

Figure. 8.3. FTIR spectra of calcite and ACC. Reproduced from Rodriguez-Blanco et al. (2011) with permission from the Royal Society of Chemistry.

S8.6 Quality assurance

It is recommended to perform the FTIR measurement at least 10 times on the same sample to increase the reliability, accuracy, and precision of the results. The average result is obtained by calculating the mean, the standard deviation, and the coefficient of variation, also known as relative standard deviation, which is defined as the ratio of the standard deviation to the mean. It is important to note that there is a peak shift between devices due to different factory calibrations. Therefore, a validation against known standards is needed.

SOP 9 – Volumetric calcimetry

S9.1 Scope and field of the application

In this SOP a quantitative method for determination of the total carbonate content (wt. %) of mineral samples by volumetric calcimetry is provided (based on British Standards Institution (1995)). Carbonate minerals in the sample are digested using acid. The volume of CO_2 released is then measured using a calcimeter, at constant temperature and pressure. A standard material (e.g. pure $CaCO_3$) is also analysed using procedure as a standard. The volume change obtained with the standard can then be used to determine the volume of carbonates in the sample. The volume of CO_2 released is related to the mass of carbonates digested.

S9.2 Principle

Carbonates within samples are reacted with an excess of acid (commonly HCl) which produces CO_2 gas (Eq. 9.1).

$$XCO_{3(s)} + 2HCl_{(l)} \rightarrow XCl_{2(aq)} + H_2O_{(l)} + CO_{2(g)} \quad \text{Eq. 9.1}$$

Where X is Ca and/or Mg. The CO_2 gas released is measured in a closed system by measuring the gas's volume (volumetric calcimetry), or the pressure change (manocalcimetry) from which the mass (wt. %) of carbonate minerals in the sample can be determined using a standard material as reference.

S9.3 Instrumentation

A range of instrument designs can be used for volumetric calcimetry including Chittick, Eijkelkamp, Scheibler and Bernard. A volumetric calcimeter consists of a glass reaction flask (recommended 250 mL), a three-way stop cock, burette, levelling bulb, and tubing. Other apparatus includes stirring plate and stirrer, electronic balance with high weighing precision, pipette or volumetric dispenser. Reagents include HCl (~4 mol L^{-1}), distilled (or deionized) water, analytical grade (>98%) $CaCO_3$.

S9.4 Sample preparation

Samples should be pre-dried at 105°C to constant mass, or the moisture content of a sub-sample should be determined and used to adjust for the determination of carbonate content. Samples should be finely ground and passed through a 10 µm mesh (samples are ground to enable fast and complete reaction with the acid). Acid digestion methods, such as a wet-oxidation method (Bao, 2000; Li et al., 2020; Walkley and Black, 1934) employ oxidation of organic carbon into CO_2 under a strong oxidant ($K_2Cr_2O_7$) in the presence of H_2SO_4.

S9.5 Calibration

The instrument is calibrated by measuring the volume of CO_2 evolved by acid digestion of several different masses of finely ground, high purity calcium carbonate (mesh size <10 µm). Carbonate bearing reference materials can be used to check the accuracy of the instrument, e.g., WEPAL reference material ISE 930 2004:1 (Clay soil, Ivory Coast) and NCS DC 73307 (Stream Sediment, Beijing, China).

S9.6 Procedure

Preparation. If an approximation of the sample's carbonate content is unknown, it can be predicted by placing ~2.5 g of sample on a watch glass and adding a few drops of acid (~1 mL), the intensity of effervescence of the sample can then be used as an indication as to the quantities of sample that should be used in the procedure. If the sample effervesces intensely, less of the sample will need to be tested (see Table 9.1).

Table 9.1. Estimation of sample quantity based on effervescence time and intensity.

Intensity of effervescence	Carbonate content (g kg^{-1})	Estimated mass of sample to be used (g)
None or limited	<20	10
Clear, but for a short time	20-80	5
Strong, for a long time	80-160	2.5
Very strong, for a long time	>160	<1

Blank determination. A blank determination can aid in the detection of system leaks and determine a zero reference. This is performed with the same method as the calibration with only water (no acid or $CaCO_3$).

Sample analysis. Once the appropriate amount of sample is determined, it is then weighed out (to 4 d.p.) into the reaction vessel (e.g., Erlenmeyer flask) which has been rinsed 4 times with deionised water. 20 mL of deionised water is also added to the flask containing the sample. 7 mL of 4 M HCl is measured into a flat-bottomed glass vial and placed into the flask containing the sample using tweezers or tongs, taking extra care and attention to not spill any acid on the sample prior to attaching the Erlenmeyer flask to the calcimeter apparatus. A wet bung rinsed with deionised water should be firmly inserted into the opening of the reaction vessel to ensure a gas tight seal. Once the apparatus is closed with no leaks in the system, a reading on the burette can be taken, this can be noted down as volume 1. The Erlenmeyer flask can be gently tipped until the acid is completely poured from the test tube onto the sample, the flask can then be swirled to assist the reaction. Shake the flask

occasionally until the reading on the burette remains stable, do not take readings after 1 hour. The volume can be read off the burette as volume 2.

Carbonate content is usually reported as wt. %. Triplicate analyses should be performed on each sample, the results averaged, with the error reported as the standard deviation.

S9.7 Calculation and expression of the results

The carbonate content $w(CaCO_3)$ in g kg^{-1} of the oven-dried material is calculated using Eq. 9.2.

$$w(CaCO_3) = 1000 * \frac{m_2(V_1 - V_3)}{m_1(V_2 - V_3)} * \frac{100 = w(H_2O)}{100} \quad \text{Eq. 9.2}$$

Where m_1 is the mass (g), of the test portion, m_2 is the mean mass (g) of the calcium carbonate standards, V_1 is the volume (mL) of carbon dioxide produced by reaction of the test portion, V_2 is the mean volume (mL) of carbon dioxide produced by the calcium carbonate standards, V_3 is the volume change (mL) in the blank determinations (this value can be negative), and $w(H_2O)$ is the water content, expressed as a percentage by mass, of the dried sample, determined according to (British Standards Institution, 1995).

S9.8 Advantages and disadvantages

Volumetric calcimetry is a simple and inexpensive method. It only provides only a measure of the total carbonate content and cannot easily distinguish between different types of carbonates. This method is destructive and can cause the decomposition of other minerals such as sulphates, releasing SO_2, or H_2S or H_2, causing overestimation of the total carbonate content. Further, another key source of uncertainty is from temperature and pressure fluctuations.

S9.9 Quality assurance

Standardisation using a known concentration of HCl and a certified standard. A blank determination should be performed as described above to correct for any background gaseous contribution. The water reservoir should be regularly saturated with CO_2, which limits CO_2 transfer during measurements. Running replicate analyses on the same solid sample or different aliquots of the same sample can help assess the precision of the method and identify potential outliers or errors in the data. Solid samples should be thoroughly homogenised to ensure that they accurately represent the entire mass. Using an appropriate amount of solid sample is crucial for accurate results. Too little sample might lead to lower precision, while too much sample could result in excessive CO_2 production, leading to errors in measurement.

SOP 10 – Thermogravimetric analysis (TGA)

S10.1 Scope and field of the application

This SOP describes the general use of thermogravimetric analysis (TGA) for analysing thermal behaviour of materials as well as multiple methods for determining specific mineral contents using TGA. These methods include determining carbonate content of alkaline materials (Campbell, 2019) and determining brucite ($Mg(OH)_2$) content of alkaline materials (Turvey et al., 2022). In some cases, TGA can be used to distinguish between different carbonates. And is also suitable for the determination of organic material in a sample (Coats and Redfern, 1963). This SOP also contains information on TGA-MS which is a combined method with mass spectrometry that allows more detailed forms of analysis and differential scanning calorimetry (DSC) which is a similar technique (discussed in Box 10.1).

S10.2 Principle

Thermogravimetric analysis is an analytical method that measures the mass of a material as a function of temperature (and time) as a sample undergoes heating (Coats and Redfern, 1963). The heating causes physical and chemical transformations to occur within the sample which result in mass loss or gain, such as the decomposition reactions that minerals undergo at specific temperature ranges. The mass changes resulting from these reactions can be quantified, and the reaction rates studied. For example TGA can be used to determine the carbonate content of alkaline materials since Mg- and Ca- carbonates decompose during heating, releasing CO_2, with magnesite decomposing between 620–650°C and calcite decomposing between 700–800°C depending on heating rate, and other experimental conditions (Földvári, 2011). As the decomposition reactions occur in a consistent predictable way determined by the stoichiometry of the mineral the mass loss during the reaction can be used to calculate the abundance of the mineral in question.

S10.3 Instrumentation

TGA is conducted on an instrument referred to as a thermogravimetric analyser. The instrument consists of a sample holder (pan) attached to a highly sensitive balance (accurate to +/−0.001 % on some instruments) (see Figure 10.1). A thermocouple (accurate to +/−0.1°C) is positioned ~1 mm above the sample such that the sample temperature can be represented as accurately as possible without touching the material and potentially interfering with mass measurement. Instruments with a temperature range from ambient to 1000°C are typical, and sufficient for the uses described herein. Open top pans, often composed of platinum or a ceramic, are used to hold the sample. The furnace atmosphere is controlled by flowing purge gas which removes evolved gases from the chamber. Gas also flows through the balance mechanism to prevent evolved gases from damaging the balance. The balance purge is typically at least 10 mL min^{-1} higher than the sample purge. This balance gas positive

purge differential prevents evolved gases from entering the balance area. The balance and furnace purge gas flow rate are controlled by mass flow controllers. For the furnace, different gases are usually available including air, N_2, Ar, or CO_2. The balance purge gas is fixed as N_2. With some instruments, the rate of mass loss can be kept constant by temperature control, which is useful for studying reactions which are sensitive to the build-up of evolved gases (Criado et al., 1990). Vacuum TGA can be used but is less commonly found in standard laboratories (Jurczyk et al., 2022). Some instruments can even perform TGA and DSC measurements simultaneously. For more on DSC see Box 10.1.

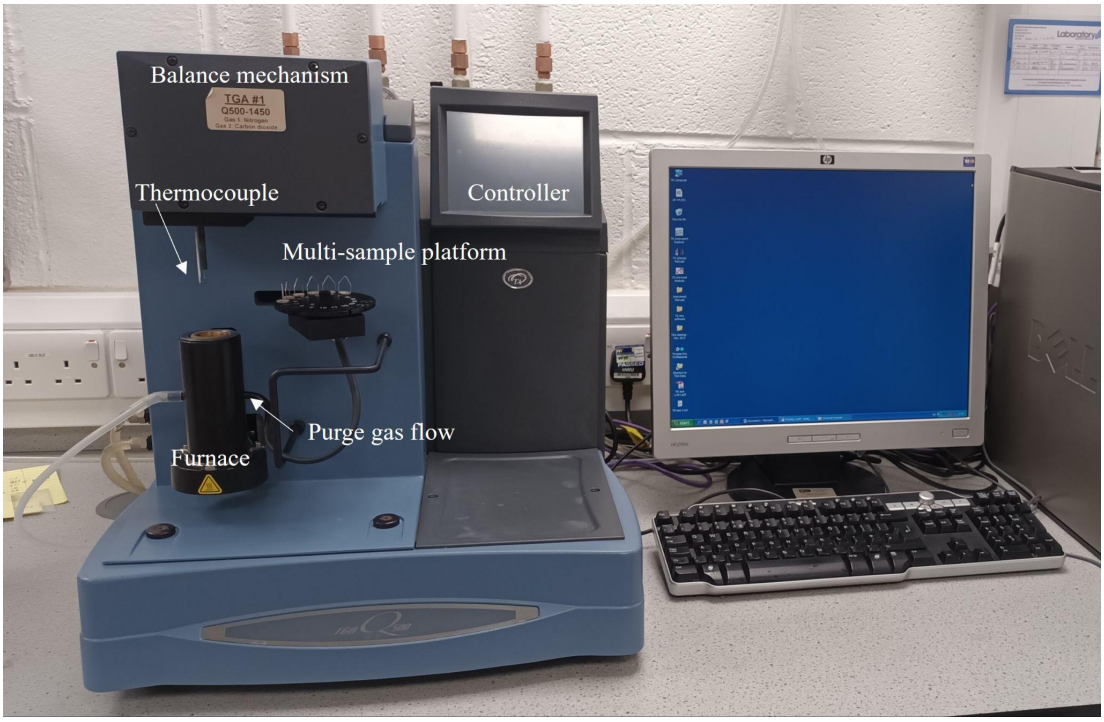

Figure 10.1. Annotated photograph of a TGA instrument.

Box 10.1 – Differential Scanning Calorimetry (DSC)

Differential Scanning Calorimetry (DSC) heat flow is measured as a function of time/temperature to study chemical processes, for example, dehydration and carbonate decomposition, but also physical processes like phase changes, like melting (Kodre et al., 2014). Differential thermal analysis (DTA) is an alternative technique whereby the heat flow is kept constant and temperature difference between the sample and the reference material is recorded. In DSC, the sample and the reference material are kept at near the same temperature, as the temperature increases linearly with time. The reference material has a well-defined heat capacity. The amount of heat that must flow to the sample depends on whether the processes occurring are exothermic or endothermic. DSC is particularly useful when coupled with TGA for additional understanding on carbonate decomposition processes, providing information which is not visible in the TGA signal, such as phase transformations. Figure 10.2 shows the DSC curve for thermal decomposition of hydromagnesite. The peaks at 309°C, 446°C and 554°C, are proposed to be due to the release of hydration shell water, decomposition of the hydroxide group and carbon dioxide loss and finally breakdown of magnesite into MgO and CO_2. The exothermic peak at 518°C is suggested to be due to cubic formation of MgO. Such DSC information can aid in deducing the mechanism of decomposition. If needed, the enthalpy of the transition can be calculated by integrating the area under the curve and using $\Delta H = K.A$ where ΔH is the enthalpy change of the transition, K is the calorimetric constant and A is the area. The constant K is obtained by studying reference materials with known transition enthalpies and is specific to each instrument.

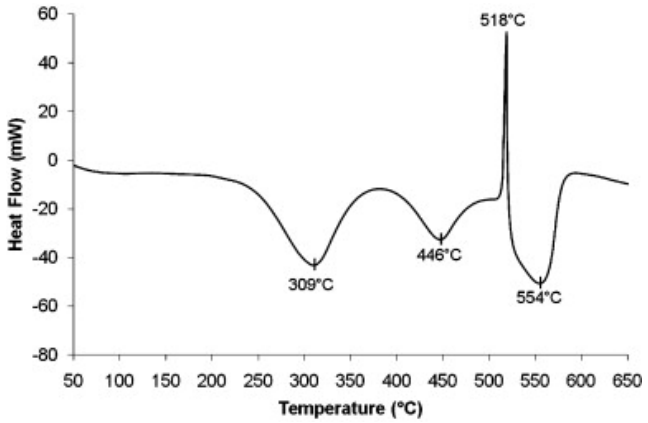

Figure 10.2. Decomposition of hydromagnesite measured by DSC at 20°C min^{-1} in air. Republished with permission from Hollingbery and Hull (2010). Copyright 2023 Elsevier.

S10.4 Calibration

Mass. The TGA balance is calibrated by weighing standard calibration weights of various masses between 1 mg and 1 g. Calibration weights of known mass (to 0.001 mg) are usually

provided by the instrument manufacturer. The calibration should be performed once per month.

Temperature. The thermocouple cannot record the actual sample temperature because touching the sample would interfere with the mass measurement. Temperature calibration largely helps alleviate this issue. Temperature calibration is achieved using materials such as Ni, Fe, CrO_2 or various alloys (traceable reference materials available from ICTAC and NIST) which have a known Curie point (Blaine and Fair, 1983). Curie point materials lose their affinity for magnetism upon heating to a certain temperature, which is observed as a sharp mass gain on the thermogravimetric analyser. The exact temperature calibration method depends on the instrument. Some modern instruments have an internal electromagnetic coil for automated calibration, while others require an electromagnet to be manually positioned beneath or above the furnace. A clean pan is tared, and the first reference material placed into the pan and loaded into the furnace. The magnetic field makes the material seem lighter than it is. The material is heated at a constant heating rate, with inert gas at flow rates as recommended by the instrument manufacturer. When the material reaches its Curie point, it loses its magnetic properties and the mass increases sharply. The temperature of the transition can be obtained by taking the first derivative of the mass loss curve and selecting the temperature of the peak. This temperature and the theoretical Curie point temperature are entered into the system. The system applies the correction to all future data. This process is repeated for another material with a different Curie point. Several Curie reference materials are needed to calibrate the temperature over a wide range. The calibration should be performed at least once per year or after any maintenance on the instrument.

In addition to calibration the furnace should be cleaned on a monthly basis by ramping the temperature to 1000°C (or the maximum temperature of the instrument and heating it for 1 hr open in air).

S10.5 Procedure

General method. Place a clean sample pan into the sample holder (or autosampler depending on instrument), and load into the furnace for taring. Tare the pan, to determine its empty weight and unload. Add the alkaline material sample to the pan. Load the pan containing the sample into the furnace. Set the heating program (equilibrate, ramp, isothermal, etc), the gas type(s) and gas flow rate(s), and any other operating conditions. At the end of the test, unload the sample, clean the pan, and save the data. It is advisable to do an initial test run, from ambient to 1000°C using a heating rate of 30°C, in order to identify the approximate temperature ranges where the mass losses occur, before using lower heating rates for data collection.

Gas purge. For determination of carbonate content dry, high-purity N_2 or another inert gas can be used as a purge gas with a cross-flow of and a down-flow depending on the

instrument. Note that the pressure in the furnace environment of most instruments is not controlled and will increase with increasing temperature. Usually, the cross-flow and down-flow are set to the recommended by the TGA manufacturer. Air should not be used as the purge gas because the CO_2 and O_2 present in the stream can interfere with the decomposition reaction. The CO_2 concentration of the feed stream should be known. Air or CO_2 atmospheres are sometimes used to shift carbonate decomposition to higher temperatures enabling CO_2 losses to be more easily distinguished from other mass losses. However, users should be aware that CO_2 atmospheres can cause carbonation of samples (mass gain), pushing carbonate decomposition to higher temperatures, while using air purge gas allows for oxidation reactions to occur for certain minerals which could complicate the analysis.

Accounting for buoyancy effects. An empty pan is heated under the same conditions as the sample. The resulting apparent mass data are subtracted from the corresponding values in the sample runs, to correct for buoyancy effects (Vyazovkin et al., 2011).

Sample size and heating rate selection. Heat transfer effects, e.g. "thermal lag", (Khawam and Flanagan, 2005) and "self-cooling" (Brown and Galwey, 1989), and mass transfer effects e.g., CO_2 build up in interstitial spaces in the sample with reverse reaction, must be minimised (Criado et al., 1990). Typically, this is achieved using small masses, low heating rates and sufficient gas flow, and by spreading the sample thinly on the bottom of the pan (Lyon et al., 2012). Small particles also aid in minimising heat and mass transfer effects. Sample masses and heating rates should not be so low that the signal to noise ratio is low. Recommended sample mass of 1-50 mg and heating rates of 5-30 K min^{-1} are recommended. It is advisable to study a sample multiple times with different parameters to study the effect of mass and heating rate on the decomposition. The calculated carbonate content should not change considerably with the sample mass or heating rate. If it does, then it is likely that the mass loss is not due to carbonate decomposition alone but is complicated by other overlapping mass loss reactions (Turvey et al., 2022).

Warnings and precautions. Sharp spikes in the mass data usually indicate that the sample pan has touched the thermocouple or the side of the furnace. If this is the case, there may be too much sample, or the hangdown wire or thermocouple may be bent, or in the wrong position. Sharp spikes can also be due to sample falling off the furnace (molten material), or explosive reactions which eject sample from the pan, common with sodium carbonate decomposition (Campbell, 2019). It is important not to disturb the TGA during operation (e.g., through impacting the bench or vibration from other laboratory activities) in the vicinity of the TGA lab as these vibrations can create noise in the data.

Box 10.2 – Thermogravimetric analysis with mass spectrometry (TGA-MS)

TGA can be combined with various methods of evolved gas analysis (EGA) – such as infrared (TGA-IR), gas chromatography (TGA-GC) or mass spectrometry (TGA-MS) – in order to identify, and quantify, in real time, the product gases released during thermal decomposition of a sample. In TGA-MS, which is the most commonly used, this is achieved by feeding the outlet gases of the TGA furnace into a quadrupole mass spectrometer where they are plasmolysed and separated according to their mass-to-charge ratios as described in SOP 5. The area under the fragment ion peak in the mass spectrograph is proportional to the mass lost. For effective operation of TGA-MS there are several key things to implement (beyond the scope of this document but see Kemp et al. (2022) for further details).

TGA-MS is especially useful for analysis of samples where the mass loss is a summation of multiple gas-producing reactions. Figure 10.3 shows TGA-MS data for partially (5 min) and extensively (90 min) carbonated serpentine. For the former, the mass spectrograph data show that CO_2 is lost in five stages during heating, whereas for the latter CO_2 is lost in just one stage (Farhang et al., 2016). This pattern is explained by the fact that the partially carbonated sample contains mainly hydromagnesite, and the extensively carbonated sample contains mainly magnesite. These data, along with SEM and XRD evidence, can be used to show that carbonation of serpentine to form magnesite proceeds via the hydromagnesite precursor, and ultimately enables the quantification of the stored carbon, and identification of its mineral form.

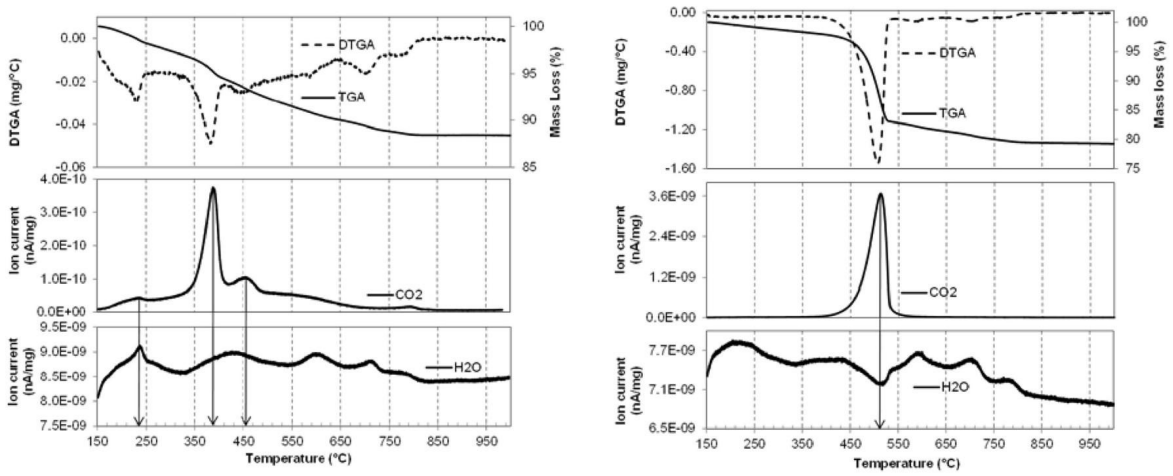

Figure 10.3. TGA-MS data vs. temperature for samples of partially (left) and extensively (right) carbonated serpentine (150°C; 140 barg; 90 min). Republished with permission from Farhang et al. (2016). Copyright 2023 Elsevier.

S10.6 Data processing, interpretation, and presentation

After correcting for buoyancy effects, data are plotted as temperature (and/or time) along the x-axis, and with weight (mg) or weight (%) along the y-axis. The first derivative of the weight or mass (with respect to time or temperature) is also usually plotted on the same figure using a secondary y axis. Since noise is amplified in the derivative signal, particularly where mass changes are small (<1 mg), data smoothing may be needed. The data can then be annotated to highlight the mass losses of interest to the user. Depending on the nature of the sample, further tests may be needed at various masses, heating rates (or even isothermal), or different purge gas compositions to gather further information. Where needed evolved gas analysis (e.g., TGA-MS, see Box 10.2) can be employed to provide additional data. By using the mass loss over certain temperature increments and multiplying them by a stoichiometric ratio it is possible to estimate the mineral abundance of certain minerals, as shown below (Campbell, 2019; Földvári, 2011; Turvey et al., 2022).

Determining Carbonate Content. If a sample is known to contain Mg- or Ca- carbonates it is possible to use TGA to estimate their abundance. Figure 10.4 shows a sample of steel slag before and after carbonation. The mass loss that occurs from the carbonated sample between 400 and 700°C is due to the presence of calcite. The quantity of calcite can be determined knowing that these decompose releasing 1 mol of CO_2 according to Eq. 10.1.

$$CaCO_3 \rightarrow CaO + CO_2 \qquad \text{Eq. 10.1}$$

By taking the mass losses (Δm) of ~ 3.8 wt % multiplied by the stoichiometric ratio of $CaCO_3$ to CO_2 of 2.27 (100.09 g mol^{-1} /44.01 g mol^{-1}) estimates a calcium carbonate content of 8.63 wt. %. However, TGA data are rarely as straightforward as that given in Figure 10.4. Other processes, such as oxidation of organic matter, dehydration and dehydroxylation, and thermal reduction of metal oxides also release gases which can overlap with those of the CO_2 released by carbonate decomposition. Prior knowledge of the composition and mineralogy of the sample is useful in such cases, and mass spectrometry (Box 10.2) or DSC (Box 10.1) can provide additional information.

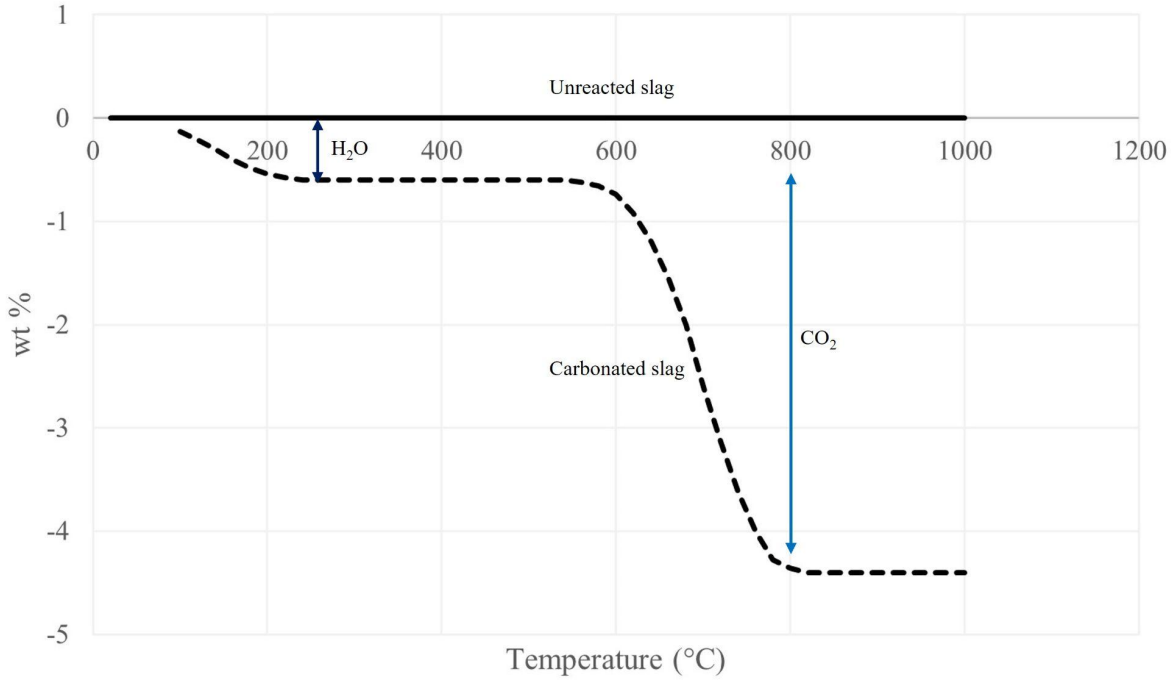

Figure 10.4. Weight loss (%) vs. temperature for slag before and after carbonation obtained via TGA.

Determining brucite content. Similar methods can be employed to determine the brucite content of an ultramafic rock sample (Turvey et al., 2022), brucite abundance is important because it represents one of the most easily reacted sources of divalent cations for carbonation in ultramafic rocks and mine tailings (Lu et al., 2022). Brucite decomposes according to reaction 10.2 between 400 and 550°C in a N_2 atmosphere (Eq. 10.2).

$$Mg(OH)_2 \rightarrow MgO + H_2O \qquad \text{Eq. 10.2}$$

Once the mass loss due to brucite has been identified it can be measured and then multiplied by the stoichiometric ratio of H_2O to $Mg(OH)_2$ (x3.24) to estimate the original brucite content of the sample before analysis (Földvári, 2011).

In complex samples that contain multiple minerals losing mass over the same temperature range, e.g., brucite and serpentine, it can be possible to separate out the contributions from different minerals. This is best done using a combined technique such as TGA-MS but can also be achieved by peak fitting to separate mass contributions from different minerals Turvey et al. (2022).

S10.7 Advantages and disadvantages

TGA is a destructive analytical method, and the sample will be physically and chemically altered over the course of the test. TGA does not by itself provide information on the types of

gases released/gained during mass change or of the minerals present. For this, TGA can be combined with mass spectrometry (TGA-MS) or another evolved gas analysis technique, and it can be combined with other analytical techniques such as XRD for determining the mineralogy of the sample.

TGA is preferable to the loss on ignition (LOI) method for carbonate quantification (see Box 10.3). TGA data can also be used to study the kinetics by collecting and processing mass loss data vs. temperature data using three or more heating rates (non-isothermal kinetic analysis) or constant temperatures (isothermal kinetic analysis) (Ptáček et al., 2010a, 2010b).

S10.8 Quality assurance

Triplicate analyses should be made to generate a mean and standard deviation for carbonate quantification. Frequent mass and temperature calibration, and furnace cleaning, is required as described above.

Box 10.3 – Loss on Ignition (LOI)

Loss on ignition (LOI) uses similar principles as the TGA method described in this section. It determines the mass of different components of a sample based on mass loss at certain temperatures. LOI requires the predetermined temperature to be known for certain analytes within the sample and weighing is performed independently to heating (unlike in TGA where mass is recorded whilst heating commences). Furthermore, instead of using a specialised machine it is performed using standard laboratory equipment, a furnace, crucibles, and an accurate balance. This allows LOI to be cheap, accessible, and easily performed in most laboratories. LOI is a good choice if the sample's composition is already approximately known and if there are multiple similar samples to be tested be run simultaneously. The TGA method can only analyse one sample per heating run.

SOP 11 – Scanning electron microscopy with energy dispersive X-ray analysis (SEM-EDX)

S11.1 Scope and field of the application

This SOP describes how to capture high-resolution images of alkaline mineral samples at the sub-micron level, as well as identifying and quantifying their surface elemental compositions using an analytical technique known as scanning electron microscopy energy dispersive X-ray analysis (SEM-EDX). SEM-EDX provides information on particle size, chemistry, and surface morphology, revealing data that cannot be obtained through bulk chemical analysis techniques such as X-ray fluorescence (XRF).

S11.2 Principle

Scanning electron microscopy utilises a beam of high-energy electrons, adjustable between 500eV and 30kV. The electron beam is generated by heating a source such as a tungsten hairpin filament, a block of LaB_6 crystal with a sharpened facet, or through the use of a field emission gun (FEG) unit. The beam is collimated and focused through a series of magnetic lenses within the column of the SEM, into the chamber where it is scanned (rastered) across the surface of a sample placed on the SEM stage to produce an image (Figure 11.1). Computer control of the size of the area scanned determines both effective magnification and resolution. Achievable magnifications can be in the area of 100,000x or more, and SEM maximum resolution is typically around 1 to 4 nm depending on specifications. For in-depth discussion see (Goldstein et al., 2017). Electron source, column and chamber are pumped to and operated at a high vacuum level (6e-6 mbar), although in many SEM's the chamber can be operated in low-vacuum (~0.80 Torr), or in wet-mode / ESEM mode (3–6.5 Torr) (see S11.3 Instrumentation).

Interaction of the primary electron beam with a sample on the SEM stage results in a variety of emissions from the interaction volume (Figure 11.2), these being secondary electrons (SE) from at or near the surface, higher energy backscattered electrons (BSE) from deeper within the sample, and light photons from the surface. These signals can be collected individually or synchronously, with SE, BSE and cathodoluminescence (CL) detectors respectively. Images generated by SE detectors are primarily used to illustrate surface topography and surface detail (Figure 11.3), while BSE detectors provide information on atomic number (density) of the substrate, with low atomic number material appearing darker than high atomic number material. CL imaging is often employed in the imaging of crystal zonation due to the presence of variability in trace amounts of elements such as Fe, Mn and Mg (Boggs and Krinsley, 2006).

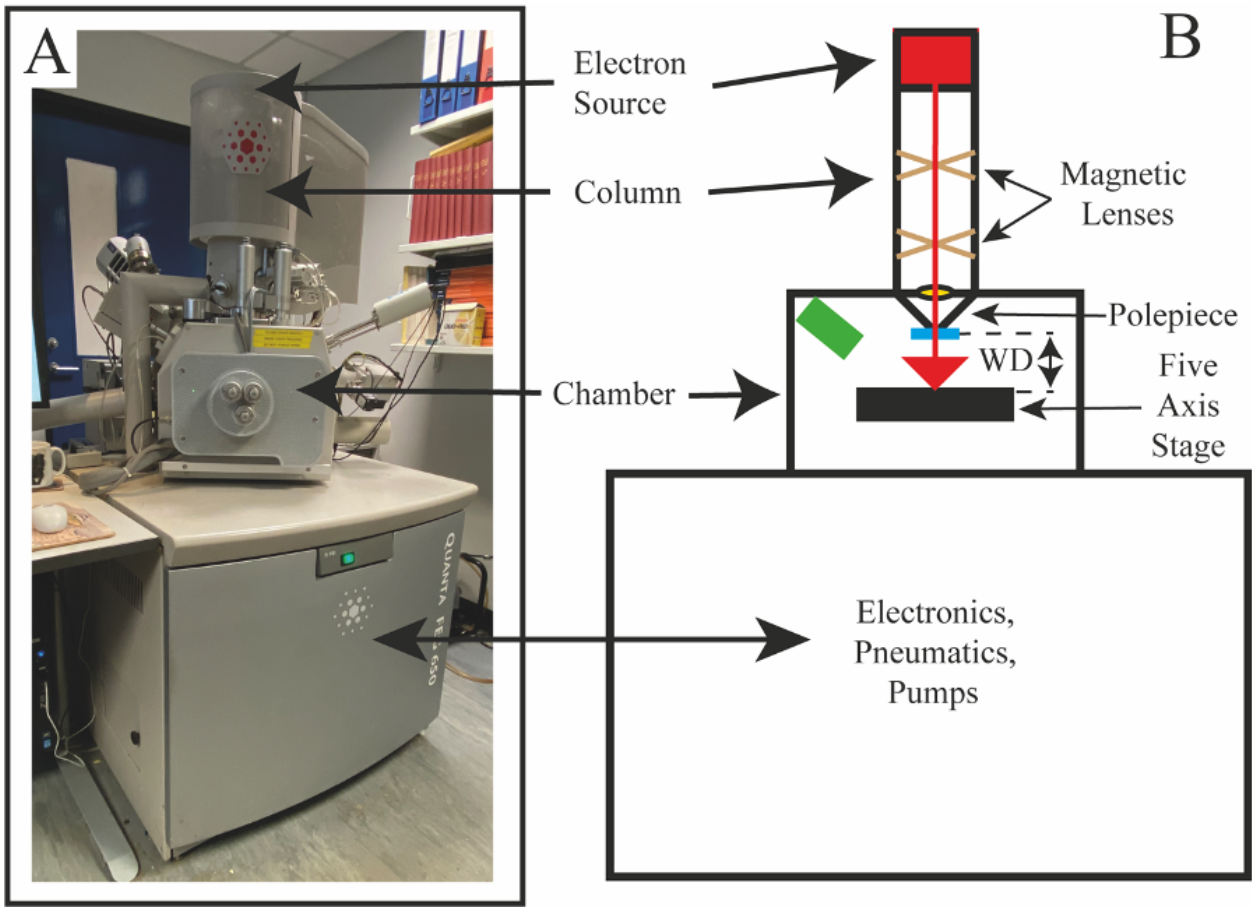

Figure 11.1. A) Image of typical SEM (Quanta FEG 650), and B) schematic sketch of SEM, illustrating the main components of SEM. Green box = Etherhardt-Thornley high-vacuum SE detector. Blue box = axial pole mounted BSE detector. Yellow ellipse = aperture. Red arrow = path of electron beam.

In addition to SE, BSE and CL emissions, beam interaction also produces Bremsstrahlung and characteristic X-rays from the whole of the interaction volume. Bremsstrahlung forms a broad continuous X-ray background, while characteristic X-rays have energies that are indicative of particular elements. The latter can be used in conjunction with an EDX detector and associated software to generate an elemental spectrum, from a spot, a defined area, or whole field of view (Figure S11.4), elemental maps (Figure S11.4), line scans (Figure S11.5) or automated grain / particle analysis (beyond scope of this SOP). EDX spectroscopy can provide rapid, qualitative, semi-quantitative or quantitative analysis of elemental composition. Full quantitative analysis requires regular calibration using suitable standards and a Faraday cup to accurately measure beam energy at the sample surface. However, modern detectors equipped with virtual standards are generally adequate to acquire representative semi-quantitative data. Where a higher degree of accuracy is important for quantitative analysis, it is also additionally important that the sample should be flat and highly polished, which is often not the case, and orientated perpendicular to the electron

beam. For such cases it is more practical to utilise an electron probe microanalysis facility, equipped with 3 or 4 wavelength diffractive X-ray (WDX) detectors. EDX data can be used in conjunction with SE, BSE or CL images to fully characterise the material.

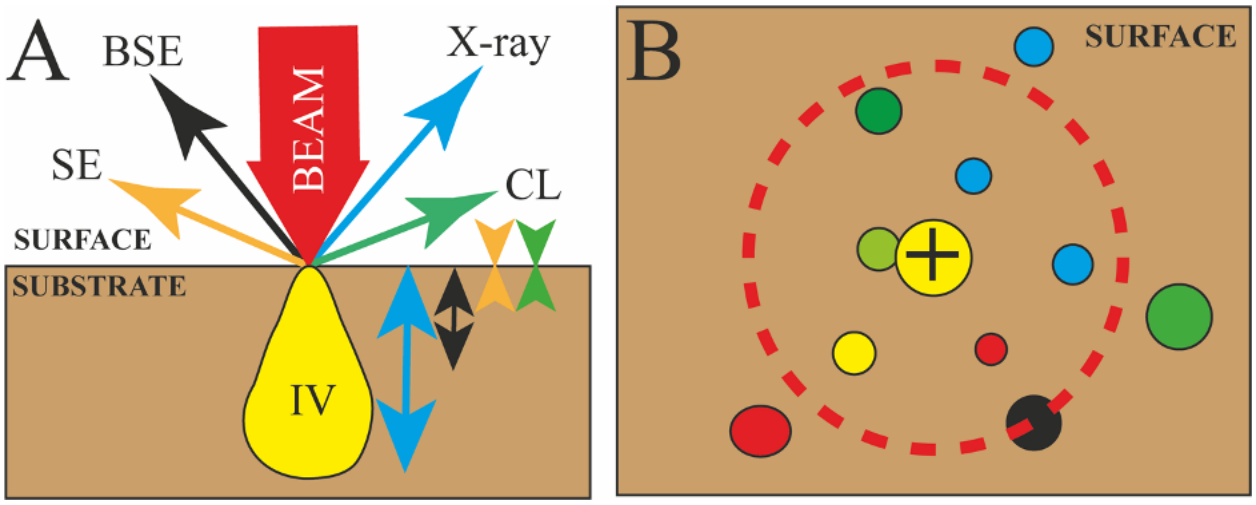

Figure 11.2. A) Cross-section through surface of polished thin-section, illustrating shape and depth of beam interaction volume (IV), and the nature of signals emitted from the interaction (SE, BSE, CL and X-ray arrows), and the relative range of depth from which the different signals originate (colour coded double-headed arrows). B) Schematic cartoon showing plan view of a sample comprising multiple particles of varying composition (shown by colour), illustrating the skirt-effect on EDX analysis in low-vacuum. Plus (+) marks the beam position on the central particle, red-dashed circle = extent of the skirt effect. Note, the majority of X-rays are generated at the point of beam interaction with sample surface (+), but some X-rays will also be developed within the skirt area and may contribute minor peaks to the spectrum acquired.

The EDX detection limit for elements Na to U in bulk materials and in individual particles larger than about 2 µm is on the order of 0.1 wt. % (Buseck and Bradley, 1982). For smaller particles, there is an increased likelihood that additional characteristic X-rays will be detected from the substrate below the particle due to the nature of beam penetration (see Figure 11.2a). In addition, it is worth noting that when using low-vacuum or ESEM mode, X-rays may be analysed from the surrounding area due to the skirt effect (Figure 11.2b), leading to the potential inclusion of minor peaks for elements that may not be within the particle under analysis.

In order to minimise surface charge build-up due to interaction with the electron beam, samples to be examined by SEM-EDX must be electrically conductive, coated in a conductive medium, or examined either in low-vacuum or ESEM mode (see S11.3 Instrumentation).

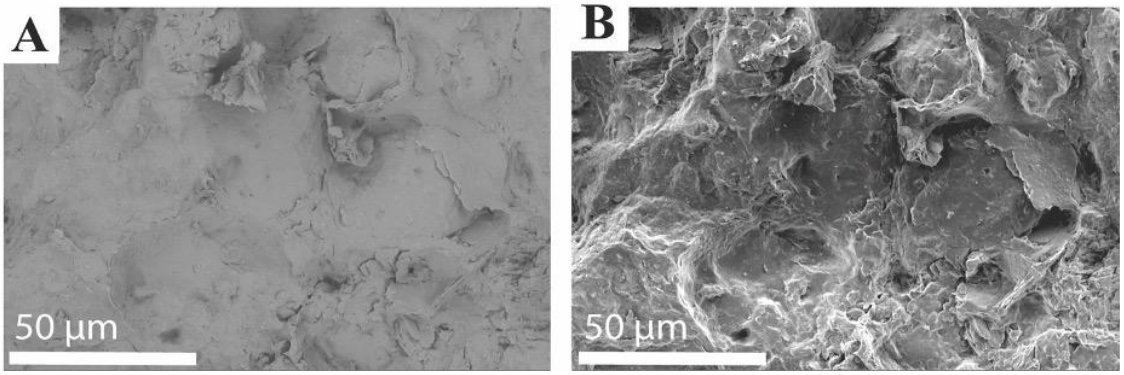

Figure 11.3. Pair of corresponding photomicrographs of natural broken surface of red Devonian sandstone, illustrating the difference in appearance of BSE and SE images (A, B respectively). A) BSE image showing some surface detail, but signal mainly illustrating a similar grey level from quartz and dolomite. B) SE image illustrating higher degree of surface detail and morphology.

S11.3 Instrumentation

In terms of SEM, two types of electron source are available, these being i) a simple tungsten hairpin filament or LaB_6 crystal, or ii) a more sophisticated field emission gun (FEG) system. The first option has the advantage of being relatively cheap to run, although having a limited lifetime (generally less than 100 hours), while FEG systems are much more expensive, but have longer lifetimes (1 to 2 years dependant on use), have extremely stable beam emissions, as well as typically providing better image resolution and ease of use compared to the first type.

SEM instruments can be further subdivided into three types: a) traditional high-vacuum SEM, b) low-vacuum SEM and c) wet-mode SEM (also known as environmental scanning electron microscopy (ESEM)). High-vacuum SEM requires that samples are electrically conductive or coated in a conductive medium such as carbon or gold, and generally involves a number of preparatory steps to perform SEM-EDX analysis (see Sample Preparation). Low-vacuum SEM and ESEM analysis work under a lower partial vacuum typically in the region of 0.80 Torr and 6.5 Torr respectively, within a water vapour atmosphere. In both cases this allows imaging and EDX analysis of uncoated non-conductive samples with little or no preparation. ESEM also has the additional benefit of allowing the examination and maintenance of partially hydrated samples within the vacuum chamber through use of a Peltier cooling stage, and operation as an experimental chamber under varying temperatures and gas environments. In this way it is also possible to examine wettability (contact angles), the effects of wetting and drying, carbonation (within a CO_2 atmosphere) and heating at temperatures up to 1000°C. Use as an experimental chamber does not form part of the current SOP, but can be further explored in (Stokes, 2008).

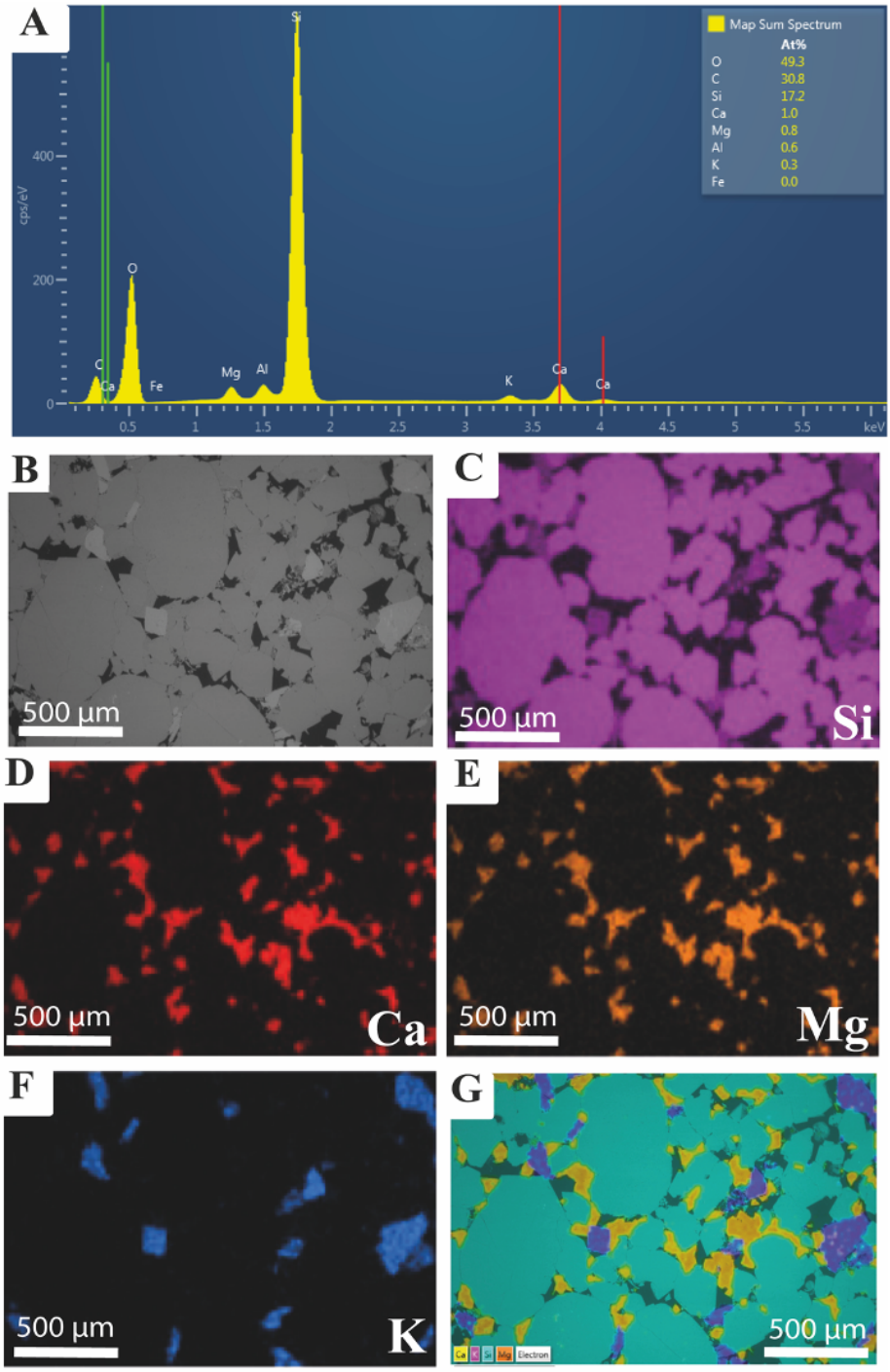

Figure 11.4. A) Characteristic X-ray spectrum of the whole image area in (B), including semi-quantitative atomic percentage data (inset top right). B) BSE image of polished thin-section of red Devonian sandstone. C)-F) X-ray elemental maps for silica, calcium, magnesium and potassium respectively from the same area as in (B). G) Composite elemental map of area in (B). Quartz (teal), feldspar (purple), dolomite cement (orange and yellow).

EDX detectors can be supplied with no window, a thin window, or a thick window depending on the requirements of the user. Thick window detectors have poor transmission of low-energy X-rays and are insensitive to elements lighter than Na. Thin window Peltier cooled EDX detectors are currently the most common form of detector offered by multiple manufacturers. In combination with larger sized detectors (i.e., 150–170 mm diameter), and improvements in detector electronics, modern detectors can process in the region of 1,000,000 cps. The inclusion of multiple EDX detectors, 2 or 3 per SEM system, has the advantage of increasing X-ray count rates, but also minimising shadowing effects where samples have a rough surface.

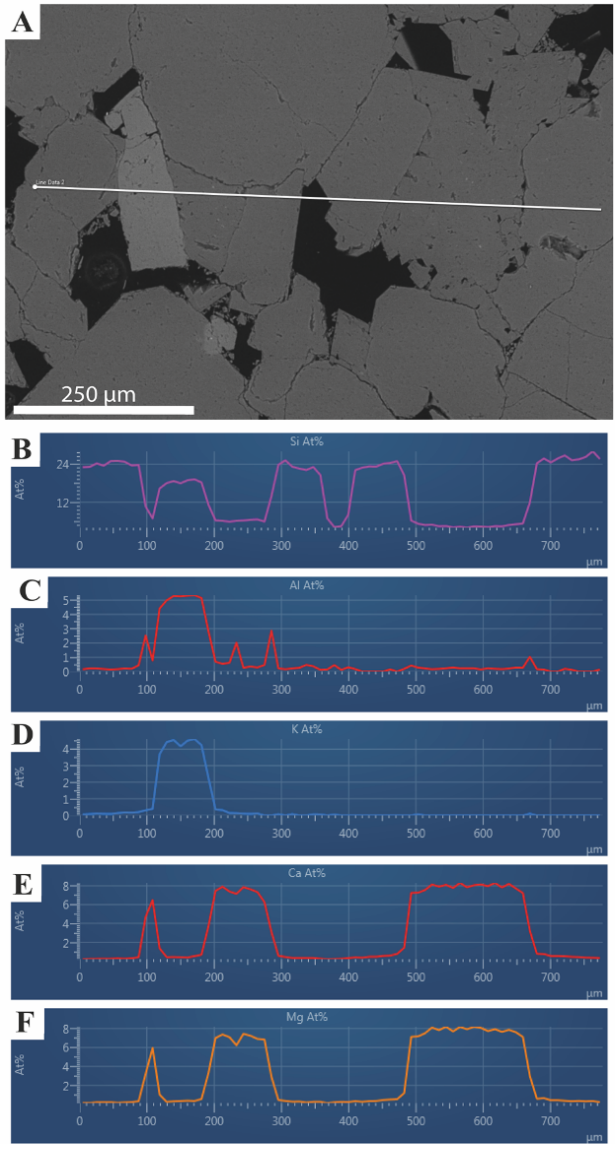

Figure 11.5. A) BSE image of polished thin-section of red Ordovician sandstone, with white line illustrating the position of the elemental line scans in B to F. B-F) Semi-quantitative elemental line scans for silica, aluminium, potassium, calcium and magnesium respectively, with results presented as atomic percentage values.

S11.4 Sample Preparation

Samples may be irregular rough surfaced grain mounts, natural broken sample surfaces, or mounted in resin and polished flat with a mirror finish as either a block or polished thin-section:

Grain & Powder Mounts (Figure 11.6a)**.** Acceptable grain and powder mounts for SEM-EDX analysis can be made by mounting double sided carbon sticky tabs to standard aluminium SEM stubs of a suitable size and design for use in the SEM model being used (e.g., pin or screw type). Make sure that the base of the stub is clearly marked with a unique identification number or code. Place the grains or powder on a suitable clean surface, then gently press the upper surface of the stub into the sample. Knock off any surplus material, then place the stub in an SEM stub storage-box. If using high-vacuum SEM, coat with gold or carbon following manufacturer instructions.

Broken Surface Mounts (Figure 11.6b)**.** Break up sample using mechanical means, to form a fragment approximately 1 cm^2 and 5 mm thick. Ideally, the sample should be as flat as possible to minimise the risk of damage to the polepiece or more importantly any BSE detector mounted on the polepiece. Sample should be securely mounted to a labelled aluminium SEM stub using a two-part epoxy resin. If the sample is to be used under high-vacuum, once the resin mounting medium has set, silver dag can be applied between the sample and the SEM stub prior to carbon or gold coating. At each stage, resin and dag should ideally be left for 24 hours to prevent outgassing during SEM examination. Stubs should be kept within a suitable storage box until required for analysis.

Polished Blocks & Thin Sections (Figure 11.6c)**.** Material should be placed within a suitably sized and shaped flexible mould and impregnated in a specialist resin designed for SEM analysis. Where an analysis of porosity is also likely or required by optical microscopy, then blue resin can be used for impregnation. Impregnation should be carried out under vacuum, with vacuum cycling at least 5 times to ensure that resin is fully drawn into any pores present. After curing of the resin, samples are removed from the moulds and a diamond saw should be used to cut a suitable section in the orientation that it is desired to image and analyse the sample. For polished blocks the cut surface can then be polished using a series of decreasing polishing media, or further processed to produce polished thin sections suitable for SEM. The quality of any SEM analysis is directly proportional to the degree of polishing. Therefore, although samples can be hand polished, it is highly recommended that block and thin-section production is undertaken at a suitably qualified facility provider. Both types of sample can be examined under high-vacuum after coating with carbon. However, where possible, samples should be examined uncoated by SEM under low-vacuum, which allows for subsequent optical microscopy without the need for coating removal and repolishing.

Unprepared stable samples (Figure 11.6d)**.** Due to the low-vacuum capability of being able to image non-conductive samples without coating (i.e., gold or carbon etc.) alkaline-mineral containing natural and man-made materials can be imaged and analysed by SEM without any form of preparation, the only limit being size. Samples should ideally be no larger than a couple of square centimetres, so as to limit potential pump down problems and imaging artefacts. Material can be placed directly on the SEM stage without the need for the use of SEM stubs.

Unstable, hydrated samples (Figure 11.6e). Unstable samples, such as specimens that are hydrated, are unstable under normal high-vacuum conditions. Such materials can be examined under high-vacuum through further preparation: freeze fracturing and examination using cryogenic-SEM, or freeze drying under vacuum (Trewin, 1988), neither of which is covered within the SOP. Alternatively, such samples can be examined fully hydrated in wet-mode (ESEM), with the use of a Peltier cooling stage. In this case a small sample less than 10 mm in diameter is placed onto an ESEM stub located on the Peltier stage (Figure 11.6e). The Peltier stage is set to 5°C, pressure to cycle 5 times between 4 and 6.5 Torr, and once cooled the sample is pumped to 5 Torr, then slowly increased to between 6 and 6.5 Torr. At the set temperature of 5°C and pressure of 6.5 Torr, the water vapour used as the chamber imaging gas maintains the sample in its hydrated state and allows the condensation of water onto the cooled ESEM stub. Adjustment of pressure in the range of 6 and 6.5 Torr allows the equilibrium point for water condensation versus evaporation, and examination of the sample in its full hydrated state.

For standard high-vacuum SEM-EDX analysis samples must be conductive. Non-conductive objects can be coated with carbon or metal (typically gold or gold-palladium). Carbon is either applied to samples by producing an electrical arc between two sharpened carbon rods, or from the instantaneous evaporation of a heated carbon fibre (Figure 11.7a). In the case of gold or other metals, a thin coat is sputtered onto the sample surface through the formation of a plasma cloud in the coater chamber (Figure 11.7b). Both carbon and metal coating are carried out under vacuum, and in the case of carbon rod evaporation and metal sputter coating, coverage can be increased by rotation of the stage during coating and in some models coating thickness can be actively controlled. Instructions concerning the operation of individual coaters should be obtained from manufacturers and made readily available next to the coater, so that consistent reproducible results are obtained. Carbon coating is usually applied to samples where EDX analysis is required, while gold sputter coating is typically applied where imaging is the priority, or where the coating does not interfere with the characteristic X-rays of the elements present. Gold coating may in some cases additionally enhance image quality. As carbon evaporators produce an extremely bright arc light, users should wear eye protection, or preferably not look at the sample during coating.

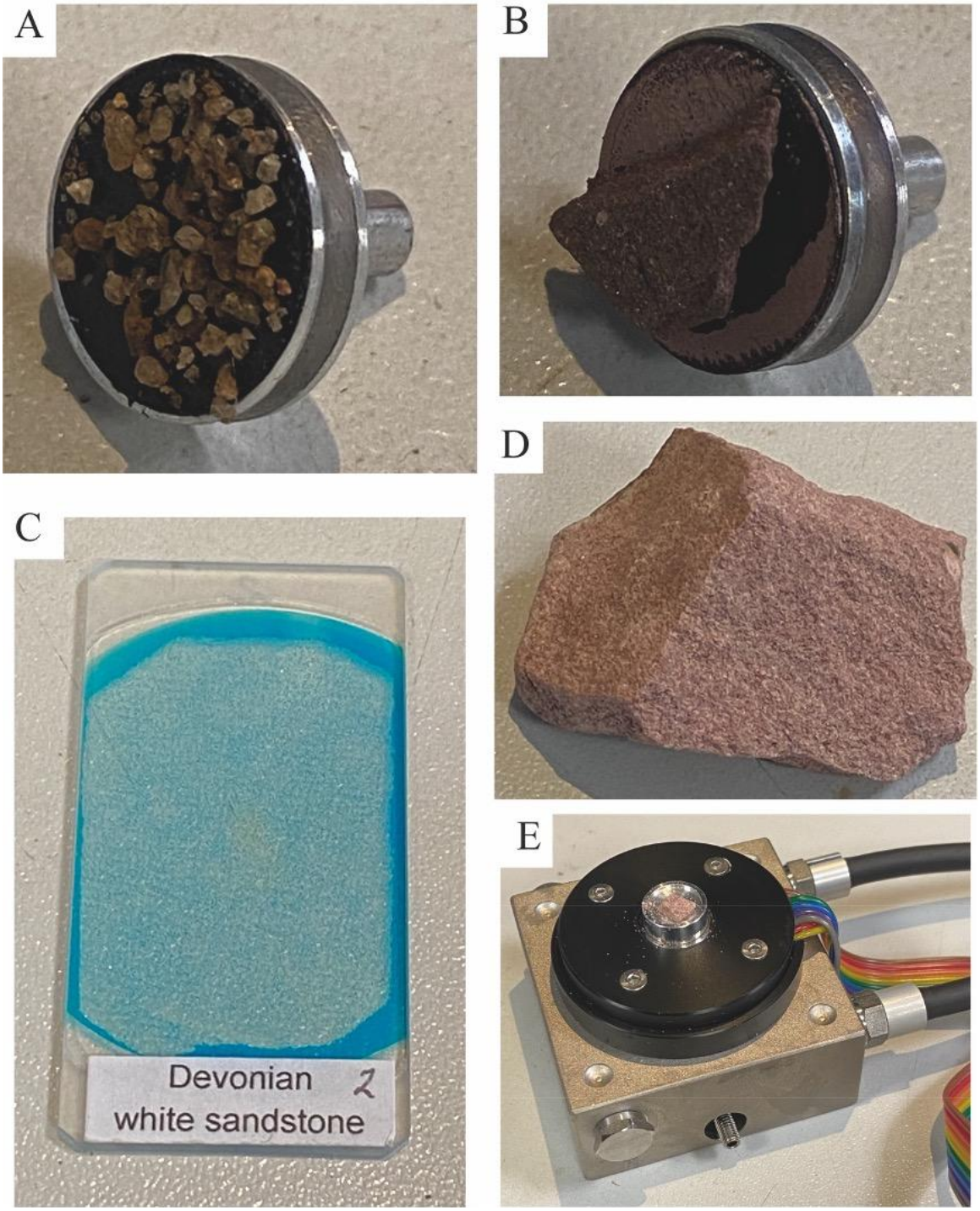

Figure 11.6. Specimen preparation for SEM-EDX analysis. A) Grain mount on SEM stub. B) Rock chip on SEM stub. C) Polished thin-section of sandstone, impregnated with blue resin. D) Unprepared and unmounted sandstone sample for low-vacuum SEM analysis. E) Peltier cooling stage, used in wet-mode ESEM analysis of unstable samples.

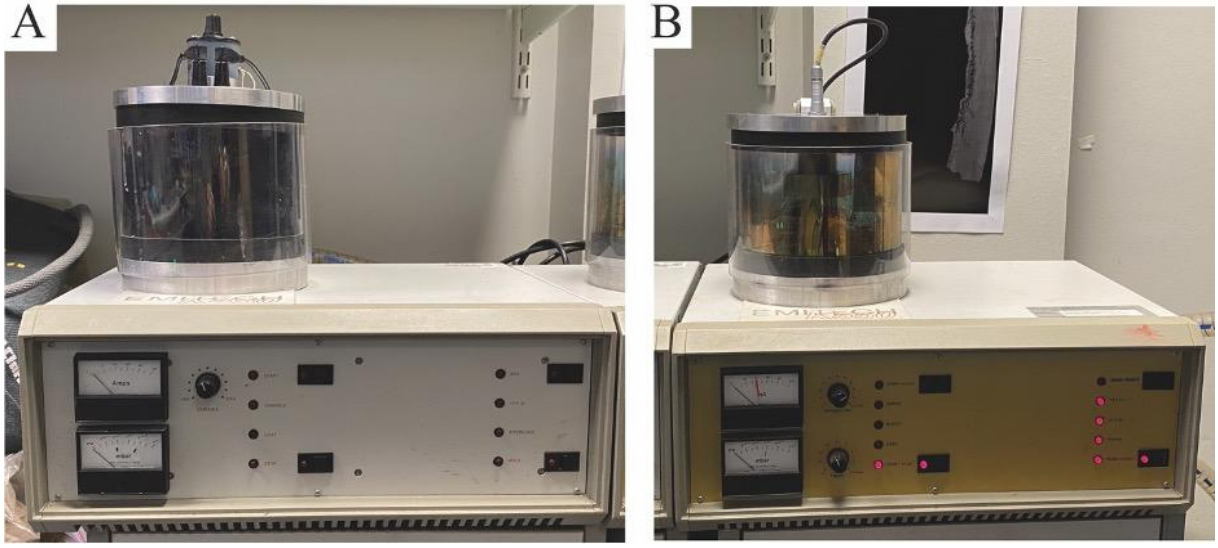

Figure 11.7. Images of specimen coating systems. A) Carbon coating using carbon fibre. B) Gold sputter coater, with Au target foil.

S11.5 Standards and calibration

Qualitative EDX analysis within SEM requires the use of standards of known, certified, composition, which are used to calibrate the EDX detector under the operational parameters being used to acquire elemental spectral data. This requires regular calibration using a set of standards suitable for the type of material being examined, and a Faraday cup to measure the beam energy implanted at the sample surface. Detailed instructions for calibration of EDX systems is not part of the present SOP, for further information refer to manufacturer manuals. In addition, for accurate quantitative analysis it is necessary for samples to be highly polished, flat, and perpendicular to the electron beam, which is not the case for many samples analysed by SEM-EDX, making any quantitative analysis semi-quantitative in nature. All manufacturers of EDX detectors supply these with factory calibrated virtual standards, which require no user intervention, providing reliable semi-quantitative data that is suitable for approximate stoichiometric calculation of mineral phases analysed. Therefore, in general SEM-EDX analysis should be seen as qualitative or more semi-quantitative in nature. Where more fully quantitative elemental analysis is required, polished samples should be examined by electron probe microanalysis (EPMA). The latter utilises 3 or 4 wavelength diffraction X-ray (WDX) detectors and is more quantitative, with improved detection limits compared to that of EDX analysis. However, WDX takes longer, and requires frequent system calibration using standards. For detailed information the user should refer to other publications (Goldstein et al., 2017), as this does not form part of the current SOP.

S11.6 Procedure

A general workflow for SEM and EDX analysis is given below:

Depending on the nature of the sample, requirement for EDX analysis, and type of SEM available, choose mode of SEM operation: high-vacuum, low-vacuum, wet-mode (ESEM). Note that although not all facilities offer the possibility of ESEM analysis, most modern SEM manufacturers offer machines that operate in both high- and low-vacuum modes, which are readily available in many facilities;

1. Where necessary prepare sample for SEM analysis (see S11.4 Sample Preparation);
2. Place sample into SEM chamber and pump to vacuum;
3. Once vacuum is achieved, select appropriate operating voltage (kV), and turn the beam on. Note that a higher kV (15–20 kV) is a typical value for BSE imaging and EDX work, and works well for polished blocks and thin-sections, while lower values of 10 kV or less can be used in conjunction with an SE detector to maximise surface details on natural (uncut, unpolished) surfaces;
4. Focus the SEM image;
5. Adjust stigmator (X and Y) settings to ensure optimal beam shape and improve image quality;
6. Optimise the distance between the polepiece and sample surface, known as working distance (WD). On many machines WD is 10 mm, and this is the optimal distance for imaging, while also offering reasonable protection for BSE detectors placed on the polepiece;
7. Select appropriate spot size. Larger spot sizes are typically used for lower magnification images, while smaller sizes are generally used for higher magnifications;
8. Select suitable final aperture size. Smaller apertures generally provide better image quality and larger depth of field. Note that depth of field can also be increased by using a longer working distance, but this will potentially be to the detriment of detector contrast and brightness;
9. If necessary, refocus the image and readjust stigmators;
10. Select detector for imaging: BSE for compositional contrast, SE for topography and fine surface details, CL for cathodoluminescence variation in polished samples. Use appropriate line scan speed and pixel resolution. Higher pixel resolution and slower scan speeds generally improve image quality, but may induce surface charging or image drift;
11. Adjust image contrast and brightness;
12. Save images. Note that many SEM's allow for multiple synchronous detector acquisition and saving, which can save time and provide valuable additional correlative information.

Where EDX analysis is being performed a number of additional stages may be necessary:

1. If necessary, change WD to optimal distance for EDX analysis. This is often the same as for imaging, but in some cases may be longer. Use of the optimal WD is important for maximising X-ray flux;
2. Spot size should be adjusted to optimise dead time for efficient X-ray count rate;
3. Aperture size can be increased to maximise X-ray generation from the sample surface, and speed up data acquisition – particularly important for elemental mapping and automated particle analysis;
4. Follow individual manufacturer procedures for obtaining EDX analysis: spectrum acquisition, elemental mapping, line scans and particle analysis.

In addition, there are a number of useful automated in-house image acquisition programmes and add-on third-party image analysis software packages that are commonly available on a range of SEM platforms. One of these is automated image acquisition, that allows for collection of a series of images over a user defined grid. Such software can generate several thousand images or more, which can be used individually or stitched into one large area high-resolution image (Buckman et al., 2017, 2018, 2019) (Figure 11.8). In this way, large numbers of images can be acquired in an efficient and cost-wise fashion. Backscattered images collected using this method can be processed by image analysis and graphing programmes such as 'ImageJ' and 'Matlab', where large-area maps can be constructed for 2D spatial variation in distribution of porosity, or particular mineral phases, based on BSE grayscale levels (Buckman et al., 2017, 2019).

In low-vacuum mode, a low vacuum SE detector can be used to collect Charge Contrast Images (CCI), which provide similar results to those acquired through CL imaging. Typically, this will be information on mineral compositional zoning (calcite and dolomite) and cement overgrowths (quartz and feldspars). In addition, CCI can help in the differentiation of some mineral phases that have similar BSE grey-scale levels, such as dolomite and quartz (Figure 11.9). Further information on the use of low-vacuum SEM, and CCI can be found in (Stokes, 2008) and (Buckman et al., 2016).

S11.7 Data presentation and analysis

Both SEM image acquisition and EDX analysis provide the opportunity to generate and store digital data that can be easily included in a range of presentation packages (Word, Excel, PowerPoint). Data can comprise SEM images, EDX spectrums, EDX maps, as well as potentially EDX elemental line scans, particle analysis and data tables. Here we consider SEM images, EDX spectra and EDX elemental maps and line scans only.

For each SEM image it is recommended that a scale bar be included on each image to calibrate feature size. Although magnification is often recorded on the databar of SEM micrographs, this value refers to the screen magnification at the time of image acquisition, and therefore is unlikely to be applicable to any final printed media or projected form of the work. Therefore, use of magnification in any report should be avoided. In addition, if not

recorded on the image databar, clear information should be included on the SEM mode used, the operating voltage during image acquisition, as well as the detector used, as these affect the nature of the image, and may be useful when comparing images.

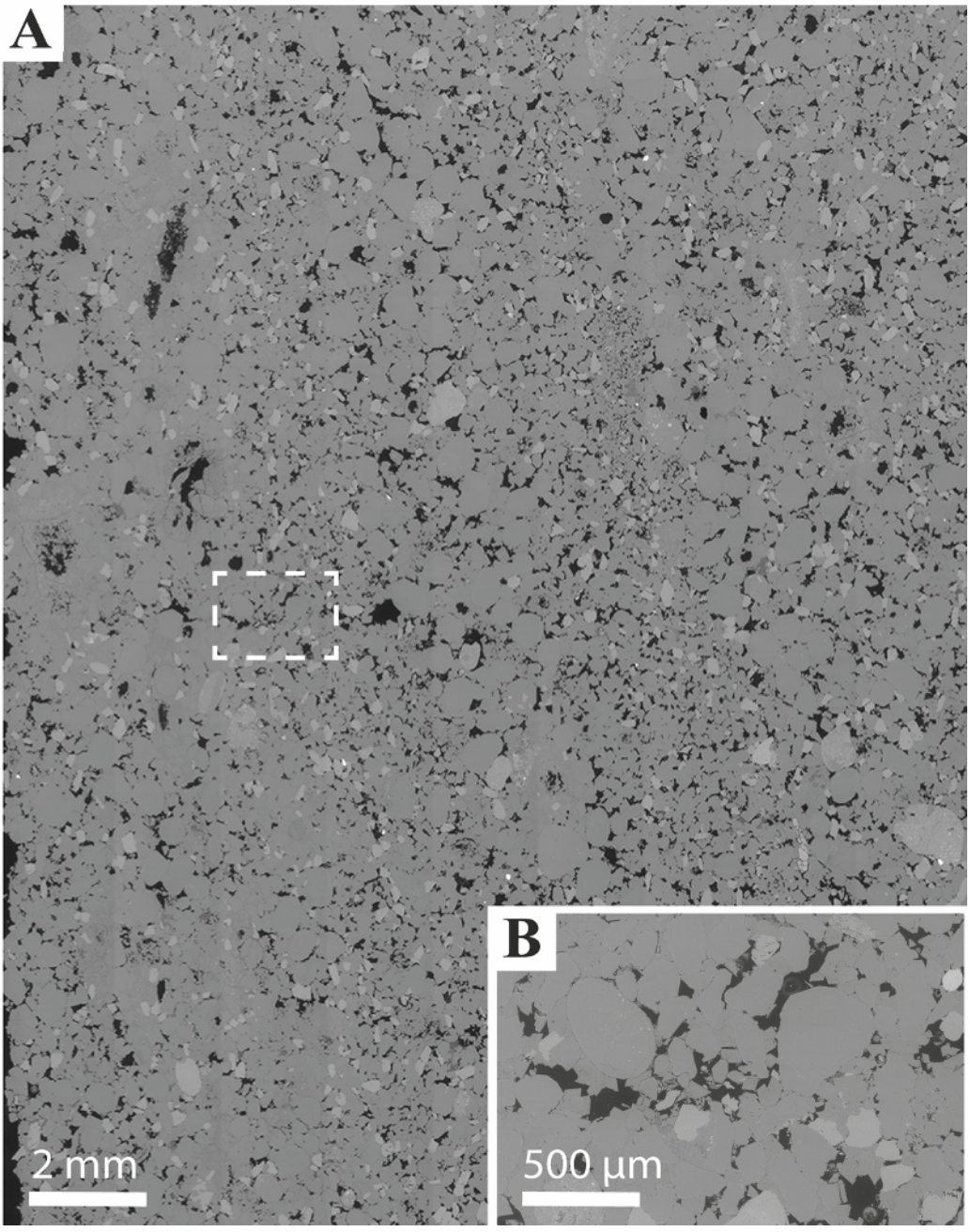

Figure 11.8. A) Large-scale high-resolution BSE montage of polished thin-section of red Devonian sandstone cemented with dolomite. White dashed box indicates location of a single image tile shown in (B). B) BSE image shows pores (black), feldspars light grey, and quartz and dolomite (darker grey).

EDX Spectral data can be presented as qualitative X-ray voltage against intensity as spectrum graphs (Figure 11.4a), or as quantitative data expressed as atomic percentage, or weight percentage. It is important to record if the data was collected from a single spot, a defined reduced area, or the whole field of view, and ideally the location should be indicated on a photomicrograph.

To avoid clutter, only elemental X-ray maps that display information of significance (e.g., Ca, Mg, Si, Al, etc) should be presented. If required, other elements that are present can be included in appendices or supplementary information. Again, it is important to include information on the mode of SEM operation, and the operating voltage (kV), as well as making sure that a scale bar is always present. A record of kV is particularly important as this will affect the characteristic X-rays that are developed and is good practice in terms of interpreting presented data; as a rule of thumb, the operating kV should be twice that of the energy of the characteristic X-rays of the elements of interest.

In addition, EDX software packages commonly offer the option to obtain elemental line scan data from selected transects across a surface. These can be displayed as individual elemental line scans of intensity versus scan position (Figure 11.5b-f), as stacked line scans or as a data table. To aid in interpretation, it is always good practice to include a BSE image illustrating the position represented by line scan (Figure 11.5a)

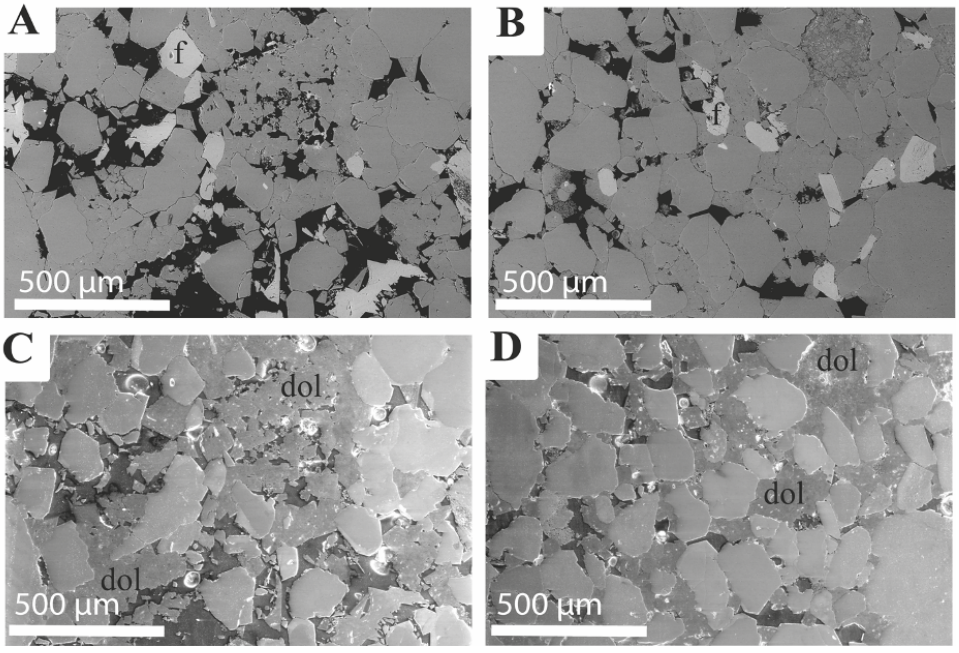

Figure 11.9. Images of polished thin-section of red Devonian sandstone cemented with dolomite. A), B) BSE images of selected areas, which shows pores (black), feldspars (light grey, f), and quartz and dolomite (darker grey). C), D) SE Charge Contrast Image (CCI) of the same areas as in (A, B). Note that feldspars and quartz are not differentiated in these images, but the dolomite (dol) cement is clearly separated (darker grey).

S11.8 Advantages and disadvantages

SEM-EDX is non-invasive and non-destructive. Some SEMs can achieve imaging resolutions better than 1 nm, with information on surface topography and fine surface detail (SE imaging) and compositional contrast being shown by BSE imaging. EDX analysis applies to the surface layer, with a typical penetration depth of several micrometres, and can resolve spatial variation in elemental distribution at the micron-scale and is particularly sensitive to lighter elements. The use of large area image acquisition and elemental mapping allows for 2D spatial mapping from the micron to centimetre scale.

SEM-EDX analysis can be used for elements from Boron (B) to Uranium (U), while other analytical techniques such as XRF, although capable of analysing a wider range of elements, beryllium (Be) to Americium (Am), only provide bulk chemical information, is often destructive in nature (requiring the production of a powder from crushed material), and does not provide information on the physical nature of the material being analysed. Some exceptions to this include handheld XRF detectors, which do not require sample preparation, and newer XRF systems that offer 2D elemental mapping similar to that of SEM-EDX (Scruggs et al., 2000). The detection limit and peak resolution for XRF is better than that of EDX, and XRF provides fully quantitative information as compared to the semi-quantitative nature of data produced using the EDX technique. Another alternative to SEM-EDX is electron probe microanalysis (EPMA) (see Llovet (2019)). The latter provides imaging as well as quantitative elemental mapping, which has a higher resolution than SEM-EDX due to the use of multiple WDX detectors. EPMA however is restricted to well-polished samples and due to the technique requiring the use of multiple diffraction crystals is more time consuming and requires regular calibration with standards. Other techniques such as Raman and FTIR spectroscopy can also offer non-destructive geochemical analysis (see Xu et al. (2019)), and provide additional direct mineral identification (e.g., aragonite, dolomite, etc.) as well as information on the hydration or oxide state of phases present, representing an additional technique that can be used in conjunction with SEM-EDX.

SOP 12 – Particle size distribution by laser diffraction or sieve method

S12.1 Scope and field of the application

The rate of mineral dissolution can be enhanced through the reduction of mineral particle size. However, no comminution technology produces a single particle size, and it is important to be able to measure a particle size distribution (PSD). For particle sizes >63 um, dry sieving can be used, which involves introducing a sample into the top of a mechanically agitated stack of decreasing aperture sieves. For reference, there are nationally produced standards for dry sieving (British Standards Institution, 2021).

Laser diffraction is an analytical method used to obtain PSDs of dry powders with particle sizes in the range of 10 nm to a few millimetres (but most useful for samples that cannot be assessed through dry sieving). Laser diffraction has a greater range of measurement but is more complicated to undertake and requires more expensive specialist equipment.

S12.2 Principle (laser diffraction)

Laser diffraction particle size analysis is based on the Mie theory of light scattering. Small particles cause more light scattering than larger particles. The angular scattering intensity data is then analysed to calculate the size of the particles in the sample. [At the molecular level, Rayleigh scattering dominates]. Particle sizes are reported as volume equivalent diameters. This means experimentally estimating the volume of the particle, which is usually non-spherical, normalising this volume to that of a sphere, and calculating the corresponding diameter. For the Mie scattering method, the complex refractive index of the alkaline material must be known in advance. The complex refractive index is composed of a real (refractive index) and an imaginary component (absorption index). Table 12.1 shows some estimated values for the refractive index for some common alkaline materials. It should be noted that there may be no universal refractive constant and these may need to be determined by optical spectroscopy (Becke Line method). In the case of fly ash and blast furnace slag the complex refractive index can be estimated based on the CaO content (Jewell and Rathbone, 2009). Some instruments provide the option of obtaining PSDs using a method based on Fraunhofer diffraction theory, rather than Mie scattering. The Fraunhofer method may be preferred when the refractive properties of the sample are unknown but is only valid for particles >50 µm.

S12.3 Sample preparation

Samples should be dried prior to sieving (to prevent agglomeration) or laser diffraction analysis (so that it can be easily entrained and dispersed by the carrier gas).

For dry sieving the amount of sample introduced into the top of the sieve stack is proportional to the maximum particle size. For 10 mm particle size, approximately 500 g is required, for < 2 mm, 100 g is sufficient.

For laser diffraction. Large particles should be removed by passing through a 2 mm sieve. Samples should be mixed by the coning and quartering method (ISO, 2008) to obtain a representative subsample. Some instruments operate by suspending the particles in a liquid suspension. [Agglomerates may need to be disaggregated by suspension in a fluid such propan-2-ol followed by sonication]. Without prior sonication, PSDs may be biassed to larger sizes (Jewell and Rathbone, 2009).

S12.4 Instrumentation

For dry sieving. A set of sieves with aperture sizes that are consistent with the particle size range that will be measured. Given that particle size is often represented on a logarithmic scale, it is convenient to increment the sieve apertures on the order of 2x (for instance 20 mm, 10 mm, 5 mm, 2 mm, 1.18 mm, 600 µm, 300 µm, 150 µm, 63 µm). A pan should be placed under the smallest increment sieve, and a lid placed onto the top of the stack. The stack should be mounted into a mechanical shaker. The shaking time must be carefully selected to allow enough time for particles to pass through the sieves while not causing extensive attrition of the particles.

For laser diffraction. A light source generates a monochromatic beam. After passing through several optical components, the raw beam creates an expanded, collimated beam that illuminates particles in the scattering volume. The particles scatter light, generating unique angular scattering patterns which are transformed into a spatial intensity pattern that is detected by a multi-element photo-detector array. A photocurrent is subsequently processed and digitised, creating an intensity flux pattern that is converted into a particle size distribution. Most instruments can operate in a dry or wet mode. In the dry mode, the carrier gas, aka the dispersant, is usually compressed air. In the wet mode, the fluid is often water or propan-2-ol. The sample is fed into the flowing air stream by vibration of the sample tray. The feed rate can be controlled by the instrument software. The wet mode is usually selected when there is very little sample mass available.

S12.5 Procedure

Dry sieving:

1. Weigh an oven dried mass of soil to be used in the test (record mass).
2. Assemble sieves into a stack of decreasing aperture size, including a lid for the top and a pan for the base.

3. Pour the sample into the top of the sieve stack and replace the lid.
4. Place the sieve stack onto the mechanical shaker, tighten screws to secure the stack, and set the timer to no less than 10 min.
5. Following the test, measure the mass retained on each sieve and in the base pan. Only use the coarse brushes on the coarse sieves. Take care not to damage the finer sieves.
6. The material retained in the pan could be analysed using laser diffraction to extend the particle size distribution analysis.

There is a limit on the maximum amount of material that can be retained on each sieve. see British Standard 1377-2 for details (British Standards Institution, 2021). This is a problem if you have introduced a large mass of fine material into the sieve stack to account for the presence of large particle sizes. If your sieve becomes overloaded, you will need to riffle a sub sample of this and the passing material and undertake another separate test on this material.

Laser diffraction:

1. Switch on the laser diffraction instrument, open the instrument software and select the dry or wet operation mode. Set up a new "sequence file", or load a pre-existing one. Input the refractive index and imaginary component for the sample, and any other necessary input data and operating instructions.
2. For dry mode: Ensure the mode is "Dry type". Switch on the compressor and vacuum cleaner. Perform a background run. Then, place the sample into the sample tray. Start the run. The run will end when the sample is depleted. Clean the system by purging with air. Repeat the process three times. Save the data file.
3. For the wet mode: Ensure the mode is "Wet type". Fill the sample holder, or cuvette, with a suitable solvent, and turn on the magnetic stirrer. Perform a background run. Inject the sample through the sample inlet port. For more efficient dispersal of the material, first wet it with the solvent. Start the run. Clean the system by purging with solvent. If possible, repeat the process. Save the data file.

Table 12.1. Refractive indices for some common alkaline materials adapted from Jewell and Rathbone (2009).

Material	Refractive index range
Blast furnace slag	1.60–1.67
Gasification slag	1.54–1.63
Limestone	1.49–1.66
Fly ash	1.53–1.66

S12.6 Laser Diffraction Calibration

Ensure lenses are clean and free of scratches. Laser diffraction instruments can be calibrated quarterly using a standard reference material as recommended by the instrument manufacturer. The reference material is typically composed of glass beads of a specific particle size (refractive index of 1.520 and absorption of 0.00). Vacuum plastic tubing may become coated with powders over time. Tubes need to be replaced regularly and the instrument cleaned.

S12.7 Data interpretation and presentation

Particle size distributions can be interpreted and represented numerous ways. A histogram of % volume retained (Eq. 12.1) for a specific size interval (typically the sieve increment) can be useful for showing the distribution of particle sizes. Alternatively, a common method is to calculate the 'cumulative percentage passing' (Eq. 12.2 and 12.3), which shows the cumulative change in mass passing a given size fraction. This is particularly useful for interpreting the particle sizes for a given passing percent (P_{80} – particle size for which 80% of the material passes, P_{50} – the median particle size).

$$A_i = 100 \cdot \frac{m_i}{m_{total}} \quad \text{Eq. 12.1}$$

$$B_i = A_i + B_{i-1} \quad \text{Eq. 12.2}$$

$$C_i = 100 - B_i \quad \text{Eq. 12.3}$$

A particle size distribution can be classified using the coefficient of uniformity (Eq. 12.4) as 'well-graded' (a wide range of sizes, $C_U > 5$) or 'poorly-graded' (a narrow distribution of sizes $C_U < 5$).

$$C_U = \frac{P_{60}}{P_{10}} \quad \text{Eq. 12.4}$$

Log-normal and gamma functions (Eq. 12.5) can typically be fit to particle size distribution curves (particularly for applying to dissolution models, (Gbor and Jia, 2004), with reasonable fit with particle size data (Figure 12.1).

$$\Gamma(D) = \frac{D^{\alpha-1} \cdot e^{-D/\beta}}{\beta^{\alpha}\Gamma(\alpha)} \quad \text{Eq. 12.5}$$

where α and β are empirically derived coefficients that describe the particle size distribution (Gbor and Jia, 2004).

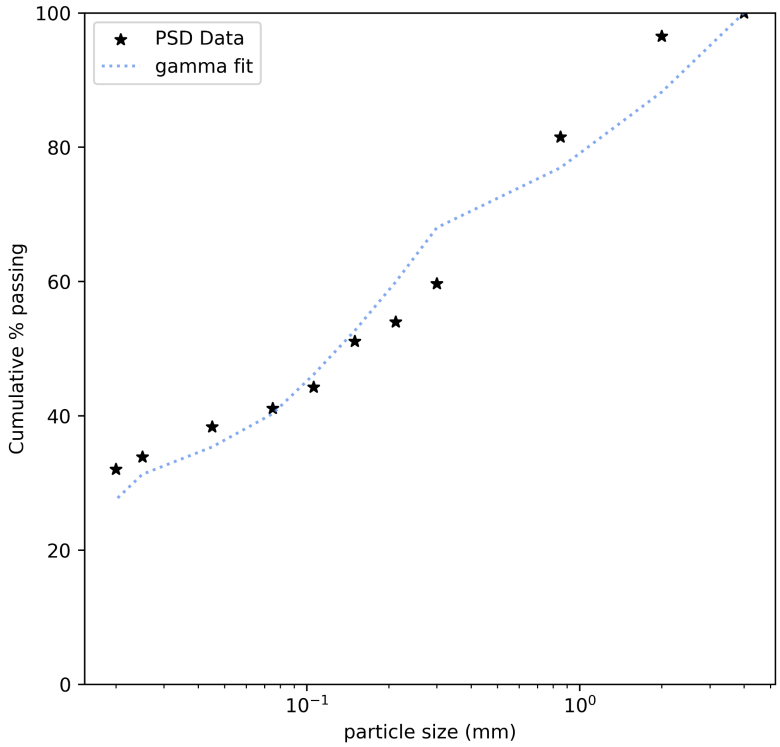

Figure 12.1. For illustration, the particle size distribution of a crushed rock showing measured particle size distribution data, which was fit with a gamma distribution.

S12.8 Advantages and disadvantages

Sieve analysis: The equipment for dry sieve analysis is ubiquitous, and relatively inexpensive to purchase and maintain. The method is straightforward and provides useful results within ~30 minutes. However, the minimum particle size is 63 µm, which may not be sufficient for some geochemical CDR materials.

Laser diffraction: The method is rapid (1 to 10 mins), has a large measurement range (nm to mm) with better resolution than traditional sieve analysis. Another advantage over sieve analysis is the time saved in not having to clean sieves, which often require acids and other hazardous cleaning reagents. Some laser diffraction instruments are non-destructive; however, most are destructive, requiring grams of sample. Although Mie theory is valid only for spherical particles, some manufacturers have included algorithms in their software, which can partly compensate for non-spherical particles. Laser diffraction requires more skill in data collection and interpretation.

S12.9 Quality assurance

Ensuring sample homogeneity is important to obtain representative results. Quality assurance involves thorough sample mixing or blending to achieve a homogeneous sample

before analysis. Adequate sample dispersion techniques, such as ultrasonication or sonication, or riffling can also be employed.

Regular calibration checks for laser diffraction using certified reference materials or traceable standards are advisable. A harmonised standard provides step-by-step instructions on sample preparation, instrument operation, data collection, and analysis (e.g., ISO (2020)).

Performing replicate analysis and calculating mean, standard deviation, and coefficient of variation, can be applied to evaluate the consistency of results.

SOP 13 – Surface area measurements: geometric vs. BET surface area

S13.1 Scope and field of the application

When a reaction is surface controlled, measured overall reaction (dissolution) rates are directly proportional to the moles of reactive sites on a mineral surface available to contact with the reacting gas or solution, and thus must be normalised by a surface area term to obtain the rate constant. The requirement is to define a representative starting value for the accessible and reactive surface area of the material particles of interest, such as a mineral or powdered rock, prior to any reaction taking place (e.g., CO_2-induced dissolution or precipitation reactions). Surface area measurements are typically calculated by two main methods: specific geometric surface area, a geometry-based approximation calculated from particle diameter (A_{geo}), and specific surface area determined by laboratory means by the BET method (Brunauer-Emmett-Teller, A_{BET}; (Brunauer et al., 1938). Other methods of determination that may be considered include image resolution techniques (e.g., SEM, TEM and atomic force microscopy (AFM)) that utilise two- and three-dimensional approaches (e.g., (Nagy et al., 1999; Penn et al., 2001; Peters, 2009; Qin and Beckingham, 2021), crystallographic in-situ X-ray diffraction approaches (e.g., Cho et al., 2019), thermal electrochemical activity approaches (Ren et al., 2020), computational software-based means (Osterrieth et al., 2022) and data-driven machine learning methods (Datar et al., 2020). Here, the use of the two most established and commonly implemented methods of estimation is considered: A_{BET} and A_{geo}. One of the difficulties encountered when estimating surface area values is the wide range of results that can be produced for a given material, which may span several orders of magnitude for different methods, or even within a single method. Therefore, understanding and justifying the choice of surface area determination, and knowledge of the strengths and limitations of the method utilised, are key considerations for calculating dissolution rates of a material.

S13.2 Principle

The experimental method of A_{BET} is based on a gas adsorption isotherm approach, whereby the coverage of the grain is quantified using monolayer (Langmuir theory) to multilayer adhesion of non-reactive gases (e.g., nitrogen, argon, krypton, carbon dioxide) to a surface. The amount of adsorption is dependent upon several controlling factors, including surface exposure, temperature, gas pressure and the strength of interaction between the gas and solid (Hwang and Barron, 2011). Nitrogen (N_2) is typically used due to its relative low-cost availability in high purity, and due to its strong interaction with solid materials (Hwang and Barron, 2011).

Methods of surface area determination by A_{geo} typically assume that the targeted grains are smooth edged, spherical (or cubic) and of uniform size, though in the case of some minerals (e.g., clays), an additional smaller grain size may also be assumed (Anbeek, 1992; Beckingham et al., 2016; Qin and Beckingham, 2021; White et al., 2005).

Generally, A_{BET} methods are used in most studies, due to its robustness as a measurement tool compared to A_{geo} measurements (Brantley, 2008). A_{geo} is typically calculated from crystal dimensions, using an assumed shape, whereas by using gas adsorption, A_{BET} considers surface roughness, such as pits, cracks and pores, giving a higher measurement. Surface area values, and by proxy, calculated dissolution rates, will differ based on the method of determination. Despite its widespread acceptance and use as a practised standard for surface area determination, a common finding from methodological comparison studies is that A_{BET} may significantly overestimate surface areas, in some cases, by several orders of magnitude. This may be the product of the invalid inclusion of non-monolayer molecules in the computed coverage from heterogeneous surface and porous regions, known as the pore-filling contamination issue (Datar et al., 2020; Gómez-Gualdrón et al., 2016; Sinha et al., 2019), lack of gas molecule mobility (and resultant preferential adsorption locations; (Bardestani et al., 2019), or through any inherent flexibility present in a material (Osterrieth et al., 2022). The A_{BET} method also neglects lateral interactions between adsorbed molecules, and assumes all adsorption sites are energetically equivalent (Bardestani et al., 2019).

S13.3 Sample preparation and procedure

***A_{BET}* determination.** An example of common sample preparation and experimental setup is presented here, based on approaches outlined in the methodological reviews of (Hwang and Barron, 2011) and (Bardestani et al., 2019) (Figure 13.1). Methods may vary depending on individual instrumental setup, and the physical or chemical properties of the material of interest. A minimum amount of 50 mg up to 1 g dry material is generally required for A_{BET} determination. For A_{BET} laboratory-based determination, samples are degassed in a high temperature vacuum to remove any water or other volatiles and contaminants, with temperatures sufficiently high as to limit the degassing time but not damage the sample structure. Degassed samples are analysed by BET instrumentation, containing glass or quartz cells and rods of variable size (cell size selection is dependent upon the particle size of the starting materials). The cell is then placed into a heating mantle, connected to a gas outport. Following degassing, the cell is moved to the analysis port, where the sample is cooled and maintained at a constant temperature using liquid nitrogen. Prior to analysis, the dead volume of the cell is determined for means of calibration using helium (which does not adsorb onto the sample). The low, maintained temperature of the cell permits measurable adsorption interactions between gas molecules and the sample surface to be detected, which is conducted when the adsorbate gas (e.g., N_2) is incrementally injected into the sample cell. Layers of gas molecules interact with the exposed and accessible surface to give

the surface area value, where the difference between the empty cell and the measured pressure correlates with the number of moles of adsorbed nitrogen. The absolute precision of A_{BET} values is generally considered to not be higher than 5%, with reproducibility in the range of 1%. The final calculation is made in accordance with ISO 9277:2022 (Determination of the specific surface area of solids by gas adsorption – BET method (ISO, 2022)), with the Eq. 13.1.

$$\frac{P/P_0}{v[1-(P/P_0)]} = \frac{c-1}{v_m c}\left(\frac{P}{P_0}\right) + \frac{1}{v_m c} \qquad \text{Eq. 13.1}$$

where v is the adsorbed gas volume, P is applied pressure, P_0 is saturation pressure, v_m is the gas volume needed to create a monomolecular layer of nitrogen, and c is the BET constant.

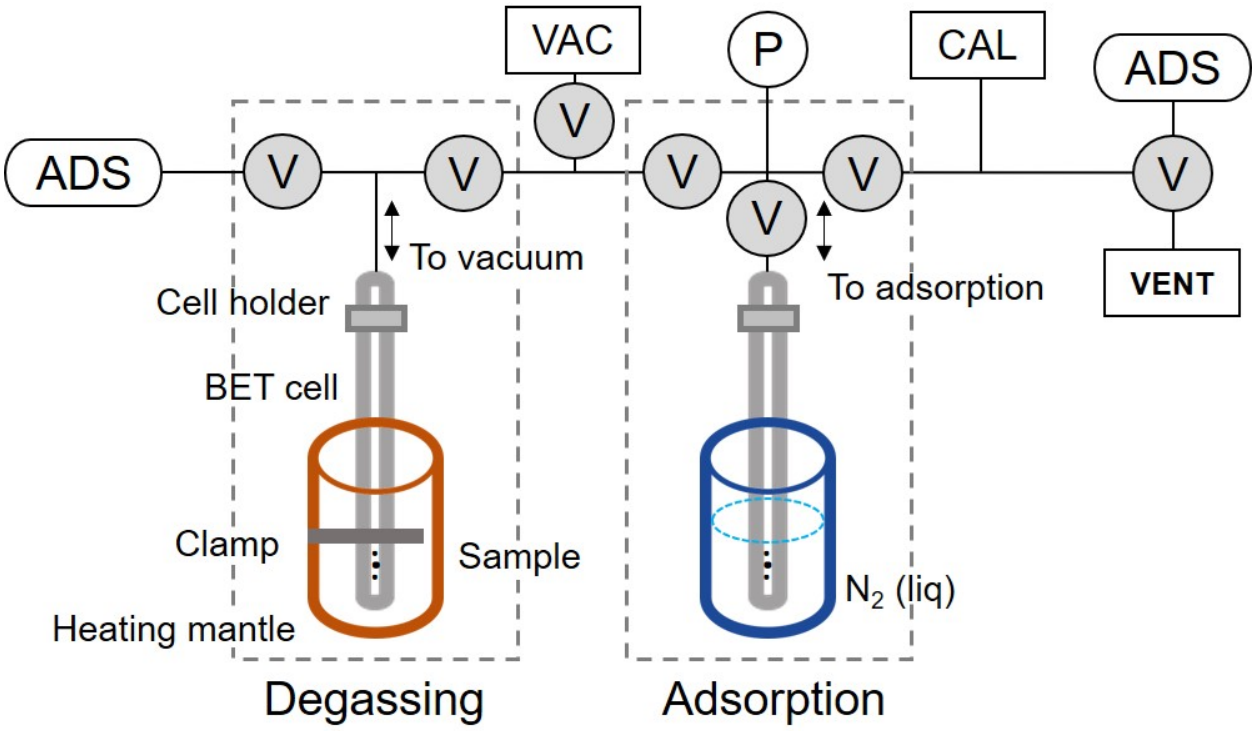

Figure 13.1. Gas physisorption instrumental setup (degassing and adsorption stations) to obtain adsorption-desorption isotherm, showing vacuum (VAC), calibration (CAL), adsorbate (ADS), pressure gauge (P) and valves (V).

***A_{geo}* determination.** Geometric determination of surface area requires imaging and/or physical characterisation of particle dimensions by methods such as scanning electron microscope (SEM), laser (particle size distribution) or X-ray diffraction (XRD) particle analysis, with assumed perfect geometric shapes (e.g., cubes, spheres) used for axial dimensions, such as particle diameter. A_{geo} can then be calculated using area equations for a given assumed shape and grain material density. For instance, when assuming a spherical particle, A_{geo} can be calculated by Eq. 13.2.

$$A_{geo} = \frac{6}{(p-d)}$$ Eq. 13.2

where A is total area (cm^2/g), d is the average particle diameter (cm) and ρ is the bulk density (g/cm^3) (Cubillas et al., 2005; Gautier et al., 2001; Guy and Schott, 1988; Marieni et al., 2020; Wolff-Boenisch et al., 2004). Other examples, where shapes such as inscribed cubes are assumed, have calculated A_{geo} using Eq. 13.3.

$$A_{geo} = 8r^2$$ Eq. 13.3

where r is half of the measured long axis of a given particle (Wygel et al., 2019). Specific sample preparation and procedure for quantifying the particle diameter is dependent upon the method utilised, such as by SEM, XRD or laser particle analysis, and are outlined in their respective supplementary sections.

S13.4 Quality assurance

It is generally considered that suitable certified reference materials for A_{BET} procedures and measurements are seldom available for establishing the absolute calibration of A_{BET} instrumentation, due in part to the lack of smooth materials (or materials with no surface roughness on a scale of Angstroms) that can serve as standards. Approaches to limit operational errors include regular maintenance and checking of vacuum pumping equipment (e.g., degassing filters), O-rings and cell conditions prior to use. The use of gloves is also recommended to avoid contamination to the cells. To address some of the encountered differences in results, many studies that utilise both methods consider grain roughness for data assessment. Grain roughness, or surface roughness, gives an indication of etch pits, macropores and mesopores, surface steps and secondary mineral coatings of a grain. This phenomenon is typically quantified as a roughness factor (Anbeek, 1992; Anbeek et al., 1994; Wolff-Boenisch et al., 2004), shown as A_{BET} / A_{geo}. This roughness factor scaling was also applied by (Beerling et al., 2020), using the Eq. 13.4:

$$\lambda = (\frac{\beta}{\alpha})^d$$ Eq. 13.4

where λ is the roughness, a is the spatial constant related to the scale of BET surface area measurement (10^{-10} m), β is the particle radius and d is the fractal dimension. In general, roughness increases as minerals dissolve (White and Brantley, 2003), and naturally weathered surfaces show higher roughness factors than freshly created surfaces (e.g., by crushing, grinding and milling) (Anbeek, 1992). A number of experimental studies on both natural and freshly ground rocks and minerals have also made an assessment on the suitability of each method for dissolution rate determinations. The discrepancies that are often encountered indicate that neither method gives a wholly accurate measurement of the concentration of reactive surface sites, as surface reactivity is not homogenous. The

selection of the surface area normalising term brings with it an inherent "term of convenience" rather than measuring at the molecular scale the surface area that is actually reacting with ions and dissolving at the moment in time (Hodson, 2006). It can therefore be concluded that no particular method is universally favoured for normalisation. However, depending on the sample type and method of rate determination, or for practical purposes (e.g., resource and time allocation), it is often still mandatory to select the most appropriate normalisation method for a given study.

S13.5 Advantages and disadvantages

The studies of Brantley and Mellott (2000), Renforth et al. (2015) and Delerce et al. (2023) indicate that A_{geo} may be an order of magnitude smaller than those determined through A_{BET} gas adsorption methods. Rimstidt et al. (2012) reviewed forsterite dissolution rate data measured by both A_{geo} and A_{BET}. The rates based on A_{geo} were on the average 5.2 times faster than those based on A_{BET}. Bulk rock dissolution rates determined by Matter et al. (2007) were ~30 times faster than rates determined for forsterite dissolution at the same pH by (Pokrovsky and Schott, 2000), in part attributed to differences in methods used for surface area determination (A_{BET} for Pokrovsky and Schott (2000); A_{geo} for Matter et al. (2007)). Marieni et al. (2020) stated that comparison between their A_{geo}-derived rates could not be made with certain literature rates because the literature examples were normalised to A_{BET} rather than A_{geo}, which may decrease the rates up to two orders of magnitude, depending on grain roughness. The use of different adsorbate gases can also cause different results from A_{BET} measurements (Anbeek, 1992; Brunauer et al., 1969; Chow and Grant, 1988; Gregg and Sing, 1982; Vidick, 1987). Values measured with N_2 may be up to 50% larger than values measured with Kr; Ar may also give lower values than N_2. Findings of these studies indicate that N_2 should be avoided in surface area measurements of mineral samples with specific surface areas below 5 $m^2 g^{-1}$ (Anbeek, 1992).

Due to A_{geo} values typically giving size fraction results that are notably lower than corresponding A_{BET} values, A_{geo}-normalised dissolution rates are often high compared to A_{BET}-normalised rates. It is considered that A_{BET} will incorporate non-accessible surfaces (e.g., pores and voids, etches, surface topography) in the calculations, thus accounting for the "true" complex nature of a given surface. However, the studies of quartz dissolution by Gautier et al. (2001) and Tester et al. (1994) suggest that A_{geo} values correlate as well as, or even better than rate equations based on A_{BET} values. The different approaches of the two methods means that A_{geo} are much less likely to contain large errors in accuracy that are found with A_{BET}, and A_{geo} is considered by many studies to be a more appropriate normalisation method for estimating dissolution rates compared to A_{BET} (Gautier et al., 2001; Hodson, 2006; Marieni et al., 2020; Wolff-Boenisch et al., 2004), particularly for natural samples (Wolff-Boenisch et al., 2004). This is partly due to natural sample surface areas, as measured by A_{BET}, changing as a function of time and sample preparation prior to experiments (Brantley and Chen, 1995). The comparability of A_{BET}-normalised dissolution

rates generated by different researchers or laboratories on the same material may therefore be problematic (Wolff-Boenisch et al., 2004). Analytical errors and discrepancies arising by using different adsorbate gases are also cited as further complications for comparison of A_{BET} normalised dissolution rates from the literature (Brantley and Mellott, 2000; Wolff-Boenisch et al., 2004). As A_{BET} is a laboratory-based method, there are also possibilities to encounter instrumental issues, as well as errors relating to sample preparation and handling.

A_{BET} may overestimate reactive surface area by identifying non-reactive external surfaces (e.g., etch pit walls, coatings and micropores) as reactive. Anbeek (1992) demonstrated that even after grinding, samples from large, naturally weathered mineral fragments may still contain substantial proportions of weathered surfaces (identified as "fresh" reactive surfaces by A_{BET} methods), and thus, previous dissolution studies in terms of fresh A_{BET} may have been misinterpreted. The author also cited literature data that suggests that A_{BET} N_2 measurement of actual surfaces of samples should be avoided. Surface areas as determined by A_{BET} are inherently high due to the effects of non-reactive surface coatings and alteration products, which may be passive or sequester the underlying reactive surface, but ultimately their presence lowers the calculated dissolution rates more so than those of the dissolving mineral (Wolff-Boenisch et al., 2004). In reality, such a non-reactive coating may not affect the overall dissolution rate compared to a more pervasive coating. Anbeek (1992, 1993) noted that the A_{BET} of quartz and feldspar dramatically increases during natural weathering, and that this additional A_{BET} is due to internal non-reactive micropores. Gautier et al. (2001) also observed that an increase in A_{BET} arising during laboratory dissolution of quartz was due to the development of non-reactive etch pit walls.

Variable internal connected porosity of grains also means A_{BET} values may not be appropriately scaled (Brantley and Mellott, 2000). The compilation of kinetic models of White and Peterson (1990) showed that when compared to A_{BET} values, the corresponding least square fits of the A_{geo} normalised dissolution rates with silica content were significantly better. The scatter among the data points shown in the compilation illustrates the difficulty in defining an unambiguous trend among A_{BET} normalised rates, which was not the case for A_{geo} normalised rates (White and Peterson, 1990; Wolff-Boenisch et al., 2004). Additionally, Hodson (2006), noted that, in field studies, it is not possible to measure initial surface area, and only current (or experimental final) areas are available. The author determined that, of the normalising terms tested for anorthite and biotite dissolution rates, A_{geo} and geometric edge surface area respectively, yielded rates that were closest to being constant across the different grain sizes. Hodson (2006) suggested that the initial A_{BET} was the most appropriate for normalising laboratory determined dissolution rates, as this approach best integrated the differences in dissolution rate and area for the basal and edge sites. However, due to the control of edge sites on dissolution (in this instance, biotite dissolution), the final A_{geo} should be the normalising term when comparing laboratory (either closed or open systems) and/or field-based dissolution rates. While initial A_{BET} is suitable before any dissolution occurs, once preferential dissolution begins and grain geometry alters, the constant of proportionality

will vary with number of reactive sites and thus the ratio between a true reactive surface area and A_{BET} will vary with grain size (Hodson, 2006).

Finally, Marieni et al. (2020) experimentally determined A_{geo}-normalised dissolution rates of basaltic rocks. The authors concluded that, between the two surface area measurements, A_{geo} was more consistent with SEM observations of particle size than A_{BET} carried out with N_2. Rates determined by Wolff-Boenisch et al. (2004) were also normalised to A_{geo}, as the method for determination of natural glass dissolution rate was found to be more consistent than normalising rates to A_{BET} (see also Wolff-Boenisch et al. (2004)).

SOP 14 – Determination of total alkalinity of a solution

S14.1 Scope and field of application

The total alkalinity of a solution is a quantity that has had, and continues to have, numerous definitions. A comprehensive definition is provided by (Dickson, 1981) who suggest it is the proton deficiency of a solution relative to an arbitrary acid dissociation zero point of pK 4.5 (at 25°C). Total alkalinity specifically refers to the dissolved aqueous species in a solution. A related property is the 'acid neutralising capacity' of a solution which includes total alkalinity and the acid neutralising properties of suspended sediments. The measurement of total alkalinity is typically expressed in terms of equivalents of acid required to neutralise the alkaline substances in the solution to this dissociation point and defined through Eq. 14.1.

$$TA = \left[HCO_3^-\right] + 2\left[CO_3^{2-}\right] + \left[B(OH)_4^-\right] + \left[OH^-\right] + 2\left[PO_4^{2-}\right] + \left[H_3SiO_4^-\right] + \left[HS^-\right] + 2\left[S^{2-}\right] + \left[NH_3^-\right] - \left[H^+\right] - \left[HSO_4^-\right] - \left[HF\right] - \left[H_3PO_4\right] \quad \text{Eq. 14.1}$$

Total alkalinity is an important parameter in water chemistry and is often used to assess the buffering capacity of natural waters, such as rivers, lakes, and oceans. It helps in maintaining stable pH levels and preventing rapid changes in acidity, which can be harmful to aquatic organisms. For a large number of environmental applications, total alkalinity will largely be derived from HCO_3^-, CO_3^{2-} and OH^- ions (Rounds and Wilde, 2012; Stumm and Morgan, 1981, 1996).

Total alkalinity is measured in a range of environmental monitoring and management applications. It is used to assess soils and sediments, in which it can affect nutrient availability, plant growth, and microbial activity. Monitoring alkalinity levels helps in understanding the impact of pollutants, such as acid rain or industrial waste, on soil and sediment quality (Mayes et al., 2008, 2018). It helps in maintaining appropriate pH levels and alkaline conditions necessary for the health and well-being of aquatic organisms (Hull et al., 2014; Koryak et al., 1998). Industries such as water and wastewater treatment, chemical manufacturing, and food and beverage production require accurate alkalinity measurements to ensure proper process optimisation and product quality.

S14.2 Principle

The measurement of total alkalinity is typically performed through titration using a strong acid, such as sulphuric (H_2SO_4), hydrochloric (HCl) or nitric (HNO_3) acid, and an appropriate method of pH measurement (potentiometric or an indicator). The acid is gradually added to the solution in small increments until the alkaline substances are completely neutralised,

and the point of neutralisation is indicated by a calibrated pH metre of a colour change in the indicator. Best practice for titrating seawater is reported in (Dickson et al., 2007).

S14.3 Sample preparation and procedure

Apparatus and Reagents: The acid can be added manually through a burette or a handheld titrator. Alternatively, there are a range of automatic titrators with the ability to add acid through a calibrated syringe or dosing unit. The receiving vessel containing the sample is conventionally a conical flask, however for the most accurate results, a temperature controlled (e.g., a glass jacketed reactor), well-mixed (automatic stirring) vessel should be used. For pH determination, the most accurate method is through potentiometric using a glass electrode. However, methyl orange indicator is commonly used in Gran titration. For the titrant, a strong acid (e.g., sulphuric, hydrochloric, or nitric), of known concentration (on the order of 0.1 mol kg^{-1} is typical). For the most accurate results, the salinity of the acid should match that of the sample.

Standardisation: The titrant (acid) is standardised by titrating a known volume of the standardisation solution (sodium carbonate). By determining the volume of the titrant required to neutralise the known amount of sodium carbonate, the concentration of the titrant is calculated.

Procedure: A representative filtered (<0.45 µm) water sample is collected in a conical flask (or temperature-controlled vessel). The pH electrode is immersed in the sample solution, or a few drops of the pH indicator are added. The indicator turns yellow in acidic conditions and orange in alkaline conditions. If a stirrer is being used, this should be inserted. The titration begins by slowly adding the titrant from the burette to the water sample, (while swirling the flask continuously if manually stirring). Initially, the alkaline substances in the water sample react with the acid, resulting in the formation of aqueous salts.

The addition of the titrant is continued until the colour of the indicator changes from yellow to a distinct orange, or the measured pH has progressed through its equivalent point (usually between pH 5 and 3). Continued recording of pH is required to identify this. This indicates that the alkalinity has been neutralised and excess acid is present. The volume of the titrant used is recorded for methods that use an indicator.

Calculation: For potentiometric titration, a gran plot can be constructed that plots both the acid and alkaline gran functions (Eq. 14.2 and 14.3).

$$f_{acid} = \left(v_0 + v_i\right) \cdot 10^{-pH_i} \quad \text{Eq. 14.2}$$

$$f_{alkaline} = \left(v_0 + v_i\right) \cdot 10^{pH_i} \quad \text{Eq. 14.3}$$

The total alkalinity of the water sample is calculated based on the volume of the titrant used and its known concentration. The alkalinity should be expressed as equivalents per mass (Eq kg^{-1}) but it is also frequently expressed in milligrams per litre (mg L^{-1}) or parts per million (ppm) of calcium carbonate ($CaCO_3$) equivalent. For automatic titration, it is common for software to identify the largest inflection point on titration curves which will be assigned the titration end-point.

S14.4 Quality assurance

If automated instruments are used for alkalinity analysis, calibration errors (particularly in uncertainties in the dosing increment/volume) or malfunctions in the equipment can introduce errors. Regular maintenance and calibration of instruments are necessary to minimise these uncertainties. User error associated with dosing amount, manual mixing, or judging the change in indicator colour and impact the final results. Water composition can vary spatially and temporally, such that alkalinity levels can change over time or at different locations within a water body. Variations in alkalinity can introduce uncertainties in the measurement, especially when trying to determine the total alkalinity of a large body of water. Inadequate mixing of the water sample during acquisition, contamination from the sampling equipment, or improper storage conditions.

To minimise these errors and uncertainties, it is important to follow standardised procedures for sampling, analysis, and calibration. Certified reference materials should be used to check the accuracy of the measurements. Quality control measures, such as duplicate analyses and regular proficiency testing, can also help ensure the accuracy and reliability of alkalinity measurements.

SOP 15 – Metal, carbon, and oxygen isotopes

S15.1 Scope and field of application

Isotopes fall into two buckets, stable and radiogenic, both of which are useful for quantifying CDR. Radiogenic isotopes undergo spontaneous radioactive decay, with a given half-life. Radiogenic isotopes are not otherwise fractionated by natural processes, such as carbonate formation, making them good provenance tracers as well as dating tools. Stable isotopes do not decay, and are fractionated by secondary processes. Isotope fractionation is a process during which certain isotopes are preferentially taken up by natural processes, such as secondary mineral (e.g., carbonates, clays) formation, but also plants or microorganisms, which then become enriched in the preferentially incorporated isotope. The capability to unmix sources of cations (with radiogenic isotope systems, such as Sr), date sources of carbon (with radiocarbon), and quantify the impact of carbonate and clay formation (using stable metal, carbon and oxygen isotopes) makes isotope geochemistry a powerful tool for monitoring in geochemical CDR, hence CDR efficacy.

The use case of isotope mass spectrometry in CDR is centred on the principle that isotopes are useful for tracing and quantifying sources of carbon contributing to DIC in, for example, an enhanced rock weathering setting. Measuring alkalinity (outlined in SOP 14) provides information on the charge balance constituent made up by CO_2 in solution, and combined with pH (or another carbonate system parameter) can be used to determine the concentration of DIC in a sample. However, not all of this DIC may be derived from the modern atmosphere, a portion of it may be from a geological source of carbon (e.g., shale oxidation Soulet et al. (2021)). Therefore, it is necessary to apportion sources of carbon accurately, such that additionality from a CDR method can be proven to a required level of accuracy. Similar approaches can also be used to examine the sources of other elements critical to carbon sequestration and the alkalinity charge balance. This SOP will focus on the measurement of radiogenic and stable isotopes to carry out this task, which are measured by a series of different types of mass spectrometers, including multi collector inductively coupled plasma mass spectrometers (MC-ICP-MS see SOP 5) for metal isotopes, accelerator mass spectrometers for radiocarbon, and gas-source mass spectrometry for stable oxygen and carbon isotopes.

S15.2 Principle for metal isotopes

MC-ICP-MS involves the ionisation of liquid or solid samples, by introducing the sample particles (either via solution, or as particles from a laser ablation system) into an inductively coupled plasma, which strips electrons and creates M^+ ions, similar to previously explained ICP instruments described in SOP 4 and 5. Ions are accelerated through an electric potential gradient, and focused by slits and electrostatically charged plates. An energy filter ensures a static energy spectrum is passed to the magnetic field. A magnetic sector mass analyzer

then accelerates positively charged ions through a flight tube, allowing them to be separated by mass-to-charge ratios. The mass discriminated beams are then collected by Faraday cups. The high ionisation efficiency of MC-ICP-MS instruments enables measurements of most elements in the periodic table, which other mass spectrometry techniques lack. For example, thermal ionisation mass spectrometry (TIMS) cannot analyse samples with high ionisation potentials, whereas MC-ICP-MS can. In contrast, TIMS can provide better analyses of, for example, the isotopes of some alkaline earth metals (e.g., Ca or Sr isotopes).

S15.3 Instrumentation

A typical MC-ICP-MS has a similar sample introduction system to ICP-OES (SOP 4). Briefly, sample particles are passed through a nebuliser to create a fine aerosol. This aerosol is ionised in an argon plasma, and passed through a series of slits, cones, and plates to filter out undesired ions. Once in the flight tube, a magnetic sector mass analyser accelerates ions, which diffract and are collected separately by Faraday cups. Upon contacting the cup, each ion creates a small voltage. Isotope ratios are calculated by comparing the voltages collected by each Faraday cup. Because mass bias variation across the mass range analysed is constant, adjacent elements can be used to calculate mass bias for elements with more than two isotopes.

S15.3 Sample preparation

Purified, mono-elemental solutions of the isotopes of interest are required for accurate measurement via MC-ICP-MS. Typically, this requires a column chromatography step, to separate the element of interest from the sample matrix. In some cases specialised resins can be used, e.g., Sr can be separated from sample matrices using Eichrom Sr spec resin (Deniel and Pin, 2001), which makes column chromatography very efficient. However, in most cases specialised resins are not available or prohibitively expensive, and non-specialised cation-exchange resins are preferred. After samples are purified by column chromatography they should be dried to a salt, and redissolved in the same solution used for blank measurements during analysis via MC-ICP-MS (typically 2% HNO_3). Laser introduction systems do not have this purification method, and typically are therefore measurements are less precise.

S15.4 Procedure

Sample-standard bracketing (SSB). Mass-bias relationships will change during a given run, usually as a result of environmental factors, this is often referred to as ‘drift’. Mass bias refers to deviation of a measured isotope ratio from the accepted value, resulting from changing transmission of ions according to their masses. Because of this drift it is important to bracket each sample with a standard of a known composition, otherwise known as a bracketing standard. This way, the mass bias relationship is defined before and after a given sample is run, providing a good constraint on how the machine is behaving. Often most drift

is confined to the beginning of a run, and settles with time. If drift is predictably confined to the beginning of a run, it can be prudent to measure a set of standards during this time, rather than samples, sometimes referred to as a 'spin-up' period. This has two benefits i) it allows the machine to stabilise to run conditions, and ii) potentially precious samples are measured after the machine has stabilised, leading to better data.

Double-spike. Sample-standard bracketing has some inherent problems, including that it assumes a linear development of mass bias between the bracketing standards, and that the resulting sample isotope ratios can be strongly affected by both column recovery, and by sample matrix. The first of these, column recovery, is because stable metal isotopes fractionate during column purification. Therefore, it is essential that as close as possible as 100% recovery is achieved, otherwise additional uncertainties will creep in (e.g., observed at ~1.7‰ per 1% loss of yield for Li isotope ratios (Pogge von Strandmann et al., 2021). The second problem with SSB, sample matrix, is when the sample has not been purified to the same degree as the bracketing standards, and other elements or molecules (the matrix) remain. Matrix changes the efficiency of sample ionisation by the plasma torch, which means that an insufficiently purified sample, measured by SSB, may also exhibit additional isotope fractionation.

The most common solution to this problem is to use the double-spike method, which circumvents both column recovery and sample matrix issues. The technique has been available for a while (Dodson, 1963), but only really gained widespread use more recently in metal stable isotope analyses.

The requirement for using double spike is that an isotope system has four or more stable isotopes (e.g., Ca), and, more recently, for some systems that only have three stable isotopes (known as "critical mixture double spiking", as demonstrated for Mg isotopes (Hin et al., 2017). The basic principle of the double spike method is to add a "spike" to the sample, consisting of two artificially enriched isotopes. This sample-spike combination is then passed through the purification columns, and analysed by mass spectrometry (either MC-ICP-MS or TIMS). If the spike composition is known, then the sample composition can then be calculated, without concerns about column yield, sample matrix or mass bias (Rudge et al., 2009).

S15.5 Principle for stable oxygen and carbon isotopes

The measurement of these two isotope systems is one of the keystones of isotope geochemistry, and has been measured via gas source isotope ratio mass spectrometry (IRMS) since the 1940s (Nier, 1940). As the analysis is routine for waters and carbonates, little space is needed. Briefly, oxygen isotope ratios ($^{18}O/^{16}O$, but also $^{17}O/^{16}O$) are analysed on CO_2 or O_2 liberated from the sample. The normalising standard is by convention either Vienna Mean Standard Ocean Water (VSMOW) or the PeeDee Belemnite (PDB) (e.g., Grossman and Klein (1994)).

Stable carbon isotopes ($^{13}C/^{12}C$) are analysed in much the same way, on CO_2 liberated from a sample. Carbon is typically extracted from carbonate by dissolution with H_3PO_4 at a specified temperature, while organic carbon is processed with the use of an oxidising agent (typically CuO or O_2; e.g., Hoefs (2021)). The international normalising standard for stable carbon isotopes is the PeeDee Belemnite (PDB).

S15.6 Principle for radiocarbon analysis

Radiocarbon, ^{14}C, is a radioactive cosmogenic isotope of carbon, with a half-life of 5,730 years. It is continuously produced in the atmosphere from the impact of cosmogenic rays on nitrogen-14 isotopes, and was developed as a dating method in the 1940s. Although originally measured by beta counting, the standard method by now is accelerator mass spectrometry (AMS). This type of mass spectrometry accelerates ions to a very high kinetic energy, which allows both separation and analysis of a minor isotope (in this case ^{14}C, which makes up ~10^{-10} % of all carbon), and can also separate atomic isobars (e.g., ^{14}N from ^{14}C).

Initially during the analysis negative ions are created (which already separates ^{14}N from ^{14}C, because N does not form negative ions). Ions are then further separated in a sector-field mass spectrometer, in much the same way as described above for MC-ICP-MS. The ions then enter an Tandem van de Graaff Accelerator, in which, as well as acceleration, the ions change charge from negative to positive, by passing through a thin foil (a process known as "stripping"). This breaks apart molecules (e.g., ^{13}CH), which would otherwise interfere with the ^{14}C measurements. The positive ions are then further accelerated, to several % of the speed of light, and the ion beam is then multiply focused, and finally analysed by single-ion counting.

S15.7 Data presentation

Absolute measurements of individual isotope concentrations can be difficult to make. Therefore, isotopic abundances are generally expressed as a ratio of different isotopes of the same element. For stable isotopes, the heavier isotope is by convention reported relative to the lighter isotope e.g., $^{13}C/^{12}C$, $^{18}O/^{16}O$, $^{7}Li/^{6}Li$.

A measured isotope ratio of a sample is reported as the difference between the measured isotope ratio and a reference standard of known composition. The standards used are universal, and are determined by the scientific community. For example, stable magnesium isotopes rely on comparison to the dead-sea magnesium 3 (DSM-3) standard (Galy et al., 2003). This is referred to as delta notation (δ), and is expressed as Eq. 15.1.

$$\delta_{sample/STD} = ((R_{sample}/R_{STD}) - 1) \times 1000 \quad \text{Eq. 15.1}$$

where R is the isotope ratio of the sample or standard. Delta notation is reported in per mille (‰). For radiogenic isotopes (e.g., Sr isotopes), the radiogenic isotope is reported relative to a

stable isotope of the same element. For Sr isotopes, that is the radiogenic Sr-87 relative to the stable Sr-86: $^{87}Sr/^{86}Sr$.

S15.8 Quality assurance

Best practice for optimising machine performance will vary between laboratories. Often, reproducible results are obtained by tuning for i) beam sensitivity and ii) beam stability. In this instance, tuning refers to the process of tweaking hardware parameters to produce stable, sensitive beams. Similar to ICP-MS (SOP 5), parameters such as torch position, gas flows and lens position should be optimised. Prior to beginning any run of real samples, a short test to check replicability of a machine standard should be performed.

SOP 16 – Isotope dilution inductively coupled plasma mass spectrometry (ID-ICP-MS)

S16.1 Scope and field of application

Isotope dilution is a technique to reduce the analytical uncertainty on a measurement of the elemental concentration of a sample using inductively coupled plasma mass spectrometry (ICP-MS, see SOP 5). Isotope dilution involves "spiking" a sample with a known amount of an artificially enriched isotope of the element of interest, as with the "double-spike" method in isotope measurement (see SOP 15). The concentration of the element of interest in the sample may then be calculated from the intensity of both isotopes (artificially enriched and naturally abundant) of the element, without the need to use calibration standards. This overcomes most drift and matrix effect issues with ICP-MS that increase analytical uncertainty. ID-ICP-MS is therefore useful where there is a need to limit analytical uncertainty to a minimum in order to resolve a signal of interest. An example of this is in calculating mass loss of a feedstock (such as basalt) that has been mixed into soil and has undergone weathering. The amount of the feedstock, and the difference in the amount of mobile cations within the feedstock as a result of loss through dissolution, is very small relative to the soil background. This means that the resolvability of mass loss signals are significantly improved with reduced analytical error, assuming that a soil sampling protocol is used that can overcome variability in soils (Reershemius et al., 2023).

S16.2 Principle

Isotope dilution involves calculating the concentration of an element of interest in a sample by doping that sample with an isotope spike. This involves making simultaneous measurements of a naturally abundant isotope and an artificially enriched isotope within the sample-spike mixture, as well as measuring the isotopic composition (the ratio of the isotopes in question) of both the sample and the spike. The amount of the element of interest in the sample, n_{sample}, is given by Eq. 16.1:

$$n_{sample} = n_{spike} * \frac{R_{spike} - R_{mixture}}{R_{mixture} - R_{sample}} * \frac{\Sigma^i R^i_{sample}}{\Sigma^i R^i_{spike}} \quad \text{Eq. 16.1}$$

where R is the ratio of the naturally abundant and artificially enriched isotopes of the element of interest, and $\Sigma^i R^i$ is the sum of ratios of all isotopes of the element of interest to a reference isotope, i (Evans and Clough, 2005; Inghram, 1954). As this relies on measuring two

stable isotopes of an element, isotope dilution cannot be used for mono-isotopic elements (e.g., Na).

S16.3 Instrumentation

ID-ICP-MS can be done using any ICP-MS capable of measuring multiple stable isotopes of an element of interest. This is true of most magnetic sectors and multi-quadrupole ICP-MS. See SOP 5 for more details.

Initial characterisation and calibration of the isotope spike used for ID-ICP-MS (typically a digested carbonate or oxide) usually requires higher precision and should therefore be carried out on a multi-collector ICP-MS (see SOP 15).

S16.4 Procedure

Samples are prepared for ID-ICP-MS in the same way as for other ICP-MS analysis (usually a strong acid digest of a solid sample; see SOP 3), but with the addition of a known amount of isotope spike during the digestion step. This homogenises the mixture and equilibrates the spike with the sample (Stracke et al., 2014). Multi-element spikes may be used, though care should be taken to ensure that the ratio of concentrations of elements in the spike solution approximates that found in the sample to avoid error magnification, should the isotope ratio in the sample-spike mixture be similar to that in the spike or sample itself (Willbold and Jochum, 2005). The ratio in elemental concentration of the sample and added spike is key to minimising uncertainty; the optimum sample/spike ratio is a function of the isotopic composition of both the sample and the spike, and can be solved for (Webster, 1960); and see Stracke et al. (2014).

Following digestion and homogenisation, samples are brought up in dilute strong acid to run on ICP-MS (see SOP 5). In most cases, it is not necessary to separate elements using column chromatography before analysis (see SOP 15), as it is possible with ID-ICP-MS to analyse multiple elements simultaneously to the degree of precision and accuracy required (Willbold and Jochum, 2005).

S16.5 Data presentation

As in SOP 5, data is returned as an intensity signal for each measured isotope. Because calculating the concentration of an element in the sample relies only on the measured isotopic ratio of the naturally abundant isotope and the artificially enriched isotope, no conversion from intensity to concentration is required. As a result, ID-ICP-MS can be considered a primary method of analysis (Stracke et al., 2014).

S16.6 Quality assurance

See SOPs 5 and 15 for best practice with ICP-MS. As for other ICP-MS methods, a blank correction should be performed prior to using intensity data; and standards, prepared in the same way as samples, should be run alongside samples throughout a run. Additionally, if other elements are being measured using more conventional approaches to calculating concentration from ICP-MS alongside those measured with ID-ICP-MS, the spike solution should be analysed for trace element concentration; if blanks are prepared without addition of a spike, then a correction for the spike should be also applied.

SOP 17 – Ion chromatography

S17.1 Scope and field of application

Ion chromatography (IC) is an analytical technique used for the separation, identification, and quantification of charged ions in water samples. It is based on the principles of liquid chromatography, where the separation is achieved by exploiting interactions between analyte ions and a stationary phase. IC is commonly used in the analysis of natural water samples to determine the concentration of various cations and anions. For instance, the measurement of common anions such as chloride (Cl^-), sulphate (SO_4^{2-}), nitrate (NO_3^-), and phosphate (PO_4^{3-}) in drinking water to assess water quality and compliance with regulatory standards (Hautman and Munch, 1997). Analysis of anions like bromide (Br^-), iodide (I^-), and fluoride (F^-) in groundwater and surface water (Neal et al., 2007). Monitoring of anions in wastewater and industrial effluents to assess pollution levels and compliance with discharge limits (Jackson, 2000). Analysis of ions, including nitrate, ammonium and phosphate, in agricultural runoff and surface water to evaluate the impact of fertilisers and agricultural practices on water quality and potential eutrophication (Han et al., 2012). Identification and quantification of anions, including chlorate (ClO_3^-), perchlorate (ClO_4^-), and chromate (CrO_4^{2-}) in water samples to assess contamination from industrial activities, mining operations, and landfill leachates (Jackson, 2001).

Ion chromatography has two primary uses in geochemical CDR:

1. the identification of solutes (particularly HCO_3^-, CO_3^{2-}, SO_4^{2-}, NO_2^-, NO_3^-) in drainage or pore waters associated with a geochemical CDR approach (Larkin et al., 2022). This information is useful for quantifying CO_2 removal as carbonate and bicarbonate, assessing the contribution of other base weathering agents, and calculating charge balance of a solution with cations determined through ICP for data quality control (Appelo and Postma, 2004).
2. the identification of organic acid molecules (e.g., citrate, malate) in weathering environments (both in the laboratory and the field) to assess their contribution to mineral dissolution (Bylund et al., 2007; Krevor and Lackner, 2011; Renforth and Manning, 2011; Teir et al., 2007).

S17.2 Principle

IC relies on the different interactions between analyte ions and a stationary phase (e.g., an exchange resin) to achieve temporal separation. The stationary phase of an ion chromatography column contains ion exchange sites. These sites can be either positively charged (to interact and exchange with anions) or negatively charged. For example, diethylaminoethyl-cellulose is commonly used for anion exchange. The ion exchange sites

interact selectively with analyte ions based on their charge and affinity, allowing for separation.

The mobile phase in ion chromatography is typically an aqueous solution containing an eluent. The eluent is carefully chosen to facilitate the separation of target analyte ions. It may consist of a buffered solution, an ion-pairing reagent, or an ion-suppressing reagent. The eluent interacts with the stationary phase and helps to control the retention and elution of analyte ions. For major anions, Br^-, Cl^-, F^-, NO_3^-, NO_2^-, PO_4^{3-}, SO_4^{2-}, Lobato (2010) suggest a 0.5 molar solution of sodium carbonate/bicarbonate.

The sample is injected into the ion chromatography system using an injector or autosampler. It is then carried by the mobile phase onto the separation column. As the sample flows through the column, the analyte ions interact with the stationary phase. Analyte ions that have a stronger affinity for the ion exchange sites will have longer retention times, leading to their separation from other ions in the sample.

Elution is achieved by manipulating the composition and strength of the mobile phase. This can be done through the use of gradient elution, where the eluent composition is changed over time, or isocratic elution, where a constant eluent composition is maintained throughout the analysis. Elution conditions are optimised to ensure efficient and complete separation of analyte ions.

Once the analyte ions elute from the column, they are detected by a suitable detector. Commonly used detectors in ion chromatography include conductivity detectors, UV-Vis detectors, and amperometric detectors. The choice of detector depends on the specific analyte ions and their detection requirements. The detector generates a signal proportional to the concentration of the analyte ions, which is recorded for further analysis.

S17.3 Instrumentation

IC instruments are designed to perform the separation, detection, and analysis of ions in various samples. While specific features and configurations may vary among different manufacturers and models, here is a detailed description of the typical form and function of ion chromatography instruments.

Exchange column. The IC instrument is built around the exchange column. It consists of a tube packed with a stationary phase that facilitates the separation of analyte ions based on their interactions with the ion exchange sites.

Mobile phase handling. A pump is used to deliver a mobile phase from a reservoir to and through the exchange column at a controlled flow rate. It ensures the consistent movement of the sample through the separation column. A manual or automatic injector is used to introduce the sample into the mobile phase.

Detector. A sensor is used for detecting the separated analyte ions. Commonly used detectors include conductivity and UV-Vis metres. The detector generates a signal proportional to the concentration of the analyte ions.

Data acquisition system and software. IC instruments are typically equipped with a data acquisition system that records and processes the signals from the detector allowing for collection and analysis of the chromatographic data. Dedicated software is used to control the instrument, acquire, and process data, and perform data analysis. The software enables method development, calibration, and quantification of analyte concentrations.

S17.4 Sample preparation

Proper sample preparation involves filtration, dilution, and removal of interfering substances. Filtration is often necessary to remove particulate matter and ensure a clear sample. Use a suitable filter, such as a syringe filter or a membrane filter, with an appropriate pore size (<0.45 µm) to remove particles. Select the filter material based on the analytes of interest and the sample matrix to avoid adsorption or interference (e.g., cellulose acetate for major anions). Approximately 1–10 mL of sample is required for the analysis.

Depending on the analytes and the separation conditions, it may be necessary to adjust the pH of the water sample. This is done to optimise the separation and retention of target analyte ions on the ion exchange column. Use acids (e.g., hydrochloric acid) or bases (e.g., sodium hydroxide) to adjust the pH, if needed. It is essential to carefully monitor and control the pH adjustment process. This pH may result in a change in the concentration of carbonate/bicarbonate anions. The pH of the sample can be modified by carefully and slowly adding small drops of acid/base while continuously mixing and monitoring the pH (e.g., with a glass electrode pH metre).

Dilution may be necessary if the analyte concentrations in the sample exceed the linear range of the calibration curve or fall outside the detection limits of the instrument. Determine the appropriate dilution factor based on the expected analyte concentrations and the desired detection range. Perform dilutions using deionized water or a suitable blank matrix.

Some water samples may contain interfering substances, such as organic matter, surfactants, or metal ions, which can affect the IC analysis. These substances can cause peak distortion, loss of resolution, or detector interference. Additional sample pretreatment techniques may be useful, such as solid-phase extraction or liquid-liquid extraction, to remove interfering substances before the IC analysis. These techniques selectively retain the analytes of interest while removing unwanted compounds.

S17.5 Procedure

1. Ensure that the IC instrument is properly set up, calibrated, and in good working condition.
2. Check the mobile phase composition and its compatibility with the separation column and detector.
3. Verify that the detector is functioning correctly and that the appropriate detection parameters (e.g., wavelength, sensitivity) are set.
4. Prior to sample analysis, it is necessary to equilibrate the separation column with the mobile phase to establish stable and reproducible chromatographic conditions.
5. Run the mobile phase through the column at the desired flow rate for a sufficient time (typically 15–30 minutes) to achieve equilibrium.
6. Prepare the sample for injection according to the sample preparation guidelines specific to the analysis (as detailed in the previous response).
7. Use an autosampler or manual injection to introduce the prepared sample into the IC system.
8. Ensure that the injection volume is appropriate for the sensitivity and dynamic range of the method, considering the target analyte concentrations.
9. The mobile phase carries the sample onto the separation column, where the separation of analyte ions occurs.
10. Monitor the separation process using real-time chromatographic data displayed on the instrument's control software or monitor.
11. Adjust the eluent composition or gradient program if necessary to optimise the separation and achieve good resolution between analyte peaks.
12. As the analyte ions elute from the separation column, they pass through the detector, which generates signals corresponding to their concentrations.
13. Ensure that the detector settings, such as sensitivity, wavelength, or electrode potentials, are appropriately adjusted for the specific analytes and detection techniques being used.
14. The data acquisition system records the detector signals, creating a chromatogram that represents the separation and detection of analyte peaks.

S17.6 Data presentation

The recorded signals from the detector are processed and analysed using dedicated software or chromatography data systems. Quantification of analyte ions is typically performed by comparing their peak areas or heights to calibration standards or internal standards. The concentration of each analyte ion in the sample is then calculated based on calibration curves or known standards.

S16.7 Quality assurance

Implement appropriate quality control measures throughout the measurement process, including replicate analyses, spike recovery tests, and analysis of certified reference materials. Verify that the obtained results fall within acceptable limits and meet the required precision and accuracy criteria. A final report should summarise the analysed sample information, identified analytes, and their respective concentrations, as well as any relevant quality control information. It is important to follow the specific guidelines and operating instructions provided by the instrument manufacturer, as instrument setup, method parameters, and software functionalities may vary depending on the specific IC system being used. Regular maintenance and periodic calibration of the instrument are also essential to ensure reliable and consistent measurements.

Symbols and abbreviated terms

σ	Standard deviation
A_{BET}	Specific surface area determined by BET
A_{geo}	Specific geometric surface area
AAS	Atomic absorption spectroscopy
ACC	Amorphous calcium carbonate
AFM	Atomic force microscopy
AMS	Accelerator mass spectrometry
AMU	Atomic mass units
BEC	Background equivalent concentration
BECCS	Bioenergy with carbon capture and storage
BES	Backscattered electrons
BSI	British Standards Institute
C_{pot}	Carbonation potential
C_U	Coefficient of uniformity
CCS	Carbon capture and storage
CCU	Carbon capture and utilisation
CDR	Carbon dioxide removal
CL	Cathodoluminescence
CRMs	Certified reference materials
d	Distance between planes of atoms within the crystal structure
DSM-3	Dead-sea magnesium 3

DI	Deionised water
DIC	Dissolved inorganic carbon
DRIFTS	Diffuse reflectance infrared Fourier transform spectroscopy
DSC	Differential scanning calorimetry
e	Void ratio
E_{avoided}	CO_2eq prevented from reaching the atmosphere
E_{LC}	CO_2eq generated during activity life cycle
$E_{removed}$	CO_2eq removed from the atmosphere
E_{pot}	Enhanced weathering potential
EDXRF	Energy dispersive X-ray fluorescence
EPMA	Electron probe microanalysis
EW	Enhanced weathering
ESEM	Environmental scanning electron microscopy
FEG	Field emission gun
FTIR	Fourier transform infrared spectroscopy
ΔG_f	Free energy change of formation
G_s	Specific gravity
GHGs	Greenhouse gases
GSC	Geological Survey of Canada
ΔH_f	Enthalpy change of formation
HDPE	High-density polyethylene
IC	Ion chromatography
ICP-MS	Inductively coupled plasma mass spectrometry
ICP-OES	Inductively coupled plasma optical emission spectroscopy

ID-ICP-MS	Isotope dilution inductively coupled plasma mass spectrometry
IAEA	International Atomic Energy Agency
ISO	International Organisation for Standardisation
λ	Wavelength
LCA	Life cycle assessment
LCIA	Life cycle impact assessment
LoD	Limit of detection
LOI	Loss on ignition
M_x	Molar mass of substance *X*
MQ	Milli-Q water
MRV	Monitoring, reporting and verification
MSDS	Material safety data sheet
MS	Mass spectrometry
η	Parameter to correct for CO_2 buffering effects during EW
n	Porosity
NET	Negative emissions technology
NIST	National Institute of Standards and Technology
OAE	Ocean alkalinity enhancement
ρ_b	Bulk density of solid
ρ_w	Water density
P_{80}, P_{10}, etc.	Particle size for which 80% (10%, etc.) of the material passes
PDB	PeeDee Belemnite
PDF	Powder diffraction file
PSD	Particle size distribution
PXRD	Powder X-ray diffraction
QEMSCAN	Quantitative evaluation of materials by scanning electron

	microscopy
S_r	Saturation ratio
SDD	Silicon drift detectors
SE	Secondary electrons
SEM	Scanning electron microscopy
SEM-EDX	Scanning electron microscopy energy dispersive X-ray analysis
SOP	Standard operating procedure
SSB	Sample-standard bracketing
θ	Angle between the incident X-ray and the plane of the crystal surface
TA	Total alkalinity
TDS	Total dissolved solids
TGA	Thermogravimetric analysis
TGA-MS	Thermogravimetric analysis mass spectrometry
TIMS	Thermal ionisation mass spectrometry
USGS	United States Geological Survey
VSMOW	Vienna Mean Standard Ocean Water
VVB	Validation and verification body
w	Moisture content
WDX	Wavelength-dispersive X-ray spectroscopy
XRD	X-ray diffraction
XRF	X-ray fluorescence
Z	Atomic number

Glossary

Accuracy is the closeness of agreement between a single test result and the accepted reference value. However, for a set of values, accuracy has contributions from *bias* and *precision*.

Additionality refers to the extent to which a CDR project or activity achieves removals that are additional to what would have occurred in the absence of the project.

Bias difference between the mean value of a large number of test results and the accepted reference value for a test material.

Carbonate minerals means minerals characterised by the presence of the carbonate ion (CO_3^{2-}) in their structure. Carbonate minerals include calcite ($CaCO_3$), aragonite ($CaCO_3$), magnesite ($MgCO_3$), siderite ($FeCO_3$), ankerite ($Ca(Fe,Mg,Mn)(CO_3)_2$), and dolomite ($CaMg(CO_3)_2$).

Carbon Dioxide Removal means anthropogenic activities that seek to remove CO_2 from the atmosphere and durably store it in geological, terrestrial or ocean reservoirs, or in products. CO2 is removed from the atmosphere by enhancing biological or geochemical carbon sinks or by direct capture of CO_2 from air and storage (DAC+S).

Carbon mineralisation is the process of turning CO_2 into carbonate minerals (aka mineral carbonation). There are three forms of carbon mineralisation: in situ, ex situ and surficial.

Characteristic value That value of a property corresponding to an acceptable percentage of defects, generally 10 %, but 5 % for the lower strength limits.

Direct Air Capture is a technological process for removing and concentrating CO_2 from air.

Dynamic range refers to the range of concentrations an instrument can read, from the minimum to the maximum detectable. The minimum detectable concentration is determined by signal-to-noise and signal-to-blank ratios. The maximum detectable concentration is determined by the compound's chemistry and instrument capabilities.

Enhanced weathering process that aims to accelerate the natural weathering by spreading finely ground rock, usually silicates.

Fluorescence is brought about by absorption of photons in the singlet ground state promoted to a singlet excited state. The spin of the electron is still paired with the ground state electron, unlike phosphorescence. As the excited molecule returns to ground state, it involves the emission of a photon of lower energy, which corresponds to a longer wavelength, than the absorbed photon.

Inter-laboratory reproducibility studies refer to experiments or tests conducted by multiple laboratories or research groups to evaluate the consistency and reliability of scientific findings across different settings.

Limit of detection is a signal that is three times greater than the standard deviation of blank runs. $LoD = 3 * SD_{blanks}$

Limit of quantitation is a signal that is three times greater than the standard deviation of blank runs. $LoQ = 10 * SD_{blanks}$

Linear range is the range over which there is a directly proportional relationship between analyte concentration and the signal.

Measurand A quantity, object, or property intended to be measured.

Measurement, reporting, and verification refers to the multi-step process to measure the amount of greenhouse gas (GHG) emissions reduced by a specific mitigation activity, over a period of time, and report these findings to an accredited third party. The third party then verifies the report so that the results can be certified, and carbon credits can be issued.

Mineral carbonation, also known as carbon mineralisation, is a process that involves the long-term storage of CO_2 by converting it into a solid mineral form.

Morphology The size, shape and physicochemical structure of particles.

Ocean alkalinity enhancement is an approach to carbon removal that involves adding alkaline substances to seawater to accelerate the ocean's natural carbon sink.

Precision is the closeness of results obtained under stipulated repeat conditions. Precision only relates to the distribution of random errors and not the true value. Precision is determined by calculating the standard deviation of repeat measurements.

Qualitative The determination of non-numerical information about a chemical species, or physical property.

Quantitative The determination of numerical information about a chemical species, or physical property.

Quality assessment The overall system of activities whose purpose is to provide assurance that quality control is being done effectively. It provides a continuing evaluation of the quality of the analyses and of the performance of the analytical system.

Quality assurance constitutes the system by which an analytical laboratory can assure outside users that the analytical results they produce are of proven and known quality.

Quality control The overall system of activities whose purpose is to control the quality of a measurement so that it meets the needs of users. The aim is to ensure that data generated are of known accuracy to some stated, quantitative degree of probability, and thus provides quality that is satisfactory, dependable, and economic.

Resolution The shortest distance between two points that can be independently resolved.

Repeatability is a measure of the ability of the method to generate similar results for multiple tests of the same test material under identical conditions.

Reproducibility is a measure of the ability of the method to generate similar results for multiple tests of the same sample under different conditions (e.g., different operators, different apparatus, different laboratories, different time).

Robustness (or ruggedness) The extent to which a method can be changed without seeing significant changes in the results.

Selectivity refers to the extent to which a method can be used to determine particular analytes in mixtures or matrices without interference from other components of similar behaviour.

Spiking refers to the act of adding a known amount of a known substance to a sample in order to evaluate the performance of an analytical method.

Working range The working range is the range where the method gives results with an acceptable uncertainty. A working range can be wider than a linear range.

X-rays are a short wavelength (high energy-high frequency) form of electromagnetic radiation inhabiting the region between gamma rays and ultraviolet radiation.

References

Alexander L and Klug HP (1948) Basic Aspects of X-Ray Absorption in Quantitative Diffraction Analysis of Powder Mixtures. *Analytical chemistry* 20(10). American Chemical Society: 886–889. DOI: 10.1021/ac60022a002.

AlKhatib M and Eisenhauer A (2017a) Calcium and strontium isotope fractionation during precipitation from aqueous solutions as a function of temperature and reaction rate; II. Aragonite. *Geochimica et cosmochimica acta* 209. Elsevier: 320–342. DOI: 10.1016/j.gca.2017.04.012.

AlKhatib M and Eisenhauer A (2017b) Calcium and strontium isotope fractionation in aqueous solutions as a function of temperature and reaction rate; I. Calcite. *Geochimica et cosmochimica acta* 209. Elsevier: 296–319. DOI: 10.1016/j.gca.2016.09.035.

Amacher MC and Brown RW (2000) Chapter 13 Mine waste characterization. In: BarcelÓ D (ed.) *Techniques and Instrumentation in Analytical Chemistry*. Elsevier, pp. 585–622. DOI: 10.1016/S0167-9244(00)80019-0.

Amann T and Hartmann J (2022) Carbon Accounting for Enhanced Weathering. *Frontiers in Climate* 4. DOI: 10.3389/fclim.2022.849948.

Amann, T, Hartmann, J, Struyf, E, et al. 2020. Enhanced Weathering and related element fluxes–a cropland mesocosm approach. Biogeosciences, 17(1), pp.103-119.

Anbeek C (1992) Surface roughness of minerals and implications for dissolution studies. *Geochimica et cosmochimica acta* 56(4). Elsevier: 1461–1469. DOI: 10.1016/0016-7037(92)90216-6.

Anbeek C (1993) The effect of natural weathering on dissolution rates. *Geochimica et cosmochimica acta* 57(21). Elsevier: 4963–4975. DOI: 10.1016/S0016-7037(05)80002-X.

Andrews JE (2006) Palaeoclimatic records from stable isotopes in riverine tufas: Synthesis and review. *Earth-Science Reviews* 75(1). Elsevier: 85–104. DOI: 10.1016/j.earscirev.2005.08.002.

Andrews, JE, Gare, SG and Dennis, PF, 1997. Unusual isotopic phenomena in Welsh quarry water and carbonate crusts. Terra Nova, 9(2), pp.67-70.

Appelo CAJ and Postma D (2004) *Geochemistry, Groundwater and Pollution*. CRC Press. Available at: https://play.google.com/store/books/details?id=cKq2DQAAQBAJ.

Arcusa S and Sprenkle-Hyppolite S (2022) Snapshot of the Carbon Dioxide Removal certification and standards ecosystem (2021–2022). *Climate Policy* 22(9-10). Taylor & Francis: 1319–1332. DOI: 10.1080/14693062.2022.2094308.

Ausra R (2023) Certification of carbon removals. EPRS: European Parliamentary Research Service. Available at: https://policycommons.net/artifacts/3834624/certification-of-carbon-removals/4640531/ (accessed 25 July 2023).

Bach LT (2023) The additionality problem of Ocean Alkalinity Enhancement. *Biogeosciences Discussions*. DOI: 10.5194/bg-2023-122.

Balaram V and Subramanyam KSV (2022) Sample preparation for geochemical analysis: Strategies and significance. *Advances in Sample Preparation* 1. Elsevier: 100010. DOI: 10.1016/j.sampre.2022.100010.

Bao SD (2000) Soil and agricultural chemistry analysis. Beijing: China agriculture press.

Bardestani R, Patience GS and Kaliaguine S (2019) Experimental methods in chemical engineering: specific surface area and pore size distribution measurements—BET, BJH, and DFT. *The Canadian journal of chemical engineering* 97(11). Wiley: 2781–2791. DOI: 10.1002/cjce.23632.

Barros AI, Pinheiro FC and Nóbrega JA (2020) Space charge effects and internal standardization in a four ion lenses interface: What is changing in quadrupole inductively coupled plasma mass spectrometry? *Spectrochimica acta. Part B: Atomic spectroscopy* 167. Elsevier: 105825. DOI: 10.1016/j.sab.2020.105825.

Becker J. Sabine, Zoriy M, Matusch A, et al. (2010) Bioimaging of metals by laser ablation inductively coupled plasma mass spectrometry (LA-ICP-MS). *Mass spectrometry reviews* 29(1). Wiley: 156–175. DOI: 10.1002/mas.20239.

Beckingham LE, Mitnick EH, Steefel CI, et al. (2016) Evaluation of mineral reactive surface area estimates for prediction of reactivity of a multi-mineral sediment. *Geochimica et cosmochimica acta* 188. Elsevier: 310–329. DOI: 10.1016/j.gca.2016.05.040.

Beerling DJ, Kantzas EP, Lomas MR, et al. (2020) Potential for large-scale CO_2 removal via enhanced rock weathering with croplands. *Nature* 583(7815): 242–248. DOI: 10.1038/s41586-020-2448-9.

Beerling DJ, Epihov DZ, Kantola IB, et al. (2023) Enhanced weathering in the U.S. Corn Belt delivers carbon removal with agronomic benefits. *arXiv [physics.soc-ph]*. Available at: http://arxiv.org/abs/2307.05343.

Benhelal, E, Rashid, MI, Rayson, et al. 2018. Study on mineral carbonation of heat activated lizardite at pilot and laboratory scale. Journal of CO_2 Utilization, 26, pp.230-238.

Benhelal, E., Rashid, M.I., Rayson, et al. 2019a. Direct aqueous carbonation of heat activated serpentine: discovery of undesirable side reactions reducing process efficiency. Applied Energy, 242, pp.1369-1382.

Benhelal, E, Rashid, MI, Rayson, et al. 2019b. "ACEME": Synthesis and characterization of reactive silica residues from two stage mineral carbonation Process. Environmental Progress & Sustainable Energy, 38(3), p.e13066.

Bijma, J, Smet, I, Hagens, M, Hartmann, J, Steffens, R and Paessler, D, 2021, July. Field trials of enhanced weathering combined with corn farming in Germany. In Goldschmidt2021 Virtual Conference (4-9 July).

Black JR, Yin Q-Z and Casey WH (2006) An experimental study of magnesium-isotope fractionation in chlorophyll-a photosynthesis. *Geochimica et cosmochimica acta* 70(16). Elsevier: 4072–4079. DOI: 10.1016/j.gca.2006.06.010.

Blaine RL and Fair PG (1983) Estimate of the 'true' magnetic transition temperatures for the ICTA reference materials GM761. *Thermochimica acta* 67(2). Elsevier: 233–240. DOI: 10.1016/0040-6031(83)80103-8.

Blight GE (2009) *Geotechnical Engineering for Mine Waste Storage Facilities*. CRC Press.

Bobicki ER, Liu Q, Xu Z, et al. (2012) Carbon capture and storage using alkaline industrial wastes. *Progress in Energy and Combustion Science* 38(2). Elsevier: 302–320. DOI: 10.1016/j.pecs.2011.11.002.

Bodénan F, Bourgeois F, Petiot C, et al. (2014) Ex situ mineral carbonation for CO_2 mitigation: Evaluation of mining waste resources, aqueous carbonation processability and life cycle assessment (Carmex project). *Minerals engineering* 59. Elsevier: 52–63. DOI: 10.1016/j.mineng.2014.01.011.

Boggs S and Krinsley D (2006) *Application of Cathodoluminescence Imaging to the Study of Sedimentary Rocks*. Cambridge University Press. Available at: https://play.google.com/store/books/details?id=4F6d-LzYObYC.

Brantley SL (2008) Kinetics of Mineral Dissolution. In: Brantley SL, Kubicki JD, and White AF (eds) *Kinetics of Water-Rock Interaction*. New York, NY: Springer New York, pp. 151–210. DOI: 10.1007/978-0-387-73563-4_5.

Brantley SL and Chen Y (1995) Chemical weathering rates of pyroxenes and amphiboles. *Reviews in Mineralogy and Geochemistry* 31(1). GeoScienceWorld: 119–172. Available at: https://pubs.geoscienceworld.org/msa/rimg/article-abstract/31/1/119/110588 (accessed 31 July 2023).

Brantley SL and Mellott NP (2000) Surface area and porosity of primary silicate minerals. *The American mineralogist* 85(11-12). GeoScienceWorld: 1767–1783. DOI: 10.2138/am-2000-11-1220.

Briggs PH (2002) The determination of forty elements in geological and botanical samples by inductively coupled plasma-atomic emission. *US Geological Survey Open-File Report*.

Brimhall GH and Dietrich WE (1987) Constitutive mass balance relations between chemical composition, volume, density, porosity, and strain in metasomatic hydrochemical systems: Results on weathering and pedogenesis. *Geochimica et cosmochimica acta* 51(3). Elsevier: 567–587. DOI: 10.1016/0016-7037(87)90070-6.

British Standards Institution (1995) *Soil Quality. Chemical Methods. Determination of Carbonate Content. Volumetric Method*. BS 7755-3.10:1995, 15 October. London, UK: British Standards Institution. Available at: https://play.google.com/store/books/details?id=cLu-PQAACAAJ.

British Standards Institution (2009) *Characterization of Waste and Soil. Determination of Elemental Composition by X-Ray Fluorescence*. BS EN 15309:2007, 31 May. London, UK: British Standards Institute. Available at: https://play.google.com/store/books/details?id=abzXnAEACAAJ.

British Standards Institution (2015) *Code of Practice for Ground Investigations*. BS 5930. London, UK: British Standards Institution.

British Standards Institution (2018) *Water quality - general requirements and performance test procedures for water monitoring equipment - measuring devices*. BS EN 17075. London, UK: British Standards Institution.

British Standards Institution (2021) *Methods of Test for Soils for Civil Engineering Purposes: Part 2. Classification tests and determination of geotechnical properties*. BS 1377-2. London, UK: British Standards Institution. Available at: https://www.bsigroup.com/en-GB/standards/bs-1377-2/.

British Standards Institution (2023) *Water quality. Performance requirements and conformity test procedures for water monitoring equipment. Automatic sampling devices (samplers) for water and waste water*. BS EN 16479. London, UK: British

Standards Institution.

Brown ME and Galwey AK (1989) Arrhenius parameters for solid-state reactions from isothermal rate-time curves. *Analytical chemistry* 61(10). ACS Publications: 1136–1139.

Bruckman VJ and Wriessnig K (2013) Improved soil carbonate determination by FT-IR and X-ray analysis. *Environmental chemistry letters* 11(1): 65–70. DOI: 10.1007/s10311-012-0380-4.

Brunauer S, Emmett PH and Teller E (1938) Adsorption of Gases in Multimolecular Layers. *Journal of the American Chemical Society* 60(2). American Chemical Society: 309–319. DOI: 10.1021/ja01269a023.

Brunauer S, Skalny J and Bodor EE (1969) Adsorption on nonporous solids. *Journal of colloid and interface science* 30(4). Elsevier: 546–552. DOI: 10.1016/0021-9797(69)90423-8.

Buckingham, FL, Henderson, GM, Holdship, P et al. 2022. Soil core study indicates limited CO2 removal by enhanced weathering in dry croplands in the UK. Applied Geochemistry, 147, p.105482.

Buckman J, Bankole SA, Zihms S, et al. (2017) Quantifying Porosity through Automated Image Collection and Batch Image Processing: Case Study of Three Carbonates and an Aragonite Cemented Sandstone. *Geosciences Journal* 7(3). Multidisciplinary Digital Publishing Institute: 70. DOI: 10.3390/geosciences7030070.

Buckman J, Mahoney C, Bankole S, et al. (2018) Workflow model for the digitization of mudrocks. *Geological Society, London, Special Publications* 484: 165–187. DOI: 10.1144/SP484.2.

Buckman J, Charalampidou E-MC, Zihms S, et al. (2019) High-resolution large area scanning electron microscopy: an imaging tool for porosity and diagenesis of carbonate rock systems. In: *Carbonate Pore Systems: New Developments and Case Studies*. Society for Sedimentary Geology. Available at: https://research-portal.uws.ac.uk/en/publications/high-resolution-large-area-scanning-electron-microscopy-an-imagin (accessed 31 July 2023).

Buckman JO, Corbett PWM and Mitchell L (2016) Charge Contrast Imaging (CCI): Revealing Enhanced Diagenetic Features of A Coquina Limestone. *Journal of Sedimentary Research* 86(6). GeoScienceWorld: 734–748. DOI: 10.2110/jsr.2016.20.

Bui M and Mac Dowell N (2022) *Greenhouse Gas Removal Technologies* (M Bui and N Mac Dowelleds). Energy and Environment Series. Royal Society of Chemistry.

Buseck PR and Bradley JP (1982) Electron beam studies of individual natural and anthropogenic microparticles: Compositions, structures, and surface reactions. In: *Heterogeneous Atmospheric Chemistry*. Geophysical monograph. Washington, D. C.: American Geophysical Union, pp. 57–76. DOI: 10.1029/gm026p0057.

Bylund D, Norström SH, Essén SA, et al. (2007) Analysis of low molecular mass organic acids in natural waters by ion exclusion chromatography tandem mass spectrometry. *Journal of chromatography. A* 1176(1-2). Elsevier: 89–93. DOI: 10.1016/j.chroma.2007.10.064.

Campbell JS (2019) Decomposition of carbonates in capture of carbon dioxide from ambient air. open.library.ubc.ca. Available at: https://open.library.ubc.ca/soa/cIRcle/collections/ubctheses/24/items/1.0387012.

Campbell JS, Foteinis S, Furey V, et al. (2022) Geochemical Negative Emissions Technologies: Part I. Review. *Frontiers in Climate* 4. frontiersin.org. DOI: 10.3389/fclim.2022.879133.

CarbonPlan (2022) CDR verification framework. Available at: https://carbonplan.org/research/cdr-verification (accessed 25 July 2023).

CarbonPlan (2023) Industry call for CDR Standards Initiative. Available at: https://carbonplan.org/blog/cdr-standards-call (accessed 25 July 2023).

Caserini S, Pagano D, Campo F, et al. (2021) Potential of Maritime Transport for Ocean Liming and Atmospheric CO_2 Removal. *Frontiers in Climate* 3(April): 1–18. DOI: 10.3389/fclim.2021.575900.

Chadwick OA, Brimhall GH and Hendricks DM (1990) From a black to a gray box — a mass balance interpretation of pedogenesis. *Geomorphology* 3(3-4). Elsevier BV: 369–390. DOI: 10.1016/0169-555x(90)90012-f.

Charles B and Fredeen KJ (1997) Concepts, instrumentation and techniques in inductively coupled plasma optical emission spectrometry. *Perkin Elmer Corp* 3(2). researchgate.net. Available at: https://www.researchgate.net/profile/Gunawan-Indrayanto/post/Can_anybody_provide_notes_for_AAS_and_ICP-OES_spectroscopy_in_brief_format/attachment/59d633fe79197b8077991a97/AS%3A377365747257344%401466982413427/download/ICP-OES-Booklet.pdf.

Chow KY and Grant DJW (1988) Surface analysis of griseofulvin powders by krypton adsorption: Evaluation of specific surface area, BET constant C and polanyi adsorption potential. *Powder Technology* 56(3). Elsevier: 209–223. DOI:

10.1016/0032-5910(88)80031-7.

Chrissafis K (2007) Multicyclic study on the carbonation of CaO using different limestones. *Journal of thermal analysis and calorimetry* 89(2). Springer Science and Business Media LLC: 525–529. DOI: 10.1007/s10973-006-7678-z.

Chung FH (1974) Quantitative interpretation of X-ray diffraction patterns of mixtures. I. Matrix-flushing method for quantitative multicomponent analysis. *Journal of applied crystallography* 7(6). International Union of Crystallography: 519–525. DOI: 10.1107/S0021889874010375.

Cipolla G, Calabrese S, Noto LV, et al. (2021) The role of hydrology on enhanced weathering for carbon sequestration I. Modeling rock-dissolution reactions coupled to plant, soil moisture, and carbon dynamics. *Advances in water resources* 154. Elsevier: 103934. DOI: 10.1016/j.advwatres.2021.103934.

Cline JP, Black D, Windover D, et al. (2013) The calibration of laboratory X-ray diffraction equipment using NIST standard reference materials. In: *Modern Diffraction Methods*. Weinheim, Germany: Wiley-VCH Verlag GmbH & Co. KGaA, pp. 399–438. DOI: 10.1002/9783527649884.ch13.

Coats AW and Redfern JP (1963) Thermogravimetric analysis. A review. *The Analyst* 88(1053). Royal Society of Chemistry (RSC): 906. DOI: 10.1039/an9638800906.

Craig H (1953) The geochemistry of the stable carbon isotopes. *Geochimica et cosmochimica acta* 3(2). Elsevier: 53–92. DOI: 10.1016/0016-7037(53)90001-5.

Criado JM, Real C, Ortega A, et al. (1990) Influence of mass-transfer phenomena on the shape of EGA traces of solid-state reactions. *Journal of Thermal Analysis* 36(7-8). Springer: 2531–2537.

Criss JW (1985) XRF-11 Users Guide. *Criss Software Inc., Largo, Md*.

Cubillas P, Köhler S, Prieto M, et al. (2005) How do mineral coatings affect dissolution rates? An experimental study of coupled CaCO3 dissolution—CdCO3 precipitation. *Geochimica et cosmochimica acta* 69(23). Elsevier: 5459–5476. DOI: 10.1016/j.gca.2005.07.016.

D18 Committee (2016) *Test method for density and unit weight of soil in place by sand-cone method*. West Conshohocken, PA: ASTM International. DOI: 10.1520/d1556_d1556m-15e01.

Dart RC, Barovich KM, Chittleborough DJ, et al. (2007) Calcium in regolith carbonates of central and southern Australia:Its source and implications for the global carbon cycle. *Palaeogeography, palaeoclimatology, palaeoecology* 249(3). Elsevier: 322–334. DOI: 10.1016/j.palaeo.2007.02.005.

Datar A, Chung YG and Lin L-C (2020) Beyond the BET Analysis: The Surface Area Prediction of Nanoporous Materials Using a Machine Learning Method. *Journal of Physical Chemistry Letters* 11(14). ACS Publications: 5412–5417. DOI: 10.1021/acs.jpclett.0c01518.

Daval D, Martinez I, Corvisier J, et al. (2009) Carbonation of Ca-bearing silicates, the case of wollastonite: Experimental investigations and kinetic modeling. *Chemical geology* 265(1): 63–78. DOI: 10.1016/j.chemgeo.2009.01.022.

Davies M (2011) Filtered dry stacked tailings : the fundamentals. The University of British Columbia. DOI: 10.14288/1.0107683.

Davies MP, Lupo J, Martin T, et al. (2010) Dewatered tailings practice--trends and observations. In: *Proceedings of Tailings and Mine Waste*, 2010. books.google.com.

Davis MK, Jackson TL, Shackley MS, et al. (1998) Factors Affecting the Energy-Dispersive X-Ray Fluorescence (EDXRF) Analysis of Archaeological Obsidian. In: Shackley MS (ed.) *Archaeological Obsidian Studies: Method and Theory*. Boston, MA: Springer US, pp. 159–180. DOI: 10.1007/978-1-4757-9276-8_7.

de Lannoy CF, Eisaman MD, Jose A, et al. (2018) Indirect ocean capture of atmospheric CO_2: Part I. Prototype of a negative emissions technology. *International Journal of Greenhouse Gas Control* 70(November). Elsevier: 243–253. DOI: 10.1016/j.ijggc.2017.10.007.

Delerce S, Bénézeth P, Schott J, et al. (2023) The dissolution rates of naturally altered basalts at pH 3 and 120 °C: Implications for the in-situ mineralization of CO_2 injected into the subsurface. *Chemical geology* 621(121353). Elsevier BV: 121353. DOI: 10.1016/j.chemgeo.2023.121353.

Deniel C and Pin C (2001) Single-stage method for the simultaneous isolation of lead and strontium from silicate samples for isotopic measurements. *Analytica chimica acta* 426(1). Elsevier: 95–103. DOI: 10.1016/S0003-2670(00)01185-5.

Di Bonito M, Breward N, Crout N, et al. (2018) Chapter 10 - Extraction and Characterization of Pore Water in Contaminated Soils. In: De Vivo B, Belkin HE, and Lima A (eds) *Environmental Geochemistry (Second Edition)*. Elsevier, pp. 195–235. DOI: 10.1016/B978-0-444-63763-5.00011-2.

Dickson AG (1981) An exact definition of total alkalinity and a procedure for the estimation of alkalinity and total inorganic carbon from titration data. *Deep-sea research. Part A, Oceanographic research papers* 28(6): 609–623. DOI: 10.1016/0198-0149(81)90121-7.

Dickson AG, Sabine CL and Christian JR (2007) Guide to best practices for ocean CO_2 measurements. repository.oceanbestpractices.org. Available at: https://repository.oceanbestpractices.org/handle/11329/249.

Dietzel, M., Usdowski, E. and Hoefs, J., 1992. Chemical and 13C/12C-and 18O/16O-isotope evolution of alkaline drainage waters and the precipitation of calcite. Applied Geochemistry, 7(2), pp.177-184.

Dijkstra JJ, Comans RNJ, Schokker J, et al. (2019) The geological significance of novel anthropogenic materials: Deposits of industrial waste and by-products. *Anthropocene* 28. Elsevier: 100229. DOI: 10.1016/j.ancene.2019.100229.

Dodson MH (1963) A theoretical study of the use of internal standards for precise isotopic analysis by the surface ionization technique: Part I - General first-order algebraic solutions. *Journal of scientific instruments* 40(6). IOP Publishing: 289. DOI: 10.1088/0950-7671/40/6/307.

Domingo C, Loste E, Gómez-Morales J, et al. (2006) Calcite precipitation by a high-pressure CO_2 carbonation route. *The Journal of supercritical fluids* 36(3). Elsevier: 202–215. DOI: 10.1016/j.supflu.2005.06.006.

Eisaman M, Geilert S and Renforth P (2023) Chapter 3: Assessing the technical aspects of OAE approaches. *State of the Planet*. sp.copernicus.org. Available at: https://sp.copernicus.org/preprints/sp-2023-1/.

Erans M, Nabavi SA and Manović V (2020) Carbonation of lime-based materials under ambient conditions for direct air capture. *Journal of cleaner production* 242: 118330. DOI: 10.1016/j.jclepro.2019.118330.

Esson J (1983) Geochemistry of a nickeliferous laterite profile, Liberdade, Brazil. *Geological Society, London, Special Publications* 11(1): 91–99. DOI: 10.1144/GSL.SP.1983.011.01.11.

Evans EH and Clough R (2005) ISOTOPE DILUTION ANALYSIS. In: Worsfold P, Townshend A, and Poole C (eds) *Encyclopedia of Analytical Science (Second Edition)*. Oxford: Elsevier, pp. 545–553. DOI: 10.1016/B0-12-369397-7/00301-0.

Fabian M, Shopska M, Paneva D, et al. (2010) The influence of attrition milling on carbon dioxide sequestration on magnesium–iron silicate. *Minerals engineering* 23(8): 616–620. DOI: 10.1016/j.mineng.2010.02.006.

Falk ES, Guo W, Paukert AN, et al. (2016) Controls on the stable isotope compositions of travertine from hyperalkaline springs in Oman: Insights from clumped isotope measurements. *Geochimica et cosmochimica acta* 192. Elsevier: 1–28. DOI: 10.1016/j.gca.2016.06.026.

Fantle MS and Tipper ET (2014) Calcium isotopes in the global biogeochemical Ca cycle: Implications for development of a Ca isotope proxy. *Earth-Science Reviews* 129. Elsevier: 148–177. DOI: 10.1016/j.earscirev.2013.10.004.

Farhang F, Oliver TK, Rayson M, et al. (2016) Experimental study on the precipitation of magnesite from thermally activated serpentine for CO_2 sequestration. *Chemical engineering journal* 303. Elsevier: 439–449. DOI: 10.1016/j.cej.2016.06.008.

Farhang F, Oliver TK, Rayson MS, et al. (2019) Dissolution of heat activated serpentine for CO_2 sequestration: The effect of silica precipitation at different temperature and pH values. *Journal of CO_2 Utilization* 30. Elsevier: 123–129. DOI: 10.1016/j.jcou.2019.01.009.

Fernández Bertos M, Simons SJR, Hills CD, et al. (2004) A review of accelerated carbonation technology in the treatment of cement-based materials and sequestration of CO2. *Journal of hazardous materials* 112(3): 193–205. DOI: 10.1016/j.jhazmat.2004.04.019.

Ferrufino GLAA, Ferrufino GLA, Okamoto S, et al. (2018) CO_2 sequestration by pH-swing mineral carbonation based on HCl/NH4OH system using iron-rich lizardite 1T. *Journal of CO_2 Utilization*. DOI: 10.1016/j.jcou.2018.01.001.

Földvári M (2011) *Handbook of Thermogravimetric System of Minerals and Its Use in Geological Practice*. Geological Institute of Hungary (=Magyar Állami Földtani Intézet). Available at: https://play.google.com/store/books/details?id=xpxeMwEACAAJ.

Fourie A (2009) Preventing catastrophic failures and mitigating environmental impacts of tailings storage facilities. *Procedia Earth and Planetary Science* 1(1). Elsevier: 1067–1071. DOI: 10.1016/j.proeps.2009.09.164.

Fretwell BA, Short RI and Sutton JS (2006) *Guidance on the Design and Installation of Groundwater Quality Monitoring Points*. Environment Agency.

Frontier (2022) Carbon removal knowledge gaps. Available at: https://frontiergaps.softr.app/ (accessed 26 July 2023).

Furnell E, Bilaniuk K, Goldbaum M, et al. (2022) Dewatered and Stacked Mine Tailings: A Review. *ACS ES&T Engineering* 2(5). American Chemical Society: 728–745. DOI: 10.1021/acsestengg.1c00480.

Galy A, Yoffe O, Janney PE, et al. (2003) Magnesium isotope heterogeneity of the isotopic standard SRM980 and new reference materials for magnesium-isotope-ratio measurements. *Journal of analytical atomic spectrometry* 18(11). Royal Society of Chemistry: 1352–1356. DOI: 10.1039/B309273A.

Gautier J-M, Oelkers EH and Schott J (2001) Are quartz dissolution rates proportional to B.E.T. surface areas? *Geochimica et cosmochimica acta* 65(7). Elsevier BV: 1059–1070. DOI: 10.1016/s0016-7037(00)00570-6.

Gbor PK and Jia CQ (2004) Critical evaluation of coupling particle size distribution with the shrinking core model. *Chemical engineering science* 59(10). Elsevier: 1979–1987. DOI: 10.1016/j.ces.2004.01.047.

Gerdemann SJ, O'Connor WK, Dahlin DC, et al. (2007) Ex situ aqueous mineral carbonation. *Environmental Science and Technology* 41(7): 2587–2593. DOI: 10.1021/es0619253.

GHGProtocol (2023) GHG Protocol standards. Available at: https://ghgprotocol.org/standards (accessed 1 August 2023).

Goldstein JI, Newbury DE, Michael JR, et al. (2017) *Scanning Electron Microscopy and X-Ray Microanalysis*. Springer. Available at: https://play.google.com/store/books/details?id=D0I_DwAAQBAJ.

Gómez-Gualdrón DA, Moghadam PZ, Hupp JT, et al. (2016) Application of Consistency Criteria To Calculate BET Areas of Micro- And Mesoporous Metal–Organic Frameworks. *Journal of the American Chemical Society* 138(1). American Chemical Society: 215–224. DOI: 10.1021/jacs.5b10266.

Gras, A., Beaudoin, G., Molson, J., Plante, B., Bussière, B., Lemieux, J.M. and Dupont, P.P., 2017. Isotopic evidence of passive mineral carbonation in mine wastes from the Dumont Nickel Project (Abitibi, Quebec). International Journal of Greenhouse Gas Control, 60, pp.10-23.

Greenfield P (2023) Revealed: more than 90% of rainforest carbon offsets by biggest certifier are worthless, analysis shows. *The Guardian*, 18 January. The Guardian. Available at: https://www.theguardian.com/environment/2023/jan/18/revealed-forest-carbon-offsets-biggest-provider-worthless-verra-aoe (accessed 25 July 2023).

Gregg SJ and Sing KSW (1982) *Adsorption, Surface Area, and Porosity*. London: Academic Press. Available at: https://www.worldcat.org/title/adsorption-surface-area-and-porosity/oclc/8908132.

Grossman EL and Klein GD (1994) The carbon and oxygen isotope record during the evolution of Pangea: Carboniferous to Triassic. *Pangea: Paleoclimate, Tectonics, and Sedimentation during Accretion, Zenith, and Breakup of a Supercontinent: Geological Society of America, Special Paper* 288. books.google.com: 207–228.

Gupta H and Fan L-S (2002) Carbonation–Calcination cycle using high reactivity calcium oxide for carbon dioxide separation from flue gas. *Industrial & engineering chemistry research* 41(16). American Chemical Society (ACS): 4035–4042. DOI: 10.1021/ie010867l.

Guy C and Schott J (1988) Multi-site surface reaction versus transport control during the hydrolysis of a complex oxide. *Chemical geology* 70. ui.adsabs.harvard.edu: 78. DOI: 10.1016/0009-2541(88)90420-2.

Haines PJ (2002) *Principles of Thermal Analysis and Calorimetry*. Royal Society of Chemistry. DOI: 10.1039/9781847551764.

Hajdas, I., Ascough, P., Garnett, M.H., Fallon, S.J., Pearson, C.L., Quarta, G., Spalding, K.L., Yamaguchi, H. and Yoneda, M., 2021. Radiocarbon dating. Nature Reviews Methods Primers, 1(1), p.62.

Hamilton JL, Wilson SA, Morgan B, et al. (2020) Accelerating Mineral Carbonation in Ultramafic Mine Tailings via Direct CO_2 Reaction and Heap Leaching with Potential for Base Metal Enrichment and Recovery. *Economic geology and the bulletin of the Society of Economic Geologists* 115(2). GeoScienceWorld: 303–323. DOI: 10.5382/econgeo.4710.

Han C, Geng J, Xie X, et al. (2012) Determination of phosphite in a eutrophic freshwater lake by suppressed conductivity ion chromatography. *Environmental science & technology* 46(19). ACS Publications: 10667–10674. DOI: 10.1021/es300771a.

Hangx SJT and Spiers CJ (2009) Coastal spreading of olivine to control atmospheric CO_2 concentrations: A critical analysis of viability. *International Journal of Greenhouse Gas Control* 3(6): 757–767. DOI: 10.1016/j.ijggc.2009.07.001.

Haque, F., Santos, R.M., Dutta, A., et al. 2019. Co-benefits of wollastonite weathering in agriculture: CO_2 sequestration and promoted plant growth. *ACS omega*, 4(1), pp.1425-1433.

Haque, F., Santos, R.M. and Chiang, Y.W., 2020. CO_2 sequestration by wollastonite-amended agricultural soils–An Ontario field study. *International Journal of Greenhouse Gas Control*, 97, p.103017.

Harrington KJ, Hilton RG and Henderson GM (2023) Implications of the Riverine Response to Enhanced Weathering for CO_2 removal in the UK. *Applied geochemistry: journal of the International Association of Geochemistry and Cosmochemistry* 152. Elsevier: 105643. DOI: 10.1016/j.apgeochem.2023.105643.

Hartmann J, West AJ, Renforth P, et al. (2013) Enhanced chemical weathering as a geoengineering strategy to reduce atmospheric carbon dioxide, supply nutrients, and mitigate ocean acidification. *Reviews of geophysics* 51(2). Blackwell Publishing Ltd: 113–149. DOI: 10.1002/rog.20004.

Harvey PK and Atkin BP (1985) *Introduction to X-Ray Fluorescence Spectrometry*. Department of Geology, University of Nottingham.

Hautman DP and Munch DJ (1997) Method 300.1 Determination of inorganic anions in drinking water by ion chromatography. *EPA: Ohio*. 19january2017snapshot.epa.gov. Available at: https://19january2017snapshot.epa.gov/sites/production/files/2015-08/documents/method_300-1_1997.pdf.

Hellevang H, Aagaard P, Oelkers EH, et al. (2005) Can dawsonite permanently trap CO_2? *Environmental Science and Technology* 39(21): 8281–8287. DOI: 10.1021/es0504791.

Highfield J, Lim H, Fagerlund J, et al. (2012) Mechanochemical processing of serpentine with ammonium salts under ambient conditions for CO 2 mineralization. *RSC advances* 2(16). Royal Society of Chemistry: 6542–6548. DOI: 10.1039/C2RA20575K.

Hillier S (1999) Use of an air brush to spray dry samples for X-ray powder diffraction. *Clay minerals* 34(1). GeoScienceWorld: 127–135. Available at: https://pubs.geoscienceworld.org/claymin/article-abstract/34/1/127/56339 (accessed 1 August 2023).

Hills CD, Tripathi N and Carey PJ (2020) Mineralization Technology for Carbon Capture, Utilization, and Storage. *Frontiers in Energy Research* 8. DOI: 10.3389/fenrg.2020.00142.

Hin RC, Coath CD, Carter PJ, et al. (2017) Magnesium isotope evidence that accretional vapour loss shapes planetary compositions. *Nature* 549(7673): 511–515. DOI: 10.1038/nature23899.

Hodson ME (2006) Searching for the perfect surface area normalizing term—a comparison of BET surface area-, geometric surface area- and mass-normalized dissolution rates of anorthite and biotite. *Journal of Geochemical Exploration* 88(1). Elsevier: 288–291. DOI: 10.1016/j.gexplo.2005.08.058.

Ho DT, Bopp L, Palter JB, et al. (2023) Chapter 6: Monitoring, reporting, and Verification for ocean alkalinity enhancement. *State of the Planet Discussions*. DOI: 10.5194/sp-2023-2.

Hoefs J (2021) *Stable Isotope Geochemistry* (J Hoefsed.). Springer Textbooks in Earth Sciences, Geography and Environment. Berlin: Springer International Publishing. DOI: 10.1007/978-3-030-77692-3.

Hollingbery LA and Hull TR (2010) The thermal decomposition of huntite and hydromagnesite—A review. *Thermochimica acta* 509(1). Elsevier: 1–11. DOI: 10.1016/j.tca.2010.06.012.

Huang HP, Shi Y, Li W, et al. (2001) Dual Alkali Approaches for the Capture and Separation of CO_2. *Energy & fuels: an American Chemical Society journal* 15(2). American Chemical Society: 263–268. DOI: 10.1021/ef0002400.

Hudson JD (1977) Stable isotopes and limestone lithification. *Journal of the Geological Society* 133(6). GeoScienceWorld: 637–660. DOI: 10.1144/gsjgs.133.6.0637.

Hughes RE, Högberg A and Olausson D (2010) Sourcing flint from Sweden and Denmark. *Journal of Nordic Archaeological Science* 17. researchgate.net: 15–25. Available at: https://www.researchgate.net/profile/Anders-Hoegberg/publication/284192709_Sourcing_flint_from_Sweden_and_Denmark_A_pilot_study_employing_non-destructive_energy_dispersive_X-ray_fluorescence_spectrometry/links/58db500c45851578dfefa58e/Sourcing-flint-from-Sweden-and-Denmark-A-pilot-study-employing-non-destructive-energy-dispersive-X-ray-fluorescence-spectrometry.pdf.

Huijgen WJJ, Witkamp G-J and Comans RNJ (2006) Mechanisms of aqueous wollastonite carbonation as a possible CO_2 sequestration process. *Chemical engineering science* 61(13). Elsevier: 4242–4251. DOI: 10.1016/j.ces.2006.01.048.

Hull SL, Oty UV and Mayes WM (2014) Rapid recovery of benthic invertebrates downstream of hyperalkaline steel slag discharges. *Hydrobiologia* 736(1). Springer Science and Business Media LLC: 83–97. DOI: 10.1007/s10750-014-1894-5.

Huntzinger, DN, Gierke, JS, Sutter, LL, et al. 2009a. Mineral carbonation for carbon sequestration in cement kiln dust from waste piles. Journal of Hazardous Materials, 168(1), pp.31-37.

Huntzinger, DN, Gierke, JS, Kawatra, SK, et al. 2009b. Carbon dioxide sequestration in cement kiln dust through mineral carbonation. Environmental science & technology, 43(6), pp.1986-1992.

Hu Z and Qi L (2014) 15.5-Sample digestion methods. In: *Treatise on Geochemistry*. Elsevier Oxford, pp. 87–109. Available at: https://www.researchgate.net/profile/Zhaochu-Hu/publication/303802311_Sample_digestion_methods/links/5dd68404299bf10c5a26608a/Sample-digestion-methods.pdf.

Hwang N and Barron AR (2011) BET surface area analysis of nanoparticles. *The connexions project*: 1–11.

Ichikawa S and Nakamura T (2016) Solid sample preparations and applications for X-ray fluorescence analysis. *Encyclopedia of Analytical Chemistry*. Chichester, UK: John Wiley & Sons, Ltd. DOI: 10.1002/9780470027318.a9562.

Ichikawa S and Nakamura T (2023) Solid sample preparations and applications for X-ray fluorescence analysis. *Encyclopedia of Analytical Chemistry*. Wiley. DOI: 10.1002/9780470027318.a9562.pub2.

Ingamells CO (1970) Lithium metaborate flux in silicate analysis. *Analytica chimica acta* 52(2). Elsevier: 323–334. DOI: 10.1016/S0003-2670(01)80963-6.

Inghram MG (1954) Stable Isotope Dilution as an Analytical Tool. *Annual review of nuclear science* 4(1). Annual Reviews: 81–92. DOI: 10.1146/annurev.ns.04.120154.000501.

ISO (2006a) *Environmental management — Life cycle assessment — Principles and framework*. ISO 14040:2006. Geneva, Switzerland: International Organization for Standardization.

ISO (2006b) *Environmental management — Life cycle assessment — Requirements and guidelines*. ISO 14044:2006. Geneva, Switzerland: International Organization for Standardization.

ISO (2008) *Soil quality — Preparation of laboratory samples from large samples*. ISO 23909:2008. Geneva, Switzerland: International Organization for Standardization.

ISO (2010) *Cement — Test methods — Part 2: Chemical analysis by X-ray fluorescence*. ISO 29581-2:2010. Geneva, Switzerland: International Organization for Standardization.

ISO (2018a) *Greenhouse Gases: Carbon Footprint of Products: Requirements and Guidelines for Quantification*. ISO 14067:2018. Geneva, Switzerland: International Organization for Standardization.

ISO (2018b) *Greenhouse Gases--Part 1: Specification with Guidance at the Organization Level for Quantification and Reporting of Greenhouse Gas Emissions and Removals*. ISO 14064-1:2018. Geneva, Switzerland: International Organization for Standardization.

ISO (2018c) *Greenhouse gas management and related activities — Framework and principles for methodologies on climate actions*. ISO 14080:2018. Geneva, Switzerland: International Organization for Standardization.

ISO (2020) *Particle size analysis — Laser diffraction methods*. ISO 13320:2020. Geneva, Switzerland: International Organization for Standardization.

ISO (2021) *Iron ores — Determination of various elements by X-ray fluorescence spectrometry — Part 4: Performance-based method using fusion preparation method*. ISO/TS 9516-4:2021. Geneva, Switzerland: International Organization for Standardization.

ISO (2022) *Determination of the specific surface area of solids by gas adsorption — BET method*. ISO 9277:2022. Geneva, Switzerland: International Organization for Standardization.

Jackson PE (2000) Ion Chromatography in Environmental Analysis. *Encyclopedia of Analytical Chemistry*. Chichester, UK: John Wiley & Sons, Ltd. DOI: 10.1002/9780470027318.a0835.

Jackson PE (2001) Determination of inorganic ions in drinking water by ion chromatography. *Trends in analytical chemistry: TRAC* 20(6). Elsevier: 320–329. DOI: 10.1016/S0165-9936(01)00070-X.

Jariwala, H., Haque, F., Vanderburgt, S., et al. 2022. Mineral–soil–plant–nutrient synergisms of enhanced weathering for agriculture: short-term investigations using fast-weathering wollastonite skarn. Frontiers in Plant Science, 13, p.929457.

Jewell R and Rathbone R (2009) Optical properties of coal combustion byproducts for particle-size analysis by laser diffraction. *Coal combustion and gasification products* 1(1). Center for Applied Energy Research: 1–6. DOI: 10.4177/ccgp-d-09-00001.

Jurczyk J, Glessi C, Madajska K, et al. (2022) Vacuum versus ambient pressure inert gas thermogravimetry: a study of silver carboxylates. *Journal of thermal analysis and calorimetry* 147(3). Springer: 2187–2195. DOI: 10.1007/s10973-021-10616-6.

Kakizawa M, Yamasaki A and Yanagisawa Y (2001) A new CO_2 disposal process via artificial weathering of calcium silicate accelerated by acetic acid. *Energy* 26(4). Elsevier: 341–354. DOI: 10.1016/S0360-5442(01)00005-6.

Kalnicky DJ and Singhvi R (2001) Field portable XRF analysis of environmental samples. *Journal of hazardous materials* 83(1-2). Elsevier: 93–122. DOI: 10.1016/s0304-3894(00)00330-7.

Kang D, Amarasiriwardena D and Goodman AH (2004) Application of laser ablation-inductively coupled plasma-mass spectrometry (LA-ICP-MS) to investigate trace metal spatial distributions in human tooth enamel and dentine growth layers and pulp. *Analytical and bioanalytical chemistry* 378(6). Springer Science and Business Media LLC: 1608–1615. DOI: 10.1007/s00216-004-2504-6.

Kantola IB, Blanc-Betes E, Masters MD, et al. (2023) Improved net carbon budgets in the US Midwest through direct measured impacts of enhanced weathering. *Global change biology*. DOI: 10.1111/gcb.16903.

Kantzas EP, Val Martin M, Lomas MR, et al. (2022) Substantial carbon drawdown potential from enhanced rock weathering in the United Kingdom. *Nature geoscience* 15(5). Nature Publishing Group: 382–389. DOI: 10.1038/s41561-022-00925-2.

Kanzaki Y, Zhang S, Planavsky NJ, et al. (2022) Soil Cycles of Elements simulator for Predicting TERrestrial regulation of greenhouse gases: SCEPTER v0.9. *Geoscientific model development* 15(12). Copernicus GmbH: 4959–4990. DOI: 10.5194/gmd-15-4959-2022.

Kelemen P, McQueen N, Wilcox J, et al. (2020) Engineered carbon mineralization in ultramafic rocks for CO_2 removal from air: Review and new insights. *Chemical geology* 550. DOI: 10.1016/j.chemgeo.2020.119628.

Kelemen PB and Matter J (2008) In situ carbonation of peridotite for CO_2 storage. *Proceedings of the National Academy of Sciences of the United States of America* 105(45): 17295–17300. DOI: 10.1073/pnas.0805794105.

Kemp SJ, Lewis AL and Rushton JC (2022) Detection and quantification of low levels of carbonate mineral species using thermogravimetric-mass spectrometry to validate CO_2 drawdown via enhanced rock weathering. *Applied geochemistry: journal of the International Association of Geochemistry and Cosmochemistry* 146. Elsevier: 105465. DOI: 10.1016/j.apgeochem.2022.105465.

Khalid A, Anwar MS and Siddiqi SA (2011) Energy dispersive X-ray fluorescence (EDXRF) for studying coinage from the Indo-Pak subcontinent. Available at: http://physlab.lums.edu.pk/images/a/a7/Coinagepart1v7.pdf.

Khawam A and Flanagan DR (2005) Role of isoconversional methods in varying activation energies of solid-state kinetics: II. Nonisothermal kinetic studies. *Thermochimica acta* 436(1). Elsevier: 101–112.

Kheshgi HS (1995) Sequestering atmospheric carbon dioxide by increasing ocean alkalinity. *Energy* 20(9). Elsevier: 915–922.

Kim Y, Caumon M-C, Barres O, et al. (2021) Identification and composition of carbonate minerals of the calcite structure by Raman and infrared spectroscopies using portable devices. *Spectrochimica acta. Part A, Molecular and biomolecular spectroscopy* 261. Elsevier: 119980. DOI: 10.1016/j.saa.2021.119980.

Knapp WJ and Tipper ET (2022) The efficacy of enhancing carbonate weathering for carbon dioxide sequestration. *Frontiers in Climate* 4. DOI: 10.3389/fclim.2022.928215.

Knapp WJ, Stevenson EI, Renforth P, et al. (2023) Quantifying CO_2 Removal at Enhanced Weathering Sites: a Multiproxy Approach. *Environmental science & technology* 57(26). ACS Publications: 9854–9864. DOI: 10.1021/acs.est.3c03757.

Kodre K, Attarde S, Yendhe P, et al. (2014) Research and reviews: journal of pharmaceutical analysis. *Res. Rev. J. Pharm. Anal. Differ* 3. academia.edu: 11–22. Available at: https://www.academia.edu/download/45034303/DSC.pdf.

Koryak M, Stafford LJ, Reilly RJ, et al. (1998) The Impact of Airport Deicing Runoff on Water Quality and Aquatic Life in a Pennsylvania Stream. *Journal of freshwater ecology* 13(3). Taylor & Francis: 287–298. DOI: 10.1080/02705060.1998.9663621.

Krevor SCM and Lackner KS (2011) Enhancing serpentine dissolution kinetics for mineral carbon dioxide sequestration. *International Journal of Greenhouse Gas Control* 5(4): 1073–1080. DOI: 10.1016/j.ijggc.2011.01.006.

Krishnamurthy, R.V., Schmitt, D., Atekwana, E.A. et al. 2003. Isotopic investigations of carbonate growth on concrete structures. Applied Geochemistry, 18(3), pp.435-444.

Kumkrong P, Mihai O, Mercier PHJ, et al. (2021) Tessier sequential extraction on 17 elements from three marine sediment certified reference materials (HISS-1, MESS-4, and PACS-3). *Analytical and bioanalytical chemistry* 413(4): 1047–1057. DOI: 10.1007/s00216-020-03063-z.

Kump LR, Kuznetsov AB, Gorokhov IM, et al. (2013) 7.10 Chemical Characteristics of Sediments and Seawater. In: Melezhik VA, Prave AR, Hanski EJ, et al. (eds) *Reading the Archive of Earth's Oxygenation: Volume 3: Global Events and the Fennoscandian Arctic Russia - Drilling Early Earth Project*. Berlin, Heidelberg: Springer Berlin Heidelberg, pp. 1457–1514. DOI: 10.1007/978-3-642-29670-3_10.

Kwon S, Fan M, DaCosta HFM, et al. (2011) Factors affecting the direct mineralization of CO_2 with olivine. *Journal of environmental sciences* 23(8). Elsevier: 1233–1239. DOI: 10.1016/s1001-0742(10)60555-4.

Lackner, K.S., Grimes, P. and Ziock, H.J., 2001. Capturing carbon dioxide from air. Carbon Capture and Storage: CO_2 Management Technologies, pp.363-376.

Lackner KS, Wendt CH, Butt DP, et al. (1995) Carbon dioxide disposal in carbonate minerals. *Energy* 20(11). Elsevier: 1153–1170. DOI: 10.1016/0360-5442(95)00071-N.

Lammers LN, Duan Y, Anaya L, et al. (2023) Electrolytic Sulfuric Acid Production with Carbon Mineralization for Permanent

Carbon Dioxide Removal. *ACS sustainable chemistry & engineering* 11(12). ACS Publications: 4800–4812. DOI: 10.1021/acssuschemeng.2c07441.

La Plante EC, Mehdipour I, Shortt I, et al. (2021) Controls on CO_2 Mineralization Using Natural and Industrial Alkaline Solids under Ambient Conditions. *ACS Sustainable Chemistry & Engineering* 9(32): 10727–10739. DOI: 10.1021/acssuschemeng.1c00838.

Larkin CS, Andrews MG, Pearce CR, et al. (2022) Quantification of CO_2 removal in a large-scale enhanced weathering field trial on an oil palm plantation in Sabah, Malaysia. *Frontiers in Climate* 4. DOI: 10.3389/fclim.2022.959229.

León-Reina L, García-Maté M, Álvarez-Pinazo G, et al. (2016) Accuracy in Rietveld quantitative phase analysis: a comparative study of strictly monochromatic Mo and Cu radiations. *Journal of applied crystallography* 49(Pt 3): 722–735. DOI: 10.1107/S1600576716003873.

Levine M (2021) ICP-OES – ICP chemistry, ICP-OES analysis, strengths and limitations. Technology Networks. Available at: https://www.technologynetworks.com/analysis/articles/icp-oes-icp-chemistry-icp-oes-analysis-strengths-and-limitations-342265 (accessed 1 August 2023).

Lewis AL, Sarkar B, Wade P, et al. (2021) Effects of mineralogy, chemistry and physical properties of basalts on carbon capture potential and plant-nutrient element release via enhanced weathering. *Applied geochemistry: journal of the International Association of Geochemistry and Cosmochemistry* 132. Elsevier: 105023. DOI: 10.1016/j.apgeochem.2021.105023.

Li J and Hitch M (2018) Mechanical activation of magnesium silicates for mineral carbonation, a review. *Minerals engineering* 128. Elsevier: 69–83. DOI: 10.1016/j.mineng.2018.08.034.

Li J, Jacobs AD and Hitch M (2019) Direct aqueous carbonation on olivine at a CO_2 partial pressure of 6.5 MPa. *Energy* 173. Elsevier: 902–910. DOI: 10.1016/j.energy.2019.02.125.

Li N, Sack D, Sun J, et al. (2020) Quantifying the carbon content of aeolian sediments: Which method should we use? *Catena* 185. Elsevier: 104276. DOI: 10.1016/j.catena.2019.104276.

Lipp AG, Shorttle O, Syvret F, et al. (2020) Major element composition of sediments in terms of weathering and provenance: Implications for crustal recycling. *Geochemistry, Geophysics, Geosystems* 21(6). American Geophysical Union (AGU). DOI: 10.1029/2019gc008758.

Liu, G, Schollbach, K, Li, P. and Brouwers, HJH, 2021. Valorization of converter steel slag into eco-friendly ultra-high performance concrete by ambient CO_2 pre-treatment. Construction and Building Materials, 280, p.122580.

Liu W, Su S, Xu K, et al. (2018) CO_2 sequestration by direct gas–solid carbonation of fly ash with steam addition. *Journal of cleaner production* 178. Elsevier: 98–107. DOI: 10.1016/j.jclepro.2017.12.281.

Li WY, Teng FZ, Ke S, et al. (2010) Heterogeneous magnesium isotopic composition of the upper continental crust. *Geochimica et cosmochimica acta* 74(23). Elsevier: 6867–6884. DOI: 10.1016/j.gca.2010.08.030.

Llovet X (2019) Microscopy| electron probe microanalysis. Elsevier. Available at: https://scholar.google.ca/scholar?cluster=4636564822006157481&hl=en&as_sdt=0,5&sciodt=0,5.

Lobato K (2010) *SOP 205 - Anions by Ion Chromatography*. Revision 8. Albuquerque Bernalillo County Water Quality Laboratory.

Lovell HC (2010) Governing the carbon offset market. *Wiley interdisciplinary reviews. Climate change* 1(3). Wiley: 353–362. DOI: 10.1002/wcc.43.

Lundblad SP, Mills PR and Hon K (2007) Analysing archaeological basalt using non-destructive energy-dispersive x-ray fluorescence (edxrf): Effects of post-depositional chemical weathering and sample size on analytical precision. *Archaeometry* 0(0). Wiley: 071027143605002–??? DOI: 10.1111/j.1475-4754.2007.00345.x.

Lundvall F, Kalantzopoulos GN, Wragg DS, et al. (2019) Characterization and evaluation of synthetic Dawsonites as CO_2 sorbents. *Fuel* 236. Elsevier: 747–754. DOI: 10.1016/j.fuel.2018.09.057.

Luo YH, Zhu DQ, Pan J, et al. (2016) Thermal decomposition behaviour and kinetics of Xinjiang siderite ore. *Mineral Processing and Extractive Metallurgy* 125(1). Taylor & Francis: 17–25. DOI: 10.1080/03719553.2015.1118213.

Lu X, Carroll KJ, Turvey CC, et al. (2022) Rate and capacity of cation release from ultramafic mine tailings for carbon capture and storage. *Applied geochemistry: journal of the International Association of Geochemistry and Cosmochemistry* 140. Elsevier: 105285. DOI: 10.1016/j.apgeochem.2022.105285.

Lyon RE, Safronava N, Senese J, et al. (2012) Thermokinetic model of sample response in nonisothermal analysis. *Thermochimica acta* 545. Elsevier: 82–89.

MacDonald JM, Khudhur FWK, Carter R, et al. (2023) The mechanisms and microstructures of passive atmospheric CO_2

mineralisation with slag at ambient conditions. *Applied geochemistry: journal of the International Association of Geochemistry and Cosmochemistry* 152. Elsevier: 105649. DOI: 10.1016/j.apgeochem.2023.105649.

Macleod, G., Fallick, A.E. and Hall, A.J., 1991. The mechanism of carbonate growth on concrete structures, as elucidated by carbon and oxygen isotope analyses. Chemical Geology: Isotope Geoscience Section, 86(4), pp.335-343.

Maesano CN, Campbell JS, Foteinis S, et al. (2022) Geochemical Negative Emissions Technologies: Part II. Roadmap. *Frontiers in Climate* 4. frontiersin.org. DOI: 10.3389/fclim.2022.945332.

Marieni C, Matter JM and Teagle DAH (2020) Experimental study on mafic rock dissolution rates within CO_2-seawater-rock systems. *Geochimica et cosmochimica acta* 272. Elsevier: 259–275. DOI: 10.1016/j.gca.2020.01.004.

Matter JM, Takahashi T and Goldberg D (2007) Experimental evaluation of in situ CO_2-water-rock reactions during CO_2 injection in basaltic rocks: Implications for geological CO_2 sequestration. *Geochemistry, Geophysics, Geosystems* 8(2). American Geophysical Union (AGU). DOI: 10.1029/2006gc001427.

Matter JM, Stute M, Snæbjörnsdottir S, et al. (2016) Rapid carbon mineralization for permanent disposal of anthropogenic carbon dioxide emissions. *Science* 352(6291): 1312–1314. DOI: 10.1126/science.aad8132.

Mavromatis V, Gautier Q, Bosc O, et al. (2013) Kinetics of Mg partition and Mg stable isotope fractionation during its incorporation in calcite. *Geochimica et cosmochimica acta* 114. Elsevier: 188–203. DOI: 10.1016/j.gca.2013.03.024.

Mayes WM, Younger PL and Aumônier J (2008) Hydrogeochemistry of alkaline steel slag leachates in the UK. *Water, air, and soil pollution* 195(1-4): 35–50. DOI: 10.1007/s11270-008-9725-9.

Mayes WM, Riley AL, Gomes HI, et al. (2018) Atmospheric CO_2 Sequestration in Iron and Steel Slag: Consett, County Durham, United Kingdom. *Environmental Science and Technology* 52(14). American Chemical Society: 7892–7900. DOI: 10.1021/acs.est.8b01883.

McQueen N, Kelemen P, Dipple G, et al. (2020) Ambient weathering of magnesium oxide for CO_2 removal from air. *Nature communications* 11(1). DOI: 10.1038/s41467-020-16510-3.

Mervine EM, Dipple GM, Power IM, et al. (2017) Potential for offsetting Diamond mine carbon emissions through mineral carbonation of processed kimberlite. ikcabstracts.com. Available at: http://www.ikcabstracts.com/index.php/ikc/article/download/3917/3917 (accessed 29 July 2023).

Mervine EM, Wilson S, Power IM, et al. (2018) Potential for offsetting diamond mine carbon emissions through mineral carbonation of processed kimberlite: an assessment of De Beers mine sites in South Africa and Canada. *Mineralogy and Petrology* 112(S2). Springer Science and Business Media LLC: 755–765. DOI: 10.1007/s00710-018-0589-4.

Meysman FJR and Montserrat F (2017) Negative CO_2 emissions via enhanced silicate weathering in coastal environments. *Biology Letters*. DOI: 10.1098/rsbl.2016.0905.

Mikkelsen A, Andersen AB, Engelsen SB, et al. (1999) Presence and dehydration of ikaite, calcium carbonate hexahydrate, in frozen shrimp shell. *Journal of agricultural and food chemistry* 47(3). ACS Publications: 911–917. DOI: 10.1021/jf980932a.

Milonjić SK, Cerović LS, Cokesa DM, et al. (2007) The influence of cationic impurities in silica on its crystallization and point of zero charge. *Journal of colloid and interface science* 309(1). Elsevier: 155–159. DOI: 10.1016/j.jcis.2006.12.033.

Minx JC, Lamb WF, Callaghan MW, et al. (2017) Fast growing research on negative emissions. *Environmental research letters: ERL [Web site]* 12(3). IOP Publishing: 035007. DOI: 10.1088/1748-9326/aa5ee5.

Morales-Flórez V, Santos A, Lemus A, et al. (2011) Artificial weathering pools of calcium-rich industrial waste for CO_2 sequestration. *Chemical engineering journal* 166(1). Elsevier: 132–137. DOI: 10.1016/j.cej.2010.10.039.

Morgan MD (1987) Impact of nutrient enrichment and alkalinization on periphyton communities in the New Jersey Pine Barrens. *Hydrobiologia* 144(3): 233–241. DOI: 10.1007/BF00005557.

Mos YM, Vermeulen AC, Buisman CJN, et al. (2018) X-Ray Diffraction of Iron Containing Samples: The Importance of a Suitable Configuration. *Geomicrobiology journal* 35(6). Taylor & Francis: 511–517. DOI: 10.1080/01490451.2017.1401183.

Myers C and Nakagaki T (2020) Direct mineralization of atmospheric CO 2 using natural rocks in Japan Environmental Research Letters OPEN ACCESS RECEIVED Direct mineralization of atmospheric CO 2 using natural rocks in Japan. *Environmental research letters: ERL [Web site]* 15: 124018. DOI: 10.1088/1748-9326/abc217.

Nagy KL, Cygan RT, Hanchar JM, et al. (1999) Gibbsite growth kinetics on gibbsite, kaolinite, and muscovite substrates: atomic force microscopy evidence for epitaxy and an assessment of reactive surface area. *Geochimica et cosmochimica acta* 63(16). Elsevier: 2337–2351. DOI: 10.1016/S0016-7037(99)00118-0.

National Academies of Sciences, Engineering, and Medicine (2021) *A Research Strategy for Ocean-Based Carbon Dioxide*

Removal and Sequestration. Washington (DC): National Academies Press (US). DOI: 10.17226/26278.

Nduagu E, Björklöf T, Fagerlund J, et al. (2012) Production of magnesium hydroxide from magnesium silicate for the purpose of CO_2 mineralisation – Part 1: Application to Finnish serpentinite. *Minerals Engineering*. DOI: 10.1016/j.mineng.2011.12.004.

Neal M, Neal C, Wickham H, et al. (2007) Determination of bromide, chloride, fluoride, nitrate and sulphate by ion chromatography: comparisons of methodologies for rainfall, cloud water and river waters at the Plynlimon catchments of mid-Wales. *Hydrology and Earth System Sciences* 11(1). Copernicus GmbH: 294–300. DOI: 10.5194/hess-11-294-2007.

Nesbitt HW, Markovics G and Price RC (1980) Chemical processes affecting alkalis and alkaline earths during continental weathering. *Geochimica et cosmochimica acta* 44(11). Elsevier: 1659–1666. DOI: 10.1016/0016-7037(80)90218-5.

Nier AO (1940) A mass spectrometer for routine isotope abundance measurements. *The Review of scientific instruments* 11(7). AIP Publishing: 212–216. DOI: 10.1063/1.1751688.

Nikulshina V, Gálvez ME and Steinfeld A (2007) Kinetic analysis of the carbonation reactions for the capture of CO_2 from air via the Ca(OH)2–CaCO3–CaO solar thermochemical cycle. *Chemical engineering journal* 129(1). Elsevier: 75–83. DOI: 10.1016/j.cej.2006.11.003.

Omotoso O, McCarty DK, Hillier S, et al. (2006) SOME SUCCESSFUL APPROACHES TO QUANTITATIVE MINERAL ANALYSIS AS REVEALED BY THE 3RD REYNOLDS CUP CONTEST. *Clays and clay minerals* 54(6). GeoScienceWorld: 748–760. DOI: 10.1346/CCMN.2006.0540609.

O'Neil, J.R. and Barnes, I., 1971. C13 and O18 compositions in some fresh-water carbonates associated with ultramafic rocks and serpentinites: western United States. Geochimica et Cosmochimica Acta, 35(7), pp.687-697.

Opfergelt S, Burton KW, Georg RB, et al. (2014) Magnesium retention on the soil exchange complex controlling Mg isotope variations in soils, soil solutions and vegetation in volcanic soils, Iceland. *Geochimica et cosmochimica acta* 125. Elsevier: 110–130. DOI: 10.1016/j.gca.2013.09.036.

Oschlies A, Bach L, Rickaby R, et al. (2023) Climate targets, carbon dioxide removal and the potential role of Ocean Alkalinity Enhancement. *State of the Planet Discussions*. DOI: 10.5194/sp-2023-13.

Osterrieth JWM, Rampersad J, Madden D, et al. (2022) How Reproducible are Surface Areas Calculated from the BET Equation? *Advanced materials* 34(27). Wiley Online Library: e2201502. DOI: 10.1002/adma.202201502.

Palmer MR and Edmond JM (1992) Controls over the strontium isotope composition of river water. *Geochimica et cosmochimica acta* 56(5). Elsevier: 2099–2111. DOI: 10.1016/0016-7037(92)90332-D.

Park A-HA and Fan L-S (2004) CO_2 mineral sequestration: physically activated dissolution of serpentine and pH swing process. *Chemical engineering science* 59(22). Elsevier: 5241–5247. DOI: 10.1016/j.ces.2004.09.008.

Patterson AL (1939) The Scherrer Formula for X-Ray Particle Size Determination. *Physics Review* 56(10). American Physical Society: 978–982. DOI: 10.1103/PhysRev.56.978.

Penn RL, Zhu C, Xu H, et al. (2001) Iron oxide coatings on sand grains from the Atlantic coastal plain: High-resolution transmission electron microscopy characterization. *Geology* 29(9). GeoScienceWorld: 843–846. DOI: 10.1130/0091-7613(2001)029<0843:IOCOSG>2.0.CO;2.

Peters CA (2009) Accessibilities of reactive minerals in consolidated sedimentary rock: An imaging study of three sandstones. *Chemical geology* 265(1). Elsevier: 198–208. DOI: 10.1016/j.chemgeo.2008.11.014.

Pillot D, Deville E and Prinzhofer A (2014) Identification and Quantification of Carbonate Species Using Rock-Eval Pyrolysis. *Oil & Gas Science and Technology – Revue d'IFP Energies nouvelles* 69(2). Technip: 341–349. DOI: 10.2516/ogst/2012036.

Pogge von Strandmann PAE, Burton KW, Snæbjörnsdóttir SO, et al. (2019) Rapid CO_2 mineralisation into calcite at the CarbFix storage site quantified using calcium isotopes. *Nature communications* 10(1). Nature Publishing Group: 1–7. DOI: 10.1038/s41467-019-10003-8.

Pogge von Strandmann PAE, Dellinger M and Joshua West A (2021) Lithium Isotopes: A Tracer of Past and Present Silicate Weathering. In: *Elements in Geochemical Tracers in Earth System Science*. Cambridge University Press. DOI: 10.1017/9781108990752.

Pokrovsky OS and Schott J (2000) Kinetics and mechanism of forsterite dissolution at 25°C and pH from 1 to 12. *Geochimica et cosmochimica acta* 64(19). Elsevier BV: 3313–3325. DOI: 10.1016/s0016-7037(00)00434-8.

Poppe LJ, Paskevich VF, Hathaway JC, et al. (2001) A laboratory manual for X-ray powder diffraction. *US Geological Survey open-file report* 1(041). edisciplinas.usp.br: 1–88. Available at: https://edisciplinas.usp.br/pluginfile.php/5738095/mod_resource/content/1/USGS%20XRD%20Manual.pdf.

Power IM, Dipple GM and Southam G (2010) Bioleaching of ultramafic tailings by acidithiobacillus spp. for CO_2 sequestration. *Environmental science & technology* 44(1). ACS Publications: 456–462. DOI: 10.1021/es900986n.

Power IM, Harrison AL, Dipple GM, et al. (2013) Carbon Mineralization: From Natural Analogues to Engineered Systems. *Reviews in Mineralogy and Geochemistry* 77(1). GeoScienceWorld: 305–360. DOI: 10.2138/rmg.2013.77.9.

Power IM, Dipple GM, Bradshaw P, et al. (2020) Prospects for CO_2 mineralization and enhanced weathering of ultramafic mine tailings from the Baptiste nickel deposit in British Columbia, Canada. *International Journal of Greenhouse Gas Control* 94: 102895. DOI: 10.1016/j.ijggc.2019.102895.

Pretorius F (2022) *Carbon Dioxide Removal by Direct Air Capture*. 2.0. Zurich, Switzerland: Climeworks.

Prichard E and Barwick V (2007) *Quality Assurance in Analytical Chemistry*. John Wiley & Sons. Available at: https://play.google.com/store/books/details?id=g-zH-odv29EC.

Ptáček P, Kubátová D, Havlica J, et al. (2010a) Isothermal kinetic analysis of the thermal decomposition of kaolinite: The thermogravimetric study. *Thermochimica acta* 501(1). Elsevier: 24–29. DOI: 10.1016/j.tca.2009.12.018.

Ptáček P, Kubátová D, Havlica J, et al. (2010b) The non-isothermal kinetic analysis of the thermal decomposition of kaolinite by thermogravimetric analysis. *Powder Technology* 204(2). Elsevier: 222–227. DOI: 10.1016/j.powtec.2010.08.004.

Pulido C, Keijsers DJH, Lucassen ECHET, et al. (2012) Elevated alkalinity and sulfate adversely affect the aquatic macrophyte Lobelia dortmanna. *Aquatic ecology* 46(3): 283–295. DOI: 10.1007/s10452-012-9399-7.

Pullin H, Bray AW, Burke IT, et al. (2019) Atmospheric Carbon Capture Performance of Legacy Iron and Steel Waste. *eprints.whiterose.ac.uk* 53(16). American Chemical Society: 9502–9511. DOI: 10.1021/acs.est.9b01265.

PuroEarth (2022) *Enhanced Rock Weathering Methodology*. 1. Puro.earth. Available at: https://puro.earth/articles/enhanced-rock-weathering-in-soil-methodology-public-consulta-788 (accessed 25 July 2023).

Qin F and Beckingham LE (2021) The impact of mineral reactive surface area variation on simulated mineral reactions and reaction rates. *Applied geochemistry: journal of the International Association of Geochemistry and Cosmochemistry* 124. Elsevier: 104852. DOI: 10.1016/j.apgeochem.2020.104852.

Qiu Q (2020) A state-of-the-art review on the carbonation process in cementitious materials: Fundamentals and characterization techniques. *Construction and Building Materials* 247. Elsevier: 118503. DOI: 10.1016/j.conbuildmat.2020.118503.

Ratouis T (2022) *Permanent and Secure Geological Storage of* CO_2 *by In-Situ Carbon Mineralization*. 1.0, 15 June. Kopavogur, Iceland: Carbfix.

Rau GH, Knauss KG, Langer WH, et al. (2007) Reducing energy-related CO_2 emissions using accelerated weathering of limestone. *Energy* 32(8). Elsevier: 1471–1477.

Reershemius T, Kelland ME, Jordan JS, et al. (2023) A new soil-based approach for empirical monitoring of enhanced rock weathering rates. *arXiv [q-bio.OT]*. Available at: http://arxiv.org/abs/2302.05004.

Renforth P (2019) The negative emission potential of alkaline materials. *Nature communications* 10(1). Springer US. DOI: 10.1038/s41467-019-09475-5.

Renforth P and Henderson G (2017) Assessing ocean alkalinity for carbon sequestration. *Reviews of geophysics* 55(3): 636–674. DOI: 10.1002/2016RG000533.

Renforth P and Manning DAC (2011) Laboratory carbonation of artificial silicate gels enhanced by citrate: Implications for engineered pedogenic carbonate formation. *International Journal of Greenhouse Gas Control* 5(6). Elsevier: 1578–1586. DOI: 10.1016/j.ijggc.2011.09.001.

Renforth P, Manning DAC and Lopez-Capel E (2009) Carbonate precipitation in artificial soils as a sink for atmospheric carbon dioxide. *Applied geochemistry: journal of the International Association of Geochemistry and Cosmochemistry* 24(9): 1757–1764. DOI: 10.1016/j.apgeochem.2009.05.005.

Renforth P, Jenkins BG and Kruger T (2013) Engineering challenges of ocean liming. *Energy* 60: 442–452. DOI: 10.1016/j.energy.2013.08.006.

Renforth P, Pogge von Strandmann PAE and Henderson GM (2015) The dissolution of olivine added to soil: Implications for enhanced weathering. *Applied geochemistry: journal of the International Association of Geochemistry and Cosmochemistry* 61: 109–118. DOI: 10.1016/j.apgeochem.2015.05.016.

Renforth P, Baltruschat S, Peterson K, et al. (2022) Using ikaite and other hydrated carbonate minerals to increase ocean alkalinity for carbon dioxide removal and environmental remediation. *Joule* 6(12). Elsevier BV: 2674–2679. DOI:

10.1016/j.joule.2022.11.001.

Ren H, Pan Y, Sorrell CC, et al. (2020) Assessment of electrocatalytic activity through the lens of three surface area normalization techniques. *Journal of materials chemistry. A, Materials for energy and sustainability* 8(6). The Royal Society of Chemistry: 3154–3159. DOI: 10.1039/C9TA13170A.

Rietveld HM (1969) A profile refinement method for nuclear and magnetic structures. *Journal of applied crystallography* 2(2). International Union of Crystallography: 65–71. DOI: 10.1107/S0021889869006558.

Rimstidt JD, Brantley SL and Olsen AA (2012) Systematic review of forsterite dissolution rate data. *Geochimica et cosmochimica acta* 99. Elsevier: 159–178. DOI: 10.1016/j.gca.2012.09.019.

Rodriguez-Blanco JD, Shaw S and Benning LG (2011) The kinetics and mechanisms of amorphous calcium carbonate (ACC) crystallization to calcite, via vaterite. *Nanoscale* 3(1): 265–271. DOI: 10.1039/c0nr00589d.

Rounds SA and Wilde FD (2012) *Chapter A6. Section 6.6. Alkalinity and acid neutralizing capacity*. US Geological Survey. DOI: 10.3133/twri09a6.6.

Rudge JF, Reynolds BC and Bourdon B (2009) The double spike toolbox. *Chemical geology* 265(3). Elsevier: 420–431. DOI: 10.1016/j.chemgeo.2009.05.010.

Samari M, Ridha F, Manovic V, et al. (2020) Direct capture of carbon dioxide from air via lime-based sorbents. *Mitigation and Adaptation Strategies for Global Change* 25(1): 25–41. DOI: 10.1007/s11027-019-9845-0.

Scarlett NVY and Madsen IC (2006) Quantification of phases with partial or no known crystal structures. *Powder Diffraction* 21(4). Cambridge University Press: 278–284. DOI: 10.1154/1.2362855.

Scruggs B, Haschke M, Herczeg' L, et al. (2000) XRF MAPPING: NEW TOOLS FOR DISTRIBUTION ANALYSIS. *Advances in X-Ray Analysis* 42: 19–25. Available at: https://citeseerx.ist.psu.edu/document?repid=rep1&type=pdf&doi=08c54a32883cb01608623f7ab30daa1d54757626 (accessed 31 July 2023).

Sen G (2014) Alkaline and Ultra-Alkaline Rocks, Carbonatites, and Kimberlites. In: *Petrology*. Springer Berlin Heidelberg, pp. 243–260. DOI: 10.1007/978-3-642-38800-2_11.

Shelton LR (1997) *Field Guide for Collecting Samples for Analysis of Volatile Organic Compounds in Stream Water for the National Water-Quality Assessment Program*. U.S. Geological Survey. Available at: https://play.google.com/store/books/details?id=UbY6PRRedBYC.

Sinha P, Datar A, Jeong C, et al. (2019) Surface Area Determination of Porous Materials Using the Brunauer–Emmett–Teller (BET) Method: Limitations and Improvements. *Journal of Physical Chemistry C* 123(33). American Chemical Society: 20195–20209. DOI: 10.1021/acs.jpcc.9b02116.

Smith S, Geden O, Nemet G, et al. (2023) The state of carbon dioxide removal – 1st edition. research.manchester.ac.uk. Available at: https://research.manchester.ac.uk/en/publications/the-state-of-carbon-dioxide-removal-1st-edition (accessed 26 July 2023).

Snæbjörnsdóttir S, Wiese F, Fridriksson T, et al. (2014) CO_2 storage potential of basaltic rocks in Iceland and the oceanic Ridges. In: *Energy Procedia*, 2014, pp. 4585–4600. DOI: 10.1016/j.egypro.2014.11.491.

Song L and Temple J (2021) The climate solution actually adding millions of tons of CO_2 into the atmosphere. Available at: https://www.propublica.org/article/the-climate-solution-actually-adding-millions-of-tons-of-co2-into-the-atmosphere (accessed 25 July 2023).

So RT, Blair NE and Masterson AL (2020) Carbonate mineral identification and quantification in sediment matrices using diffuse reflectance infrared Fourier transform spectroscopy. *Environmental chemistry letters* 18(5). Springer: 1725–1730. DOI: 10.1007/s10311-020-01027-4.

Soulet G, Hilton RG, Garnett MH, et al. (2021) Temperature control on CO_2 emissions from the weathering of sedimentary rocks. *Nature geoscience* 14(9). Nature Publishing Group: 665–671. DOI: 10.1038/s41561-021-00805-1.

Stokes D (2008) *Principles and Practice of Variable Pressure / Environmental Scanning Electron Microscopy (VP-ESEM)*. John Wiley & Sons. Available at: https://play.google.com/store/books/details?id=GSeJEAAAQBAJ.

Stolaroff JK, Lowry GV and Keith DW (2005) Using CaO-and MgO-rich industrial waste streams for carbon sequestration. *Energy Conversion & Management* 46(5). Elsevier: 687–699.

Stracke A, Scherer EE and Reynolds BC (2014) 15.4 - Application of Isotope Dilution in Geochemistry. In: Holland HD and Turekian KK (eds) *Treatise on Geochemistry (Second Edition)*. Oxford: Elsevier, pp. 71–86. DOI: 10.1016/B978-0-08-095975-7.01404-2.

Strefler J, Amann T, Bauer N, et al. (2018) Potential and costs of carbon dioxide removal by enhanced weathering of rocks. *Environmental research letters: ERL [Web site]* 13(3). IOP Publishing: 034010. DOI: 10.1088/1748-9326/aaa9c4.

Stripe (2023) Stripe Climate. Available at: https://stripe.com/en-gb-gr/climate (accessed 25 July 2023).

Stubbs AR, Paulo C, Power IM, et al. (2022) Direct measurement of CO_2 drawdown in mine wastes and rock powders: Implications for enhanced rock weathering. *International Journal of Greenhouse Gas Control* 113. Elsevier: 103554. DOI: 10.1016/j.ijggc.2021.103554.

Stumm W and Morgan JJ (1981) Aquatic chemistry--2nd Edition, 780 pp. New York-London-Sydney-Toronto (Wiley).

Stumm W and Morgan JJ (1996) Aquatic Chemistry--chemical equilibria and rates in natural waters 3rd edition. Wiley-Interscience, New York.

Sutter B, Mcadam AC, Mahaffy PR, et al. (2017) Evolved gas analyses of sedimentary rocks and eolian sediment in Gale Crater, Mars: Results of the Curiosity rover's sample analysis at Mars instrument from …. *Journal of Geophysical Research: Planets* 122(12): 2574–2609. DOI: 10.1002/2016JE005225.

Sverdrup HU, Koca D and Schlyter P (2017) A Simple System Dynamics Model for the Global Production Rate of Sand, Gravel, Crushed Rock and Stone, Market Prices and Long-Term Supply Embedded into the WORLD6 Model. *BioPhysical Economics and Resource Quality* 2(2). Springer: 8. DOI: 10.1007/s41247-017-0023-2.

Tatzber M, Stemmer M, Spiegel H, et al. (2007) An alternative method to measure carbonate in soils by FT-IR spectroscopy. *Environmental chemistry letters* 5(1). Springer Science and Business Media LLC: 9–12. DOI: 10.1007/s10311-006-0079-5.

Taylor LL, Beerling DJ, Quegan S, et al. (2017) Simulating carbon capture by enhanced weathering with croplands: an overview of key processes highlighting areas of future model development. *Biology letters* 13(4). DOI: 10.1098/rsbl.2016.0868.

Teir S, Revitzer H, Eloneva S, et al. (2007) Dissolution of natural serpentinite in mineral and organic acids. *International Journal of Mineral Processing* 83(1): 36–46. DOI: 10.1016/j.minpro.2007.04.001.

Ten Berge, HF, Van der Meer, HG, Steenhuizen, JW, Goedhart, PW, Knops, P and Verhagen, J, 2012. Olivine weathering in soil, and its effects on growth and nutrient uptake in ryegrass (Lolium perenne L.): a pot experiment.

Tessier A, Campbell PGC and Bisson M (1979) Sequential extraction procedure for the speciation of particulate trace metals. *Analytical chemistry* 51(7). American Chemical Society: 844–851. DOI: 10.1021/ac50043a017.

Tester JW, Worley WG, Robinson BA, et al. (1994) Correlating quartz dissolution kinetics in pure water from 25 to 625°C. *Geochimica et cosmochimica acta* 58(11). Elsevier BV: 2407–2420. DOI: 10.1016/0016-7037(94)90020-5.

Tipper ET, Calmels D, Gaillardet J, et al. (2012) Positive correlation between Li and Mg isotope ratios in the river waters of the Mackenzie Basin challenges the interpretation of apparent isotopic fractionation during weathering. *Earth and planetary science letters* 333-334. Elsevier: 35–45. DOI: 10.1016/j.epsl.2012.04.023.

Totland M, Jarvis I and Jarvis KE (1992) An assessment of dissolution techniques for the analysis of geological samples by plasma spectrometry. *Chemical geology* 95(1). Elsevier: 35–62. DOI: 10.1016/0009-2541(92)90042-4.

Trewin N (1988) Use of the scanning electron microscope in sedimentology. In: Tucker M (ed.) *Techniques in Sedimentology*. Oxford: Blackwell Scientific Publications, pp. 229–273.

Turvey CC, Wilson SA, Hamilton JL, et al. (2017) Field-based accounting of CO_2 sequestration in ultramafic mine wastes using portable X-ray diffraction. *The American mineralogist* 102(6). De Gruyter: 1302–1310. DOI: 10.2138/am-2017-5953.

Turvey, CC, Wilson, S, Hamilton, JL, et al. 2018a. Hydrotalcites and hydrated Mg-carbonates as carbon sinks in serpentinite mineral wastes from the Woodsreef chrysotile mine, New South Wales, Australia: controls on carbonate mineralogy and efficiency of CO_2 air capture in mine tailings. International Journal of Greenhouse Gas Control, 79, pp.38-60.

Turvey, CC, Hamilton, JL, and Wilson, SA, 2018b. Comparison of Rietveld-compatible structureless fitting analysis methods for accurate quantification of carbon dioxide fixation in ultramafic mine tailings. American Mineralogist, 103(10), pp.1649-1662.

Turvey CC, Wynands ER and Dipple GM (2022) A new method for rapid brucite quantification using thermogravimetric analysis. *Thermochimica acta* 718. Elsevier: 179366. DOI: 10.1016/j.tca.2022.179366.

Tu Z, Liang X, Wu C, et al. (2022) Thermal decomposition characteristics of low-grade rhodochrosite ore in N_2, CO_2 and air atmosphere. *Journal of thermal analysis and calorimetry* 147(11). Springer Science and Business Media LLC: 6481–6488. DOI: 10.1007/s10973-021-10974-1.

US-EPA (2007) *Inductively coupled plasma-atomic emission spectrometry*. Method 6010C. Washington DC: United States Environmental Protection Agency.

Verified Carbon Standard (2019) *VM0043 methodology for CO_2 utilization in concrete production*. 1, 30 April. Verra. Available at: https://verra.org/methodologies/methodology-for-co2-utilization-in-concrete-production/ (accessed 25 July 2023).

Vidick B (1987) Specific surface area determination by gas adsorption: Influence of the adsorbate. *Cement and Concrete Research* 17(5). Elsevier: 845–847. DOI: 10.1016/0008-8846(87)90047-0.

Vienne, A, Poblador, S, Portillo-Estrada, M, et al. 2022. Enhanced weathering using basalt rock powder: carbon sequestration, co-benefits and risks in a mesocosm study with Solanum tuberosum. Frontiers in Climate, 4, p.72.

Vink, JPM, Giesen, D and Ahlrichs, E, 2022. Olivine weathering in field trials. Effect of Natural Environmental Conditions on Mineral Dissolution and the Potential Toxicity of Nickel; Deltares Technical Report, 11204378.

von Blanckenburg F (2006) The control mechanisms of erosion and weathering at basin scale from cosmogenic nuclides in river sediment. *Earth and planetary science letters* 242(3). Elsevier: 224–239. DOI: 10.1016/j.epsl.2005.11.017.

Vyazovkin S, Burnham AK, Criado JM, et al. (2011) ICTAC Kinetics Committee recommendations for performing kinetic computations on thermal analysis data. *Thermochimica acta* 520(1). Elsevier: 1–19.

Walkley A and Black IA (1934) AN EXAMINATION OF THE DEGTJAREFF METHOD FOR DETERMINING SOIL ORGANIC MATTER, AND A PROPOSED MODIFICATION OF THE CHROMIC ACID TITRATION METHOD. *Soil science* 37(1). journals.lww.com: 29. Available at: https://journals.lww.com/soilsci/citation/1934/01000/an_examination_of_the_degtjareff_method_for.3 (accessed 23 August 2023).

Wang F and Dreisinger D (2022) Carbon mineralization with concurrent critical metal recovery from olivine. *Proceedings of the National Academy of Sciences of the United States of America* 119(32): e2203937119. DOI: 10.1073/pnas.2203937119.

Wang X and Maroto-Valer MM (2011) Dissolution of serpentine using recyclable ammonium salts for CO_2 mineral carbonation. *Fuel* 90(3): 1229–1237. DOI: 10.1016/j.fuel.2010.10.040.

Wang X, Wang J and Zhang J (2012) Comparisons of three methods for organic and inorganic carbon in calcareous soils of northwestern China. *PloS one* 7(8): e44334. DOI: 10.1371/journal.pone.0044334.

Warne SSJ (2005) Variable atmosphere thermal analysis — methods, gas atmospheres and applications to geoscience materials. In: *Thermal Analysis in the Geosciences*. Berlin/Heidelberg: Springer-Verlag, pp. 61–83. DOI: 10.1007/bfb0010260.

Washbourne C-L, Lopez-Capel E, Renforth P, et al. (2015) Rapid Removal of Atmospheric CO_2 by Urban Soils. *Environmental science & technology* 49(9). ACS Publications: 5434–5440. DOI: 10.1021/es505476d.

Webster RK (1960) Mass spectrometric isotope dilution analysis. *Methods in Geochemistry*. Interscience. Available at: https://cir.nii.ac.jp/crid/1573387450062881024 (accessed 30 July 2023).

Wendt CH, Butt DP, Lackner KS, et al. (1998) *Thermodynamic calculations for acid decomposition of serpentine and olivine in MgCl2 melts. I. Description of concentrated MgCl2 melts*. Rep. LA-UR98-4528. Los Alamos Natl. Lab.

White AF and Brantley SL (2003) The effect of time on the weathering of silicate minerals: why do weathering rates differ in the laboratory and field? *Chemical geology* 202(3). Elsevier: 479–506. DOI: 10.1016/j.chemgeo.2003.03.001.

White AF and Peterson ML (1990) Role of Reactive-Surface-Area Characterization in Geochemical Kinetic Models. In: *Chemical Modeling of Aqueous Systems II*. ACS Symposium Series. American Chemical Society, pp. 461–475. DOI: 10.1021/bk-1990-0416.ch035.

White SP, Allis RG, Moore J, et al. (2005) Simulation of reactive transport of injected CO_2 on the Colorado Plateau, Utah, USA. *Chemical geology* 217(3). Elsevier: 387–405. DOI: 10.1016/j.chemgeo.2004.12.020.

Wilcox J, Kolosz B and Freeman J (2021) CDR primer.

Willbold M and Jochum KP (2005) Multi-element isotope dilution sector field ICP-MS: A precise technique for the analysis of geological materials and its application to geological reference materials. *Geostandards and Geoanalytical Research* 29(1). Wiley: 63–82. DOI: 10.1111/j.1751-908x.2005.tb00656.x.

Wilson SA, Raudsepp M and Dipple GM (2006) Verifying and quantifying carbon fixation in minerals from serpentine-rich mine tailings using the Rietveld method with X-ray powder diffraction data. *The American mineralogist* 91(8-9). Mineralogical Society of America: 1331–1341. Available at: https://pubs.geoscienceworld.org/msa/ammin/article-abstract/91/8-9/1331/134281.

Wilson SA, Dipple GM, Power IM, et al. (2009) Carbon Dioxide Fixation within Mine Wastes of Ultramafic-Hosted Ore Deposits: Examples from the Clinton Creek and Cassiar Chrysotile Deposits, Canada. *Economic geology and the bulletin of the Society of Economic Geologists* 104(1). GeoScienceWorld: 95–112. DOI: 10.2113/gsecongeo.104.1.95.

Wilson SA, Barker SLL, Dipple GM, et al. (2010) Isotopic disequilibrium during uptake of atmospheric CO_2 into mine process

waters: Implications for CO_2 sequestration. *Environmental Science and Technology* 44(24): 9522–9529. DOI: 10.1021/es1021125.

Wilson SA, Harrison AL, Dipple GM, et al. (2014) Offsetting of CO_2 emissions by air capture in mine tailings at the Mount Keith Nickel Mine, Western Australia: Rates, controls and prospects for carbon neutral mining. *International Journal of Greenhouse Gas Control* 25: 121–140. DOI: 10.1016/j.ijggc.2014.04.002.

Wolf A, Chang ES-H and Tank AR (2023) Verification methods and agronomic enhancements for carbon removal based on enhanced rock weathering. *US Patent*. 11644454. Available at: https://patentimages.storage.googleapis.com/ab/2d/58/dc57d23c538b83/US11644454.pdf (accessed 8 August 2023).

Wolff-Boenisch D, Gislason SR, Oelkers EH, et al. (2004) The dissolution rates of natural glasses as a function of their composition at pH 4 and 10.6, and temperatures from 25 to 74°C. *Geochimica et cosmochimica acta* 68(23). Elsevier BV: 4843–4858. DOI: 10.1016/j.gca.2004.05.027.

World Bank (2022) What you need to know about the Measurement, Reporting, and Verification (MRV) of carbon credits. World Bank Group. Available at: https://www.worldbank.org/en/news/feature/2022/07/27/what-you-need-to-know-about-the-measurement-reporting-and-verification-mrv-of-carbon-credits (accessed 25 July 2023).

Wren DG, Barkdoll BD, Kuhnle RA, et al. (2000) Field techniques for suspended-sediment measurement. *Journal of Hydraulic Engineering* 126(2). American Society of Civil Engineers (ASCE): 97–104. DOI: 10.1061/(asce)0733-9429(2000)126:2(97).

Wyatt KH and Stevenson RJ (2010) Effects of acidification and alkalinization on a periphytic algal community in an Alaskan wetland. *Wetlands* 30(6). Springer Science and Business Media LLC: 1193–1202. DOI: 10.1007/s13157-010-0101-3.

Wygel CM, Peters SC, McDermott JM, et al. (2019) Bubbles and Dust: Experimental Results of Dissolution Rates of Metal Salts and Glasses From Volcanic Ash Deposits in Terms of Surface Area, Chemistry, and Human Health Impacts. *GeoHealth* 3(11). Wiley Online Library: 338–355. DOI: 10.1029/2018GH000181.

Xu J-L, Thomas KV, Luo Z, et al. (2019) FTIR and Raman imaging for microplastics analysis: State of the art, challenges and prospects. *Trends in analytical chemistry: TRAC* 119. Elsevier: 115629. DOI: 10.1016/j.trac.2019.115629.

Yadav S and Mehra A (2017) Experimental study of dissolution of minerals and CO_2 sequestration in steel slag. *Waste management* 64: 348–357. DOI: 10.1016/j.wasman.2017.03.032.

Yatkin S, Trzepla K and McDade CE (2015) *IMPROVE Standard Operating Procedure for the X-Ray Fluorescence Analysis of Aerosol Deposits on PTFE Filters (with PANalytical Epsilon 5) SOP 301*. 2.1, 1 October. Crocker Nuclear Laboratory University of California.

Yu L, Wu K, Liu L, et al. (2020) Dawsonite and ankerite formation in the LDX-1 structure, Yinggehai basin, South China sea: An analogy for carbon mineralization in subsurface sandstone aquifers. *Applied geochemistry: journal of the International Association of Geochemistry and Cosmochemistry* 120. DOI: 10.1016/j.apgeochem.2020.104663.

Zeyen N, Wang B, Wilson SA, et al. (2022) Cation Exchange in Smectites as a New Approach to Mineral Carbonation. *Frontiers in Climate* 4. DOI: 10.3389/fclim.2022.913632.

Zhang J, Zhang R, Geerlings H, et al. (2010) A novel indirect wollastonite carbonation route for CO_2 sequestration. *Chemical Engineering & Technology* 33(7). Wiley: 1177–1183. DOI: 10.1002/ceat.201000024.

Zhang S, Planavsky NJ, Katchinoff J, et al. (2022) River chemistry constraints on the carbon capture potential of surficial enhanced rock weathering. *Limnology and oceanography* 67(S2). Wiley. DOI: 10.1002/lno.12244.

The cover image was created using Midjourney: “highly stylised book cover print in navy blue showing simplified repeating white highly translucent crystals of calcite --ar 2:3”